



Laboratoire
Génie Civil
et géo-Environnement
Lille Nord de France



UNIVERSITÉ LILLE 1 SCIENCES et TECHNOLOGIES

Laboratoire Génie Civil et géo-Environnement LGCgE

Discipline : Génie Civil

Et

UNIVERSITY of BALAMAND

Faculty of Civil Engineering

École Doctorale des Sciences pour l'Ingénieur EDSPI

THÈSE DE DOCTORAT

Développement et Élaboration de Méthodes de Traitement de Données de Terrain et de Modèles Hydrodynamiques et Hydrodispersifs dans une Optique de Développement Durable En Matière de Gestion de L'eau au Nord du Liban

Soutenu le 26/06/2014

Pour l'obtention du diplôme de

Docteur de l'Université Lille 1 Sciences et Technologies

Par

Marianne SABA

Devant le Jury :

Professeur Jalal HALAWANI
Professeur Lahcen ZOUHRI
Professeur Erick CARLIER
Professeur Najib GEORGES

Université Libanaise
Institut Polytechnique LaSalle Beauvais
Université Lille 1 Sciences et Technologies
University of Balamand

Rapporteur
Rapporteur
Directeur de Thèse
Co-Directeur de Thèse

ACKNOWLEDGEMENTS

Pursuing a PhD is a challenging experience where mixed and contradicting feeling emerged. It is just like climbing the highest peak of a mountain step by step accompanied by its bitterness, hardship and encouragement of so many people around me. When I found myself at the end of the journey, I realized that this long path toward my professional development objective would not have been possible without the support of all those people who supported me.

My outmost gratitude goes to my honorable director, Professor Erick Carlier, whose support; advice and guidance were the main drivers toward the right directions. No doubt, learning from such a professional reference has influenced my learning experience and without his sustenance this thesis would not have been possible.

My sincere gratitude goes as well to my co-director and trustworthy director, Professor Najib Georges, whose encouragement, guidance and support have enabled me to develop and accomplish my thesis.

Special thanks go as well to the Environmental Engineering Laboratory at the University of Balamand, GIS center with Dr. Amal Iaaly in person, the North Water Establishment in Lebanon and the LGCgE Laboratory at Polytech Lille.

Last but not least, I would like to mention that the accomplishment of this thesis would have not been successful without the full support of Professor Michel Najjar, Dean of Engineering and Vice President for Development.

My greatest regards is to my beloved husband Michel and two little boys Boutros and Marc. Without the personal and emotional support that my husband provided unconditionally towards me and the boys, this journey would have ended long time ago. Truly, you are the origin and essence of my happiness and success.

I would also like to convey my heartfelt thanks to my wonderful mother, whose understanding and support all through the three years have made me a stronger and more motivated individual in the pursuit of my academic degree. I am so thankful to all my family members from my father to my brother and sister as well as to my mother-, brother- and sister in laws who have encouraged me all along the way.

ABSTRACT

Keywords: Hydrochemistry, Groundwater Quality, Modeling, Visual Modflow, GIS, Sea Water Intrusion

The increasing population in Tripoli and its surrounding has placed an increase in the demand of groundwater and the random drilling of wells. This situation has resulted in a higher demand of groundwater and thus endangered the Miocene limestone aquifer that will cause problems unless serious steps for the management of water resources are implemented. These steps should include defining stringent characterization of the properties of the aquifer in order to properly manage the quality and quantity of pumped water.

Our aim in this study is to analyze the hydrochemical, hydro physical quality, and water level of groundwater in the Miocene aquifer in the North of Lebanon. The results have shown that the dominant type of groundwater in the area is highly chlorinated with sulfated calcium and magnesium with heavily charged nitrate and nitrite. The spatial distribution of anions and cations as well as electrical conductivity obeys an increasing pattern westwards towards the Mediterranean Sea. Due to the high concentrations of SO_4^{2-} , Cl^- , Mg^+ and Ca^{2+} , NO_2^- , and the presence of bacteriological contamination (E. Coli, Coliform, Salmonella) and some ions in higher concentration than the maximum allowable levels and, not all of the 65 water sampled in wet and dry seasons are categorized in suitable ranges for drinking use. During the last decades, illegal groundwater pumping mainly for domestic and agricultural use has caused groundwater quality degradation due to saline water intrusion from western areas (Tripoli and Mina area). In order to study the origin and the hydrochemical aspect of groundwater, PhreeqC and Diagram software helped us determine the properties after inputting the measured data on site; as for the water level parameters (conductivity and transmissivity) the Aquitest software was used. GIS and Visual Modflow software were used to generate maps locating the spatial distribution of all parameters, including the potentiometric map of the region.

The end result was the determination of anthropogenic and naturogenic sources of water contamination and pollution in North Lebanon. This is considered as one of the main concerns of the area; but due to the low utilities, budgets, political situation and unawareness of the population, the analysis and sampling were done in very crucial conditions in addition to the lack of studies and information on the Koura\Zgharta\Tripoli Miocene aquifer.

TABLE OF CONTENTS

ACKNOWLEDGEMENTS	iii
ABSTRACT	iv
TABLE OF CONTENTS	v
ABBREVIATIONS	xi
LIST OF TABLES	xiii
LIST OF FIGURES	xiv
INTRODUCTION	1
CHAPTER 1: HYDROLOGY AND HYDROGEOLOGY	3
Introduction	3
1.1 Hydrology and Hydrogeology	3
<i>1.1.1 Hydrologic Cycle</i>	3
<i>1.1.2 Elements of the Hydrologic Cycle</i>	5
<u>1.1.2.1 Precipitation</u>	5
<u>1.1.2.2 Infiltration</u>	6
<u>1.1.2.3 Run-Off</u>	6
<u>1.1.2.4 Evaporation and Transpiration</u>	7
<u>1.1.2.5 Evapotranspiration</u>	8
<u>1.1.2.6 Mathematical Statement for Hydrologic Cycle</u>	9
<i>1.1.3 Energy Transformations</i>	9
1.2 Hydrologic Equation	9
1.3 Geology of Groundwater	9
<i>1.3.1 Movement of Groundwater</i>	10
<i>1.3.2 Confined and Unconfined Aquifers</i>	11
CHAPTER 2: CHARACTERIZATION OF THE STUDIED AREA	13
Introduction	13

2.1 Area of Study	13
2.2 Climate of Koura, Zgharta and Tripoli Area	14
2.3 Groundwater	14
2.4 Previous Studies	15
2.5 Geology of Lebanon	16
2.6 Lithostratigraphy of the Studied Area	20
2.6.1 Location of the Studied Area	20
2.6.2 Secondary Formation	23
2.6.2.1 Middle Cretaceous	23
2.6.3 Upper Cretaceous (C6)	24
2.6.4 Eocene (E1-2a)	24
2.6.5 Vindobonian (M2)	24
2.6.6 Pontian	25
2.6.7 Pliocene (P)	26
2.6.8 Quaternary	26
2.7 Structural Features of the Studied Area	27
2.7.1 Jabal Kelhat Anticline	27
2.7.2 Jabal Tourbol Anticline	27
2.7.3 Amioun Anticline	27
2.7.4 Kousba Anticline	27
2.7.5 Koura-Zgharta Basin	27
CHAPTER 3: HYDROGEOLOGY OF THE STUDIED AREA	29
3.1 Introduction	29
3.2 Minor Aquifers in Koura Zgharta Basin	31
3.3 Miocene Aquifer of Koura Zgharta Basin	32

3.4 Potentiometric Surfaces	33
3.5 Karst in The Region	37
CHAPTER 4: MATERIALS, SAMPLING AND SAMPLING PROCEDURE (OR METHODOLOGY)	38
4.1 Criteria for Sampling (Or Sampling Protocol)	39
4.2 Field Investigation	40
4.3 Steps for Groundwater Sampling	43
<i>4.3.1 Handling Objects for Sampling</i>	43
<i>4.3.2 Washing the Sample Containers</i>	43
4.4 Sample Registration	44
4.5 Groundwater Sampling Methodology	44
<i>4.5.1 Sampling Procedure for Water Level</i>	44
<i>4.5.2 Sampling Procedure for Water Quality</i>	45
4.6 Difficulties Faced in Sampling Campaigns	46
4.7 Laboratory Measurement	49
<i>4.7.1 Procedure for Microbiological Tests: E.Coli ,Coliforms and Salmonela</i>	49
4.7.2 Procedure for Chemical Parameters	50
CHAPTER 5: ANALYSIS AND INTERPRETATIONS OF RESULTS	53
5.1 Water Level: Static and Dynamic Water Level	53
5.2 Water Chemistry Analysis	53
<i>5.2.1 The Physical Parameters</i>	75
<u>5.2.1.1 pH</u>	75
<u>5.2.1.2 Temperature</u>	76
<u>5.2.1.3 Total Dissolved Solids (TDS)</u>	77
<u>5.2.1.4 Dissolved Oxygen (DO)</u>	79

<u>5.2.1.5 Conductivity</u>	80
<u>5.2.1.6 Salinity</u>	82
<u>5.2.1.7 Wilcox Method</u>	85
5.2.2 <i>The Chemical Parameters</i>	86
<u>5.2.2.1 Hydrochemical Results Obtained With PhreeqC</u>	90
<u>5.2.2.2 Phosphate</u>	93
<u>5.2.2.3 Fluoride and Fluorite</u>	94
<u>5.2.2.4 Bromide</u>	97
<u>5.2.2.5 Nitrate, Nitrite and Ammonium</u>	99
<u>5.2.2.6 Chloride</u>	102
<u>5.2.2.7 Hardness, Calcium and Magnesium</u>	104
<u>5.2.2.8 Sodium and Potassium</u>	107
<u>5.2.2.9 Sulphate</u>	110
<u>5.2.2.10 Correlation Between Calcium, Sodium & Sulphate</u>	111
<u>5.2.2.11 Magnesium</u>	113
<u>5.2.2.12 Lithium</u>	114
<u>5.2.2.13 Bromide</u>	115
<u>5.2.2.14 E.Coli , Coliform and Salmonella</u>	116
5.3 Brief Discussion and Conclusion	117
CHAPTER 6: ESTIMATION OF GROUNDWATER RESOURCES AND GROUND WATER FLOW TO WELLS (PUMPING TEST ANALYSES)	124
6.1 Estimation of Groundwater Resources	124
6.2 Ground Water Flow to Wells (Pumping Test Analyses)	134
6.2.1 <i>Method to Approach Fractured Medium</i>	135

6.2.2	<i>Determination of Conductivity and Transmissivity</i>	135
6.2.3	<i>Theis Method (Unsteady-state flow)</i>	138
6.2.4	<i>Cooper-Jacob Method</i>	140
6.3	Interpretation of Theis and Cooper Jacob	148
6.4	Conclusion	151
	CHAPTER 7: MODELING GROUNDWATER USING VISUAL MODFLOW	152
7.1	Introduction	152
7.1.1	<i>Gridding Overview</i>	153
7.1.2	<i>Gridding Method</i>	154
7.1.3	<i>The Kriging Formula</i>	155
7.2	Geographical Information System and Visual Modflow for Our Study	158
7.2.1	<i>Procedure in Simulation of VMOD</i>	161
7.2.1.1	<u>Defining Properties</u>	164
7.2.2	<i>Boundary Condition</i>	167
7.2.3	<i>Proceed to Run or Define Optional Model Elements</i>	175
7.3	Results	177
	CHAPTER 8: MANAGEMENT OF GROUNDWATER IN MIOCENE LIMESTONE	184
	AQUIFER OF NORTH LEBANON	
8.1	Recharge and Evapotranspiration	185
8.2	Discharge	186
8.3	Groundwater Budget	186
8.4	Lifetime of the Aquifer	187
8.5	What is the Future?	189
8.5.1	<i>Water Law</i>	189
8.5.2	<i>Fundamental Principles</i>	190
8.5.3	<i>Water Shortage</i>	190
8.5.4	<i>Social Impact Analysis</i>	192
	CHAPTER 9: CONCLUSION AND RECOMMENDATIONS	199
	BIBLIOGRAPHY	196
	APPENDIX 1	217

APPENDIX 2	220
APPENDIX 3	249

ABBREVIATIONS

AET	Actual Evapotranspiration
BTD	Bureau Technique de Development
CDR	Council for Development and Reconstruction
CN	Curve Number
DEM	Digital Elevation Model
DEP	Department of Environmental Protection
DO	Dissolved Oxygen
EEL	Environmental Engineering Laboratory
EPA	Environmental Protection Agency
ETp	Evapotranspiration
FAO	Food and Agriculture Organization
Fp	Infiltration Capacity
GIS	Geographical Information System
IC	Ion Chromatography
LS	Lebanese Standard
MCL	Maximum Contaminant Level
MCM	Million Cubic Meters
MOE	Ministry of Environment
MSL	Mean Sea Level

NLWE	North Lebanon Water Establishment
SAR	Sodium Adsorption Ratio
SI	Saturation Index
SMCL	Secondary Maximum Contaminant Level
TDS	Total Dissolved Solid
USC	U.S. Soil Conservation Service
UTM	Universal Transverse Mercator
VMOD	Visual Modflow
WHO	World Health Organization

LIST OF TABLES

Table 2.1	Flow in Watercourses in Lebanese Caza's (MOE, 2011)	1
Table 3.2	Hydrostratigraphic Units of Lebanon (M. Abbud, 1986)	29
Table 3.2	The hydrogeologic Entities of the Koura- Zgharta Platform(Programme des Nations Unies pour le Développement F. C., 1972).	33
Table 4.1	Coordinates of Sampling Locations	41
Table 5.1	Results of Sampling Campaign Aug- Sept 2012	54
Table 5.2	Results of Sampling Campaign April - May 2013	65
Table 5.3	Geological Structure of the Sampling Locations	92
Table 5.4	Saturation Index (SI) for Dry Season 2012	93
Table 5.4	Bis Saturation Index (SI) for Dry Season 2012	94
Table 6.1	Density, Kinematic and Dynamic Viscosity of Water (Kruseman G.P., 2003)	136
Table 6.2	Method of Cooper-Jacob Applied for One of the Sampled Location by the Use of Aquitest Software	142
Table 6.3	Results of Conductivity and Transmissivity Obtained with Aquitest Software Wet Season 2013	145
Table 7.1	Typical Data Object Used for a Conceptual Model Workflow (Harbaugh, Banta, & Hill, 2000)	164
Table 7.2	Representative Porosity Values	167
Table 8.1	Water Sector Institutional Mapping of Responsibilities (ECODIT, Integrated Groundwater – Surface Water Management, 2003)	189

LIST OF FIGURES

Figure 1.1	Hydrological Cycle (Hydrogeologic cycle)	4
Figure 1.2	Process of the Hydrological Cycle (Kiely, 1998)	5
Figure 1.3	Saturated and Unsaturated Zones (Watershed)	11
Figure 1.4	Confined and Unconfined Aquifers (Singhal, 2007)	12
Figure 2.1	Location Map of Studied Area	13
Figure 2.2	Mean Annual Precipitation over Lebanon (MOE, 2011)	15
Figure 2.3	Simplified Geological Map of Lebanon. (Walley C. D., 1998)	17
Figure 2.4	Stratigraphic Scale of Lebanon (Programme des Nations Unies pour le Développement, 1971)	18
Figure 2.5	Stratigraphic Summary of Lebanon (Walley C. D., 1998)	19
Figure 2.6	Geologic Map of Koura Zgharta Region (FAO, 1971)	21
Figure 2.7	Cross Section AA' of the Koura Zgharta Region (Khayat Z., 2001)	21
Figure 2.8	Cross Section BB' of the Koura Zgharta Basin (Khayat Z., 2001)	21
Figure 2.9	Cross Section CC' of the Koura Zgharta Basin (Khayat Z., 2001)	23
Figure 2.10	Structural Features of the Koura-Zgharta Basin (FAO, 1971)	28
Figure 3.1	Plate II A Potentiometric Contour Map of the Miocene Aquifer (FAO, 1971)	35
Figure 3.2	Plate II B Potentiometric Contour Map of the Miocene Aquifer (FAO, 1971)	36
Figure 3.3	Modèle Conceptuel du Système Karstique (Bakalowicz M., 2010)	37
Figure 4.1	Sampling Location (GIS, 2012-2013)	39
Figure 4.2	Piezometers Used in Sampling (Hydrotechnik, 2012)	45

Figure 4.3	Horriba Apparatus and TDS meter	46
Figure 4.4	Sampled Wells	47
Figure 4.5	Sampled Wells	47
Figure 4.6	Situation in Tripoli	48
Figure 4.7	Incubators (37°C) for Bacterial Growth	50
Figure 4.8	Bacterial Colony Counter	50
Figure 4.9	Ion Chromatography	51
Figure 4.10	Scheme of Ion Chromatography (Dionex, 2003)	52
Figure 5.1	pH Variation for Dry Season 2012	79
Figure 5.2	Temperature Variation for Wet Season 2013	80
Figure 5.3	Temperature and DO Variation for Wet Season 2013	81
Figure 5.4	TDS & Temperature Variations, Done with PhreeqC Software	82
Figure 5.5	Temperature Variation for Wet Season 2013	83
Figure 5.6	TDS Variations for Dry Season 2012	83
Figure 5.7	Temperature and DO Variations for Dry Season 2012	84
Figure 5.8	Conductivity Variation for Dry Season 2012 in $\mu\text{S}/\text{cm}$ (GIS)	85
Figure 5.9	Conductivity Variation for Dry Season 2012 in $\mu\text{S}/\text{cm}$	86
Figure 5.10	Salinity Variations for Wet Season 2013	87
Figure 5.11	Salinity Variations in % for Wet Season 2013- GIS	88
Figure 5.12	Salinity Versus Elevation for Dry Season 2012	89
Figure 5.13	Wilcox Diagram for Dry Season 2012 (PhreeqC)	90
Figure 5.14	Piper Diagram for Dry Campaign 2012	91

Figure 5.15	Saturation Index of Dry Season 2012	97
Figure 5.16	Phosphate Variations for Dry Season 2012	98
Figure 5.17	Variations of Fluoride Concentrations for Wet Season 2013	99
Figure 5.18	Variations of Fluoride Concentrations for Dry Season 2012	99
Figure 5.19	Relationship Between Conductivity and Fluoride for Wet Season 2013	100
Figure 5.20	Relationship Between Sodium and Fluoride for Dry Season 2012	101
Figure 5.21	Concentrations of Bromide in the Dry Season 2012	102
Figure 5.22	Nitrate Concentrations in Dry Season 2012	103
Figure 5.23	Nitrate Concentrations in Wet Season 2013 (GIS)	104
Figure 5.24	Nitrite Concentrations for Dry Season 2012	104
Figure 5.25	Ammonium Concentrations in mg/L for Dry Season 2012	105
Figure 5.26	Ammonium Concentrations in mg/L for Wet Season 2013	106
Figure 5.27	Chloride Concentrations for Dry Season 2012	107
Figure 5.28	Chloride Variations for Wet Season 2013 (in mg/L)	107
Figure 5.29	Concentrations of Magnesium (in mg/L) for Dry Season 2012	109
Figure 5.30	Concentrations of Calcium (in mg/L) for Wet Season 2013	110
Figure 5.31	Concentrations of Sodium for Dry Season 2012	111
Figure 5.32	Sodium Variations for Wet Season 2013	112
Figure 5.33	Potassium Variations for Wet Season 2013	113

Figure 5.34	Sulfate Variations (in mg/L) for Wet Season 2013	114
Figure 5.35	Correlation Between Sodium and Calcium (PhreeqC) for Dry Season 2012	115
Figure 5.36	Correlation Between Calcium and Sulfate (PhreeqC) for Dry Season 2012	116
Figure 5.37	Correlation Between Calcium and Chloride and Sulfate and Sodium (PhreeqC) for Dry Season 2012	116
Figure 5.38	Magnesium Variation in mg/L for Dry Season 2012	117
Figure 5.39	Magnesium Variations in mg/L for Wet Season 2013	118
Figure 5.40	Lithium Variations for Dry Season 2012	119
Figure 5.41	Bromide Variation Between Wet and Dry Season	119
Figure 5.42	E.Coli and Coliform Variations for Dry Season 2012	120
Figure 5.43	E.Coli and Coliform Variations for Wet Season 2013	121
Figure 5.44	Correlation Between Sulfate & Salinity in Dry Season 2012	122
Figure 5.45	Correlation Between Chloride and Salinity for Dry Season 2012	123
Figure 6.1	Method of Theis Applied for One of the Sampled Location by the Use of Aquitest Software	139
Figure 6.2	Method of Cooper-Jacob Applied for one of the Sampled Location by the Use of Aquitest Software	140
Figure 6.3	Time Drawdown Plot with Discharge	150
Figure 7.1	Area of Study Applied with Surfer Software Using Kriging Method	156
Figure 7.2	Temperature Variations (in °C) for the Studies Area Using Kriging Method	157
Figure 7.3	Window Appearing in VMOD Upon its Creation	161
Figure 7.4	Collecting Data with VMOD	162
Figure 7.5	Creating Grid System in VMOD	163

Figure 7.6	Defining Model Properties for the Studied Area	166
Figure 7.7	Defining Boundary Conditions	168
Figure 7.8	Constant Head Condition with VMOD	169
Figure 7.9	River Boundary Condition as seen in VMOD (A. W. Harbaugh, 2000)	170
Figure 7.10	Layer View of the River Studied in our Study in VMOD	172
Figure 7.11	Running the Simulation	175
Figure 7.12	Engines used to Proceed with VMOD	176
Figure 7.13	Translating with VMOD	176
Figure 7.14	Potentiometric Map of Koura Zgharta and Tripoli Area	178
Figure 7.15	Closer view of Potentiometric Map of Koura Zgharta and Tripoli Area	179
Figure 7.16	Dynamic Water Level Map (in meters below ground) of Koura Zgharta and Tripoli Region	181
Figure 7.17	Static Water Level Map (in meters below ground) of Koura Zgharta and Tripoli Region	182
Figure 8.1	Annual Water Demand-Supply Balance, Total and Dry Seasons, 2003-2030 (World Bank, 2003)	191
Figure 8.2:	Annual Water Demand by Water Usage Category one in (MCM/year) and the Other in Percentage	191

INTRODUCTION

Nowadays, the uncontrolled development of industrialization and urbanization causes degradation of the water, whether surface or underground. This degradation is not uniform in time and space. The vast variability in water quality requires a detailed knowledge of the physical environment; hence an investigation of the interactions between the surface and groundwater as well as the flow patterns of various physiochemical pollutants in aquifer. The main objective of this PHD dissertation is to develop a model for analyzing the potentiometric groundwater indicators. This model will support decisions in management of water in a sustainable development perspective. From a socio-economic point of view, flow modeling and simulation of pollution in water are one of the tools necessary to develop an operating strategy and safeguard of this vital resource. The Lebanese context is of prominent need for this research since potable water is a scarce resource, thus the Miocene aquifer of Koura Zgharta and Tripoli will be selected. The proposed research will be based on the following phases covering experimental and theoretical aspects. The first phase covers the identification of chemical and physical parameters; the physical parameters cover conductivity, water level, temperature, pH, turbidity and hardness. As to obtain an overview on water quality, chemical parameters such as Nitrate, Nitrite, Phosphate, Fluoride, Chloride, Sulfate, Bromide, Ammonium, Magnesium, Calcium, Potassium and Sodium will allow so. A pre-climatological study to make an assessment in terms of effective rainfall and a summary of hydrochemical data will be covered as well. Building on the results of the physical and chemical analyses a distinction between the anthropogenic impact on water quality and the natural impact essentially linked to the geochemical nature of rocks and soils of the area will be made. The second phase will focus on the development of numerical model simulation with Visual Modflow and statistical models of data processing using PHREEQC that will be validated by field work. The third phase will focus on the usage of elaborated and developed models as tools to support decisions and projecting for the better management of water, restoring the quality of water and enhancing the social and economic development of the region.

In a nutshell, the objective of this study is to examine the water level and quality of the Miocene aquifer, which is considered as the main aquifer of the area under study, examine the usage of this aquifer and last but not least investigate the groundwater conditions in the Tripoli, Koura and Zgharta.

The results of this study are necessary for the proper management of the groundwater in the Koura, Zgharta and Tripoli Caza's. Thus, this research will provide scientific information's to manage water resources and to protect our quality of life. The mission is to provide hydrologic information (such as a recent water level map of the area) and water quality study for a better understanding and a better management of the water resources of the area. It will provide information needed for water -use and land-use planning since the large scale development of groundwater resources with the accompanying decline in its levels and other effects of pumping has led to concerns about the future availability of groundwater to meet domestic and public supply.

CHAPTER 1

HYDROLOGY and HYDROGEOLOGY

Introduction

Water covers about seventy percent of the planet. It is easy to assume that water is a typical liquid, much like any other; but, in fact, every physical and chemical property is unusual when compared with other liquids, and these differences are essential to life. Approximately 96 % of the water at the earth's surface is in the ocean, 3% in the form of ice, 1 %v is groundwater, 0.01 % is in streams and lakes, and only about 0.001 % is in the atmosphere (Drever, 1997). Although rivers and lakes make up only a small fraction of the hydrosphere, the rate of the water circulation through them is quite rapid. The amount of water discharging from rivers to the sea each year is equal to the amount of water available in rivers and lakes. The hydrologic cycle is a description of the way water moves through these various environments.

1.1 Hydrology and Hydrogeology

Hydrology is the study of water; it addresses the occurrence, distribution, movement, and chemistry of all waters of the earth. Hydrogeology encompasses the interrelationships of geologic materials and process with water (Fetter C.W., 2001).

1.1.1 Hydrologic Cycle

Water is a renewable resource, which is recycled in the hydrological cycle. Surface water tends to have a short residence time in the cycle while groundwater has a very long residence time. Despite the fact that water is renewable, freshwater resources are finite. Inputs of water (rainfall) are balanced by recharging groundwater and outputs from the catchment via river (surface flow).

Water is in constant motion on, under, and above earth's surface. The hydrological cycle is a continuous process with no starts or finishes. Figure1.1 shows this cycle. Precipitation begins when atmospheric moisture (water vapor) is cooled and condensed into the water droplets. The precipitation can follow different paths after it reaches the ground. Some of it may be intercepted by vegetation or small surface depressions; in other words, it is temporarily stuck on the surfaces

of leaves or grass or it is retained in puddles. Some portion of the water can infiltrate through the earth's surface and seep downward into the ground. Another portion of the water can flow over the ground's surface. Some of the intercepted water soon evaporates, and some of it is absorbed by the vegetation. A process called transpiration takes place as water is used by the vegetation and passes through the leaves of grass, plants, and trees, returning to the atmosphere as vapor. The combined process of evaporation and transpiration is called evapotranspiration. Overall, more than half the precipitation that reaches the ground is returned to the atmosphere by this process before reaching the oceans [3].

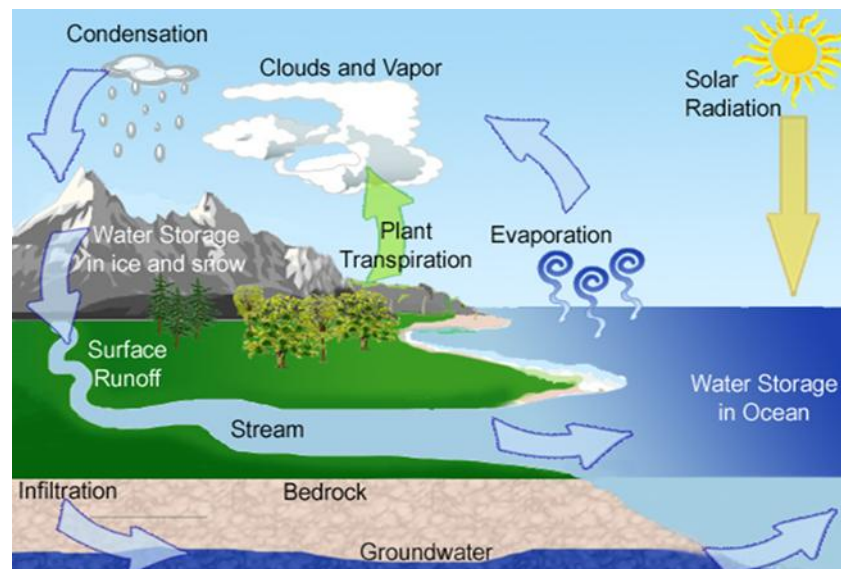


Figure 1.1 Hydrological Cycle (Hydrogeologic cycle)

Overland flow and surface runoff occur when the rate of precipitation exceeds the combined rates of infiltration and evapotranspiration. Eventually, the overland flow its way into the steam channels, rivers and lakes and finally the oceans. The ocean can be thought of as the final sink to which the water flows. The water that infiltrates the ground surface will percolate into the saturated soil and porous rock layers, forming vast groundwater reservoirs. The groundwater may later seep out to the surface in springs or into lakes. Eventually the groundwater makes its way to the ocean, either directly or by surface streams. Evaporation from the ocean surface substantially replenishes the water vapor in the atmosphere, winds carry the moist air over land, and the hydrologic cycle continues. (Fetter C.W., 2001)

The entire process is shown in Figure 1.2.

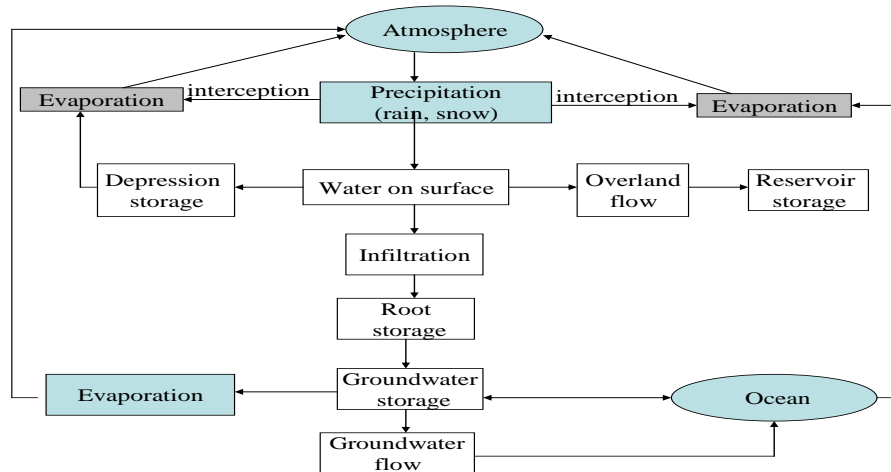


Figure 1.2 Process of the Hydrological Cycle (Kiely, 1998)

Recent changes in atmospheric temperature due to various human activities, particularly the burning of fossil fuels and deforestation, are also bound to affect the hydrological cycle. Recent records show that due to the continuous increase in the atmospheric concentration of CO₂ and other greenhouse gases worldwide, the Earth's surface temperature may rise about 2°C by 2050 and more than 3°C by 2100 (Dingman, 1994) which is likely to disturb the hydrological balance.

1.1.2 Elements of the Hydrologic Cycle

The various components of the hydrological cycle are described briefly in the following paragraphs.

1.1.2.1 Precipitation

The major types of precipitation are drizzle rain, snow and hail. Atmospheric precipitation is a consequence of condensation of water vapor around hygroscopic nuclei in the atmosphere. Rainfall is expressed in terms of depth of water in millimeters or centimeters, it is measured with the help of rain gauges. As for snow, it is as well a measure of precipitation, approximately 10 to 12 mm depth of snow equals 1 mm depth of water (Dingman, 1994). The precipitation intensity that is measured per unit of time, influences the recharge run-off relation as rainfall of moderate

intensity will be effective for groundwater recharge rather than short spells of higher intensity (because in this case, excessive run-off will lead to floods). The average depth of precipitation over a basin can be calculated by (a) arithmetic mean method, (b) isohyetal method and (c) Thiessen polygon method. The isohyetal method is considered as the most accurate one among these three since it takes into consideration the influence of topography on precipitation (Fetter C.W., 2001).

1.1.2.2 Infiltration

When rain falls on the ground, three processes are set in motion: wetting of soil and infiltration, surface runoff and evaporation. Rain leads to a significant amount of water in the ground. The moisture content is dependent on the porosity and the permeability of the soil. Below a certain elevation, the water content no longer increases with depth. The soil is said to be saturated, all the empty pores in the soil are filled with water. This water is said to belong to the water table aquifer. Above this elevation, the soil is said to be unsaturated, as the empty spaces in the soil contain both water and air simultaneously. Therefore, infiltration is the process of absorption of water into the soil; this allows the supply of water for plants growth, contributes to the base flow of streams and recharges the groundwater reservoirs. Infiltration capacity, f_p , is defined as the maximum rate at which water penetrates into the soil in a given condition. The rate of infiltration, f , is the actual rate that enters into the soil. In normal conditions, f will be less than f_p unless the rainfall intensity is greater or equal to the infiltration capacity. The maximum amount of water that soil can hold is defined as the field capacity. Infiltration is usually determined from hydrograph analysis, it depends in the soil/rock and vegetative properties of the ground under study. (Kiely, 1998)

1.1.2.3 Run-Off and Initial Abstraction

Run-off from a basin consists mainly of four components, surface run-off, interflow, channel precipitation and groundwater (base flow). A part of the precipitation infiltrates downward leading to an increase in the groundwater reservoir; another part travels laterally under the existing hydraulic gradient and is discharged into the stream with a greater time delay due to effluent seepage. After a rainstorm, water level in streams will rise as compared to the

groundwater, leading a reverse flow from the stream into the groundwater thus resulting in bank storage. Once the stream stage falls, the water flows back from the bank storage to the stream. In general, the total streamed of flow is divided into two fragments, the direct run-off and base flow. The direct run-off is made of the surface run-off, interflow and channel precipitation. On the other hand, base flow is the discharging water from the groundwater into the stream. Initial abstraction is defined as the maximum amount of rainfall absorbed without producing runoff (Karst, 2002). Curve Number CN, is defined as the coefficient that reduces the total precipitation to runoff potential, after evaporation, absorption, transpiration and surface storage. In 1972, the U.S. Soil Conservation Service SCS (SCS, 1972) , suggested an empirical model for rainfall abstractions which is based on the potential for the soil to absorb a certain amount of moisture. On the basis of field observations, this potential storage S (millimeters) was related to CN which is a characteristic of the soil type, land use and the initial degree of saturation known as the antecedent moisture condition. The SCS Runoff Equation is as follow

$$Q(t) = \frac{(P(t) - I_a)^2}{(P(t) + S - I_a)} \quad (1.1)$$

$Q(t)$ = accumulated depth of effective rainfall to time t (millimeters)

$P(t)$ = accumulated depth of rainfall to time t (millimeters)

I_a = initial abstraction (millimeters)

S = potential storage in the soil (millimeters)

$P(t)$ = accumulated precipitation depth (millimeters)

Note that the effective rainfall depth or runoff will be zero until the accumulated precipitation depth $P(t)$ exceeds the initial abstraction I_a .

From this equation the initial abstraction can be taken as equal to

$$I_a = 0.2 S \quad (1.2)$$

And the surface storage as

$$S = (1000 / CN) - 10 \quad (1.3)$$

1.1.2.4 Evaporation and Transpiration

Water molecules are constantly exchanged between the liquid and atmospheric water vapor. If the number of molecules passing to the vapor states exceeds the liquid molecules, the result is evaporation. This occurrence will proceed until the air becomes saturated with moisture, and is expressed in terms of absolute humidity (number of grams of water per cubic meter of air). When air masses are cooled and the saturated humidity drops, condensation occurs as air particles can no longer hold of its humidity. (Fetter C.W., 2001). Evaporation of water takes place in free water surfaces such as lakes, reservoirs, puddles, dew droplets etc... The rate depends on factors such as water temperature, absolute humidity of the air layer just above the free water surface, wind. Solar radiation is the driving energy behind evaporation as it warms both water and the air. Free water evaporation is only a part of the mechanism for mass transfer of water to the atmosphere. Growing plants are continuously pumping water from the ground into the atmosphere through transpiration. Water is drawn into a plant rootlet from the soil moisture to osmotic pressure, to a point that water will move from the plant to the leaves. The amount of transpiration depends on the type, density and size of the plant.

1.1.2.5 Evapotranspiration

In field conditions it is very hard to separate between evaporation and transpiration. The total loss of water from the soil surface and plants is termed Evapotranspiration (ET). Potential Evapotranspiration (PET or ETp) is a term introduced by Thornthwaite (1944); it expresses the maximum amount of water that will be removed by evapotranspiration if the soil has sufficient water to meet the demand. The majority of the water loss due to the evapotranspiration takes place during the summer months, with little or no loss during the winter. Because there is often no sufficient amount of water available from the soil water, the term Actual Evapotranspiration (AET) is used to describe the amount of evapotranspiration that takes place under field conditions. Thornthwaite's method is based upon the assumption that potential evapotranspiration was dependent only upon meteorological conditions and ignored the effect of vegetative density. The factors included are temperature, latitude and months. Thornthwaite's formula is expressed by the following equation: (Marsily D.G, 1986)

$$ET_p = 16(10\theta/I)_a \times F(\lambda) \text{ in (mm/month)} \quad (1.4)$$

Here, ET_p is the potential evapotranspiration and is given in millimeters per month

θ mean temperature of the period in question (C) measured under shelter

$$a = 6.75 \times 10^{-7} I^3 - 7.71 \times 10^{-5} I^2 + 1.79 \times 10^{-2} I + 0.49239$$

I annual thermal index, sum of twelve monthly thermal indexes, i

$$i = (\theta/5)^{1.514}$$

$F(\lambda)$ correction coefficient, function of latitude and month, given by **Appendix 1**

1.1.2.6 Mathematical Statement for Hydrologic Cycle

By remembering that the hydrological Cycle is a matter of balance between inflows, outflows and change in storage, the cycle can be summarized in a mathematical equation given in units of volume per unit time (Fetter C.W., 2001).

$$\text{Water Budget equation: } P - R - G - E - T = \Delta S \quad (1.5)$$

Where P is precipitation, R is surface runoff, G groundwater flow, E evaporation and T transpiration

1.1.3 Energy Transformations

The hydrologic cycle is an open system in which solar radiation serves as a source of constant energy; this is most evident on the evaporation and atmospheric circulation of water. For example, the energy of a flowing river is due to the work done by solar energy; the evaporating water from the ocean surface and lifting it to higher elevations, where it falls to earth. When water changes from one state to another, liquid, vapor or solid, an accompanying change on the heat energy of the water occurs. Therefore the heat energy is the amount of thermal energy contained by a substance.

1.2 Hydrologic Equation

The hydrologic cycle is a useful concept but is quantitatively rather vague. The hydrologic equation provides a quantitative means of evaluating the hydrologic cycle. This equation is a

simple statement of the law of mass conservation; it is expressed as follows (Fetter C.W., 2001):

$$\text{Inflow} = \text{outflow} \pm \text{changes in storage}$$

If we consider any hydrologic system, for example a well, it has a certain volume of water at a given time; several inflows add the volume of water: precipitation that falls on the surface of the lands and seeps into the ground with time, overflow from nearby surfaces. But water also leaves through evaporation, outlet streams and groundwater seepage from the aquifer. If, over a given time period, the total inflows are greater than the outflows, the well water is rising and more water accumulates; but if the outflow exceeds the inflow over a time period, the volume of water will decrease. Any difference between rates of inflow and outflow in a hydrologic system will result in a change in the volume of water stored in the system. In addition, the equation is time dependent, which means that the elements of inflow must be measured of a time period as the outflow. It is essential to note that the hydrologic equation can be applied to systems of any size, in other words it is as useful for a reservoir as for an entire continent. Hydrologic inputs may include precipitation, surface-water inflow from outside an area including runoff and overland flow; ground-water inflow from outside the area and artificial import of water into the area through pipes and canals. Hydrologic outputs from an area include evapotranspiration from land areas, evaporation of surface water, surface water runoff, groundwater outflow and artificial export of water through pipes and canals. The changes in storage necessary to balance the hydrologic equation include changes in the volume of surface water in streams, rivers, lakes and ponds; soil moisture in the vadose zone; ice and snow at the surface; temporary depression storage; intercepted water on plants surfaces; and groundwater below the water table.

1.3.1 Movement of Groundwater

Water movement occurs in soils under three distinct conditions, (1) saturated flow, (2) unsaturated flow and (3) vapor phase flow. All water movement beneath the water table is of the saturated flow type. However, a soil may be temporarily saturated above the water table and this occurs if all the pores are filled with water. Unsaturated flow takes place in response to gravity or moisture gradient. The mechanism of water movement in unsaturated flow is from pore to pore.

Figure 1.3 illustrates the movement of water. Water may exist in the vapor phase in the pores of a soil and be drawn upward to evaporate. The rate of movement depends on the temperature, pore size and pore continuity as well as the amount of water.

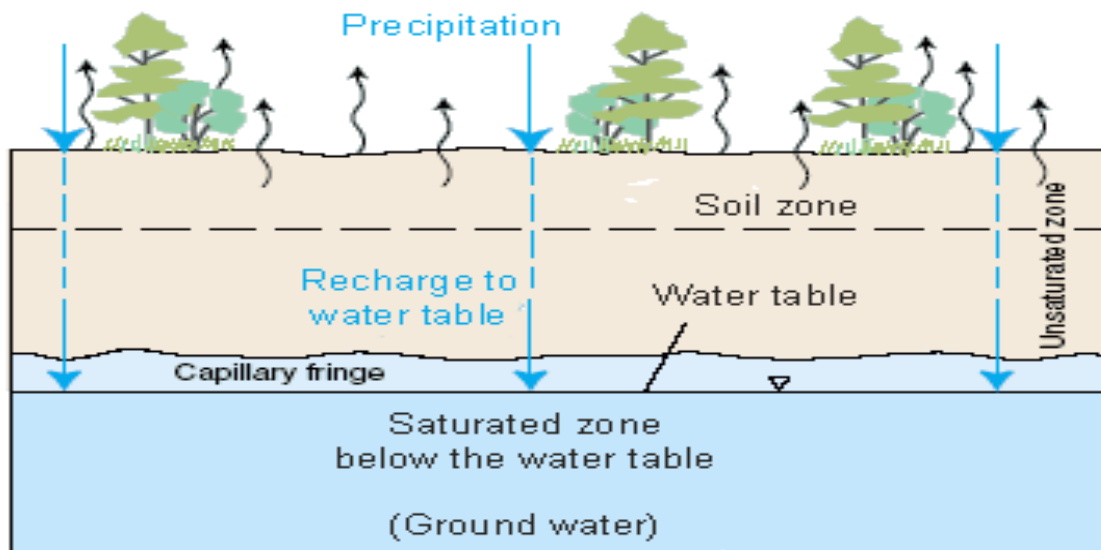


Figure 1.3 Saturated and Unsaturated Zones (Watershed)

After water first infiltrates the ground surface, it seeps downward through a layer called the zone of aeration. This is a layer of soil in which the small spaces between the solid soil particles are partially filled with air as well as water. As water percolates downward, it reaches the zone called the zone of saturation, a layer of soil or rock in which all the pore spaces or rock fissures are filled with water. The dividing line between the zone of aeration and the zone of saturation is called the water table. The water table is generally closer to the ground surface (Clair N. Sawyer, 1994).

1.3.2 Confined and Unconfined Aquifers

An aquifer is defined as a layer of soil or rock in which groundwater can move relatively freely, in other words, it is a water bearing rock formation that contains water in sufficient amounts to be exploited and brought to the surface by wells. An aquifer may be either confined or unconfined. Figure 1.4 clarifies the differences.

- The upper aquifer is unconfined, near the land surface is characterized by a natural free water table line free to move up or down. It is also called phreatic aquifer. It is recharged directly over the entire exposed surface of the aquifer.
- The confined aquifer is restrained by an upper impermeable layer, inhibiting the upward movement of water. The water here is under hydrostatic pressure (Clair N. Sawyer, 1994). This type of aquifers is also known as artesian aquifers it is overlain and underlain by a confining layer. The water in this type of aquifer is under pressure which is greater than the atmospheric pressure. The piezometric (or potentiometric) surface is an imaginary surface to which water will rise in wells tapping the confined aquifer. This surface should be on the upper surface of the aquifer, above the base of the overlying confining layer. Groundwater movement in the aquifer is similar to the conduit flow.

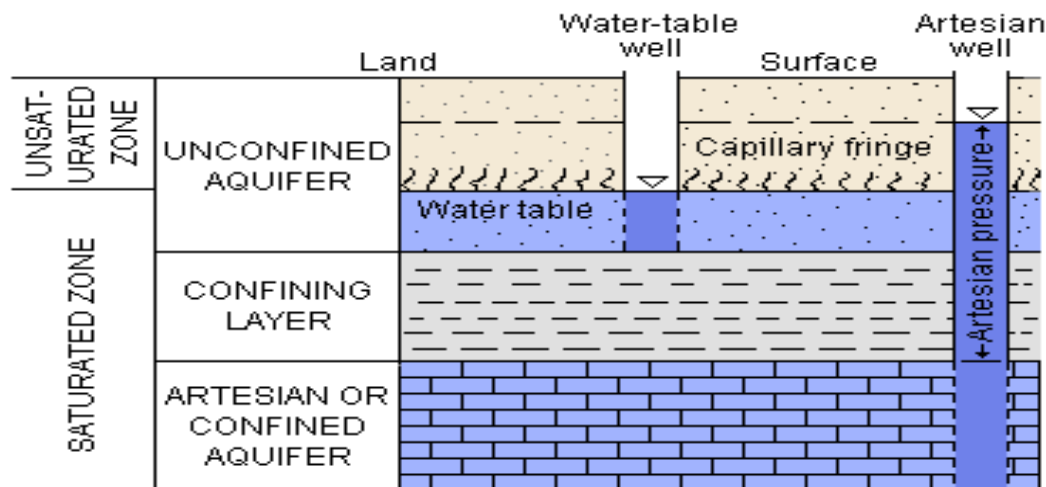


Figure 1.4 Confined and Unconfined Aquifers (Singhal, 2007)

CHAPTER 2

CHARACTERIZATION of the STUDIED AREA

2.1 Area of Study

The investigated area, about 165 km², is located between 35°46' and 35°58' E and 34°17' and 34°27' N; see Figure 2.1. The Koura-Zgharta area is bounded to the north by Jabal Qalhat, to the south by the Amioun hills, and the east by the Lebanese mountain chain. The main source of groundwater is the Miocene (Vindobonian) limestone aquifer, which is overlain in some areas by low permeability Neogene and Quaternary deposits. The Koura- Zgharta area has a mean altitude of 250 m and a slope of 1.5 to 3.5 %. The main river in the area is the Abou Ali River. Two of its major tributaries are the Rachaaïne River and the Jouaaït River. Typical agricultural uses of water in the study area are the irrigation of olive trees and vegetables.

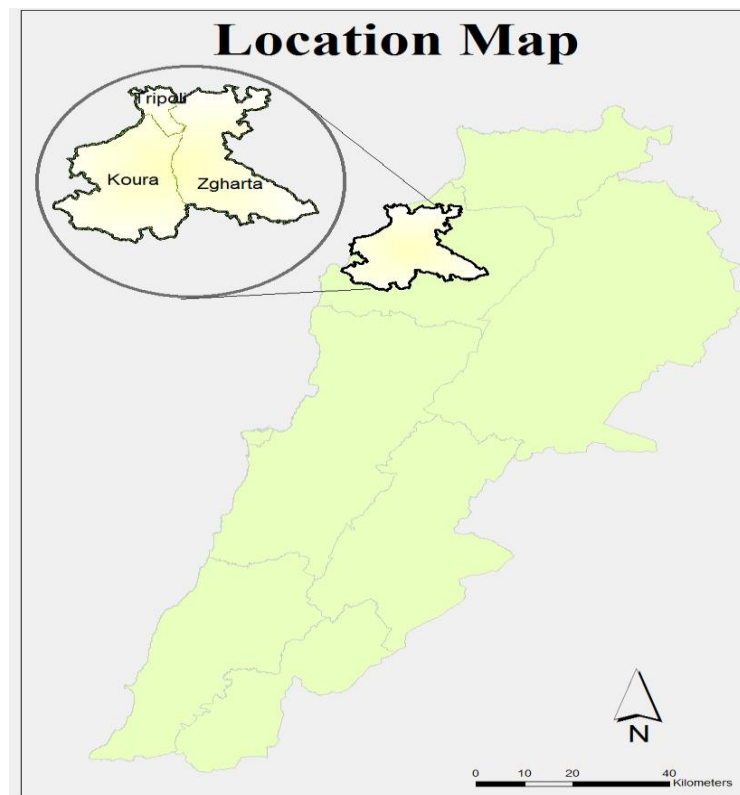


Fig 2.1 Location Map of Studied Area

2.2 Climate of Koura Zgharta and Tripoli Area

Lebanon has a typical Mediterranean climate with moderately cold, windy, wet winters and warm dry summers. From this, we can say that we have two distinctive seasonal periods, one from May to October which consists of the dry season and another rainy season that covers November up to April. This raining period results in the greatest supply of water at the time of its least demand in winter and the least supply of water at the time of its greatest demand in summer (Bou-Zeid E., September- October 2002). During the dry season, water availability is limited due to low water storage capacity, the difficulty of capturing water close to the sea, and the shortcomings of the existing water delivery systems and networks. The annual average of temperature in Koura –Zgharta is around 20°C, reaching a maximum of 31°C in August and a minimum of 8.5°C in January. These temperatures are obtained from the Tripoli weather station and were provided by Beirut International Airport Services. Precipitation records for the Tripoli area are available since 1962 up till nowadays, from this it is seen that the studied area receives an average of 821mm/year of precipitation. The seasonal and yearly fluctuations affect the groundwater storage and cause corresponding potentiometric surface fluctuations. (Traboulsi M., 2010) See table 2.1 and figure 2.2.

Table 2.1 Flows in watercourses in Lebanese Caza's (MOE, 2011)

Flows in water courses (average values) (in Mm ³)	North Lebanon	Mount Lebanon	North Bekaa	Central and Southern Bekaa	South Lebanon	Total
Entire Year	670	990	480	830	430	3,400
May to October (6 months)	270	305	240	240	25	1,080
July to October (4 months)	115	95	155	115	10	490
September	22	18	38	27	2	107

Source: Comair, 2006

2.3 Groundwater

Although surface and groundwater are dealt with separately, it should be noted that almost all surface water resources in Lebanon are attributed to ground karstic aquifers (MOE, 2011). Groundwater recharge is estimated around 3,200 MCM, of which 2,500 MCM constitute the base flow of rivers (FAO, 2008). Snow cover is the main source of groundwater recharge, in addition to rainwater percolation which is enhanced by fractures and fissures of a heavily dissected limestone karstification along the coast of Lebanon (Saadeh, 2008).

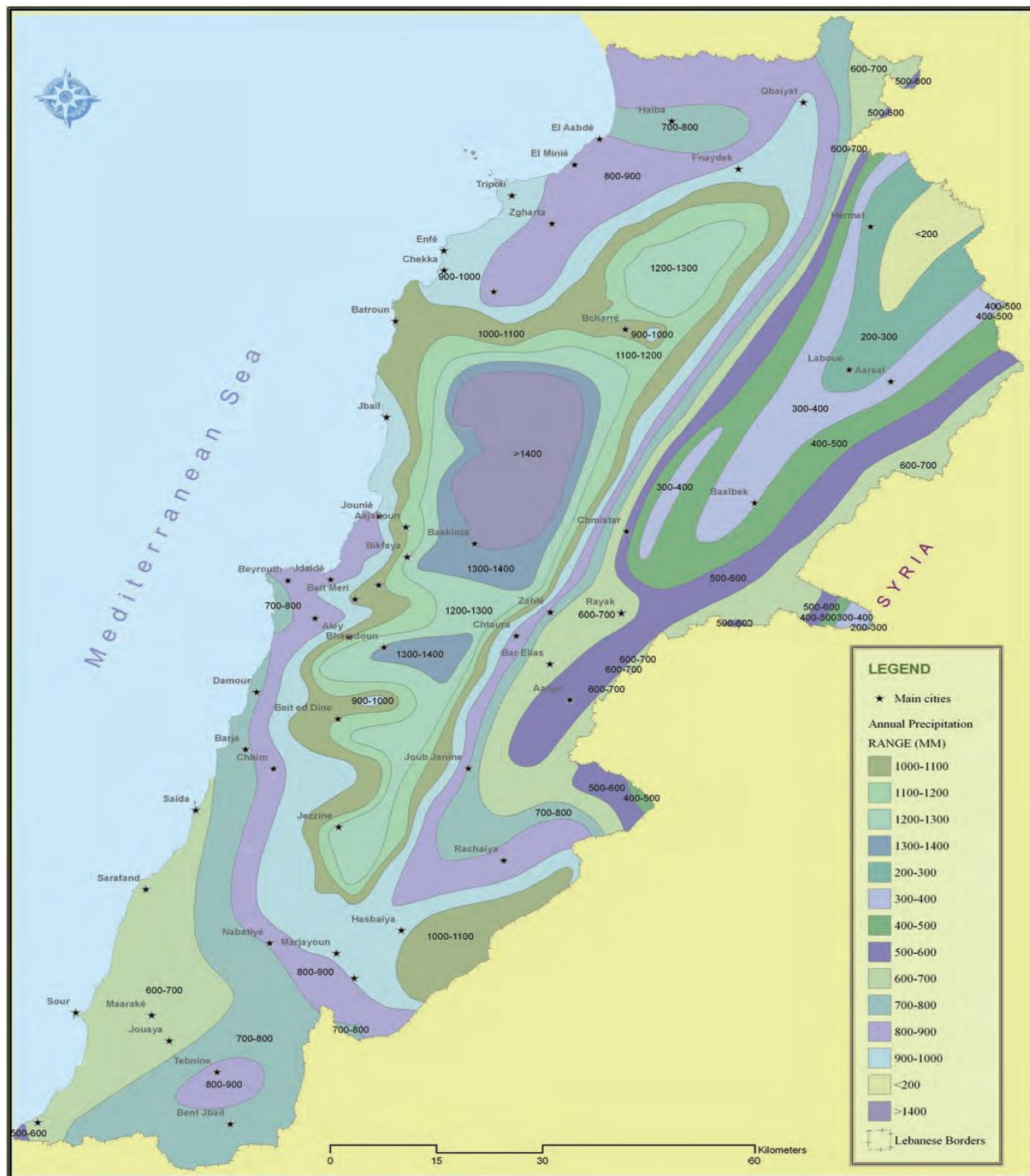


Figure 2.2: Mean Annual Precipitation over Lebanon (MOE, 2011)

2.4 Previous Studies

The geology of the Koura-Zgharta region has been studied by Dubertret and Wetzel between 1949 and 1951; and by Beydon in 1977. The Ministry of Hydraulic and Electrical Resources and the Food and Agriculture Organization (FAO) performed a detailed geological study in 1971. The hydrogeology of Lebanon including the study area was studied by the United Nations Development Program (UNDP) in 1970. Hydrogeological studies of the area are limited; FAO and the ministry of hydraulics did a hydrogeological research in 1972 on the Miocene limestone aquifer, which is the subject of this thesis. In the last decade, the Council for Development and Reconstruction (CDR) contracted several groundwater development studies and drilled many boreholes in the Koura – Zgharta as well as Tripoli area for public water supply. Most of these studies were performed by the Bureau Technique pour le Development (BTD). However these studies were limited, didn't cover the entire region and lacked the complete management approach of groundwater resources.

2.5 Geology of Lebanon

The oldest rocks exposed at the surface in Lebanon are Early Jurassic, around 200 million years old as show in Figure 2.3. In the Jurassic era, the Lebanese territory lacked tectonic activity but has coped with deposition of a thick marine limestone aquifer. The sea level gradually rose during the early to Middle Jurassic replacing the flat limestone and evaporating with shallow marine limestone muds and sand. According to FAO, the oldest tectonic activity with a trace goes back to the late Jurassic, it lead to a renewed phase of the breakup of Gondwanaland, breakup of the area into a series of blocks; some of which were risen above the sea, as well as the widespread of volcanic activities mainly lava flows (Dubertret, 1975). This short volcanic and tectonic phase was quickly replaced by a phase of flooding at the end of the Jurassic giving a way to a deposition of limestone. At the beginning of the Cretaceous, many faults emerged and erosion, this is seen in the Chouf sandstone formation of the lower Cretaceous covering unconformably on the Jurassic limestone. In the same time, swamps, rivers and deltas were born, resulting in the widespread of a sequence of shale and sand. (Oueida, 1992)

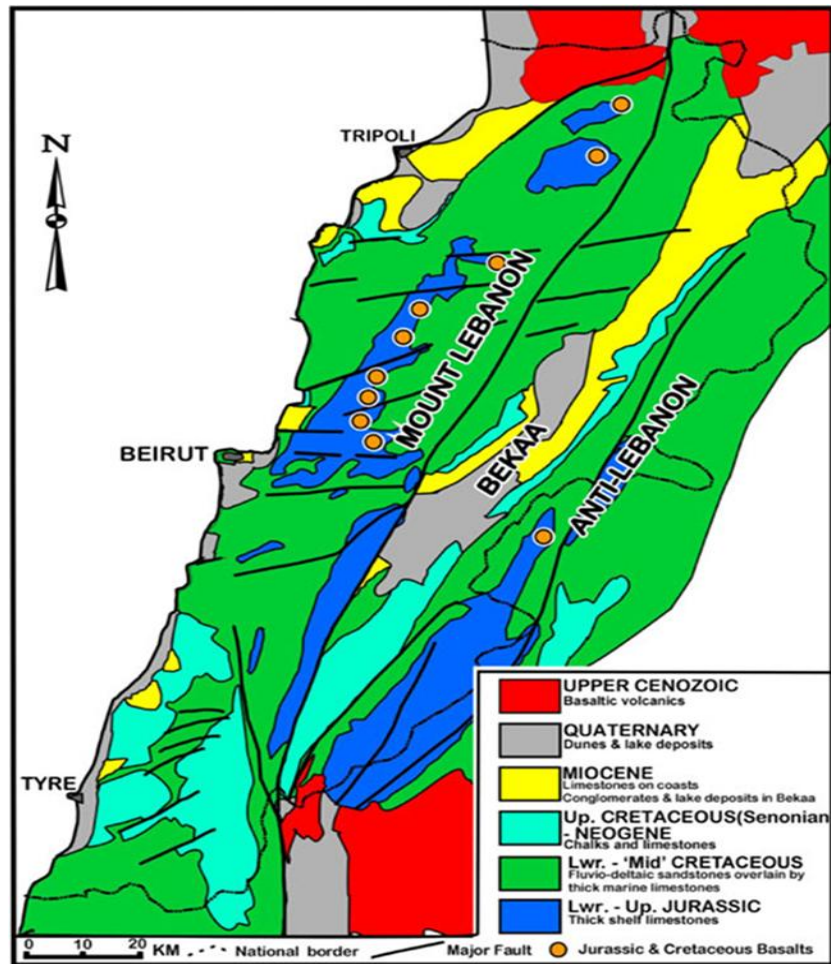


Figure 2.3 Simplified Geological Map of Lebanon. (Walley C. D., Notes on the Geology of Lebanon. AUB : Beirut , 1998)

From the later part of the Early Cretaceous to the Middle Cretaceous a sea level rise gave a widespread limestone deposition. Nevertheless this deposition was briefly interrupted by sandstone and clay deposition and then resumed as a result of further rise in sea level.

During the later Cretaceous, the closure of the Tethyan Ocean leads to a compression effect which gave rise to the first uplifting of the Mount Lebanon. The late Cretaceous and Early Tertiary were dominated by a very high sea rise, and resulted in a thick sequence of pale fine limestone and chalk formation. Through the late Eocene and Oligocene, major uplifting gave upsurge to the threefold NNE-SSW pattern of modern Lebanon. During this period, sea retreated from the Bekaa and was delimited to shallow marine incursions along the line of the present day coast. A second major uplift took around 10 million years ago along the Dead Sea fault. (Walley

C.D., The lithostratigraphy of Lebanon: A review., 1997)

During the late Miocene, carbonate were deposited along the coast, and thick conglomerates and marls over the Bekaa region. In the course of the Pliocene and Quaternary phase, many uplifts and local inclines occurred. The above sequence of events is summarized in the stratigraphic column presented in Figure 2.4 and 2.5. At the start of the Miocene, areas like Koura Zgharta saw the deposition of limestone due to the return of the sea. At the end of the Vindobonian, the continuous retrieve of the sea in the North lead to the shifting of the subsidence axe to the west. The marine system was substituted by a lacustrine environment. The Pontion era observed an uplift and emergence of the Koura Zgharta basin which experienced extensive erosion. (Oueida, 1992) A new brief marine incursion covered again the older zone of marine Vindobonian. Late tectonic activities provoked the deformation of the Neogene deposits. In the Quaternary, phases of successive degradation generated coarse deposits.

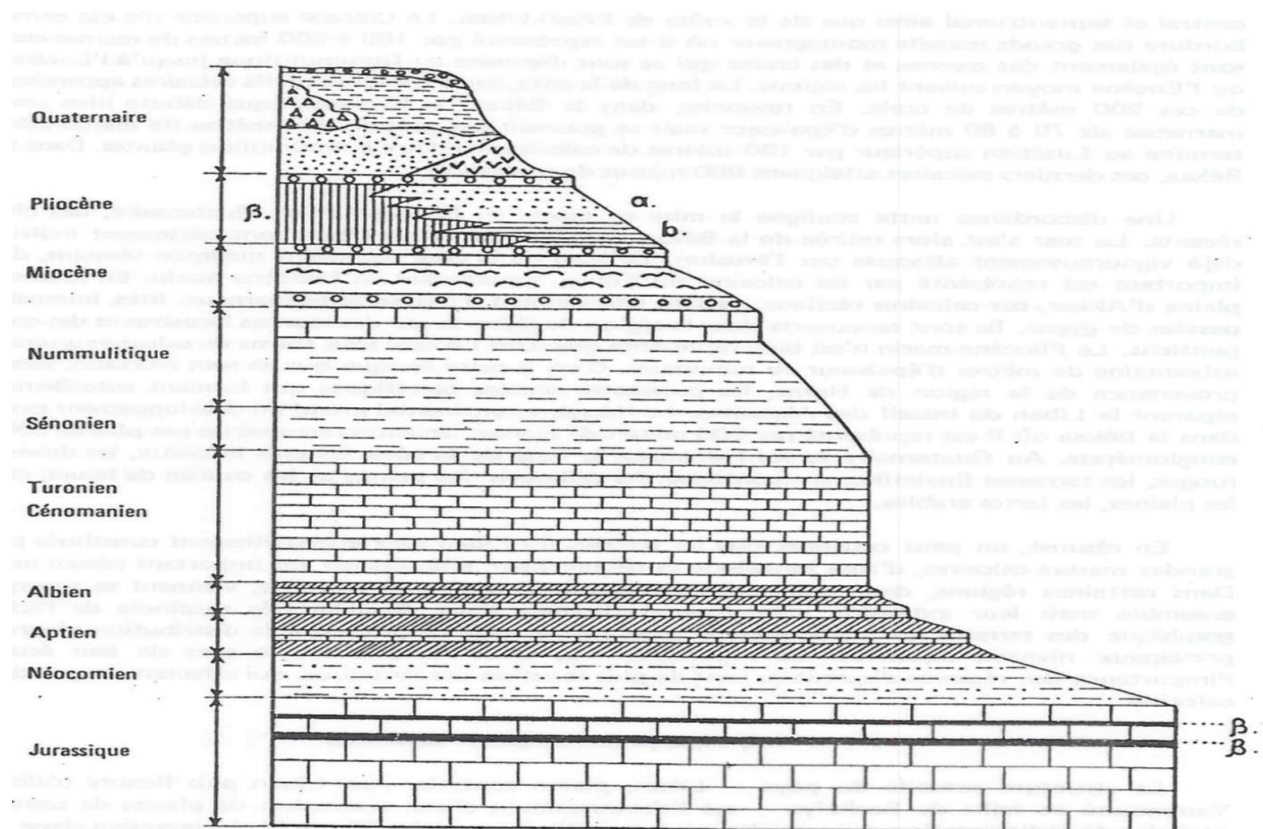
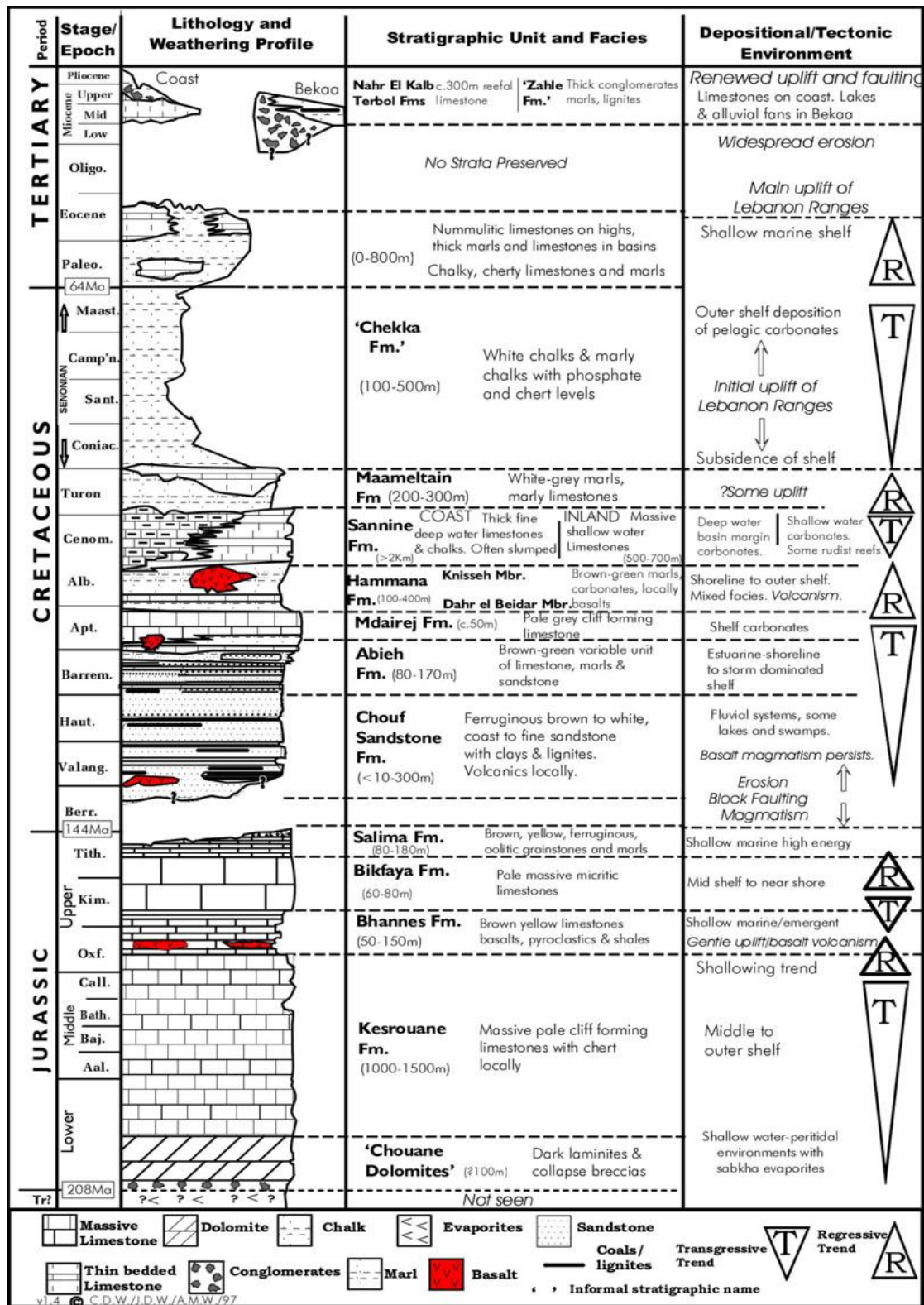


Figure 2.4 Stratigraphic scale of Lebanon (Programme des Nations Unies pour le Développement F. C., 1971)



2.6 Lithostratigraphy Of The Studied Area

2.6.1 Location of The Studied Area

The region of Koura –Zgharta is located in the North of Lebanon, it is located in the South-East of Qelhat and the North of Amioun. It is surrounded by Jabal Tourbol in the North; Mediterranean Sea in the North-West; Jabal Qalhat in the West side; Amioun hills in the South and in the East and South Est by Mount Lebanon. The principle source of groundwater is present in the Miocene Limestone Aquifer (Vindobonian). This layer was complemented by thick marine and continental deposits that were distorted at the end of the Miocene, beginning of Pliocene. In the Quaternary, successive phases of flattening the land gave the general shape of the present Koura- Zgharta platform. The geology of the area was studied by FAO in 1972, (FAO, 1971) the following units are recognized in the studied area and are listed below,(refer to Figure 2.6 to observe the geologic map of the area).

- Quaternary
 - Continental deposits: varying origins covering the platform of Koura-Zgharta
 - Marine deposits: occurring along the length of the coast and on the flanks of Jabal Qalhat and Tourbol.
- Tertiary
 - Pliocene: - Plaisancian: marl deposits of marine origin
 - Miocene: - Pontian : continental deposits conglomeratic or lacustrine
 - Vindobonian: marine deposits of limestone
 - Eocene: Marl and calcareous marl
- Secondary
 - Upper Cretaceous: - Senonian : marl and calcareous marl
 - Middle Cretaceous: -Turonian : limestone and marly limestone
 - Cenomanian: limestone and dolomite
 - Albian: dolomite and marl

For actual localities refer to Figure 2.7 ; 2.8 and 2.9.



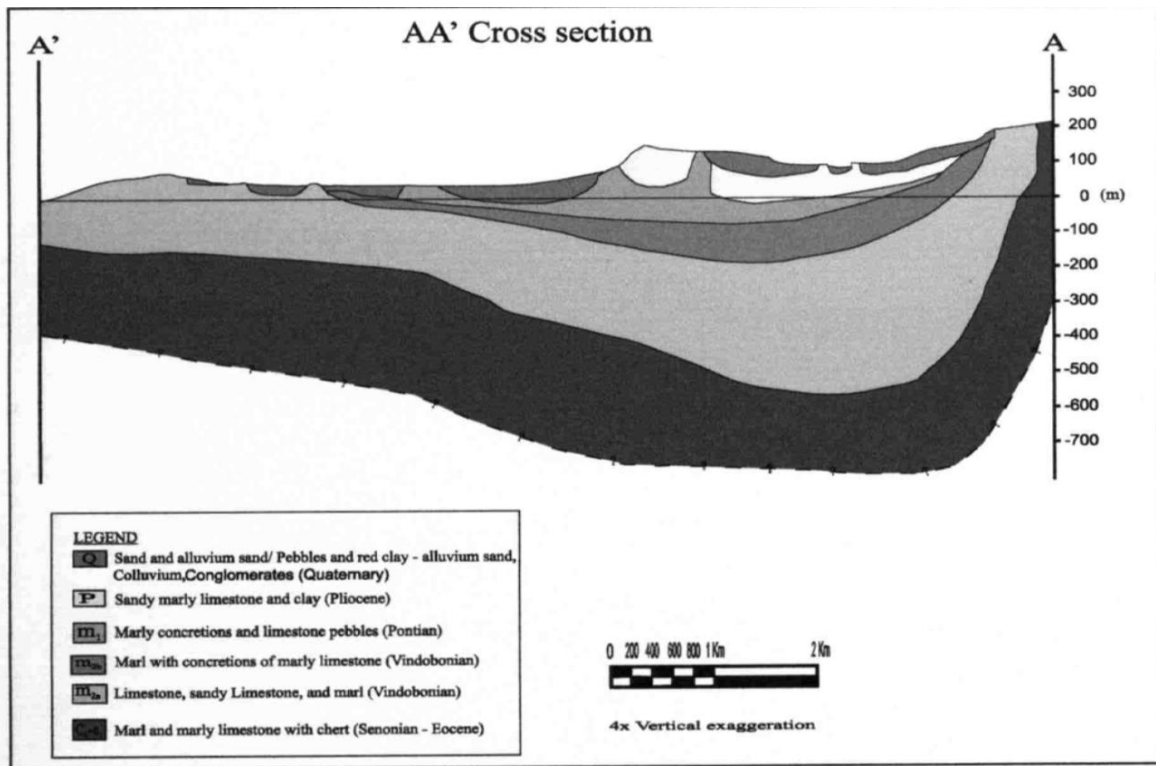


Figure 2.7- Cross Section AA' of the Koura Zgharta Region (Khayat Z., 2001)

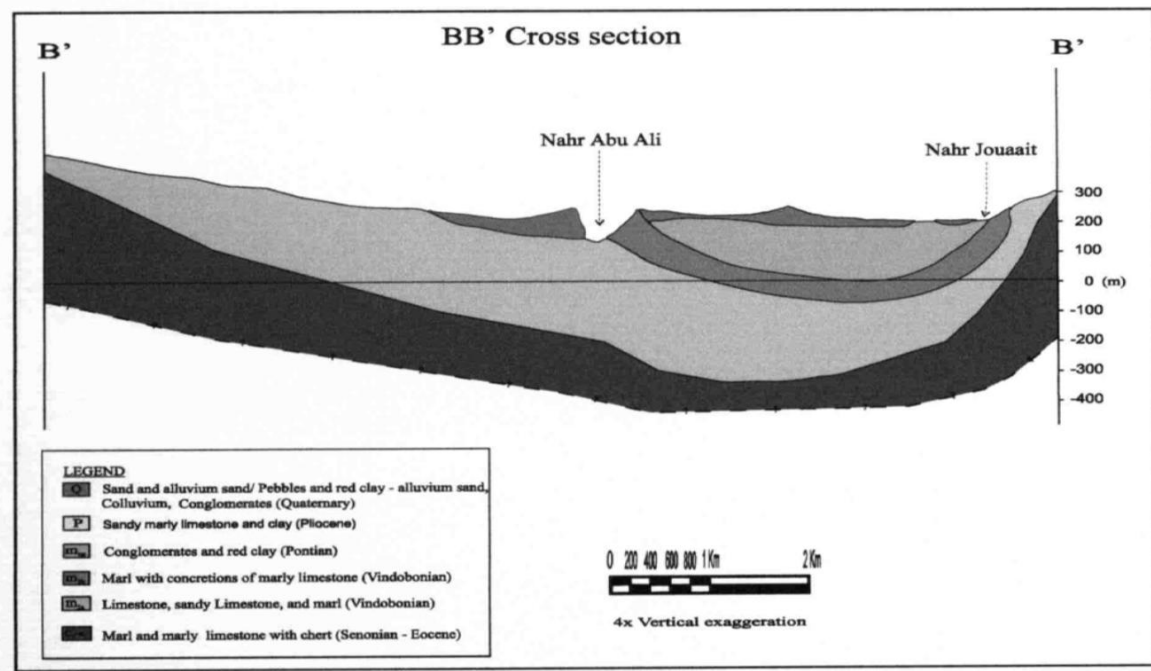


Figure 2.8- Cross Section BB' of the Koura Zgharta Basin (Khayat Z., 2001)

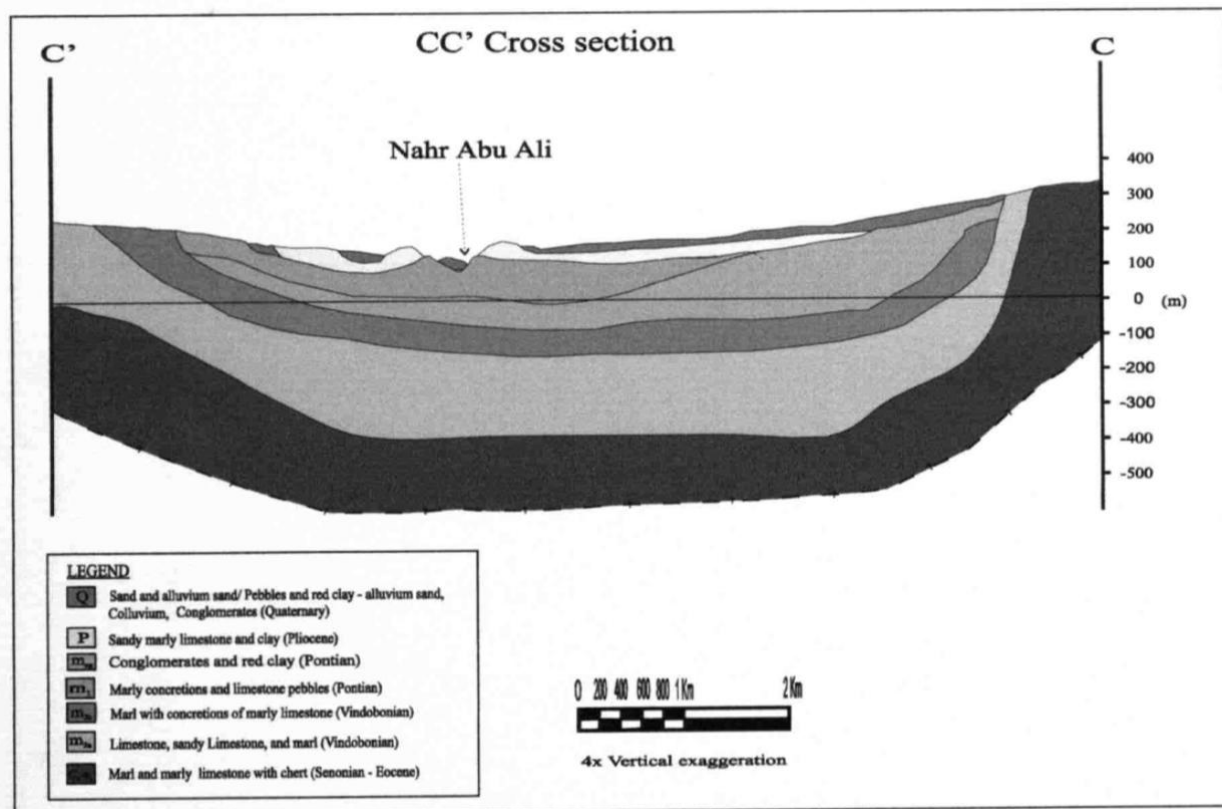


Figure 2.9- Cross Section CC' of the Koura Zgharta Basin (Khayat Z., 2001)

2.6.2 Secondary Formations

2.6.2.1- Middle Cretaceous

The middle Cretaceous is composed of succession of thick limestone and calcareous marl sequences that have an average thickness of 900m. This layer outcrops all around the eastern bordure and in the center of the Amioun anticline in the south. The units that characterize this layer are discussed from bottom to top:

- Albian (C₃): dolomite and marl that are mixed with the base of the Cenomanian with a thickness of 20 to 50 m.

- Lower Cenomanian (C_{4a}): essentially dolomite composition with a thickness of 150 m.
- Middle Cenomanian (C_{4b}): principally calcareous marl with a thickness of 300 m.
- Upper Cenomanian (C_{4c}): represented by limestone and dolomite with a thickness of 200m.
- Turonian (C_5): starts with a cover of yellowish marl with ammonites surmounted by marly limestone regularly interbedded with chert. C_5 ends up with reefal limestone largely stratified with lenses of silicified rudists. The average thickness is about 300m.

2.6.3 Upper Cretaceous (C_6)

The conditions of sedimentation change suddenly and marls and calcareous marls succeed the limestone of the Middle Cretaceous. The Senonian begins by a coat of glauconitic marl with phosphate nodules surmounted by gray marl. On top, alterations of marl and marly limestone appear with several occurrences of brown or black chert; this occurs on a thickness of around 200 m in the Koura -Zgharta basin. The thickness of the Senonian tends to decrease from south towards north and from west towards the east; a progressive substitution of marl by marly limestone takes place. (Programme des Nations Unies pour le Développement F. C., 1972)

2.6.4 Eocene (e_1-2_a)

The facies of the Eocene are comparable with those of the Senonian with alterations of gray or whitish marl and marly limestone; however they are richer in chert. These two layers are combined on the geologic map, (Plate I which is Figure 1.9) as one unit C_6-e_1 . The Senonian and Eocene continually outcrop along the south and the east of the Koura-Zgharta region. At the west, near Qalamoun, and in the north in the center of Jabal Qalahat they outcrop again due to the anticlinal structure. The average thickness of the Eocene is around 300 meters, which gives nearly 500 meters of impermeable layers between the Eocene and Senonian. (Programme des Nations Unies pour le Développement F. C., 1971)

2.6.5 Vindobonian (M_2)

This unit outcrops all around the Koura-Zgharta basin. It follows a small band to the east and the south and a much larger band to the west and north; Jabal Qalhat (on the west) is formed of Vindobonian limestone. This unit is subdivided onto two different lithologic assemblages: the lower limestone and the upper marl compositions. The first group is a lower limestone formation (m_{2a}); it was formed at the present location of Jabal Qalhat and Tourbol in shallow shoal water where reefal limestone with algae accumulated. In the east of this basin and in the shelter of this barrier reef, progressive addition of marly sand is observed. The thickness of the lower limestone formation is greatest in the region of Zgharta, 400m; it is much less at the borders, 300m and in the north it is about 265m.

The upper marl formation (m_{2b}) is the second formation. It only outcrops at the north-east border of Jabal Qalhat, at the south-east mountain side of Jabal Tourbol, in the region of Kfar Yachit and to the east of Zgharta. This layer is characterized by transitional deposits of brackish water (rich in fossils) and in limestone concretions that announce the arrival of the Pontian. The general composition is a compact; its thickness varies from 60 to 100 meters.

2.6.6 Pontian

Two formation of Pontian can be distinguished, a lower formation characterized by lacustrine deposits (just above the Vindobonian marls) and an upper formation represented by a thick accumulation of conglomerates.

The lower lacustrine formation (m_1) outcrops essentially on the south and south-west flanks of Jabal Tourbol. It is composed of lacustrine marl with interstratifications of limestone beds with an average thickness of 50 m.

The upper conglomeratic formation (m_{cg}) corresponds to an ancient piedmonts cone, which totals 300 to 400 m in thickness. It is formed of conglomerate beds more or less well cemented that include the intercalations in the form of layers and lenses of red detrital clay. This layer outcrops in the flanks of Jabal Tourbol and Nahr Abou Ali. (Programme des Nations Unies pour le Développement F. C., 1971)

2.6.7 Pliocene (P)

With the Pliocene occurs the last marine transgression in the Koura –Zgharta basin; it covers a limited surface between Zgharta, the south flank of Jabal Tourbol and the Kfar Yachit- Iaal hills. A layer of whitish limestone with algae marks the base of the Plaisancian. The rest is formed of sandy marl passing laterally to grayish clay and some layers of reefal limestone. The thickness of the Pliocene layer is around 100 m.

2.6.8 Quaternary

Two types of categories are well characterized; the continental formations associated with the colluvial or fluvial banks and the marine and dune deposits. Continental deposits are divided into three categories early Q_1 , middle Q_2 - Q_{ar} and recent Q_3 .

Early fluvial deposits Q_1 , cover the greater part of Koura Zgharta basin. This talus formed by the growing accumulation cones of different rivers unloading in the basin and principally by Nahr Abou Ali. The thickness of these deposits is variable between 100m in the axis of the ancient Abou Li valley and a few meters in other places. The grain size is also variable, blocks of several cubic meters are frequent near the base of the cones, but in general the size decreases downstream. The coarse fraction is composed of limestone pebbles, dolomite, chert and also some basalt and some pebbles which permit their differentiation from Neogene conglomerates. As for the middle and recent fluvial deposits Q_2 - Q_3 , they compose the middle and base of riverbanks. They are formed of non-consolidated pebbles; some deposits especially those of the middle bank contain pebbles coated with red clay whereas the lower bank deposits have pebbles coated with slit. The Q_{ar} formation consists of red layer of colluvial origin that covers a large part of the ancient Quaternary talus and certain Miocene outcrops; their thickness is around 15m. The marine and dune deposits Q_d , represent ancient beach deposits; they are composed of sand and calcite-cemented conglomerate.

2.7 Structural Features of The Studied Area

The structural features of the area are well characterized and contribute to the morphology of the basin and its relief. The main structures are as follows. (Walley C.D., The lithostratigraphy of Lebanon: A review., 1997)

2.7.1 *Jabal Kelhat anticline.*

It is a very flat structure where its axis oriented SW-NE plunges gently and regularly from Chekka to the south until the Tripoli corridor. It is asymmetric, the west flank slope is steeper than the east flank slope. Several fractures oriented NW-SE affect this structure.

2.7.2 *Jabal Tourbol anticline*

It is a dome of elliptical form whose major axis is oriented E-W and the minor axis is oriented SW-NE. It is crossed by the Beddaoui transversal fault which elevated the south of the flank and lowers the north side.

2.7.3 *Amioun anticline*

This is an anticlinal structure analogous to Jabal Tourbol and equally fractured by the Batroun E-W fault. To the north of this fault one can observe a half- upfold of elliptical form with two axes one oriented E-W and the other SW-NE.

2.7.4 *Kousba anticline*

This anticline is bounded to the west by a major flexure which forms the eastern boundary of the area of study.

2.7.5 *Koura-Zgharta basin*

This basin is a lowered complex structure formed by three synclinal zones whose axes form a Y. Figure 2.10 defines the general form of this basin and all of the structures discussed above.

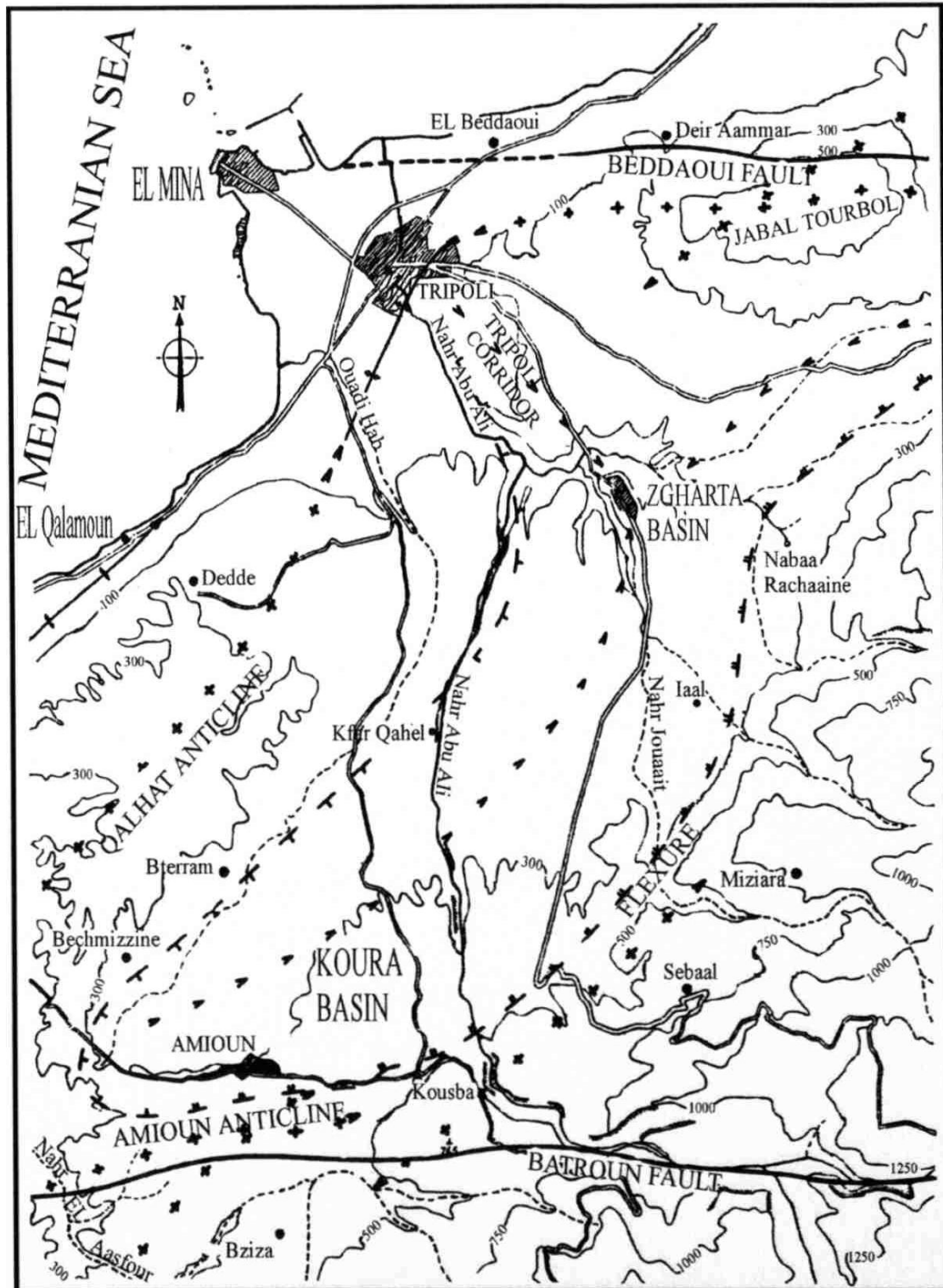


Figure 2.10 Structural Features of the Koura-Zgharta Basin (FAO, 1971)

CHAPTER 3

HYDROGEOLOGY of the STUDIED AREA

3.1 Introduction

Several hydrogeological studies of Lebanon were completed in the past as mentioned in the previous chapter, Abbud and Aker (1986) provided a hydrostratigraphy of Lebanon presented in table 3.1.

Table 3.1 -Hydrostratigraphic Units of Lebanon (Abbud M., 1986)

Period	Formation (Age)	Lithology	Hydrogeological Classification
Quaternary	Quaternary deposits "q" (Quaternary)	Coastal or alluvial loose deposits	Aquifer under favorable conditions
Tertiary	Pliocene succession "p" (Neogene)	Marl, conglomerate, basalt	Aquiclude to aquifer under favorable conditions
	Miocene successions "m and m _{cg} " (Neogene)	The marine succession (m) consists of conglomeratic limestone, sandy-silty marls, overlain by a thick sequence of fractured limestone. The continental succession (m _{cg}) consists of lacustrine conglomerates and sandy silty marl deposits	An aquifer, "m _{cg} " is an aquiclude, but aquiferous under favorable conditions
	Lower (plus Paleocene) and middle Eocene successions e ₁ -e ₂ (Paleogene)	e ₁ consists of chalky marl and marly limestone; e ₂ consists of fractured, sometimes folded beds or chalky marly limestone and hard limestone, and sometimes with chert concretions	Aquiclude Aquifer

Table 3.1 –Continued

Period	Formation (Age)	Lithology	Hydrogeological Classification
Cretaceous	Chekka Marl "C ₆ " (Senonian)	Chalky marl and chalky limestone with nodules and bands of chert	Aquiclude
	Maameltein limestone "C ₄ -C ₅ " (Cenomanian-Turonian)	Massive to thin-bedded limestone and marl	Aquifer under favorable conditions
	Sannine limestone "C ₃ -C ₄ " (Up. Albian-Cenomanian)	Fractured, folded and karstified thin and thick bedded limestone, with geodes and chert bands at different levels	Excellent aquifer
	Hammana Marl "C _{2b} -C ₃ " (Up. Aptian-Mid. Albian)	Marl and fractured limestone beds which grade toward the top into dolomitized limestone with geodes and chert bands	Aquiclude
Jurassic	Mdairej limestone "C _{2a2} " (Up.-L. Aptian)	Fractured massive limestone overlain by a sequence of limestone, marl, sandy limestone, sandstone, and/or local volcanics	The limestone member (45 m) is aquiferous
	Abeih Formation "C _{2a1} " (L. Aptian)	Argillaceous sandstone, sandy argillaceous limestone, claystone, argillaceous limestone, marls and shales	Aquiclude
	Chouf sandstone "C ₁ " (Up. Neocomian-Barremian)	Fractured quartzitic, argillaceous, almost ferruginous sands, interbedded with tuff and basalt and with horizons of lignitic coal, sometimes with horizons of sandy limestone	Aquifer under favorable conditions
	Salima Limestone "J ₇ " (Up. Portlandian)	Oolitic limestone, marls, and shales	Aquiclude
	Bikfaya Limestone "J ₆ " (Up. Portlandian)	Fractured, karstified, massive limestone, with horizons of dolomitic limestone, thin marly limestone, and with frequent horizons of chert nodules	Excellent aquifer

Table 3.1 -Continued

Period	Formation (Age)	Lithology	Hydrogeological Classification
Jurassic	Bhannes volcanic complex "J ₅ " (Kimmeridgian-Up. Portlandian)	Basalt and volcanic tuff. Volcanism was accompanied by simultaneous deposition of detrital and oolitic limestone, marls and shales assigned as Bhannes volcanic complex equivalent	Aquiclude
	Kesrouane limestone "J ₄ " (Bajocian-Kimmeridgian)	Fractured, karstified massive dolomite, dolomitic limestone, and massive to bedded limestone with some marl intercalations. This formation is characterized by a series of fault-line and fault valleys	Excellent aquifer

3.2 Minor Aquifers in Koura Zgharta Basin

There are many geologic formations in this area that serve as aquifers with wells of low productivity. These wells are mostly for domestic use but some are for agriculture use, for instance there are the conglomerates with the sandy clay matrix of the Pontian, the sandy formation of the Plaisancian and the sand matrices of the quaternary.

Basic investigations on the Pontian aquifer have ruled that the thickness of this formation reaches 300 to 400 m , however wells tapped are of much lower depth and do not exceed 100 m in depth. This unconfined aquifer is found mostly in Jabal Tourbol and along the Nahr Abou Ali valley. As for the Plaisancian unconfined aquifer, it was found that its thickness does not exceed 50 m in depth. It is found between Zgharta and the south border of Jabal Tourbol. It has been noticed that wells digged in this aquifer cannot be used all year long, as in late summer months the water table falls drastically and cannot support individual wells.

The unconfined quaternary aquifer is widespread all over the studied area and a variable lithology from unconsolidated sand to conglomerates. It is around 20 m thick and supplies very low quantities of water. This aquifer is very susceptible to pollution from sea water intrusion (in coastal areas), pesticides and untreated sewage leaking from sewage pipes.

3.3 Miocene Aquifer of Koura Zgharta Basin

As we have mentioned previously, the principal source of groundwater in this basin is the reefal limestone of the Miocene. This Miocene limestone aquifer is a fractured, karstic aquifer; and in some areas it approaches the behavior of granular aquifer due to the variable lithology. As this aquifer is the only exploitable reserve in the region, water authorities and many wells are located in this basin. It is a confined aquifer underlain by the Senonian-Eocene marl and overlain by Pontian and Quaternary clay deposits. Since this is a highly fractured aquifer, it is bound as well on the top by unfractured section of the Vindobonian limestone. Its geographic boundaries are Jabal Tourbol to the north, Jabal Kelhat to the west, Amioun to the south and by the flexure of the mountainside to the east. Some outcrops are seen on the west and north of both Jabal Kelhat and Jabal Tourbol anticlines. Due to the synclinal structure of the Koura-Zgharta platform in the central part, the Vindobonian is covered by several tens of meters of Neogene and Quaternary deposits of low permeability. The thickness and geology of the Vindobonian vary. The karstification and fracturing is manifested externally by channels on the limestone crags of Jabal Kelhat and Tourbol. In addition, profound karstification is perceived by the presence of caves and by the underground Haab River. In the central zone of Koura Zgharta platform, the dominance of the marl beds and sandy marl limits the development of karst; therefore the aquifer in the central zone approaches more the behavior of a granular aquifer. Table 3.2 summarizes the hydrogeologic units and its characteristics.

Table 3.2 The hydrogeologic Entities of the Koura- Zgharta Platform (Programme des Nations Unies pour le Développement F. C., 1972).

Formation	Symbol	Simplified Litology	Hydrologic Designation
Quaternary	Q	Clastics	Aquiclude/Aquifer
Pliocene	P	Marly limestone, sandy marl, reef carbonates, clay	Aquiclude/Aquifer
Miocene	m _{cg}	Conglomerates	Aquiclude/Aquifer
	m ₁	Marl	Aquiclude
	m _{2b}	Marl	Aquiclude
	m _{2a}	Limestone	Aquifer
Senonian-Eocene	C _{6-e1}	Marly to marly limestone	Aquiclude
Turonian	C ₅	Limestone	Aquifer
Cenomanian	C ₄	Limestone	Aquifer

3.4 Potentiometric Surfaces

A potentiometric map is a contour map based on water level measurements in wells tapping a confined aquifer. Field measurements of water level in wells tapping the Miocene- Vindobonian limestone aquifer are taken during March-April 2012, September 2012 and May –June 2013. The measurements were obtained using a water level meter provided by the Water Quality Engineering Laboratory in the faculty of Civil Engineering. These water level meter measurements are depth to water level from top of well and were converted to water level above mean sea level (hydraulic head) using the elevation of the top of the wells above the mean sea level as a datum. There are 86 wells (measurements points) occurring in the Miocene limestone aquifer, some of them were private and others were public wells sampled with the approval of the North Lebanon Water Establishment (NLEW). Previous estimated studies in the 1970's (FAO, 1971), have adapted and resulted in a potentiometric contour map, Plate II A seen Figure 2.1. Flow lines, which are imaginary lines that trace the path that a particle of groundwater would follow as it flows through an aquifer were also added. The spacing of the potentiometric contours depends upon the flow rate, aquifer thickness and hydraulic conductivity. Figure 3.1

shows area of recharge (R), areas of discharge (D). It can be observed that generally the flow is from the boundaries, areas of recharge towards the corridor of Tripoli which is the discharge area. The head values in the Tripoli area are below sea level and this is due to the high demand on water and therefore the high density of wells. These below sea level head values are serious as they could lead to sea water intrusion resulting in changing the properties of the groundwater. In addition, seawater intrusion results in the lowering of hydraulic conductivity especially in carbonate aquifers (Goldenberg et al, 1985) thus lower the productivity of the aquifer. A second general trend that can be observed in the potentiometric contour map is that equipotential lines are more widely spaced in Tripoli corridor area than in the rest of the aquifer. This movement suggests that the hydraulic conductivity values are higher in Tripoli area than in the rest of the aquifer. Figure 3.2, shows the potentiometric contour maps studied in December 1971 by FAO. Although this map is done in recharge season, the greatest variation are observed in Tripoli area, where the head values are depressed by as much as 40 m, due to normal seasonal fluctuations and the population increase thus resulting in an increase for water demand. Other areas of the aquifer show minimal variations that are most likely due to seasonal head value fluctuations; thus the effect of increased demand on the aquifer can only be detected in Tripoli area.

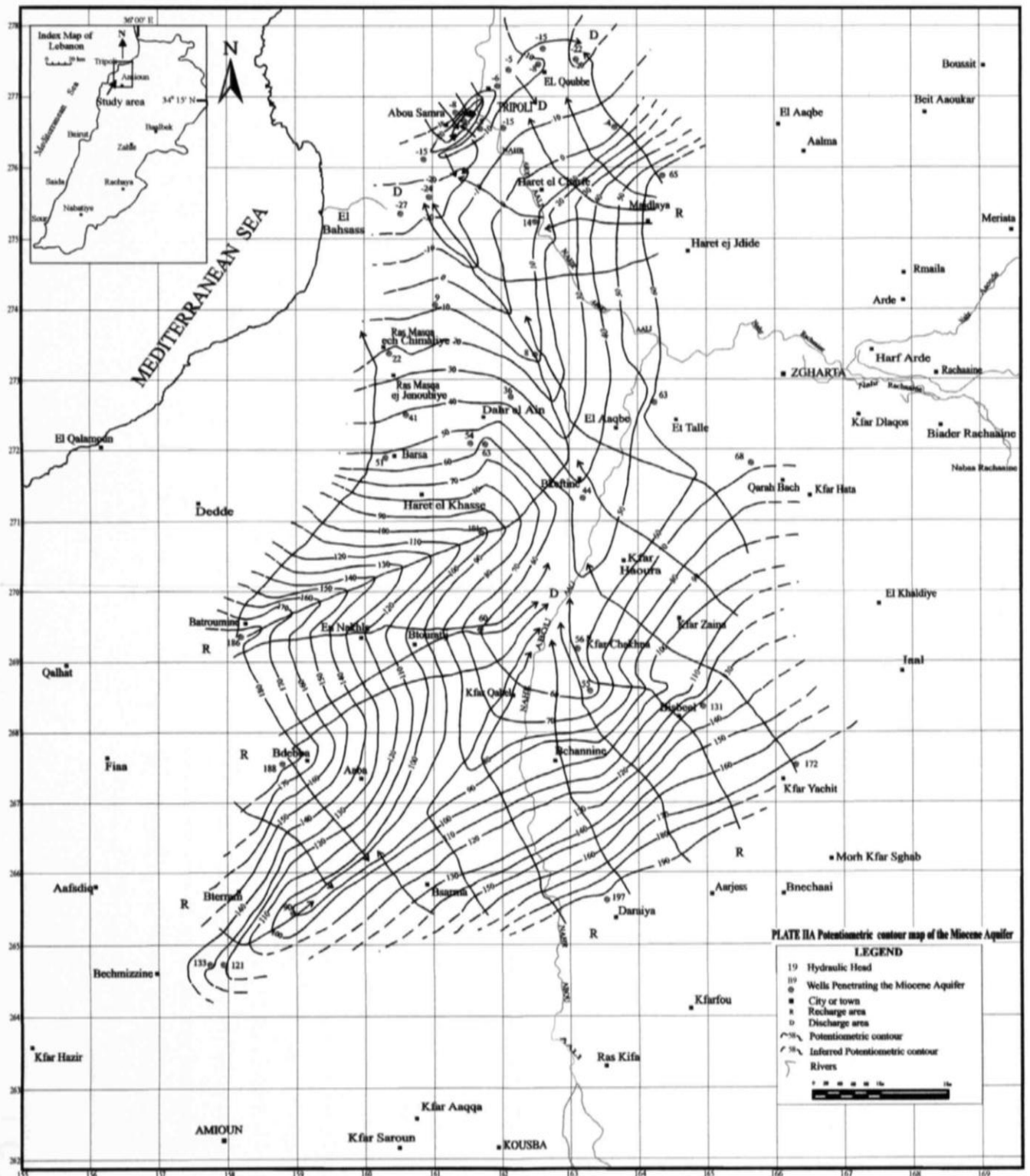
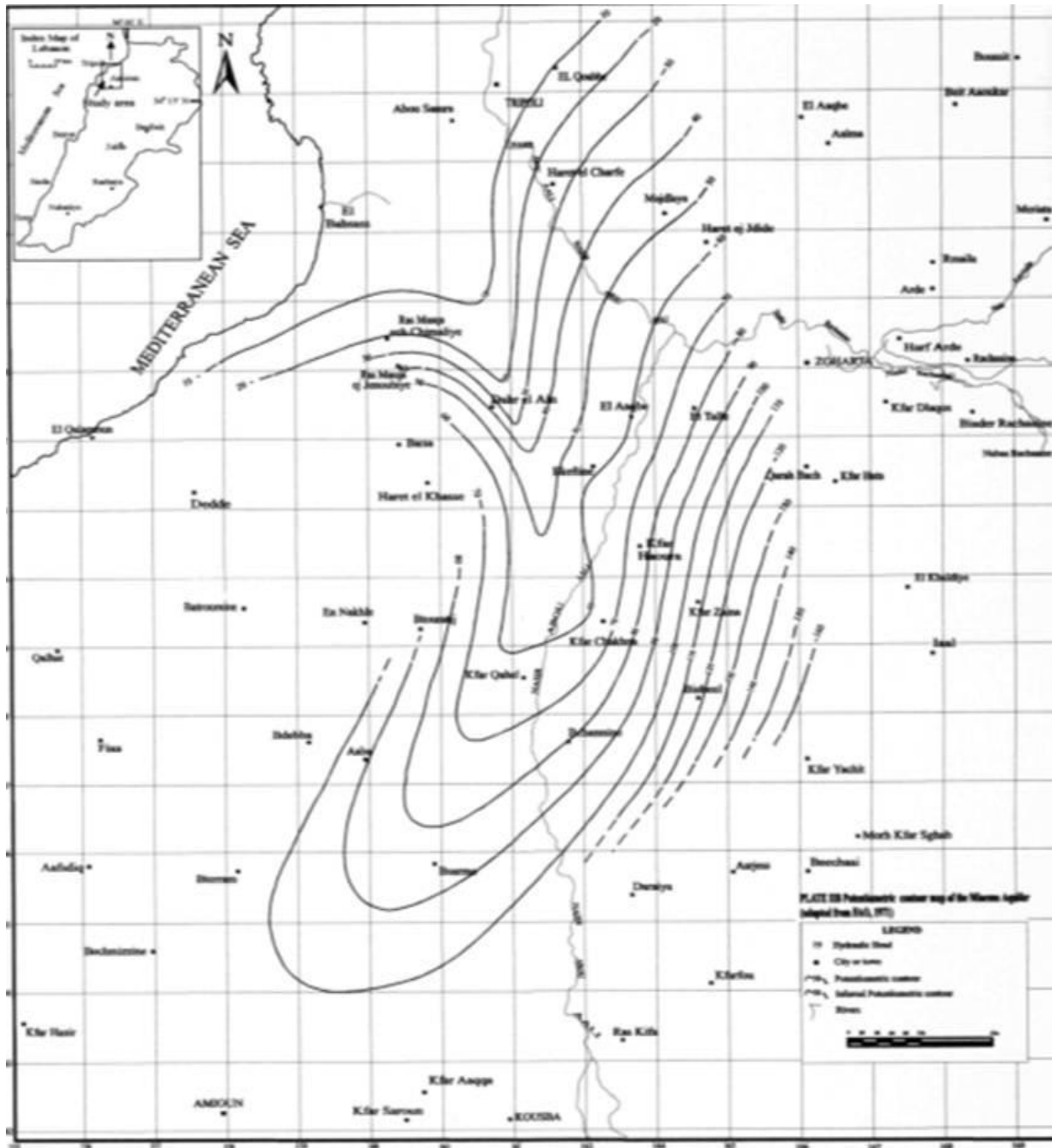


Figure 3.1- Plate II A Potentiometric Contour Map of the Miocene Aquifer (FAO, 1971)



2010)The hydrogeological characteristics of a Karstic aquifer such as the one of concern in our study is that karst systems fits well in the general conceptual model of flow structure . See Figure 3.3; Karst is identical to bassin versant in surface hydrology: a Karst system is the catchment area of a source or group of karst springs including geological formations in which develops a network conduits leading to the source. (Mangin A, 1994)

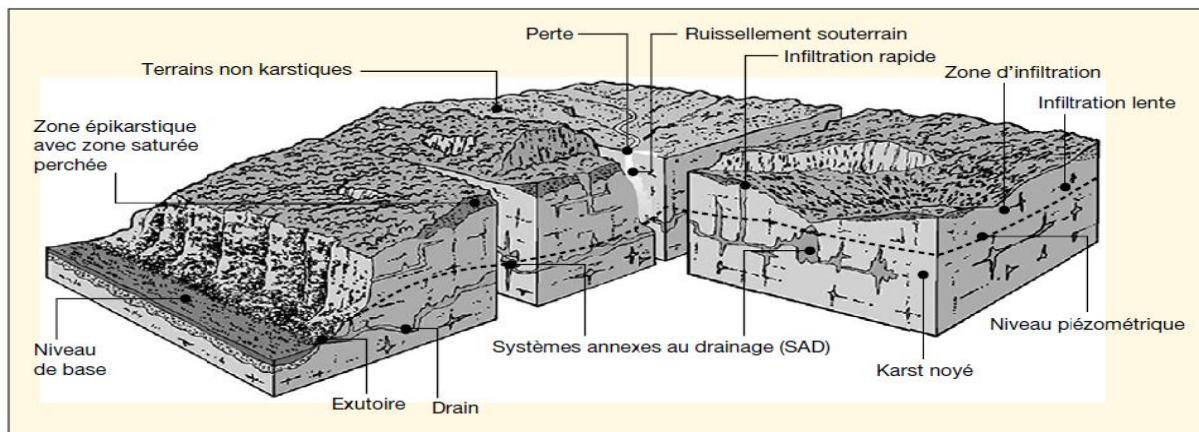


Figure 3.3 Modèle Conceptuel du Système kKarstique (Bakalowicz M., Karst et ressources en eau souterraine : un atout pour le développement des pays Méditerranéens., 2010)

The feature of karst in the Mediterranean makes groundwater resources relatively important. Firstly, these aquifers are subject to terms of complex recharge by melting of snow and infiltration in a sedimentary. Similarly, the discharge of the aquifer is often complex outputs provided by multiple, lasting or temporary presence of different stages of karstification. these outlets can occur both levels upper, ashore, and at lower levels under the sea level The issue of coastal or submarine outfalls is crucial. Indeed, due to the depth development of karstification, aquifers coasts can be directly related with the sea, where the presence of very numerous submarine springs occur. In our studied area, many submarine springs are seen offshore. Therefore, the exploitation of coastal karst aquifers is an important solution for water management but requires knowledge and detailed of the hydrogeological regional and local levels of water and requires the establishment of networks of permanent salinity control collected and flows, in accordance with a management plan very careful. (Bakalowicz M., Karst et ressources en eau souterraine : un atout pour le développement des pays Méditerranéens., 2010)

CHAPTER 4

MATERIALS, SAMPLING and SAMPLING PROCEDURE (OR METHODOLOGY)

The objective of the sampling campaigns is for analysis in order to obtain information on a given medium using representative samples. Proper planning of the campaign is needed to avoid wasted time and errors. It must take into account the context and objectives of the project in which sampling should occur; such as compliance with regulations, improvement of knowledge on the medium we are studying. Therefore planning the sampling campaign can be done taking into account the following:

- Quality control program results;
- Obtaining information about the geology, water & water level in the aquifer,
- A list of all the parameters that needs to be analyzed and associated logistics (number and type of containers, coolers, etc.).
- Locate the collection sites with maps, aerial photos, plans and specifications
- Identify cycles or hours of operation of the process in order to analyze the sample during this time.

Therefore this chapter discusses the methodologies used for the sampling campaigns. It covered hydraulic testing's, as well as chemical, physical and microbial parameters collected. Each has its own way of sampling and measurement. The depth of these wells varies from 5 to 500 meters according to the NLWE; the sampling piezometers selected goes up to 600 meters and is complimented with a portable gauge that measures temperature, conductivity and total dissolved solids on site. All the sampling campaigns were completed by myself with equipment owned by the University of Balamand. Sample analysis will be accomplished by NLWE for the public wells and by the Environmental Engineering Laboratory (EEL) for the private wells as well as the chamber of commerce of Tripoli for replication of results.

To sum up, the sampling was done twice a year to cover wet and dry seasons of year 2012-2013, and a preliminary campaign was accomplished during the wet season of year 2012 in order to

assemble general information on the sites. The total number of wells tested were 86, 34 groundwater locations were covered by the NLWE and 52 private wells. They covered Tripoli, Koura and Zgharta region. Figure 4.1 indicates the areas of sampling.

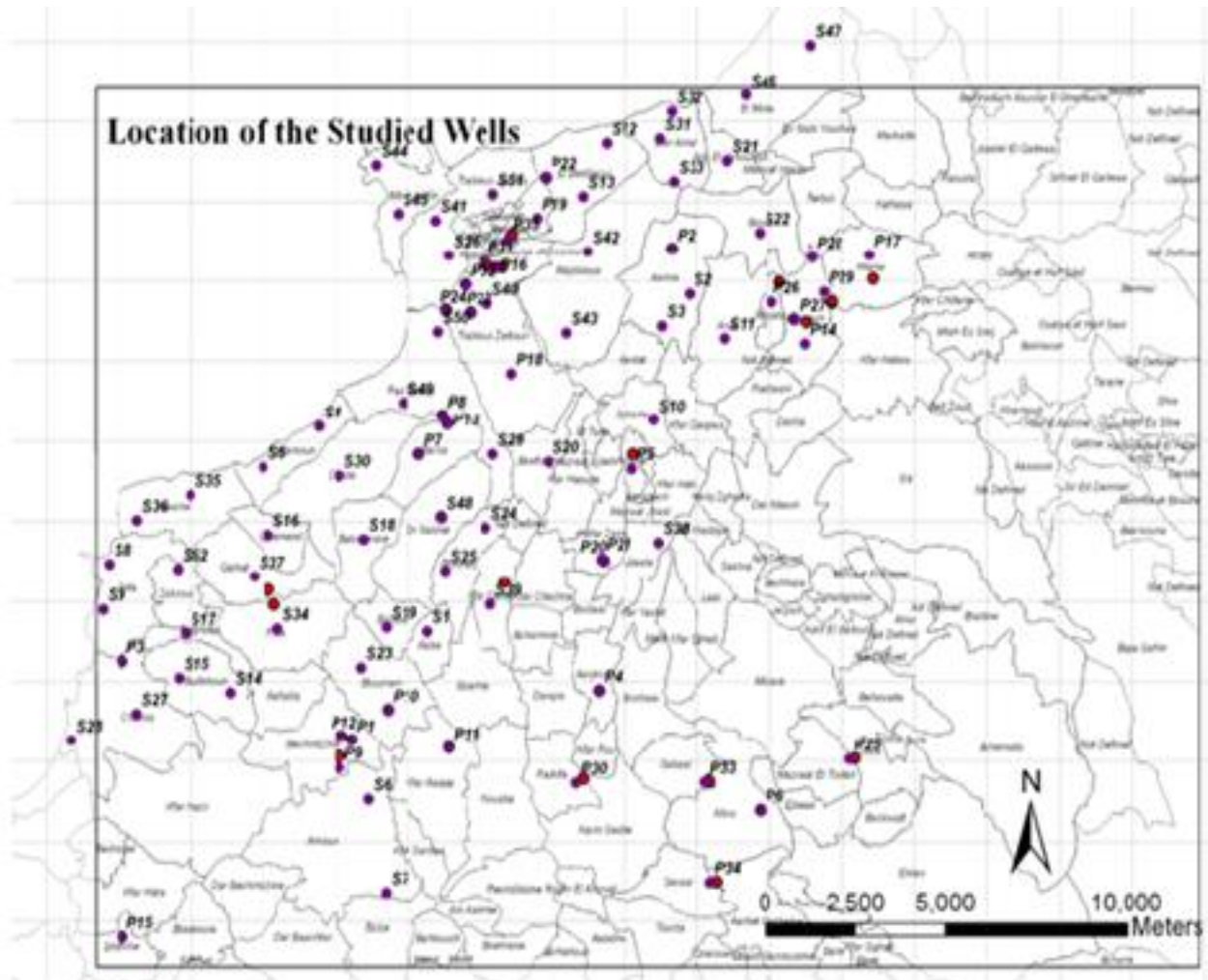


Figure 4.1: Sampling Location (GIS, 2012-2013-2014)

4.1- Criteria For Sampling (or Sampling Protocol)

Existing bores in the area largely define the potential sites for groundwater sampling; however natural features might prevent us from accessing the groundwater. Different criteria can determine which bores are to be sampled, including the:

- Spatial and depth distribution allowing reasonable representation across and within the target

aquifer

- Spatial distribution to allow development of the regional groundwater flow paths
- Depth to water level ranging from shallow to deep groundwater system. Piezometers are needed to sample from the shallow water table aquifer to deeper confined systems at a site.
- Representation of the various lands uses covering agricultural, irrigation practices, or urban areas. Sampling needs to be carried out to address the groundwater contamination potential.
- Representation of sampling to describe the recharge ,nature and extent of groundwater/surface water interaction.

In order to specify the best locations for sampling, several visits were made to make a complete survey on the conditions of the private and public wells in the studied area. The sampling locations were chosen based on the distance between each well (at least 500 meter radius between each well), the condition of the well for the insertion of the piezometer and see if the well is treated or any chemical is being inserted to it such as chlorine for example.

A total of 86 wells were measured and sampled according to DEP, EPA, WHO and APHA recommendations of the standard methods for the examination of water and wastewater (APHA, 1998) (EPA, Ground Water and Drinking Water , 2012) (WHO, 2006).

4.2 Field Investigation

As the sampling locations covered three different areas in North Lebanon, the campaign was divided into three geographical regions and was subdivided according to the distances between each well, as well as the hours in which electricity is distributed in order to measure static and dynamic groundwater level. The campaigns were done throughout a period of 10 to 14 days each, depending on the political situation in the region that allowed us to enter the areas of study especially in Tripoli. The 86 sampling locations were surveyed with a Global Position System (GPS) to determine the elevation, WGS 1980 as datum and the Universal Transverse Mercator (UTM) zone 36N (North) as projection. See table 4.1 and 4.1 continued.

Table 4.1: Coordinates of Sampling Locations

ID	Location	North	Esat	Elevation	Y	X
S1	Aaba (private)	N 34° 20' 48.0"	E 035° 49' 42.8"	241	34.34667	35.82856
P1	Agrotech	N 34° 19' 17.7"	E 035° 48' 25.0"	256	34.32158	35.80694
P2	Alma	N 34° 26' 05.0"	E 035° 53' 55.2"	254	34.43472	35.89867
S2	Alma 1	N 34° 25' 29.0"	E 035° 54' 14.9"	198	34.42472	35.90414
S3	Alma 2	N 34° 25' 31.6"	E 035° 54' 13.2"	220	34.42544	35.90367
S4	Almoun 1	N 34° 23' 31.0"	E 035° 47' 38.9"	7	34.39194	35.79414
S5	Almoun 2	N 34° 23' 07.6"	E 035° 47' 18.1"	20	34.38544	35.78836
S6	Amioun 1	N 34° 17' 55.3"	E 035° 49' 00.9"	295	34.29869	35.81692
S7	Amioun 2	N 34° 17' 05.2"	E 035° 49' 08.3"	298	34.28478	35.81897
P3	Anfe , Jrade	N 34° 20' 14.7"	E 035° 44' 13.9"	20	34.33742	35.73719
S8	Anfeh 1	N 34° 21' 03.3"	E 035° 43' 53.8"	10	34.35092	35.73161
S9	Anfeh 2	N 34° 20' 39.1"	E 035° 44' 02.3"	14	34.34419	35.73397
S10	Arabech	N 34° 23' 01.0"	E 035° 53' 45.6"	770	34.38361	35.89600
S11	Arde	N 34° 24' 33.0"	E 035° 55' 14.1"	145	34.40917	35.92058
P4	Arges	N 34° 20' 05.2"	E 035° 52' 50.1"	299	34.33478	35.88058
P5	Asnoun 2	N 34° 23' 17.3"	E 035° 53' 20.4"	149	34.38814	35.88900
P6	Ayto	N 34° 18' 32.6"	E 035° 55' 48.3"	1028	34.30906	35.93008
S12	Badawi 1	N 34° 27' 17.4"	E 035° 51' 56.1"	10	34.45483	35.86558
S13	Badawi 2	N 34° 26' 43.8"	E 035° 49' 49.1"	15	34.44550	35.83031
S14	Badebhoun 1	N 34° 20' 05.3"	E 035° 45' 32.8"	199	34.33481	35.75911
S15	Badebhoun 2	N 34° 20' 05.8"	E 035° 45' 33.6"	216	34.33494	35.75933
S16	Balamand	N 34° 22' 01.9"	E 035° 46' 48.0"	302	34.36719	35.78000
S17	Barghon	N 34° 20' 31.9"	E 035° 45' 25.8"	153	34.34219	35.75717
P7	Barsa	N 34° 23' 11.11"	E 035° 49' 28.4"	164	34.38642	35.82456
S18	Batromine	N 34° 22' 19.3"	E 035° 48' 09.2"	318	34.37203	35.80256
S19	Bdebba	N 34° 20' 28.6"	E 035° 49' 16.5"	247	34.34128	35.82125
P8	Bir Al- Ahdab (Ras Maska)	N 34° 23' 43.3"	E 035° 49' 52.3"	114	34.39536	35.83119
P9	Bir Bechmezzine, Snouba	N 34° 19' 04.3"	E 035° 48' 12.0"	270	34.31786	35.80333
P10	Bir Bterram	N 34° 19' 43.3"	E 035° 49' 02.8"	260	34.32869	35.81744
P11	Bir El mazraa – Kferaka	N 34° 19' 14.3"	E 035° 50' 09.6"	319	34.32064	35.83600
P12	Bir Kfarhazir, (Ain el Baka)	N 34° 19' 20.6"	E 035° 48' 13.4"	260	34.32239	35.80372
P13	Bir Ras Maska	N 34° 23' 36.8"	E 035° 49' 58.0"	149	34.39356	35.83278
S20	Bkeftine	N 34° 23' 08.9"	E 035° 51' 48.0"	170	34.38581	35.86333
S21	Borj Hayodiyeh (Dawle W)	N 34° 27' 15.8"	E 035° 54' 58.5"	198	34.45439	35.91625
S22	Boussit	N 34° 26' 20.9"	E 035° 55' 29.0"	596	34.43914	35.92472
S23	Bteram (private)	N 34° 19' 46.5"	E 035° 48' 33.6"	268	34.32958	35.80933
S24	Btouratij , Adnan Hassan	N 34° 22' 01.8"	E 035° 50' 34.7"	215	34.36717	35.84297
S25	Btouratij 2 , Mokhtar	N 34° 21' 42.7"	E 035° 50' 11.0"	227	34.36186	35.83639
S26	Chahal Building (Dam & F	N 34° 25' 53.6"	E 035° 49' 53.7"	23	34.43156	35.83158
S27	Chekaa 1	N 34° 19' 32.4"	E 035° 44' 14.2"	52	34.32567	35.73728
S28	Chekaa 2	N 34° 19' 47.1"	E 035° 43' 38.9"	11	34.32975	35.72747
S29	Dahel El Ain , private 1	N 34° 24' 04.4"	E 035° 50' 27.0"	79	34.40122	35.84083
P14	Deir Achach	N 34° 25' 09.3"	E 035° 56' 23.4"	187	34.41925	35.93983

Table 4.1(continued)

ID	Location	North	Esat	Elevation	Y	X
S31	Deir Amar 1	N 34° 27' 33.8"	E 035° 53' 38.2"	46	34.45939	35.89394
S32	Deir Amar 2	N 34° 27' 46.8"	E 035° 53' 46.5"	37	34.46300	35.89625
S33	Deir amar, kassarar	N 34° 27' 15.8"	E 035° 53' 59.7"	146	34.45439	35.89992
S30	Didde, Gaz Station	N 34° 22' 37.5"	E 035° 47' 54.3"	306	34.37708	35.79842
P15	Ejed Ebrin	N 34° 16' 30.9"	E 035° 44' 22.9"	247	34.27525	35.73969
S34	Fih	N 34° 21' 05.1"	E 035° 46' 56.5"	412	34.35142	35.78236
P16	Hawouz	N 34° 25' 44.3"	E 035° 50' 45.5"	56	34.42897	35.84597
P17	Hellan	N 34° 25' 46.2"	E 035° 57' 34.2"	312	34.42950	35.95950
S35	Hraiche 1	N 34° 22' 15.7"	E 035° 44' 39.6"	40	34.37103	35.74433
S36	Hraiche 2	N 34° 17' 33.5"	E 035° 55' 03.6"	10	34.29264	35.91767
P18	Jisr	-303353	30343,48	28		
P19	Kasser Mae	-303105	31161,84	89		
S37	Kelhat	N 34° 21' 16.9"	E 035° 46' 50.1"	410	34.35469	35.78058
S38	Kfarhat, Jedeide	N 34° 22' 43.3"	E 035° 53' 50.5"	129	34.37869	35.89736
S39	Kfarkahel	N 34° 21' 30.0"	E 035° 51' 05.3"	220	34.35833	35.85147
P20	Kferzayna 1	N 34° 21' 50.6"	E 035° 52' 51.3"	182	34.36406	35.88092
P21	Kferzayna 2	N 34° 21' 51.5"	E 035° 52' 49.2"	190	34.36431	35.88033
P22	Malloule	N 34° 26' 59.1"	E 035° 51' 36.5"	16	34.44975	35.86014
P23	Manar	N 34° 25' 07.3"	E 035° 50' 18.9"	70	34.41869	35.83858
P24	Massafi 7	N 34° 25' 08.7"	E 035° 49' 52.9"	28	34.41908	35.83136
P25	Mazra3et el Tefeh	N 34° 19' 17.3"	E 035° 57' 29.7"	1031	34.32147	35.95825
S40	Mervat , Abou Samra	N 34° 25' 15.4"	E 035° 50' 37.6"	138	34.42094	35.84361
S41	Mervat , House	N 34° 26' 21.6"	E 035° 49' 38.8"	99	34.43933	35.82744
P26	Meryata 1- El Blat	N 34° 25' 41.0"	E 035° 55' 53.5"	370	34.42806	35.93153
P27	Meryata 2	N 34° 25' 11.2"	E 035° 56' 10.2"	225	34.41978	35.93617
P28	Meryata 3	N 34° 25' 25.4"	E 035° 56' 49.2"	219	34.42372	35.94700
P29	Meryata 4 (Youn Achech)	N 34° 25' 27.0"	E 035° 56' 49.7"	219	34.42417	35.94714
S42	Mijdlaya 1	N 34° 26' 00.8"	E 035° 52' 23.9"	146	34.43356	35.87331
S43	Mijdlaya 2	N 34° 25' 09.2"	E 035° 52' 39.9"	148	34.41922	35.87775
S44	Mina 1	N 34° 26' 51.1"	E 035° 49' 19.2"	2	34.44753	35.82200
S45	Mina 2	N 34° 26' 51.11"	E 035° 49' 32.2"	10	34.44753	35.82561
S46	Minieh	N 34° 28' 56.2"	E 035° 56' 22.6"	38	34.48228	35.93961
S47	Minieh 2 -	N 34° 29' 01.9"	E 035° 56' 26.6"	26	34.48386	35.94072
S48	Nakhle	N 34° 22' 21.0"	E 035° 49' 54.2"	227	34.37250	35.83172
S49	Ras Maska , Private 1	N 34° 23' 51.1"	E 035° 49' 41.6"	108	34.39753	35.82822
S50	Ras Maska , Private 2	N 34° 23' 52.7"	E 035° 50' 09.3"	78	34.39797	35.83592
P30	Raskifa	N 34° 18' 53.0"	E 035° 52' 36.6"	405	34.31472	35.87683
P31	Saadoun	N 34° 25' 47.4"	E 035° 50' 34.1"	66	34.42983	35.84281
P32	Sankari	N 34° 25' 29.7"	E 035° 50' 12.9"	80	34.42492	35.83692
P33	Seb3el	N 34° 18' 54.3"	E 035° 54' 53.5"	653	34.31508	35.91486
P34	Ser3el	N 34° 17' 33.5"	E 035° 55' 03.6"	794	34.29264	35.91767
P35	Willey	N 34° 25' 45.6"	E 035° 50' 36.8"	80	34.42933	35.84356
S52	Zakroun	N 34° 21' 32.5"	E 035° 45' 05.3"	96	34.35903	35.75147

4.3 Steps for Groundwater Sampling

To demonstrate the validity of the results of a sampling campaign, it is essential to develop a quality assurance program and quality control. (WHO, 2006) The extent or completeness of the insurance and quality control program depends, among other things, objectives, environmental issues, risks and environmental heterogeneity. Quality assurance includes not only the various elements of quality control of sampling, but also notions of human resources (training and experience) and material resources (equipment calibration, maintenance) used to perform adequately a sampling campaign. The following discussion briefly deliberates an important aspect related to quality assurance.

4.3.1 Handling Objects for Sampling

The results of a sampling campaign can be disfigured by several errors related to the operations performed during sampling. A series of relatively simple techniques to minimize the number of these errors are described below (Gvt, 2002)

- Rinsing: Generally adequate rinsing is to bring together different liquids selected with all equipment surfaces that come in contact with the sample. The quantities needed are therefore depending on the surface of the equipment and accessories used for wetting. Washing the sample containers and equipment (piezometer head and Horriba) described in sections 4.4 and 4.5 requires deionized water.
- Washing sampling equipment: Different sampling equipment (Horriba, piezometers, etc...) must be cleaned between each sample; therefore deionized water bottles were carried in the cooling boxes with us. To clean each sampling equipment for each sampling location.

4.3.2 Washing the Sample Containers

Samplers do not have to wash or rinse sample containers if they are provided by the laboratory such in our case. However, we must ensure that the containers (plastic bottles for chemicals analysis) are washed and used as the control of the quality of the cleaning

was done. For chemical analyzes, the washing method is as specified three rinses with deionized water, than rinsed with acetone. Afterwards a new rinsing with purified water is done to remove all traces of acetone and drain the excess.

4.4 Sample Registration

The sample recording and labeling is the last phase in sampling in which the written data are recorded to be identified easily and bottles containing the water samples are labeled. The essential information to be provided on each bottle is listed as follow:

- Identification of the well and site (Area Code (letter+ number) and indicated if Private or Public sector)
- Date and time of sampling

All the information identifying the sample must be identical to the one worn in the file containing the test results collected by the laboratories (EEL and NLWE). For additional information on-site, the field notebook is essential to keep a neat newspaper that records the activities and all the relevant facts concerning the sampling procedures. We necessarily include in the field notes the location of sampling points, frequency and time of sampling as well as the events surrounding. In addition, we note the values of the analysis parameters measured on site, such as pH and temperature, conductivity, etc...

4.5 Groundwater Sampling Methodology

4.5.1 Sampling Procedure for Water Level

Groundwater level measurements will be conducted using a piezometer (the brand was HYDROTECHNIK) held at a reference point at the top of the well casing. It measures up to 500 meters. The piezometers selected were used to measure the aquifer water depth, temperature, and conductivity at different locations. The resulting procedure was followed

- Wash the piezometer probe to make sure it is clean and that it is working.
- Insert the piezometer into the well,

- The end of the measuring tape is lowered into the observation well until the probe touches the water level, a sound occurs indicating the presence of water.
- Write the water level detected as well as its conductivity and temperature.
- Adjust the water level value to the land-surface elevation in meters above or below sea level, and adjust it to the height of the reference point. The distance between the reference level and the water surface is read at the measuring tape of the piezometer.
- The piezometer will read the dynamic water level (level of water when pump is working and water is being withdrawn) and after, 24 hours when the pump is turned off, the static water level will be taken as well.

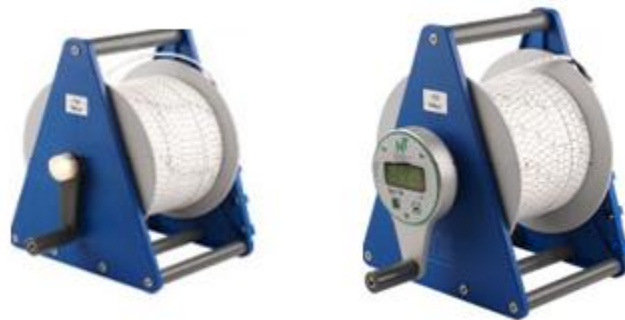


Figure 4.2: Piezometers Used in Sampling (Hydrotechnik, 2012)

4.5.2 Sampling Procedure for Water Quality

Many criteria's have to be taking in consideration when we are recuperating water from the well. In almost all of the 86 sampling points, a plastic baler was inserted in the well to obtain a water sample representative of the groundwater in the area. In order to accomplish this, we made sure to take raw untreated water, representative of the identified resource. Sample conditioning was done with the least possible source of contamination (motor vehicle, car exhaust, cigarette, roads, exhaust of a generator, or other source of potential contamination ...). Moreover, wearing gloves was crucial for filling up the water samples in the bottles. A

part of the water carried from the bailers was inserted in a beaker on-site in order to make field measurements such as pH, Salinity, TDS and DO. These parameters were handled on site with the help of Horriba apparatus and a TDS meter. The Horriba water quality checker shown in the figure4.3 is composed of six probes that are specific to each parameter. It provides quick, accurate measurement onsite simply by immersing the probe into the water in a way that the water covers the sensors. After each use, the apparatus should be rinsed in distilled water to remove if present, any sediment or residual if existing in the sample. As for the TDS meter shown in the figure 4.3, the Total Dissolved Solid (TDS) are measured by inserting the water in the cell cup and reading the value in parts per million (ppm) which is equivalent to milligrams per liter (mg/l).



Figure 4.3: Horriba Apparatus and TDS Meter.

4.6 Difficulties Faced in Sampling Campaigns

Only few of the locations contain a one inch tubing that allows the piezometers to be inserted in the well without any concerns; whereas in most wells, the lack of tubing lead to some problems in the insertions of the piezometers .The piezometer in most of the cases was inserted with high fear and excessive care because no piezometric tubing was present and therefore the piezometer sensor was inserted on our responsibility. In several locations the apparatus was stuck in the well, and therefore a winch was paid to remove the well pump were the piezometer sensor was stuck. We concluded from the campaign, that the very bad well conditions such as the well opening affected almost 85% of the wells. This general bad condition can be explained by the lack of maintenance with the

age of the wells (most of them above 25 years old); the electrical wires are let go in all sides (meaning they are not rapped on the pump tubing) allowing the insertion of the piezometer unclear and dangerous, last but not least, most of them lack a cover or a room that protects the well from external contamination such as rats etc... See figure 4.4 and 4.5 .



Figure 4.4: Sampled Wells



Figure 4.5: Sampled Wells

Other major issues faced, were the common people who feared testing because most of these wells are unlicensed. Hence convincing them in some cases was rather impossible. Another factor was the distance between wells, and their location. The presence of wells in deserted places or even in locations where no car can reach, thus a 25 minute walk was necessary in some locations (for example Meryata 3& 4), meanwhile other wells were found in buildings under construction or even inside dark places where no light is available.

To top things, the most terrifying factor was the gunshots and bad political situation that was confronted in Tripoli and its surrounding (Mina and Minieh) in each of our sampling campaigns. We were forbidden to enter many areas in our sampling in some specific days for example Malloule and Abou Samra, but in other days we were allowed only with the presence of the Lebanese army surrounding us. See Figure 4.6.



Figure 4.6: Situation in Tripoli

4.7 Laboratory Measurement

The water samples for chemical analysis were carried in 250-500 ml plastic polyethylene bottles, while for the microbial study sterilized cup were used. All of the bottles were labeled collected and stored inside two coolers. They were handled to the Environmental laboratory and NLWE laboratory for testing and analysis within 24 hours to prevent damage, degradation or contamination of the samples.

4.7.1 Procedure for Microbiological Tests: *E.Coli* and *Coliforms* and *Salmonela*

The procedure used for detecting and measuring *E.Coli* , *Coliforms* and *Salmonela* in water is membrane-filter method. It takes less time and provides more of a direct count of *E.Coli* and *Coliforms*. In this method, a measured volume of sample is drawn through a special membrane filter by applying a partial vacuum. The filter, a flat paper like disk about the size of a silver dollar, has uniform microscopic pores small enough to retain bacteria on its surface while allowing the water to pass through. After the sample is drawn, the filter is placed in a sterile container called a Petri dish. The Petri dish also contains a special cultural media that the bacteria use as a food source. This nutrient media is usually available in small glass containers called ampules, from which is readily transferred into the Petri dish. Its composition is such that it promotes the growth of *E.Coli* , *Coliforms* and *Salmonela* while inhibiting the growth of other bacteria caught on the filter. The Petri dish holding the filter and nutrient media is usually placed in an incubator Figure 4.7, with a temperature of 37°C for a period of 24 hours. After incubation, colonies of *E.Coli* , *Coliforms* and *Salmonela* can be visible. The colonies appear as dots, and each colony counted on the counter seen in Figure 4.8 represents only one bacteria in the original sample.

Escherichia Coli are used as indicator organisms whose presence suggests that the water is contaminated. Water should not contain more than one *Coliform* bacteria per hundred milliliters (mL). The assumption that the absence of *Coliforms* implies an absence of pathogens is based primarily on the fact that the excreta from relatively few individuals add pathogens to a waste stream, while the entire population contributes *Coliforms*.



Figure 4.7 Incubators (37°C) for Bacterial Growth



Figure 4.8 Bacterial Colony Counter

4.7.2 Procedure for Chemical Parameters

Once the polyethylene bottles were carried to the laboratory the samples chemical concentrations for water quality were tested using an IC (Ion Chromatography). It is commonly used for the analysis of common anion and cation. In our case, anions such as Fluoride, Phosphate, Bromide, Chloride, Nitrite, Nitrate, and Sulfate were detected as for cations the IC covered Sodium, Potassium, Calcium, Magnesium, Ammonium, Sodium and Lithium. Ion chromatography is a form of liquid chromatography; it measures concentrations of ionic species by separating them based on their interaction with a resin. Ionic species separate differently depending on species

type and size (meaning on the ion exchange rate).

The Dionex ICS-2000 Ion Chromatography System (ICS-2000) and ICS- 1500 (for cation) perform ion analyses using suppressed or non-suppressed conductivity detection. An ion chromatography system typically consists of liquid eluents, a high-pressure pump, a sample injector, a guard and separator column, a chemical suppressor, a conductivity cell, and a data collection system. Before running a sample, the ion chromatography system is calibrated using standard solutions for both anions and cations. Before injection the water samples were diluted by a factor of 5 with deionized water and then inserted into the auto sampler that will inject automatically the water vials in to the IC columns. Sample solutions pass through a pressurized chromatographic column where ions are absorbed by column constituents. The eluents (which are deionized water for anion and methane sulfonic acid for cation) run through the column; leading to the absorption of ions that will consequently be separated from the column. The retention time of different species determines the ionic concentrations in the water sample. The data collection system, typically a computer running the chromatography software (Chromelion software in our case), produces a chromatogram. The chromatography software converts each peak in the chromatogram to a sample concentration and produces a printout of the results. Figure 4.9 shows the IC used in this study.



Figure 4.9 Ion Chromatography

Moreover, the detection of anions and cations using ion chromatography follows five steps:

1. Injection,
2. Separation,
3. Suppression,
4. Detection
5. Recording

Figure 4.10 shows the scheme of the IC steps in water sampling.

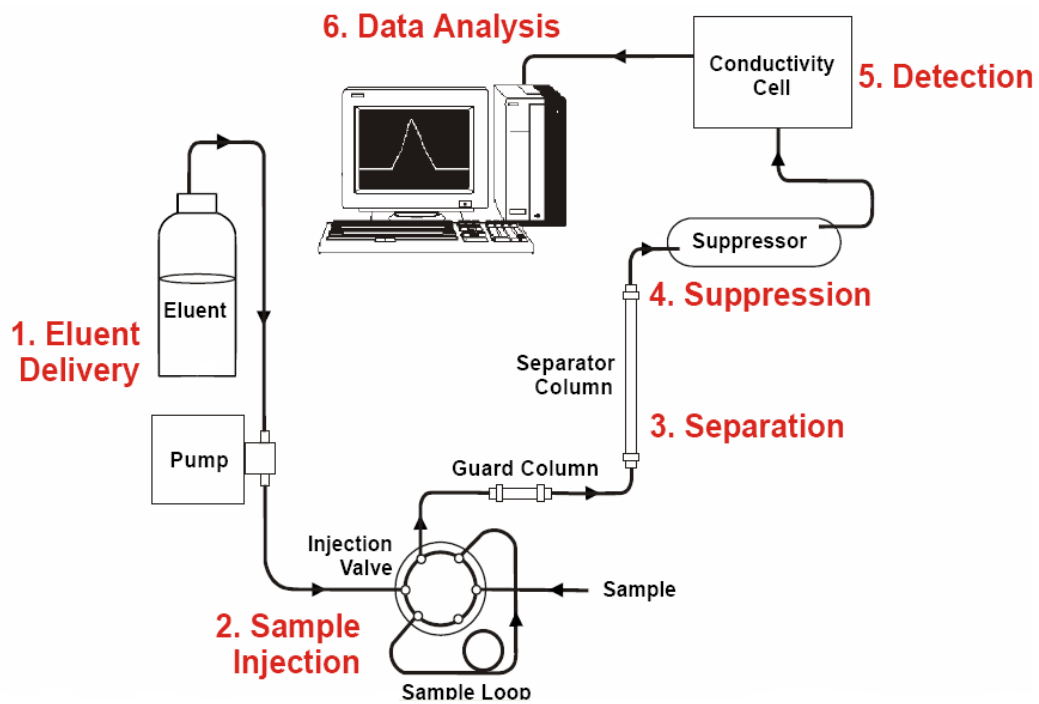


Figure 4.10 Scheme of Ion Chromatography (Dionex, 2003)

CHAPTER 5

ANALYSIS and INTERPRETATIONS of the RESULTS

In the recent years, the occurrence of pollution has led to reflect the possibilities of action to protect groundwater resources or to decontaminate after accident if occurring. Nowadays, in order to prevent the risks of pollution, it is necessary to understand the mechanisms by which water gradually acquires its chemical composition under natural conditions (Vivier J.P, October 1997). For these reasons, we thought it is necessary to study the mechanisms by which groundwater acquired its physical and chemical quality; and in a next step study the static and dynamic water levels. This chapter is based on the presentation and interpretation of the different results collected from the field and relies on different tables, graphs, diagrams and maps made .

5. 1 Water Level: Static and Dynamic Water Level

The results of measurements of water levels as well as the physio-chemical characteristics of the samples groundwater are presented in Table 5.1 and Table 5.2. It is the synthesis of the measurement points wells (Nos. 1 to 86) taken according to the geographic coordinates (latitude, longitude, and height). These tables show the static and dynamic levels in the work. It was found that 39 wells have a level between 0 and 50 m; 20 wells are between 50 to 100 meters and 25 are above 100 meters.

5.2 Water Chemistry Analysis

Groundwater has physical and chemical characteristics of its own; they vary between temperature, pH, conductivity and dissolved chemical elements. All these features are functions of many parameters such as rain water; presence of vegetation and alteration zones; the chemical nature of the reservoir and the depth of water. The hydrochemical study of the groundwater in the North relies on the water analysis from the dry season 2012 and wet season 2013 (James, 1997). In this context, the characteristics of water are presented to help develop further the chemistry of the aquifer. Different sets of water samples were taken when possible in order to provide the following elements of this research: The physio-chemical parameters such as temperature, pH, conductivity ,salinity ,TDS , and they key cations and anions Li^{2+} , Ca^{2+} , Mg^{2+} , Na^{+} , K^{+} , Cl^{-} , SO_4^{2-} , NO_2^{-} , NO_3^{2-} , PO_4^{2-} , F^{-} , and Br^{2-} .

Table 5.1: Results of Sampling Campaign Aug- Sept 2012

Sample ID	ID	Date	Static Water Level (in m)	Time in hours (off)	Dynamic Water Level (in m)
Aaba (private)	S1	9/11/2012	147.15	4	146
Agrotech	P1	9/4/2012	92.4	1	91
Alma dawle	P2	9/13/2012	230	4	238
Alma 1	S2	9/13/2012	72	6	77.7
Alma 2	S3	9/13/2012	89	5.5	96
Almoun 1	S4	9/9/2012	9	12	9
Almoun 2	S5	9/9/2012	n.a	n.a	8
Amioun 1	S6	9/9/2012	3.5	4	3.5
Amioun 2	S7	9/9/2012	2.7	24	5.3
Anfe , Jrade	P3	9/6/2012	12	12	12
Anfeh 1	S8	9/9/2012	5.5	12	5.5
Anfeh 2	S9	9/9/2012	5.3	48	5.5
Arabech	S10	9/8/2012	85	2	92
Arde	S11	9/11/2012	12.9	72	n.a
Arges	P4	9/2/2012	98	4.5	111
Asnoun	P5	9/2/2012	64.1	8	87
Ayto	P6	9/3/2012	23	2	53
Badawi 1	S12	9/1/2012	46	72	47
Badawi 2	S13	9/7/2012	82	4	85
Badebhoon 1	S14	9/12/2012	11.3	72	n.a
Badebhoon 2	S15	9/12/2012	67	4	76.4
Balamand	S16	9/7/2012			158
Barghon	S17	9/9/2012	8.3	10.3	9.3
Barsa	P7	9/4/2012	157	1	157.3
Batromine	S18	9/9/2012	185	72	188

Bdebba	S19	9/7/2012	134	72	135.5
Bir Al- Ahdab (Ras Maska)	P8	9/4/2012	84	4	90.6
Bir Bechmezzine, Snoubar	P9	9/5/2012	53	1	71
Bir Bterram	P10	9/5/2012	179	3	186.5
Bir El mazraa – Kferaka	P11	9/11/2012	212	long periode	off
Bir Kfarhazir, (Ain el Bakar)	P12	9/5/2012	88	4	90
Bir Ras Maska	P13	9/4/2012	124.5	3	127
Bkeftine	S20	9/1/2012	144	2	145
Borj Hayodiyeh (Dawle Well)	S21	9/13/2012	58.7	3.3	n.a
Boussit	S22	9/7/2012	145.5	2.5	n.a
Bteram (private)	S23	9/8/2012	127	12	127
Btouratij 1 , Adnan Hassan	S24	9/1/2012	154	2	n.a
Btouratij 2 , Mokhtar	S25	9/1/2012	2.5	12	4
Chahal Building (Dam & Farez)	S26	9/8/2012	69	4.3	71
Chekaa 1	S27	9/10/2010	35.8	2	36
Chekaa 2	S28	9/10/2010	7.9	4	8
Dahel El Ain , private 1	S29	9/8/2012	64	6	71.5
Dédde, Gaz Station	S30	9/1/2012	18	72	14
Deir Achach	P14	9/2/2012	2.6	4	3.1
Deir Amar 1	S31	9/7/2012	52	48	544
Deir Amar 2(kasser balade)	S32	9/1/2012	32	1.5	47
Deir amar 3, Kassarat	S33	9/1/2012	18	4	22
Ejed Ebrin	P15	9/6/2012	155	6	161
Fih	S34	9/7/2012	75.6	14	80
Hawouz	P16	9/1/2012	98	3.5	99
Hellan	P17	8/30/2012	52	4.3	52
Hraiche 1	S35	9/9/2012	23.5	14	46

Hraiche 2	S36	9/9/2012	35	48	n.a
Jisr	P18	not done			
Kasser Mae	P19	9/1/2012	92	long periode	off
Kelhat	S37	9/7/2012	98	12	106
Kfarhat, Jedeide	S38	9/8/2012	48	240	n.a
Kfarkahel (private)	S39	9/7/2012	153.5	1.5	162
Kferzayna 1	P20	9/2/2012	52.3	4	60.7
Kferzayna 2	P21	9/2/2012	52.8	5	60.1
Malloule	P22	9/1/2012	28	4	35
Manar	P23	9/10/2012	84	long periode	off
Massafi 7	P24	9/5/2012	34	4	37
Mazraet el Tefeh	P25	9/3/2012	101	6	122.7
Mervat , Abou Samra	S40	9/11/2012	74.8	4	75
Mervat , House	S41	9/11/2012	6.5	4	6.5
Meryata 1- El Blat	P26	8/30/2012	155	15	170
Meryata 2	P27	8/30/2012	19.2	15	21.6
Meryata 3	P28	8/30/2012	15	12	16
Meryata 4 (Youn Achech)	P29	8/30/2012	15.8	12	16.8
Mijdlaya 1	S42	9/3/2012	113	72	n.a
Mijdlaya 2	S43	9/3/2012	95	2	108
Mina 1	S44	9/7/2012	2.5	3	n.a
Mina 2	S45	9/11/2012	2.5	48	11
Minieh 1	S46	9/1/2012	11	2	19
Minieh 2 - Saleh Kheir	S47	9/9/2012	167	3	175
Nakhle (private)	S48	9/7/2012	212	0.5	225.5
Ras Maska , Private 1	S49	9/8/2012	53	2	53
Ras Maska , Private 2	S50	9/9/2012	n.a	n.a	198
Raskifa	P30	9/3/2012	214	2.3	229
Saadoun	P31	9/1/2012	92	4	96

Sankari	P32	9/1/2012	78	4	83
Sebeel	P33	9/3/2012	312	5	380
Sereel	P34	9/3/2012	20	10	25
Tripoli (200)	S51	9/11/2012	6	2.5	7
Willey	P35	9/1/2012	93	4	96
Zakroun	S52	9/12/2012	89.3	4	89.3

Sample ID	Time in hours (on)	Conductivity ($\mu\text{S/cm}$)	T ($^{\circ}\text{C}$)	TDS (ppm)	pH
Aaba (private)	0	1400	21	580	6.16
Agrotech	4	1270	20.9	655	6.72
Alma dawle	2	2460	18.3	750	7.05
Alma 1	2	779	22.2	506	6.82
Alma 2	3	855	22.1	630	n.a
Almoun 1	1	647	11.5	420	6.17
Almoun 2	72	950	18.7	560	6
Amioun 1	12	631	18.6	409	6.58
Amioun 2	5	507	20.7	328	6.29
Anfe , Jrade	12	850	21	400	7.8
Anfeh 1	10	1690	22.1	750	6.29
Anfeh 2	10	1710	24.1	820	6.12
Arabech	4	1210	20.1	615	n.a
Arde	n.a	n.a	n.a	n.a	n.a
Arges	6	620	20	320	7.36
Asnoun	1	673	21.4	499	6.44
Ayto	4	525	15	340	7.69
Badawi 1	1	854	18.7	555	5.89
Badawi 2	0.5	737	20.1	479	6.53

Badebhoon 1	n.a	n.a	n.a	n.a	n.a
Badebhoon 2	2	1260	21	710	6.42
Balamand	72	1380	21.7	740	6.12
Barghon	1	1580	20.8	890	6.32
Barsa	3.2	950	23.4	420	7.29
Batromine	1.5	510	22.7	320	6.28
Bdebba	3	685	21.8	444	6.57
Bir Al- Ahdab (Ras Maska)	2.3	1290	23.8	850	7.15
Bir Bechmezzine, Snoubar	4	1020	23	500	6.19
Bir Bterram	4	605	22.8	320	6.54
Bir El mazraa – Kferaka	off				
Bir Kfarhazir, (Ain el Bakar)	2	752	22	450	n.a
Bir Ras Maska	4	763	25.7	350	7.2
Bkeftine	4	428	20.6	278	6.89
Borj Hayodiyeh (Dawle Well)	n.a	470	18.7	305	n.a
Boussit	n.a	n.a	n.a	n.a	n.a
Bterram (private)	2	1740	22	650	6.18
Btouratij 1 , Adnan Hassan	n.a	624	21.8	409	n.a
Btouratij 2 , Mokhtar	3	2810	22.3	950	6.44
Chahal Building (Dam & Farez)	3	503	21.9	327	6.74
Chekaa 1	2	1430	20.6	820	6.46
Chekaa 2	4	1340	21.3	780	6.26
Dahel El Ain , private 1	2	499	16.9	324	6.51
Dédde, Gaz Station	4	801	19.5	520	6.08
Deir Achach	4	541	18.2	352	6.56
Deir Amar 1	20.9	354	n.a	n.a	n.a
Deir Amar 2(kasser balade)	3.5	1400	21	850	6.35

Deir amar 3, Kassarar	1	811	18.8	527	6.03
Ejed Ebrin	4	621	22	350	7.54
Fih	1	1220	20.5	550	6.45
Hawouz	2	444	17	288	7.36
Hellan	1	357	19.1	232	7.02
Hraiche 1	2	1624	23.1	835	6.51
Hraiche 2	n.a	n.a	n.a	n.a	n.a
Jisr					
Kasser Mae	off	1315	19.2	850	
Kelhat	1.5	1420	22.5	620	6.4
Kfarhat, Jedeide	n.a	n.a	n.a	n.a	n.a
Kfarkahel (private)	4	549	20.6	355	6.81
Kferzayna 1	1	2160	19.5	1406	7.16
Kferzayna 2	3	730	19.6	476	7.38
Malloule	6	1100	21	750	
Manar	off				
Massafi 7	4	730	18	350	7.43
Mazraeet el Tefeh	2	2540	11.9	950	7.3
Mervat , Abou Samra	0.5	1250	21.9	650	6.29
Mervat , House	0.5	2880	25.3	1150	6.33
Meryata 1- El Blat	3.7	481	20	313	6.42
Meryata 2	3	516	19.2	335	7.53
Meryata 3	1	465	20.3	302	7.25
Meryata 4 (Youn Achech)	1	461	20.6	300	
Mijdlaya 1	n.a	n.a	n.a	n.a	n.a
Mijdlaya 2	6	1700	19.7	865	6.18
Mina 1	n.a	2500	22.2	890	n.a
Mina 2	1	1200	22.7	850	6.37
Minieh 1	1.5	1626	20	1060	5.93

Minieh 2 - Saleh Kheir	2	524	19.9	341	7.01
Nakhle (private)	4	526	24.6	350	6.6
Ras Maska , Private 1	2	566	22.1	368	6.57
Ras Maska , Private 2	6	1590	22.2	863	6.18
Raskifa	14.2	751	18	488	6.37
Saadoun	4	1180	20.8	850	7.32
Sankari	2	1275	19.9	828	7.45
Sebeel	3.3	1233	14.6	680	7.15
Sereel	4	815	20.8	350	7.22
Tripoli (200)	4	1756	21	1141	6.98
Willey	4				
Zakroun	2	1260	23.3	720	6.44

ID	Salinity %	DO (ppm)	Fluoride (mg/L)	Phosphate (mg/L)	Calcium (mg/L)	Magnesium (mg/L)	Potassium (mg/L)
S1	0.05	3.05	3.11	15.74	78.34	10.69	11.07
P1	0.05	7.3	0.86	3.1	53.67	14.61	1.53
P2	0.04	3.17	0.88	0.901	40.31	7.65	0.63
S2	0.03	4.15	2.05	0	73.06	9.59	213.99
S4	0.02	3.91	0.89	11.38	63.64	18.97	3.34
S5	0.04	8.65	0.86	22.18	48.74	3.436	0.48
S6	0.02	4.92	1.05	10.27	66.45	19.04	2.01
S7	0.01	3.32	0.91	3.507	51.53	23.85	1.19
P3	0.04	5.21	1.13	0	72.01	13.68	2.39
S8	0.07	4.39	1.87	5.97	82.73	13.39	2.61
S9	0.08	6.48	1.43	4.24	102.86	14.02	80.16
P4	0.02	8.06					
P5	0.02	2.67	0.93	15.88	55.11	24.96	2.93
P6	0.03	7.54	1.15	5.81	27.44	31.21	2.51
S12	0.03	4.16					
S13	0.08	6.31	2.26	5.94	96.86	35.39	2.32
S15	0.05	1.54	0.63	2.36	65.37	10.02	4.55
S16	0.06	5.5	0.88	0	58.36	3.168	2.42
S17	0.09	4.73	1.16	0	77.22	14.28	2.89
P7	0.09	4.85	1.83	14.44	41.8	30.26	2.91
S18	0.02	3.23	1.04	3.95	49.45	5.67	0.72
S19	0.02	6.38	0.81		58.53	8.89	3.33
P8	0.06	4.69	0.86	3.1	53.67	14.61	1.53
P9	0.04	5.86	1.61		62.32	17.82	9.81
P10	0.02	5.71	0.83	5.02	48.36	12.9	0

P13	0.03	5.84	0.76	13.62	50.79	10	1.67
S20	0.03	5.98	0.86	0	54.61	14.47	2.73
S23	0.06	5.39	0.86	0	48.61	5.721	2.4
S25	0.13	1.7	1.15	14.62	79.33	18.99	3.01
S26	0.02	7.61	2.03	0	74.51	36.78	6.01
S27	0.06	1.98	1.83	10.96	65.38	15.9	5.26
S28	0.05	4.21	1.83	14.8	89.74	14.02	5.55
S29	0.03	8.32	0.76	15.56	43.25	16.98	1.49
S30	0.01	8.08	0.68	4.74	61.6	3.984	0.55
P14	0.03	5.64	0.55	0	52.7	7.361	2.52
S31	n.a						
S32	0.06	3.56	0.49	0	60.29	6.502	1.31
S33	0.04	8.07	1.55	0	37.76	26.54	22.2
P15	0.03	6.25	1.37	2.49	72.2	14.07	2.39
S34	0.04	3.04	2.4		51.72	33.47	5.23
P17	0.02	4.4	0.4	0	47.43	2.32	0.53
S35	0.33	4.03	1.25	10.12	77.78	96.29	21.6
S37	0.05	1.46	2.28	0	58.13	40.33	4.42
S38	n.a	n.a					
S39	0.02	5.58	1.53	0.5	56.41	9.13	1.58
P20	0.02	10.03	2.16	0	48.12	30.24	390
P21	0.02	11.03	1.47	2.72	50.4	32.42	63.7
P25	0.06	7.43	1.31	0	40.17	29.32	2.65
S40	0.05	4.62	1.04	4.264	26.45	19.16	0.85
S41	0.13	3.41	9.73	0	229.3	103.56	9.51
P26	0.02	5.27	0.63	14.46	43.91	9.63	2.34
P27	0.03	4.84	0.5	0	46.37	6.297	14.5
P28	0.02	4.11	1.1	0	59.15	3.989	1.11
S43	0.06	6.71	1.11	11.3	36.78	26.83	6.45

S44	n.a	n.a	0.6	1.01	64.59	9.39	1.63
S45	0.05	2.61					
S46	0.13	5.3	1.37	3.14	102.4	18.89	1.46
S47	0.03	5.68	2.22	0	88.17	16	5.57
S48	0.02	2.22	1.16	10.6	38.82	35.6	1.83
S49	0.02	8.19					
S50	0.02	5.28	0.78	1.903	40.84	16.09	1.69
P30	0.01	9.42	0.53	0	44.77	18.32	2.61
P31	0.05		1.64	0	83.73	32.9	2.12
P33	0.01	13.29	0.66	14.5	35.13	30.74	1.13
P34	0.02	7.02	0.58	0	60.64	23.03	1.73
S51	0.05	6.3	1.13	6.46	72.24	13.87	4.46
S52	0.05	5.51	0.64	0	59.98	4.88	0.62

ID	Ammonium in mg/L	Sodiumin mg/L	Sulfate in mg/L	Nitrate in mg/L	Bromide in mg/L	Nitrite in mg/L	Chloride in mg/L	Lithiumin mg/L
S1	3.86	50.11	20.27	24.61	0	15.94	53.11	
P1	3.52	25.45	15.06	26.23	8.22	12.79	35.25	
P2	3.15	15.14	7.68	6.17	8.21	7.604	20.47	
S2	6.69	43.25	18.61	18.61	0	15.27	237.9	
S4	3.27	30.46	25.69	17.37	6.6	10.24	45.68	
S5	2.88	12.26	5.18	2.77	0	8.205	23.94	
S6	4.18	23.46	36.67	11.93	0	11.51	28.09	
S7	4.68	35.83	3.44		9.17	11.87	67.03	1.14
P3	4.05	34.38	23.71	7.19	0	15.1	47.77	
S8	4.71	36.06	58.18	23.36	0	14.32	57.81	1.34

S9	5.64	34.98	86.39	53.34	0	13.59	127.69	1.37
P5	3.54	15.99	16.35	17.27	10.7	10.05	30.83	
P6	4.06	52.33	32.63	4.53	3	13.22	17.05	0.62
S13	8.73	150.42	76.81	56.46	1.31	16.96	235.78	
S15	4.42	41.56	26.15	2.18	0	12.52	32.07	
S16	3.46	16.94	5.013	11.29	0	8.827	26.26	
S17	6.85	16.95	72.47	15.51	0	10.06	28.36	1.35
P7	4.86	17.67	15.73	6.54	0	11.26	22.84	
S18	3.57	18.21	3.197	7.45	0	8.547	27.74	
S19	5.17	17.35	9.92	18.51	8.81	9.28	30.25	1.03
P8	3.5	25.45	15.06	26.23	8.22	12.79	35.25	
P9	8.23	27.29	9.67	27.76	0	18.26	32.47	
P10	4.57	17.97	9.42	16.75	0	8.95	26.36	
P13	3.07	19.95	10.02	22.17	3.52	8.828	33.71	
S20	3.9	20.02	9.24	24.62	0	9.428	39.31	0.52
S23	3.46	13.55	4.571	11.17	0	8.52	22.69	
S25	6.04	83.31	36.94	43.72	1.72	11.85	149.19	
S26	4.33	44.15	49.22	39.17	0	13.1	121.54	
S27	4.07	64.11	29.95	24.83	0	12.85	90.63	
S28	6.75	57.72	41.46	56.72	0	15.18	60.96	
S29	3.69	27.68	14.24	12.26	8.22	8.14	38.88	
S30	2.92	19.76	3.24	20.74	0	8.84	34.31	
P14	3.12	12.94	13.42	26.14	0.77	8.21	22.34	0.53
S32	3.29	17.44	12.18	3.719	0	9.64	25.65	
S33	5.03	46.17	17.96	14.47	0	14.23	65.79	1.49
P15	4.24	7.191	23.05	7.19	0	16.28	47.3	
S34	7.12	31.67	48.5	0.49	0	16.4	43.52	1.42
P17	2.87	10.17	6.78	5.76	0	6.05	16.92	
S35		659.2	225.52	4.91	3.32	9.64	1154.25	

S37	5.68	33.71	36.45	2.63	8.63	19.53	39.63	1.54
S39	3.53	20.38	5.41	11.21	0	8.9	43.55	0.55
P20	6.79	47.64	13.96	35.93	2.99	18.62	391.53	
P21	6.31	29.04	13.15	36.84	0	13.58	96.91	
P25	4.17	8.738	14.45	9.015	0	11.67	12.76	0.74
S40	3.57	15.36	9.544	5.48	8.2	7.67	26.15	
S41	21.8	447.6	100.1	20.31	3.2	25.49	1101.89	
P26	2.73	12.72	6.411	9.033	0	8.66	20.73	0.56
P27	3.74	19.27	12.6	10.16	0	9.08	37.22	
P28	3.23	15.17	11.7	19.92	0	8.68	19.18	
S43	4.58	36.77	18.7	5.109	0	11.71	38.06	1.17
S44	3.72	24.03	16.6	5.235	0	11.37	34.37	
S46	5.1	26.07	75.92	65.54	0	14.34	28.69	
S47	10.1	27.01	64.18	53.42	0	13.88	26.74	
S48	4.07	16.88	17.35	2.347	0	12.64	23.95	
S50	3.36	22.1	12.54	22.53	1.5	9.07	30.59	
P30	3.2	11.78	6.723	8.144	0	9.67	18.65	
P31	5.08	24.91	42.06	0.379	0	18.44	33.96	1.03
P33	3.13	11.19	12.99	1.491	0	10.32	16.75	
P34	3.39	13.21	15.42	2.729	0	12.55	19.35	
S51	8.24	40.97	23.16	7.23	0	18.66	47.71	
S52	3.26	20.82	3.72	6.19	0	9.102	37.31	

ID	Salinity %	DO (ppm)	Fluoride (mg/L)	Phosphate (mg/L)	Calcium (mg/L)	Magnesium (mg/L)	Potassium (mg/L)
S1	0.05	3.05	3.11	15.74	78.34	10.69	11.07
P1	0.05	7.3	0.86	3.1	53.67	14.61	1.53
P2	0.04	3.17	0.88	0.901	40.31	7.65	0.63
S2	0.03	4.15	2.05	0	73.06	9.59	213.99
S4	0.02	3.91	0.89	11.38	63.64	18.97	3.34
S5	0.04	8.65	0.86	22.18	48.74	3.436	0.48
S6	0.02	4.92	1.05	10.27	66.45	19.04	2.01
S7	0.01	3.32	0.91	3.507	51.53	23.85	1.19
P3	0.04	5.21	1.13	0	72.01	13.68	2.39
S8	0.07	4.39	1.87	5.97	82.73	13.39	2.61
S9	0.08	6.48	1.43	4.24	102.86	14.02	80.16
P4	0.02	8.06					
P5	0.02	2.67	0.93	15.88	55.11	24.96	2.93
P6	0.03	7.54	1.15	5.81	27.44	31.21	2.51
S12	0.03	4.16					
S13	0.08	6.31	2.26	5.94	96.86	35.39	2.32
S15	0.05	1.54	0.63	2.36	65.37	10.02	4.55
S16	0.06	5.5	0.88	0	58.36	3.168	2.42
S17	0.09	4.73	1.16	0	77.22	14.28	2.89
P7	0.09	4.85	1.83	14.44	41.8	30.26	2.91
S18	0.02	3.23	1.04	3.95	49.45	5.67	0.72
S19	0.02	6.38	0.81		58.53	8.89	3.33
P8	0.06	4.69	0.86	3.1	53.67	14.61	1.53
P9	0.04	5.86	1.61		62.32	17.82	9.81
P10	0.02	5.71	0.83	5.02	48.36	12.9	0
P13	0.03	5.84	0.76	13.62	50.79	10	1.67
S20	0.03	5.98	0.86	0	54.61	14.47	2.73

S23	0.06	5.39	0.86	0	48.61	5.721	2.4
S25	0.13	1.7	1.15	14.62	79.33	18.99	3.01
S26	0.02	7.61	2.03	0	74.51	36.78	6.01
S27	0.06	1.98	1.83	10.96	65.38	15.9	5.26
S28	0.05	4.21	1.83	14.8	89.74	14.02	5.55
S29	0.03	8.32	0.76	15.56	43.25	16.98	1.49
S30	0.01	8.08	0.68	4.74	61.6	3.984	0.55
P14	0.03	5.64	0.55	0	52.7	7.361	2.52
S31	n.a						
S32	0.06	3.56	0.49	0	60.29	6.502	1.31
S33	0.04	8.07	1.55	0	37.76	26.54	22.2
P15	0.03	6.25	1.37	2.49	72.2	14.07	2.39
S34	0.04	3.04	2.4		51.72	33.47	5.23
P17	0.02	4.4	0.4	0	47.43	2.32	0.53
S35	0.33	4.03	1.25	10.12	77.78	96.29	21.6
S37	0.05	1.46	2.28	0	58.13	40.33	4.42
S38	n.a	n.a					
S39	0.02	5.58	1.53	0.5	56.41	9.13	1.58
P20	0.02	10.03	2.16	0	48.12	30.24	390
P21	0.02	11.03	1.47	2.72	50.4	32.42	63.7
P25	0.06	7.43	1.31	0	40.17	29.32	2.65
S40	0.05	4.62	1.04	4.264	26.45	19.16	0.85
S41	0.13	3.41	9.73	0	229.3	103.56	9.51
P26	0.02	5.27	0.63	14.46	43.91	9.63	2.34
P27	0.03	4.84	0.5	0	46.37	6.297	14.5
P28	0.02	4.11	1.1	0	59.15	3.989	1.11
S43	0.06	6.71	1.11	11.3	36.78	26.83	6.45
S44	n.a	n.a	0.6	1.01	64.59	9.39	1.63
S45	0.05	2.61					

S46	0.13	5.3	1.37	3.14	102.4	18.89	1.46
S47	0.03	5.68	2.22	0	88.17	16	5.57
S48	0.02	2.22	1.16	10.6	38.82	35.6	1.83
S49	0.02	8.19					
S50	0.02	5.28	0.78	1.903	40.84	16.09	1.69
P30	0.01	9.42	0.53	0	44.77	18.32	2.61
P31	0.05		1.64	0	83.73	32.9	2.12
P33	0.01	13.29	0.66	14.5	35.13	30.74	1.13
P34	0.02	7.02	0.58	0	60.64	23.03	1.73
S51	0.05	6.3	1.13	6.46	72.24	13.87	4.46
S52	0.05	5.51	0.64	0	59.98	4.88	0.62

Table 5.2: Results of sampling campaign April - May 2013

Sample ID	ID	Date	Static Water Level (in m)	Time in hours (off)	Dynamic Water Level (in m)	Time in hours (on)	Conductivity ($\mu\text{S}/\text{cm}$)	T ($^{\circ}\text{C}$)	TDS (ppm)	pH
Aaba (private)	S1		147.15							
Agrotech	P1	4/4/2013	90	3	92	2	940	19.8	280	7.44
Alma dawle	P2	24/03/2013	211	1	210	1	507	20.4	200	8.3
Alma 1	S2	24/03/2013	58	72	70	1	940	19.9	425	7.6
Alma 2	S3	24/03/2013	92	3	98	3	750	20.2	500	
Almoun 1	S4	1/4/2013	8.5	1	8.5	1	690	21	300	7.5
Almoun 2	S5	1/4/2013	7.5	1	7.5	72	437	20.9	200	7.4
Amioun 1	S6	4/4/2013	4.6	72	4.2	2	1000	14.4	300	8.58
Amioun 2	S7	4/4/2013	1.8	24	2	3	930	15.6	300	8.11
Anfe , Jrade	P3	3/4/2013	8	48	8	12	510	20.5	300	8.84

Anfeh 1	S8	3/4/2013					1130	17.8	390	7.15
Anfeh 2	S9	3/4/2013	6.2	2	6.6	2	n.a	n.a	n.a	n.a
Arabech	S10	41160	80	2	85	4	1260	18.1	550	7.08
Arde	S11	5/4/2013	9	100	n.a	n.a	n.a	n.a	n.a	n.a
Arges	P4	1/4/2013	92	3	105	4	750	18.3	450	7.54
Asnoun	P5	1/4/2013	76.5	7	91	2				
Ayto	P6	26/04/2013	18	4	35	4	525	13.2	320	8.01
Badawi 1	S12	31/04/2013	10.5	72	19	1.5	1780	22.5	900	7.55
Badawi 2	S13	31/04/2013	42	200	43	1	1080	18.3	400	5.3
Badebhoun 1	S14	14/04/2013	8	340	n.a	n.a	n.a	n.a	n.a	n.a
Badebhoun 2	S15	14/04/2013	58	4.2	64	1.8	1060	20.3	350	7.83
Balamand	S16	15/04/2013	128.1	6	107.4	72	619	20.6	650	7.74
Barghon	S17	14/04/2013	8	48	8.8	1.8	1350	18.4	450	7.57
Barsa	P7	22/04/2013	105.5	1	104	3.5	542	23.3	200	8.1
Batromine	S18	29/04/2013	183	90	185	1.5	500	21.7	250	6.93
Bdebba	S19	16/04/2013	128	48	126.1	5	623	21.1	400	6.66
Bir Al- Ahdab (Ras Maska)	P8	8/5/2013	82	3	88.23	3	620	22.4	280	6.01
Bir Bechmezzine, Snoubar	P9	2/4/2013	143	3.5	150	2	628	19.8	300	8.55
Bir Bterram	P10	3/4/2013	176	3.21	181	4	920	19.2	300	6.96
Bir El mazraa – Kferaka	P11	4/4/2013	204	long periode	222	1.5	701	18.2	250	8.52
Bir Kfarhazir, (Ain el Bakar)	P12	3/4/2013	86	4	90	2.5	391	18	350	8.54
Bir Ras Maska	P13	8/5/2013	101.2	3	122	2.5	475	25.7	220	7.72
Bkeftine	S20	25/03/2013	133	15.5	142	3	622	20.4	300	6.4
Borj Hayodiyeh (Dawle Well)	S21	6/4/2013	28	4	31	2.2	503	18.5	200	7.08
Boussit	S22	23/03/2013	35.5	2.8	37.2	2	526	18.7	250	7.81
Bteram (private)	S23	22/04/2013	125	10	126.2	2.2	535	18.7	510	6.16
Btouratij 1 , Adnan Hassan	S24	9/4/2013	142	6	145	1	494	20.1	230	8.5

Btouratij 2 , Mokhtar	S25	9/4/2013	2.5	6	4	1	1601	20.8	760	8.68
Chahal Building (Dam & Farez)	S26	9/4/2013	9.5	120	10.5	3	1430	20	550	7.7
Chekaa 1	S27	41337	32.5	2	36.1	2	1490	19.6	300	7.32
Chekaa 2	S28	41337	5.4	4	6.2	3	1480	21.9	600	6.78
Dahel El Ain , private 1	S29	27/03/2013	53.5	2	61.2	2	638	24.6	340	7.12
Dédde, Gaz Station	S30	9/1/2012	13	72	18	4	801	19.5	520	6.08
Deir Achach	P14	24/03/2013	3.2	4	3.2	2	625	18.2	300	8.36
Deir Amar 1	S31	2/4/2013	49	long periode	52	10	n.a	n.a	n.a	n.a
Deir Amar 2(kasser balade)	S32	2/4/2013	30.5	1	37	1	1160	20.5	400	8.13
Deir amar 3, Kassarat	S33	2/4/2013	79	long periode	81	1	1130	20.1	350	6.21
Ejed Ebrin	P15	4/4/2013	237	1.5	240	3	518	18.5	250	7.34
Fih	S34	29/03/2013	72	14	78	2	671	19	300	7.41
Hawouz	P16	9/4/2013	93.5	3	95	3	n.a	n.a	n.a	n.a
Hellan	P17	26/04/2013	46	long periode	46	1	n.a	n.a	n.a	n.a
Hraiche 1	S35	41161	18	12	32	3	10200	21.9	3800	5.99
Hraiche 2	S36	41161	27	78	29	1	n.a	n.a	n.a	n.a
Jisr	P18	not done	81	150	89	4				
Kasser Mae	P19	9/4/2013					1120	21.8	750	8.64
Kelhat	S37	9/4/2013	92	10	104	2	910	21.8	425	7.17
Kfarhat, Jedeide	S38	21/04/2013	38	long periode	n.a	n.a	n.a	n.a	n.a	n.a
Kfarkahel (private)	S39	26/03/2013	147.5	2	149	3	662	21	300	7.23
Kferzayna 1	P20	8/4/2013	55	4	59	2	1727	19.2	800	6.4
Kferzayna 2	P21	9/4/2012	51.5	4	52.5	2	930	19.1	400	7.82
Malloule	P22	31/03/2013	27	1	31	2	950	19.5	750	n.a

Manar	P23	9/10/2012	84	long periode	off	off				
Massafi 7	P24	14/04/2013	34	4	37	4	730	18	350	7.43
Mazraet el Tefeh	P25	31/03/2013	121	4	128	2	1150	16.7	750	7.5
Mervat , House	S41	16/04/2013	6.5	4	7	0.5	3180	22.3	1500	7.12
Meryata 1- El Blat	P26	24/03/2013	153.6	1.5	156	29	508	16.8	250	7.11
Meryata 2	P27	24/03/2013	13.7	2	15.5	3	682	19.5	300	7.45
Meryata 3	P28	24/03/2013	12	15	13	4	538	19	230	7.8
Meryata 4 (Youn Achech)	P29	24/03/2013	12.6	12	13	4	471	20.3	200	7.45
Mijdlaya 1	S42	7/4/2013	86	240	93	2	1060	16	650	7.94
Mijdlaya 2	S43	7/4/2013	49	260	53	2.9	960	20	350	6.5
Mina 1	S44	7/4/2013	2	6	2.5	1	2470	20.3	1200	7.15
Mina 2	S45	7/4/2013	2	long periode	4	0.5	3240	19.7	1700	7.44
Minieh 1	S46	26/03/2013	14	2	16	2	1530	19.6	950	6.03
Minieh 2 - Saleh Kheir	S47	26/03/2013	28	240	32	2	1034	21	400	7.87
Nakhle (private)	S48	24/03/2013	162	120	165.5	2	920	22.4	400	6.67
Ras Maska , Private 1	S49	3/4/2013	53	2	53	2	566	22.1	368	6.57
Ras Maska , Private 2	S50	3/4/2013	190	2	198	6	1590	22.2	863	6.18
Raskifa	P30	26/04/2013	208	2	215	5	750	17.5	380	7.55
Saadoun	P31	1/4/2013	90	3	95	4	1350	17.9	550	8
Sankari	P32	31/03/2013	75	3.5	85	24	1275	19.9	828	7.45
Sebeel	P33	31/03/2013	234	5	243	2	545	18.2	300	7.5
Sereel	P34	9/4/2013	18	24	23	3	751	18.3	400	7.35
Tripoli (200)	S51	27/03/2013	5.5	2.5	5.5	3	1756	21	1141	6.98
Willey	P35	13/04/2013	89	2	90	0.5	679	17.7	400	8.9
Zakroun	S52	14/04/2013	84.1	3	85	2	552	19.5	260	8.72

ID	Salinity %	DO (ppm)	Fluoride (mg/L)	Phosphate (mg/L)	Calcium (mg/L)	Magnesium (mg/L)	Potassium (mg/L)
S1			2.524		83.97	19.54	5.45
P1	0.02	0.68	2.01		123.68	11.42	7.56
P2	0.02	3.59	1.266		76.485	5.91	1.98
S2	0.03	4.39	1.399		135.97	12.77	2.43
S3					79.18	8.82	1.79
S4	0.04	3.91			159.98	17.17	5.45
S5	0.01	1.22	1.158		105.07	4.2	3.03
S6	0.04	4.44	5.786		157.79	24.66	6.48
S7	0.04	3.4	4.831		145.01	20.91	4.84
P3	0.02	1.01			139.89	28.91	3.65
S8	0.05	4.05	1.184		157.86	15.03	5.124
S9	n.a	n.a					
S10	0.02	3.5	4.027		86.8	19.44	6.02
S11	n.a	n.a					
P4	0.02	6.78					
P5			4.966		81.6	19.94	16.7
P6	0.03	8.07			81.4	18.08	2.12
S12	0.08	5.78			196.32	40.64	5.25
S13	0.04	4.6			142.15	30.89	
S14	n.a	n.a					
S15	0.04	1.04			151.85	5.31	425.69
S16	0.04	5.64	0.721		141.57	3.97	7.11
S17	0.06	4.06	1.012		198.71	27.59	5.51
P7	0.02	1.25			110.46	10.58	4.46
S18	0.02	3.06			115.76	6.55	5.67
S19	0.02	6.66			120.68	4.27	3.57
P8	0.02	4.69			140.55	18.12	4.6

P9	0.03	5.49	3.746		129.59	19.52	11.35
P10	0.04	5.42			121.25	19.52	7.2
P11	0.02	0.38	2.415		132.32	39.33	10.58
P12	0.02	0.69	4.269		78.19	15.34	5.78
P13	0.02	5.31	2.564		104.87	39.98	7.09
S20	0.02	5.41			95.94	13.776	12.896
S21	0.02	6.19			87.03	24.878	8.23
S22	0.02	0.48			63.93	2.71	2
S23	0.04	5.62			155.82	7.83	6.45
S24	0.02	1.21	0.97		102.27	2.48	1.92
S25	0.04	6.12			84.3	16.26	2.69
S26	0.06	6.29			174.68	42.1	8.16
S27	0.04	6.26			89.47	15.99	5.68
S28	0.05	5.28			178.73	155.07	35.81
S29	0.03	8.26	2.234		95.72	22.09	5.79
S30	0.01	8.08			118.23	8.99	2.63
P14	0.02	5.46	1.8		95.39	6.25	5.08
S31	n.a						
S32	0.05	3.02	3.757		143.23	16.56	5.44
S33	0.04	8.09	3.257		103.49	22.99	23.93
P15	0.02	6.28	6.07		110.03	16.67	7.36
S34	0.03	3.26			152.43	30.19	5.13
P16	n.a	n.a					
P17	n.a	n.a					
S35	0.6	0.8	0.478		166.49	169.62	43.13
S36	n.a	n.a					
P18					65.734	30.15	4.93
P19	0.04	6.08	8.574		105.05	31.05	10.83
S37	0.03	1.12	0.755		152.85	27.42	7.99

S38	n.a	n.a			135.25	2.17	1.99
S39	0.02	5.5	0.859		98.03	8.17	14.24
P20	0.03	10.3			75.25	25.61	7.61
P21	0.03	10.4			94.18	72.87	7.67
P24	0.05				123.67	32.53	0
P25	0.03	6.03			68.86	48.43	6.19
S41	0.16	4.96			227.93	73.13	10.37
P26	0.02	5.69			80.2	6.93	10.62
P27	0.03	4.69	1.232		99.53	6.36	2.55
P28	0.02	4.45			85.56	3.62	3.57
P29	0.01	4.64			91.4	2.97	3.03
S42	0.04	4.04	3.124		97.52	46.86	17.63
S43	0.04	4.12			105.79	26.52	7.05
S44	0.12	8.2			197.34	66.13	17.63
S45	0.16	8.21			292.69	80.32	11.19
S46	0.12	6.4	3.347		191.13	21.18	141.35
S47	0.05	8.35			105.53	18.534	4.911
S48	0.04	2.02	5.689		68.73	58.3	3.56
S49	0.02	8.19			93.72	19.08	9.22
S50	0.02	5.28	1.411		99.96	17.14	3.34
P30	0.01	8.05			27.23	9.42	15.99
P31	0.06	9.14			144.44	96.43	19.6
P32	0.06		1.195	5.265	111.37	21.73	4.66
P33	0.02	8.27			74.87	70.83	4.59
P34	0.02	6.5			69.07	16.77	2.16
S51	0.05	6.3			173.89	18.14	1.63
P35	0.02	2.2			79.66	61.115	10.13
S52	0.02	0.74			121.71	23.77	4.431

ID	Ammonium (mg/L)	Sodium (mg/L)	Sulfate (mg/L)	Nitrate (mg/L)	Bromide (mg/L)	Nitrite (mg/L)	Chloride (mg/L)	Lithium (mg/L)
S1		22.15	26.37	4.07		12.04	42.23	
P1		15.94	13.52	41.72		17.37	32.3	
P2		13.18	12.98	24.32		12.45	21.05	
S2		31.44	38.46	51.56		20.92	52.32	
S3		23.61	26.35	40.96		9.275	36.75	
S4		32.75	33.12	54.1		19.98	59.27	
S5		16.2	12.53	24.72		13.4	31.26	
S6		38.12	64.88	31.37		19.36	46.67	
S7		24.16	62.45	26.72		14.36	40.62	
P3		30.12	28.82	26.21		19.49	63.97	
S8	0.262	41.47	80.69	49		17.16	69.86	
S10		22.74	27.31	4.916		12.12	47.12	
P5		24.71	25.61	5.848		6.384	49.38	
P6		18.04	24.78	5.147		12.58	37.59	
S12		174.5	121.5	87.43		22.15	333.9	
S13		39.92	7.564	24.37		18.88	93.98	
S14								
S15		66.44	43.3	36.86		15.09	55.53	
S16	0.62	20.25	16.16	34.97		17.29	38.82	
S17	0.63	32.78	163.3	50.12		19	65.23	
P7		23.8	17.85	49.05		14.01	41.92	
S18	0.66	20.9	9.098	26.55		15.2	41.26	
S19	0.53	18.65	27.17	10.8		14.22	34.76	
P8		31.79	29.49	63.64		17.4	55.69	
P9		22.1	18.92	64.81		21.27	47.25	
P10		19.7	19.82	45.69		17.44	39.81	
P11		29.73	34.11	59.52		24.15	53.2	

P12		12.86	14.02	23.32		12.6	17.95	
P13	0.38	22.76	26.28	33.49		18.73	43.78	
S20		22.57	17.14	48.84		15.54	48.93	
S21		21.79	31.85	31.06		14.36	37.46	
S22		11.36	10.84	31.65		7.786	21.95	
S23	0.36	18.46	14.02	32.47		18.41	37.89	
S24		12.42	11.63	31.75		14.84	19.69	
S25		18.35	17.65	20.16		12.38	38.29	
S26		50.34	91.4	87.72		19.52	133.5	
S27	0.72	22.17	23.98	35.2		11.32	39.59	
S28		924.5	333	31.37	7.075	23.09	2031	
S29		32.96	41.16	28.89		17.46	46.32	
S30		23	9.579	54.27		15.3	43.54	
P14		12.64	22.97	41		14.54	25.43	
S32		55.91	37.54	63.86		18.32	122.4	
S33		44.21	20.96	45.19		18.03	82.58	
P15		18.39	21.73	40.62		17.94	36.72	
S34		25.98	75.41	17.96		18.04	50.97	
S35		1078	362.2	37.03	9.95	21.8	2361	
P18		36.88	33.13	38.55		10.18	81.79	
P19		45.81	35.34	54.86		16.84	95.35	
S37	0.57	30.52	61.19	30.61		17.82	54.96	
S38		9.859	31.76	31.54		16.4	26.16	
S39		20.71	9.317	25.58		14.97	57.08	
P20	1.83	20.15	41.49	64.35			37.59	
P21		41.93	36.36	123		17.61	105.1	
P24		35.91	47.95	9.086		15.06	68.6	
P25		15.15	50.3	38.65		6.729	26.32	
S41		306.1	121.5	63.92	2.72	18.85	889.8	

P26		13.86	11.74	29.92		13.77	32.87	
P27		14.76	48.65	32.27		13.92	26.26	
P28		9.9	68.78	33.53		12.11	18.26	
P29		9.831	17.93	30.99		13.08	20.98	
S42	1.77	38.48	100.1	31.64		4.717	68.14	
S43		31.75	30.07	27.72		17.52	41.11	
S44		237.9	107.9	39.65	2.63	18.86	689.2	
S45		308.1	182.5	51.14	3.46	18.23	1030	
S46	0.29	23.86	117.4	146.6		19.66	49.98	
S47		17.76	94.02	94.7		9.761	35.35	
S48		18.46	57.35	17.95		19.77	30.17	
S49	0.59	20.59	16.74	27.38		15.09	42.23	
S50		22.99	19.68	45.69		15.97	37.39	
P30		21.37	7.457	25.36		8.105	64.43	
P31		284.8	105.1	113.4		19.62	667.9	
P32		47.33	97.66	40.95		14.78	99.21	
P33		22.42	39.46	15.86		18.1	47.81	
P34		6.297	33.49	23.51		10.48	12.58	
S51		25.89	104.5	27.86		15.17	75.44	
P35		81.12	57.19	63.47		15.13	175.5	
S52		20.28	10.92	34.19		14.43	43.43	

5.2.1 The Physical Parameters

5.2.1.1 pH

Water acidity is governed by what is referred to as pH. pH stands for "potential hydrogen." When water has a low pH, it is referred to as soft water, it is more acidic, therefore, it can be corrosive and harmful to any metals it comes into contact with. When the water corrodes the metal, this corrosion can then seep into the water.

When water has high levels of pH, it is considered to be hard water. Hard water isn't necessarily harmful to humans; however, it is known to make water have a bad taste and it causes lime scale to build up on plumbing fixtures and pipes. The pH level can be affected by several factors, including soil and bedrock, and some forms of pollution. According to the Lebanese Standards and WHO, (WHO, 2006) the pH varies between 6.5 and 8.5. Whether the samples are located in Zgharta, Tripoli or Koura areas, the pH values are not all present within the standards. pH values vary with proximity to urban areas in addition to the caustic substances coming from industry and soil additives in agriculture such as lime $\text{Ca}(\text{OH})_2$. Consequently, we can see clearly from the dry campaign of 2012 that slightly acidic pH is seen in areas closer to the sea such as in Anfe (P3, S8 & S9) or Mina (S44 & S45), see Figure 5.1. The pH values alone are not sufficient to indicate the presence of contamination in Tripoli, Zgharta and Koura areas; therefore, other parameters are required to assume the occurrence of any groundwater pollution.

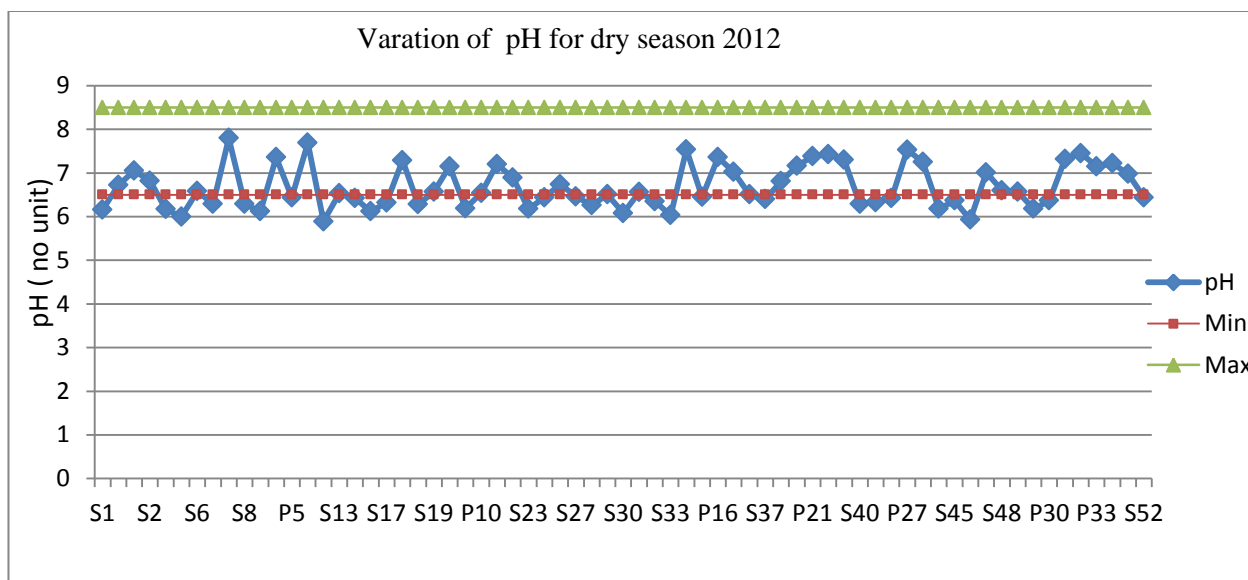


Figure 5.1: pH Variation for Dry Season 2012

5.2.1.2 Temperature

Temperature affects many of the physical, chemical, and biological characteristics of groundwater. If seasonal variations are to be discussed in the three locations Koura, Zgharta and Tripoli area, it is noticeable that the temperature deviation is almost absent; groundwater temperatures vary slightly from one season to another. The groundwater temperature had a mean average of 20.57 °C for the dry season 2012 and an average of 19.7°C for the wet season 2013. International reference standards (WHO and EU standard) as well as The Lebanese Standard (LS) set the Temperature standard as 18°C. Any value above could lead to drastic changes in the quality of groundwater. Advocate temperature thresholds values for drinking water is set at 25 ° C. In the aquifer, not all values are below the threshold and therefore acceptable. Some are above either in wet or dry season. Knowledge of water temperature and its variation is quite important, for instance in the dry season it varied between 11.9°C and 25 °C , whereas in the wet season it varied between 13.2° C and 25.7° C . The lowest values seen were always observed in P 25(Mazraat Al Tefeh)and its surrounding (Sebeel P33, and Zgharta region such as in P5 & P6) and the highest temperatures were seen in the Tripoli area either in Ras Maska or in Abou Samra such as in P13 or S41 etc... The trivial increase in temperature could be explained by the urban activities that warm up the soil (Foley D., 2009) and thus warming up the underground including groundwater. In addition, the presence of more ions in the water due to agricultural activities or even seawater intrusion, increases the presence of chemicals in the groundwater that induces drastic changes to the physical and chemical properties of the groundwater (Grassi & Cortecchi, 2007). See figure 5.2 and 5.3.

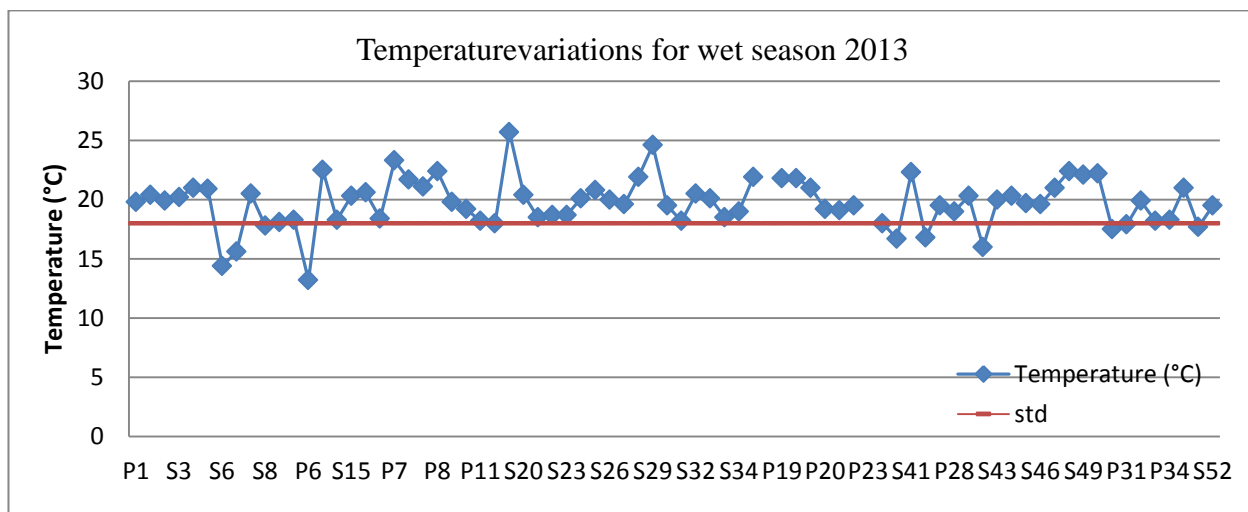


Figure 5.2: Temperature Variation for Wet Season 2013

Temperature affects many of the physical, chemical, and biological characteristics of groundwater. For instance, an increase in temperature could decrease the amount of dissolved oxygen (DO). If the variations of Temperatures versus DO have to be discussed, ideally no major temperature variation occurs, DO values should vary scarcely, but in our case we observe an increase of DO values in Tripoli area. Refer to figure 5.3. This situation is due to urban runoff that can add salts thus increasing the DO levels (El-Hoz, 2007, May). As for Koura and Zgharta regions, moderate temperature values should lead to an increase in DO values theoretically, but as shown in the figure 5.3, some values are higher than expected; this has to do with the agriculture and fertilizers used in the North specially olive culture that will slightly increase the rate of DO.

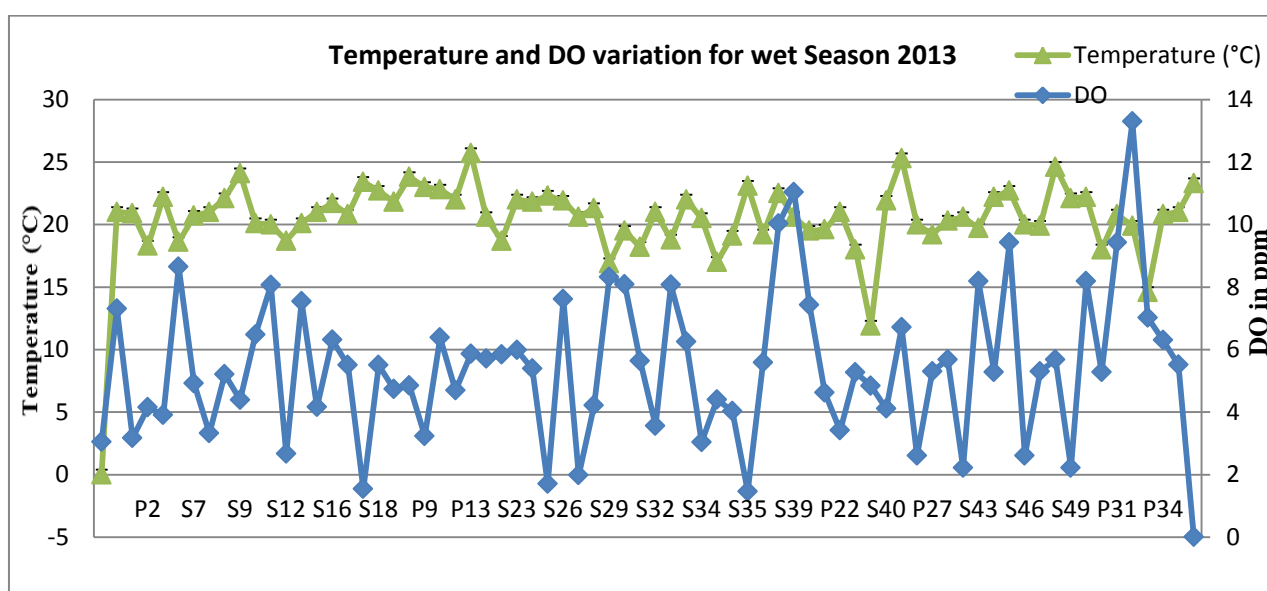


Figure 5.3: Temperature and DO Variation for Wet Season 2013

5.2.1.3 Total Dissolved Solids (TDS)

TDS is a measure of material dissolved in water (solid matter) such as chloride Cl^- , sulfate SO_4^{2-} , phosphate PO_4^{2-} , nitrate NO_3^{2-} , calcium ion Ca^{2+} , magnesium ion Mg^{2+} , and other ions. The maximum allowable levels range from 500 ppm to 1500 ppm. In this study, almost all the samples values range between the allowable levels in the exception of some locations such as S35, S45 etc... As seen in Figures 5, 4 and 5.5, the highest values are observed mostly in Tripoli and it's surrounding such as S35, S45, S51, and P19, P22, P25, P31, P32. Some of these locations are quite close to the sea therefore; the high values could be due to run off from the salts, and excessive salinity from seawater intrusion that increases the percentage of salts in the groundwater like in P31 Tripoli. This assumption was confirmed in the dry season in S35, S41. In the two other main regions, high levels within the standard are seen, as observed

in P20, this can be explained by the soil structure, runoff of salts and land use. If agricultural activities occur, fertilizers increase the level of salts in the soil thus increasing the value of TDS in the groundwater (Li Y., 2011). As a consequence, an area like P26 & P27 (Meryata 1 & 2) which is used as an agricultural land will face a higher TDS value as seen. A relation is formed between TDS and Temperature, TDS and temperature values are proportional; the increase in TDS leads to an increase in temperature and vice versa. See Figure 5.4. As a result, the highest temperatures observed in Tripoli led to the highest TDS values in Tripoli. The TDS values in Southern Tripoli are high due to excessive salinity from seawater intrusion that increases the percentage of salts in the groundwater (Grassi & Cortecchi, 2007), for instance S45 is the closest site to the coast, which explains the most abundant amounts of TDS in water while the lowest are seen in P24. Therefore, the sample distance from the sea is an important indication of the presence of Total Dissolved Solids. Therefore, TDS in all of the three regions shown in Figure 5.5 and 5.6 indicate that the groundwater is acceptable in almost all sampling locations because it is far from exceeding the standard issued.

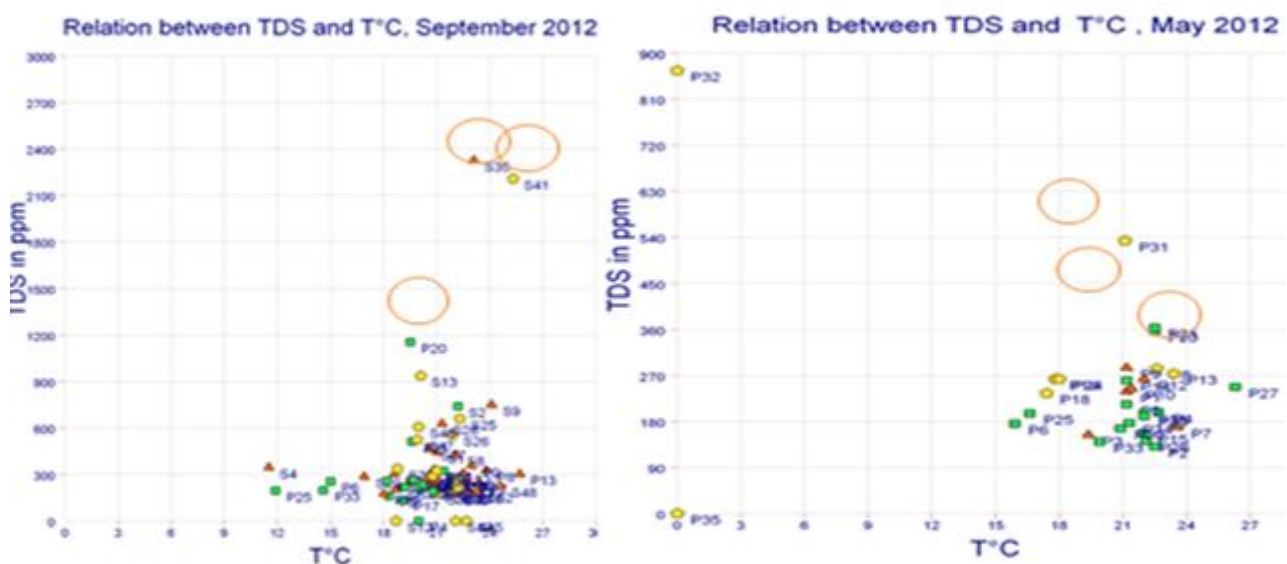


Figure 5.4: TDS and Temperature Variations using PhreeqC

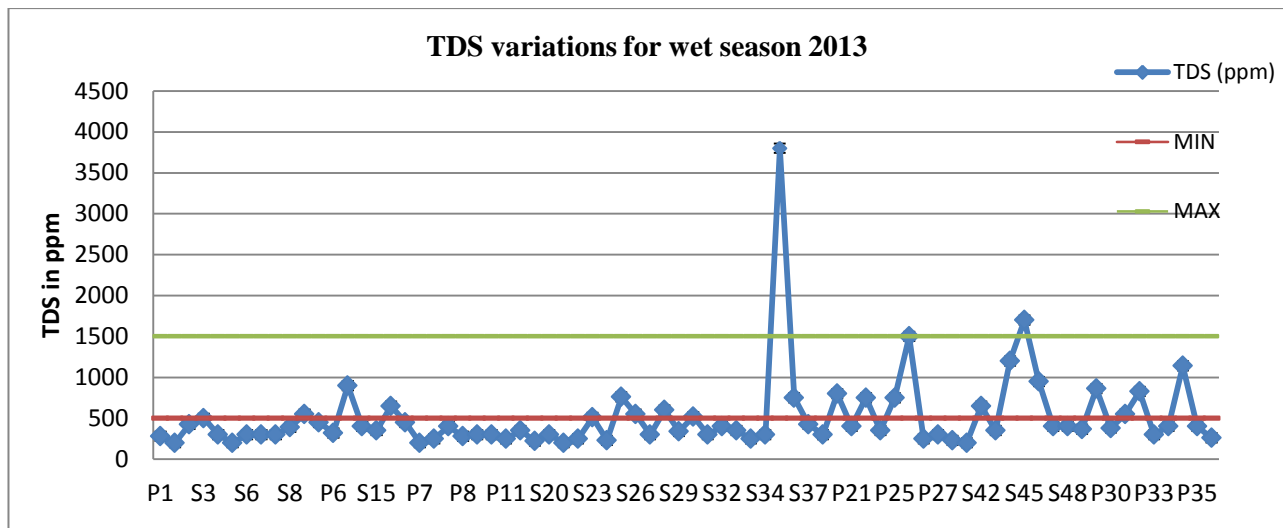


Figure 5.5: TDS Variations for Wet Season 2013

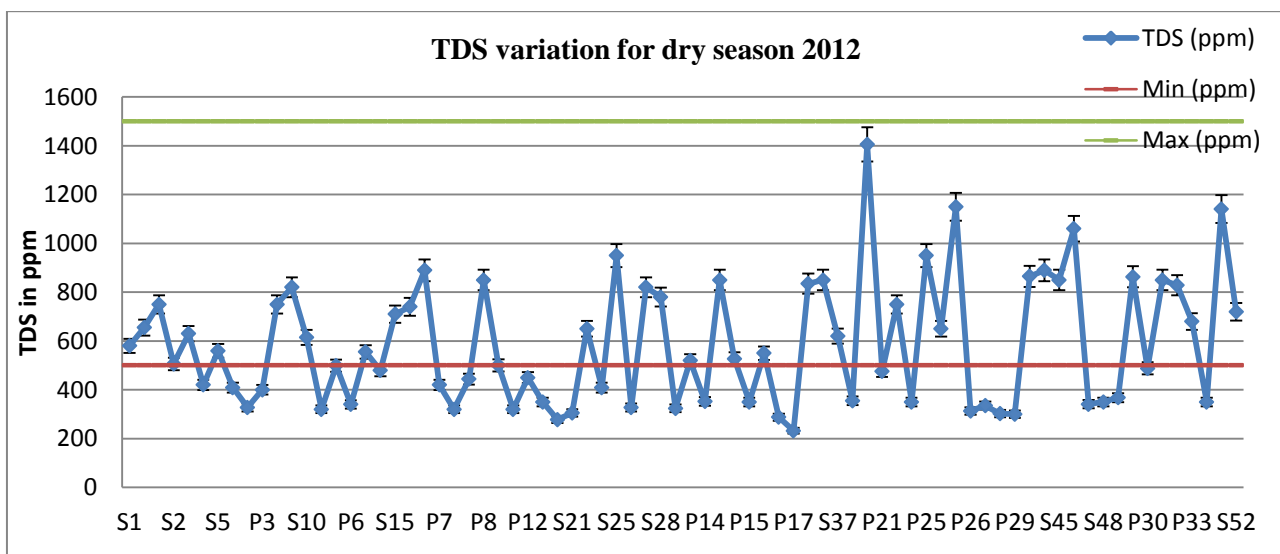


Figure 5.6: TDS Variations for Dry Season 2012

5.2.1.4 Dissolved Oxygen (DO)

Dissolved oxygen levels above 8 ppm in groundwater are considered unsafe. Figure 5.7 indicates that all samples have levels of DO lower than 8 ppm with some exceptions. The high values of DO are due to fertilizers, sea water intrusion etc... the following figure illustrates the interrelation between DO and temperature. It is delineated that Zgharta and Koura regions have lower temperature values, therefore leading to higher DO values; whereas in Tripoli, elevated temperatures are seen; thus leading to a

decrease in DO levels. Dissolved Oxygen is one of the parameters that gets affected by different factors such as temperature conductivity and TDS (Fadoua Hamzaoui-Azaza, 2011). As temperature increases, oxygen levels decrease and vice versa. The actual quantity of oxygen that can be present in solution is governed by temperature and the purity of the water. For instance, the lowest DO values are seen in Zgharta instead of Tripoli, this is explained by the fact that the actual amount of oxygen present in the groundwater is governed not only by temperature but also by the purity (salinity and suspended solids) of the water. As TDS and salinity values are the highest in the Caza of Tripoli, there effect is of great importance to the amount of dissolved oxygen. Other factors affecting the amount of dissolved oxygen are the anthropogenic aspect that includes the absence of wastewater treatment plant thus increasing the DO levels, as well as the presence of pesticides and fertilizers in the groundwater coming from upper and surrounding regions of Zgharta and Koura.

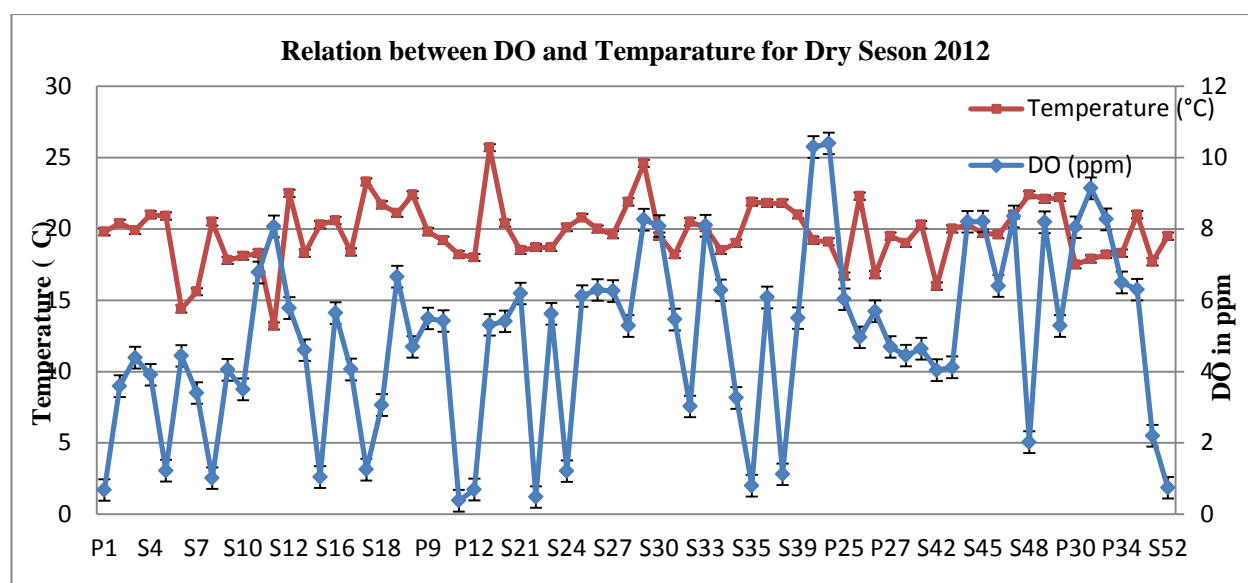


Figure 5.7 Temperature and DO Variations for Dry Season 2012

5.2.1.5 Conductivity

Conductivity is a measure of the ability of water to conduct an electrical current; it depends on the presence of dissolved ions. According to Lebanese and WHO standards, groundwater conductivity varies between 250 and 1500 $\mu\text{S}/\text{cm}$ in groundwater (WHO, 2006). The highest values seen in Figure 5.8 and 5.9 can be explained by several factors such as the high levels of inorganic compounds present due to the seawater intrusion in coastal regions (Zektzer I.S., 1973); or its closeness to the sea. To add up, the increase in temperature and TDS leads to an increase in conductivity values and most

importantly the general and different types of soils affect the values of conductivity. The high levels of conductivity are described in our case by the dominating Miocene limestone formation in the area as well as the quaternary deposits made mostly of sedimentary rock formed by a mixture of carbonates and clay minerals.

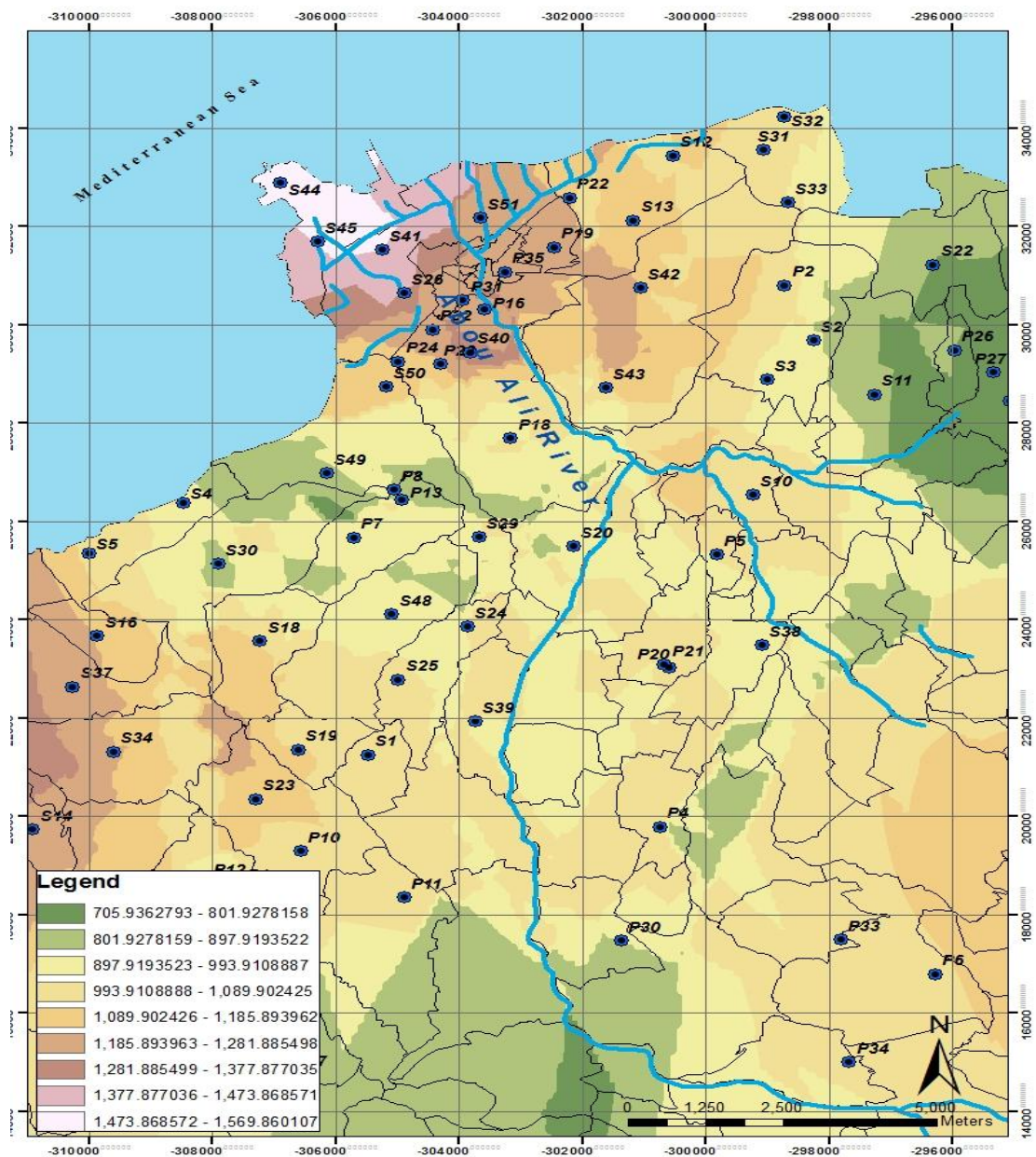


Figure 5.8 Conductivity Variation for Dry Season 2012 in $\mu\text{S}/\text{cm}$ (GIS)

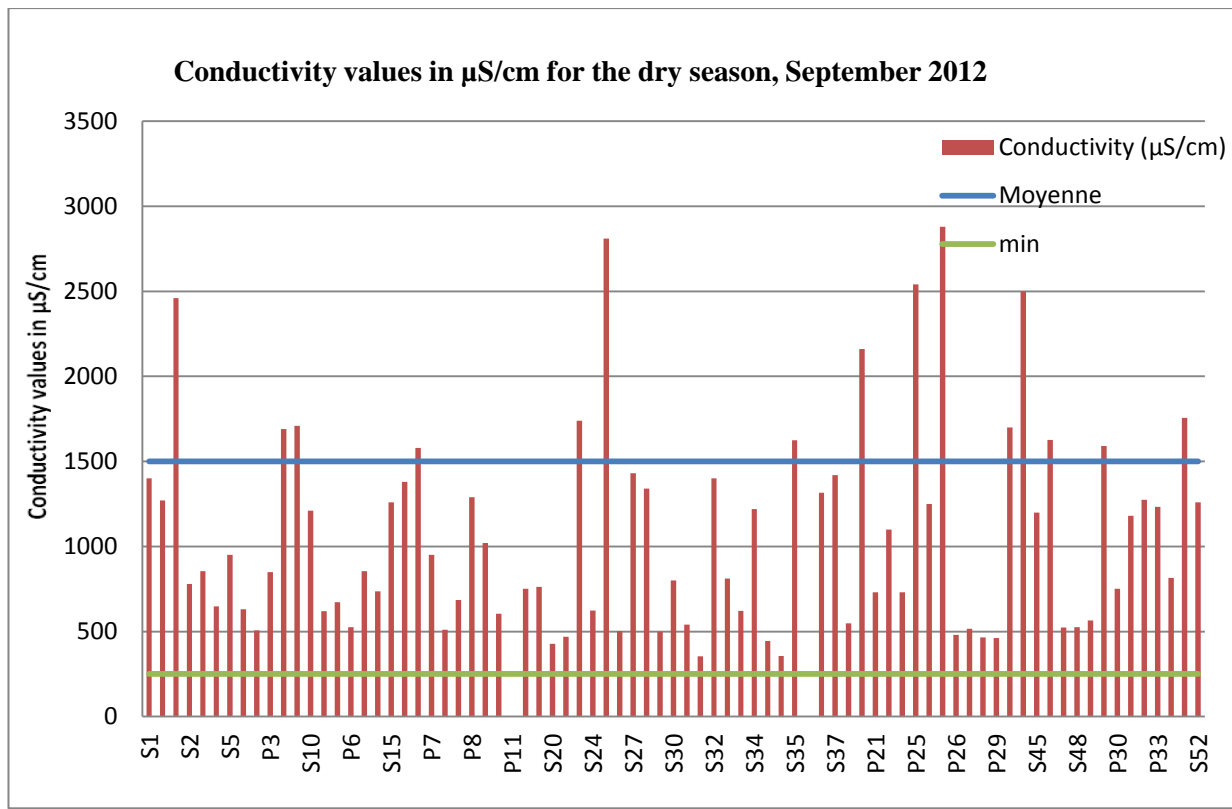


Figure 5.9 Conductivity Variation for Dry Season 2012 in $\mu\text{S/cm}$

5.2.1.6 Salinity

Salinization is a process that is becoming more and more familiar when it comes to groundwater. Agricultural activities such as irrigation could with time increase the salinity of the soil and therefore with the infiltration of the groundwater, these high levels of salts will end up in the water leading to its contamination. Another reason is the seawater intrusion that increases the salinity of the water, thus instead of having drinking water, groundwater will be mixed with sea water (Mijatović B., 2006). This is mostly the case of Tripoli and its surrounding. Moreover, other sites facing high salinity percentages superior to 0.05 %, implies that the geology of the land, such as the limestone affect the salinity of the land (Mehnert E., 1985). As the land has low porosity potential, many impurities will infiltrate the ground, thus increasing the salinity percentage. From this concept, Figure 5.10 and 5.11 presents the salinity values observed in the wet season 2013, which could be an indication of seawater intrusion. The closer to the coast, the higher is the salinity, based on this phenomenon; salinity reaches 0.6% in S35 (Hraiche) while it reaches 0.05% in Tripoli area such as in Tripoli 200 and many others. This is also due

to the presence of groundwater on very shallow elevation leading to easier intrusion of saline water. See Figure 5.12 that links salinity % to elevation of the sampling locations, it indicates that in addition to the geological structure of the soil, the water level affects the percentage of salts in the groundwater.

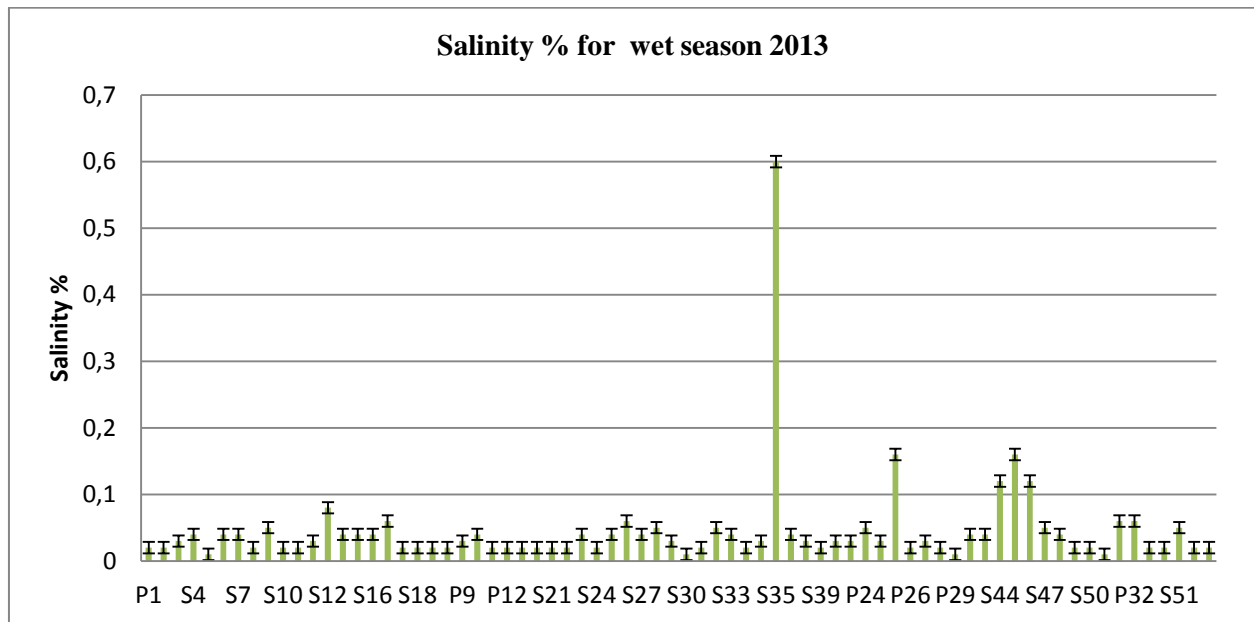


Figure 5.10 Salinity Variations for Wet Season 2013

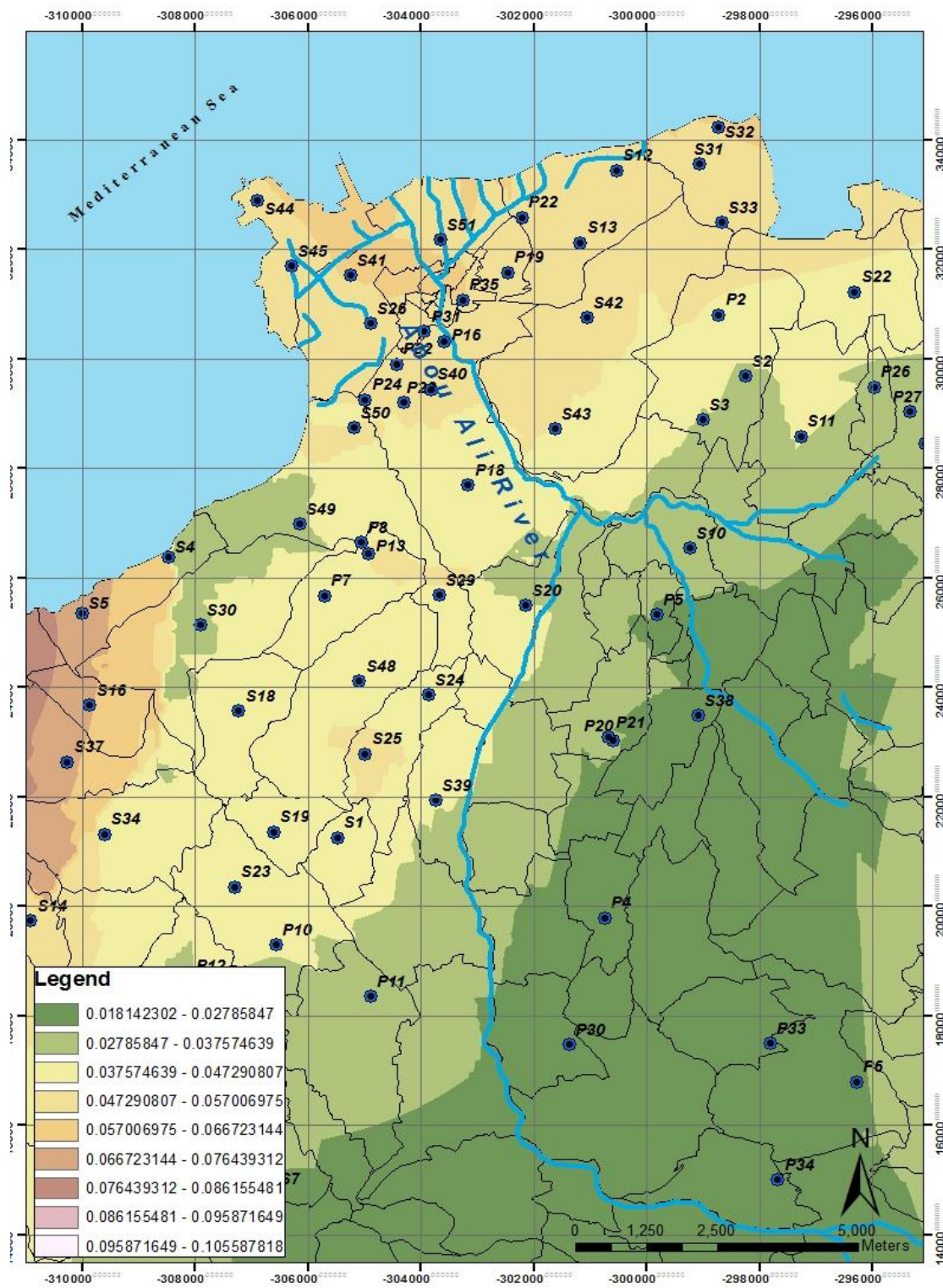


Figure 5.11 Salinity Variations in % for Wet Season 2013 (GIS)

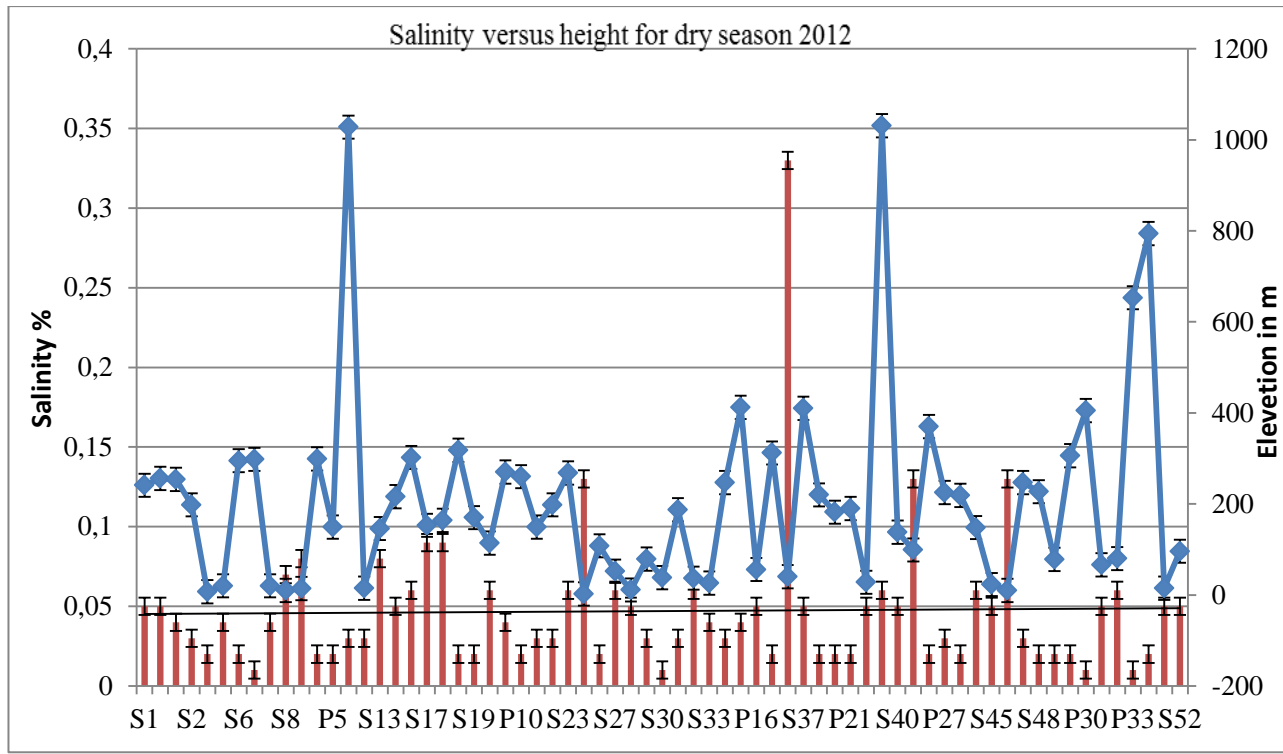


Figure 5.12 Salinity Versus Elevation for Dry Season 2012

5.2.1.7. Wilcox Method

The SAR (Sodium Adsorption Ratio) is a measure that assesses the danger posed by the existence of a given content in sodium it is calculated by the following formula:

$$SAR = \frac{Na^+}{\sqrt{(Ca^{2+} + Mg^{2+})}}$$

SAR values were calculated from Na^+ , Ca^{2+} , Mg^{2+} concentrations in mg / L.

Wilcox method is based on the combination of two methods: SAR and electrical conductivity. The following diagram (Fig 5.13) shows that these water samples are of a low saline content, and therefore can be used for agricultural uses.

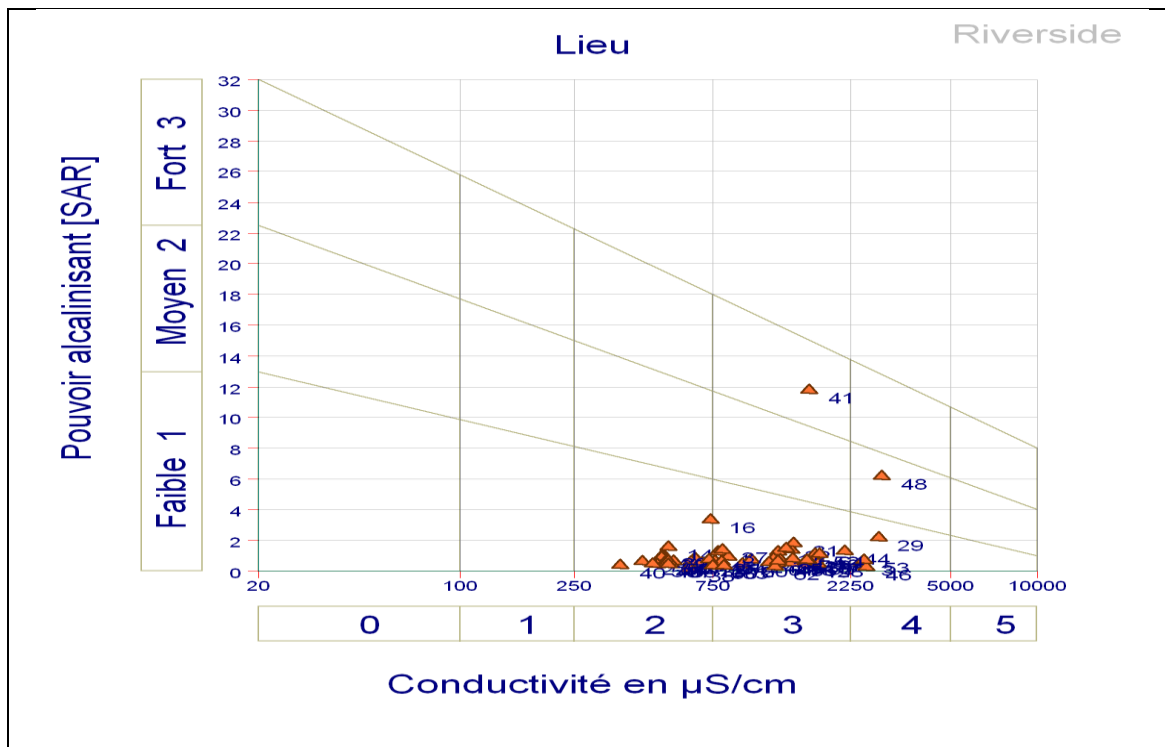


Figure 5.13 Wilcox Diagram for Dry Season 2012 (PhreeqC)

5.2.2 The Chemical Parameters

Representing all the chemical elements of the different samples on Piper diagram (see Figure 5.14) for the two major campaigns accomplished shows that the majority of the samples correspond to the poles characterizing traces of sulfated magnesium and sodium sulfate, hyper chlorinated calcium, and hyper sulfated and calcium samples, which is probably due to the dissolution of evaporates (Aquilina L., 2003). The facial distribution of 65 samples indicates the following:

- The chemical facials are predominant is chlorinated and sulfated calcium and magnesium heavily charged with Nitrate
- 04 samples faces chemically high sulfated – potassium concentrations
- 04 samples facials are chemically highly chlorinated and sulfated with calcium samples
- 2 samples facials are sodium chlorinated chemical samples
- Generally the origin of the dissolved salts in groundwater is due to the migrations of the minerals in the enclosing rock reservoir. Thus giving a general idea of the good correlation between the soil composition and the chemical elements in the groundwater.

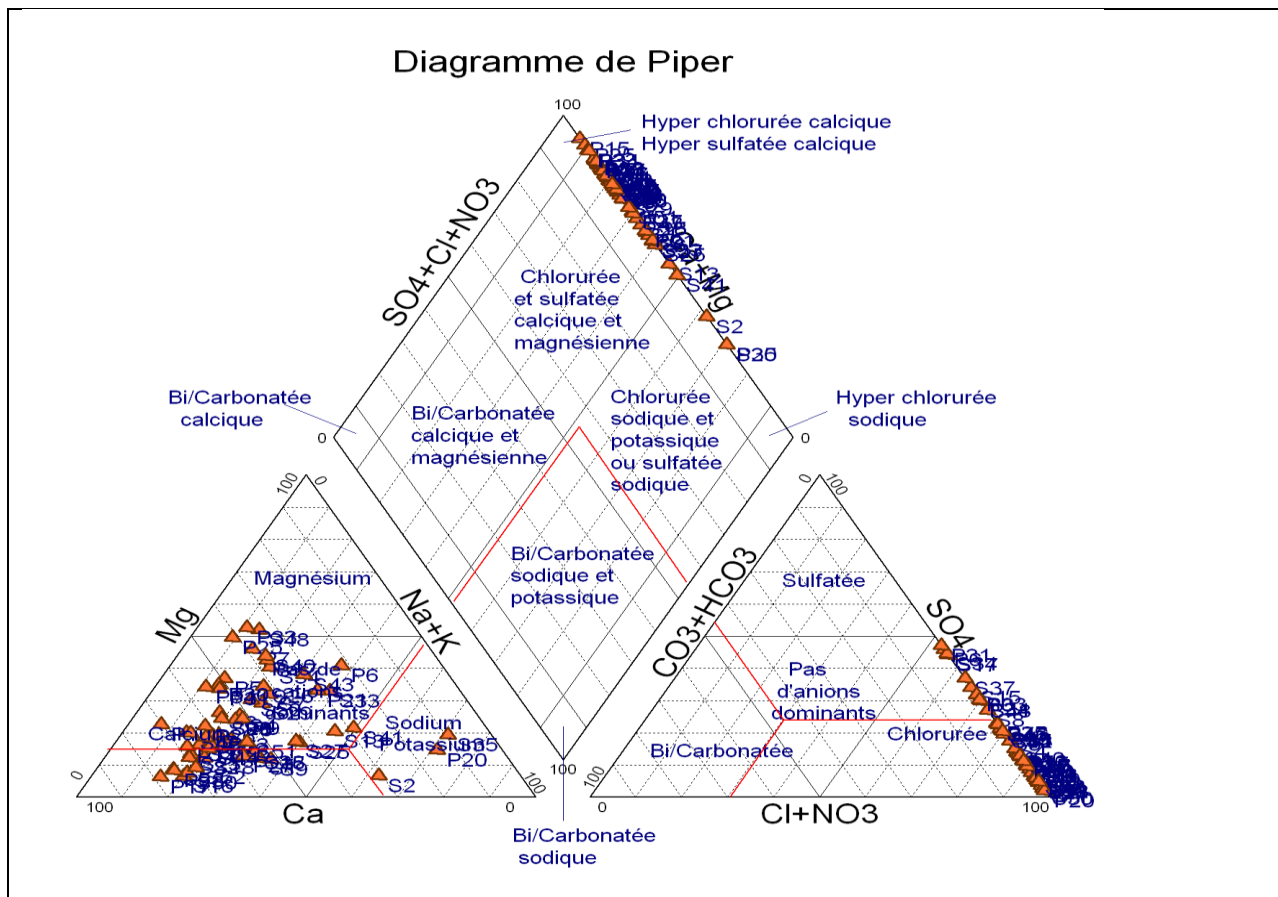


Figure 5.14 Piper Diagram for Dry Campain 2012

In order to study the origin of the chemicals in water , PhreeqC software determined after entering the measured on site data the hydrochemical properties of the water samples studied.to this we needed to know and summ up as seen in Table 5.3 the geolglical structures of the studied locations.In the upcoming step , the geological structure will be linked to the chemical parameters obtained from the campain to see the source of the ions prensent in the groundwater.

Table 5.3 Geological Structure of the Sampling Locations

Sample ID	Abbreviation	Geological formation	Sample ID	Abbreviation	Geological formation
Aaba (private)	S1	m2a	Deir Amar 1	S31	m2
Agrotech	P1	m2a	Deir Amar 2(kasser balade	S32	mL
Alma dawle	P2	m2a	Deir amar 3, Kassarar	S33	quaternaire, cone de deje
Alma 1	S2	mL	Ejed Ebrin	P15	
Alma 2	S3	m2a	Fih	S34	c6
Almoun 1	S4	m2a	Hawouz	P16	a quaternaire
Almoun 2	S5	m2a	Hellan	P17	mL
Amioun 1	S6	m2a	Hraiche 1	S35	m2
Amioun 2	S7	ml1	Hraiche 2	S36	m2
Anfe , Jrade	P3	q1	Jisr	P18	ad quaternaire
Anfeh 1	S8	q1	Kasser Mae	P19	a quaternaire
Anfeh 2	S9	qd	Kelhat	S37	c6
Arabech	S10	p	Kfarhat, Jedeide	S38	p
Arde	S11	p	Kfarkahel (private)	S39	m2
Arges	P4	c6	Kferzayna 1	P20	q
Asnoun	P5	m2b	Kferzayna 2	P21	q
Ayto	P6	c4	Malloule	P22	m2
Badawi 1	S12	a quaternaire	Manar	P23	a
Badawi 2	S13	m2	Massafi 7	P24	ad quaternaire
Badebhoon 1	S14	qd	Mazraet el Tefeh	P25	c4
Badebhoon 2	S15	c6	Mervat , Abou Samra	S40	m2
Balamand	S16	m2	Mervat , House	S41	a quaternaire
Barghon	S17	c6	Meryata 1- El Blat	P26	p
Barsa	P7	m2	Meryata 2	P27	a quaternaire
Batromine	S18	m2	Meryata 3	P28	a quaternaire
Bdebba	S19	m2	Meryata 4 (Youn Achech)	P29	a quaternaire
Bir Al- Ahdab (Ras Maska)	P8	m2	Mijdlaya 1	S42	mL
Bir Bechmezzine, Snouba	P9	m2	Mijdlaya 2	S43	mL
Bir Bterram	P10	m2	Mina 1	S44	a quaternaire
Bir El mazraa – Kferaka	P11	c6-e1	Mina 2	S45	a quaternaire
Bir Kfarhazir, (Ain el Baka	P12	m2	Minieh 1	S46	a quaternaire
Bir Ras Maska	P13	m2	Minieh 2 - Saleh Kheir	S47	p
Bkeftine	S20	m2	Nakhle (private)	S48	m2
Borj Hayodiyeh (Dawle W	S21	c6	Ras Maska , Private 1	S49	q
Boussit	S22	mcg	Ras Maska , Private 2	S50	m2
Bteram (private)	S23	m2	Raskifa	P30	c4
Btouratij 1 , Adnan Hassar	S24	m2	Saadoun	P31	a quaternaire
Btouratij 2 , Mokhtar	S25	m2	Sankari	P32	ad quaternaire
Chahal Building (Dam & F	S26	a quaternaire	Sebeel	P33	c4
Chekaa 1	S27	a quaternaire	Sereel	P34	
Chekaa 2	S28	ad quaternaire	Tripoli (200)	S51	a
Dahel El Ain , private 1	S29	q	Willey	P35	ad quaternaire
Dédde, Gaz Station	S30	m2	Zakroun	S52	m2
Deir Achach	P14	p			

Table 5.4 Saturation Index (SI) for Dry Season 2012

nom/Wateq	Libellé	Anhydrite	Aragonite	Calcite	Dolomite	Gypsum	H2(g)	H2O(g)	Si2(g)	Halite	Mirabilite	Natron	CO2(g)	Fluorite	Hydroxapatite
S1	Aaba (privat)	-2.49	-1.45	-1.31	-3.75	-2.25	-20.12	-1.62	-43.84	-7.15	-8.04	-10.81	-1.02	0.06	-0.26
P1	Agrotech	-2.75	-1.18	-1.04	-2.91	-2.49	-21.44	-1.62	-41.64	-7.61	-8.72	-10.97	-1.74	-1.18	0.46
P2	Alma dawle	-3.07	-1.1	-0.95	-2.94	-2.82	-22.1	-1.69	-41.22	-8.05	-9.27	-11.11	-2.19	-1.2	0.14
S2	Alma 1	-2.59	-0.85	-0.7	-2.51	-2.36	-21.64	-1.58	-40.75	-6.58	-8.3	-10.35	-1.7	-0.38	
S4	Almoun 1	-2.43				-2.18	-20.34	-1.88	-47.19	-7.4	-7.86			-0.95	-1.85
S5	Almoun 2	-3.18	-1.88	-1.74	-4.94	-2.91	-20	-1.68	-45.28	-8.08	-9.65	-12.17	-0.95	-1.15	-1.82
S6	Amoun 1	-2.28	-1.35	-1.2	-3.25	-2.04	-21.16	-1.68	-43	-7.74	-8.31	-11.18	-1.67	-0.91	1.12
S7	Amoun 2	-3.4	-1.54	-1.89	-3.39	-3.16	-20.58	-1.62	-43.41	-7.18	-9.07	-11.01	-1.21	-1.16	-2.17
P3	Anfe , trade	-2.42	0	0.15	-0.7	-2.25	-23.6	-1.61	-17.28	-7.35	-8.28	-9.66	-2.83	-0.83	
S8	Anfeh 1	-2.02	-1.32	-1.18	-3.35	-1.75	-20.58	-1.59	-42.94	-7.26	-7.93	-11.03	-1.17	-0.38	-0.52
S9	Anfeh 2	-1.82	-1.35	-1.2	-3.49	-1.6	-20.34	-1.53	-42.94	-6.35	-7.93	-11.24	-0.94	-0.6	-1.63
P4	Arges						-22.72	-1.64	-35.35				-2.07		
P5	Asnoun	-2.65				-2.46	-20.88	-1.6	-42.58	-7.87	-8.12			-1.13	0.96
P6	Ayto	-2.68				-2.43	-21.38	-1.78	-39.84	-7.59	-7.45			-1.16	4.18
S12	Badawi 1						-15.78	-1.68	-45.72						
S13	Badawi 2	-1.95	-1.23	-1.08	-2.89	-1.71	-21.06	-1.64	-42.67	-6.05	-6.57	-9.65	-1.57	-0.23	0.77
S15	Badebhoon	-2.39	-1.68	-1.53	-4.15	-2.16	-20.84	-1.61	-42.8	-7.43	-8.05	-11.14	-1.72	-1.36	-1.25
S16	Balamand	-3.09				-2.86	-20.34	-1.6	-43.76	-7.5	-9.54			-1.07	
S17	Barhon	-1.94	-1.2	-1.05	-3.11	-1.71	-20.64	-1.62	-43.27	-7.89	-8.41	-11.47	-1.07	-0.81	
P7	Barsa	-2.82				-2.59	-22.58	-1.55	-38.5	-7.96	-9.14			-0.69	5.1
S18	Batromine	-3.38	-1.51	-1.37	-3.92	-1.13	-20.56	-1.57	-42.78	-7.85	-9.72	-11.65	-1.19	-1.01	-1.8
S19	Bdebbi	-2.85	-1.22	-1.08	-3.21	-2.61	-21.14	-1.59	-41.91	-7.84	-9.26	-11.43	-1.53	-1.18	
P8	Bir Al- Ahdal	-2.73	-0.56	-0.42	-1.63	-2.51	-22.3	-1.54	-38.92	-7.62	-8.86	-10.48	-1.99	-1.23	3.02
P9	Bir Bechmez	-2.87	-1.72	-1.57	-3.93	-2.64	-20.38	-1.56	-43.04	-7.62	-8.97	-11.62	-1.29	-0.61	
P10	Bir Bteram	-2.94	-1.4	-1.26	-3.33	-2.71	-21.08	-1.57	-41.7	-7.88	-9.29	-11.54	-1.58	-1.26	0.05
P13	Bir Ras Mask	-2.91	-0.69	-0.55	-2	-2.69	-22.4	-1.48	-38.09	-7.74	-8.31	-10.87	-2.21	-1.38	5.29
S20	Bkeftine	-2.92	-0.99	-0.85	-2.55	-2.69	-21.78	-1.63	-41.06	-7.86	-8.12	-10.99	-1.9	-1.16	
S23	Bteram (priv	-3.22	-1.64	-1.5	-4.18	-2.99	-20.36	-1.59	-43.42	-8.07	-9.75	-12	-1.11	-1.19	
S25	Btourati 2, 1	-2.27	-1.41	-1.26	-3.39	-2.04	-20.88	-1.58	-42.28	-6.49	-7.44	-10.37	-1.53	-0.86	1.43

non/Azoo	Libra	Anhydra	Argonia	Calcia	Solenita	Gypsum	K2O	H2O(g)	CO2(g)	Li2O	Muscovita	Selen	CO2(g)	Fluorita	Hydroxapatite
525	Chrysotil 2	-1.27	-1.4	-1.35	-1.25	-2.67	-26.68	-1.58	-12.18	-6.11	-7.45	-10.25	-1.11	-6.38	1.0
526	Chrysotil 3	1.17				1.54	21.48	1.59	41.11	6.84	7.88			6.39	
527	Chrysotil 1	-1.37				-3.17	-26.13	-1.78	-42.38	-6.81	-7.18			-6.47	3.1
528	Chrysotil 2	-1.15	-1.5	-1.35	-1.25	-1.41	-26.13	-1.61	-41.14	-7.04	-7.85	-11.5	-1.11	-6.38	1.2
529	Calcit B. Als	-1.84	-1.36	-1.41	-1.75	-2.21	-21.62	-1.75	-43.88	-7.31	-8.45	-11	-1.16	-1.35	3.48
530	Calcit, Sup	-1.38				-1.14	-26.16	-1.66	-44.68	-7.71	-5.5			-1.75	-1.77
531	Carbact	-1.75				-2.45	-21.12	-1.69	-43.12	-8.01	-8.18			-1.5	
532	Carbact 2	-1.15	-1.5	-1.35	-1.25	-2.45	-21.12	-1.69	-43.68	-7.1	-9.11	-11.4	-1.15	-1.58	
533	Coronar 1	1.21				2.54	20.66	1.67	43.11	7.67	8.12			6.11	
535	Cjed Calc	-1.44	-0.67	6.35	-0.11	-2.21	-21.68	-1.55	-32.58	6.84	-1.7	-11.15	-2.15	-6.53	5
536	Flu	-1.25	-1.15	-1.11	-0.68	-0.17	-20.5	-1.03	-42.83	-7.41	-8.34	-11.5	-1.12	-4.58	
537	Fluor	-1.45	-0.81	-6.35	-0.58	-2.21	-22.64	-1.67	-41.68	-8.11	-9.71	-11.5	-1.14	-1.81	
538	Fluor 2	-1.1	-1.15	-1.11	-0.11	-1.51	-21.12	-1.56	-41.12	-4.71	-5.15	-8.38	-1.15	-1.15	3.61
539	Fluor	-1.15	-1.36	-1.11	-0.22	-2.15	-20.8	-1.58	-42.17	-7.48	-8.18	-11.2	-1.12	-6.38	
539	Fluor 2	-1.12	-0.98	-6.35	-1.16	-2.15	-21.62	-1.63	-41.18	-7.61	-8.12	-10.95	-1.78	-6.18	-1.21
540	Fluor 2	-1.96	-0.9	-6.75	-2	-3.71	-21.12	-1.68	-41.16	-6.31	-8.15	-10.03	-1.1	-6.55	
541	Fluor 2	-1.87				-1.61	-20.78	-1.63	-39.7	-7.11	-8.45			-6.77	1.8
542	Fluor 2	-1.86	-0.8	-6.35	-1.65	-2.81	-22.6	-1.68	-42.12	-6.41	-7.2	-10.05	-2.11	-6.15	
543	Fluor, Als	-1.17	-2.02	-1.11	-0.15	-2.81	-26.18	-1.59	-43.61	-7.31	-9.15	-12	-1.14	-1.5	-1.04
544	Fluor, Als	1.15	2.98	5.61	2.2	1.45	26.16	1.2	48.7	9.31	3.98	9.01	1.14	1.18	
545	Fluor 1-2	-1.16	-1.8	-1.11	-0.25	-1.21	-20.14	-1.68	-43.15	-8.11	-7.5	-11.18	-1.11	-1.48	3.25
547	Fluor 2	-1.5				-1.14	-21.16	-1.66	-43.98	-7.48	-8.5			-1.58	
548	Fluor 2	-1.14	-0.46	-1.1	-0.45	-1.41	-21.75	-1.61	-41.75	-8.61	-4.15	-10.78	-1.11	-6.38	
549	Fluor 2	-1.11	-1.75	-1.11	-0.68	-2.17	-20.16	-1.65	-41.11	-7.41	-8.15	-11	-1.14	-1.11	-2.21
549	Fluor 2	1.15				2.14	22	1.58	42.67	7.64	8.75			1.4	1.2
549	Fluor 2						26.74	1.67	42.42						
549	Fluor 2	-1.84				-1.61	-19.85	-1.68	-43.11	-7.7	-8.12			-6.15	-1.5
547	Fluor 2-1	-1.96	-0.7	-6.35	-2.15	-1.71	-22.62	-1.68	-43.12	-7.71	-8.34	-10.55	-2	-6.15	
548	Fluor 2	-1.1				-2.51	-21.2	-1.52	-43.15	-7.91	-8.2			-1.11	3.98

Table 5.4 and 5.4 bis indicate the Saturation index (SI) of the dry sampling campaign of year 2012 with the use of PhreeqC software. The SI permits to specify the sources of the ions, if it is naturogenic or anthropogenic. To do so, allow us to define SI (Mineral saturation index,), the Saturation index SI, is an index showing whether water will tend to dissolve or precipitate a particular mineral. If the value is negative, this means that the mineral is dissolved therefore the chemicals will seep from the rock to the water, however if SI is positive, this indicates that the minerals will precipitate and therefore the chemicals will percolate from the water to the rock. A value of zero is seen when the water and mineral are at chemical equilibrium with each other. The saturation index (SI) is calculated by comparing the chemical activities of the dissolved ions of the mineral (ion activity product, IAP) with their solubility product (K_{sp}). In equation form, $SI = \log(IAP/K_{sp})$

Factors affecting ground water chemistry:

If the geological formation is to be discussed, it is obvious from the geological map of the region and the table 5.3 that the soil is composed mainly from sedimentary rocks, either it is marl, clay, flint (silex) or poudingues. All of these rocks contain Calcium Carbonate CaCO_3 with additional compounds depending on the layer in which the H_2O is available. It could be MgCO_3 ; SiO_2 etc... (Drever, 1997). The chemical composition of ground water varies because of many complex factors that change with depth and over geographic distances. Groundwater quality can be affected by the composition and solubility of rock materials in the soil or aquifer, water temperature, partial pressure of carbon dioxide, acid-base reactions, oxidation-reduction reactions, loss or gain of constituents as water percolates through clay layers, and mixing of ground water from adjacent strata. (Hess J.W, 1993). The extent of each effect will be determined in part by the residence time of the water within the different subsurface environments (Bakalowicz M. E. H.-H., 2008). Rain and snow is the major sources of recharge to groundwater. They contain small amounts of dissolved solids and gases such as carbon dioxide, sulfur dioxide, and oxygen. As precipitation infiltrates through the soil, biologically-derived carbon dioxide reacts with the water to form a weak solution of carbonic acid. The reaction of oxygen with reduced iron minerals such as pyrite is an additional source of acidity in ground water. The slightly acidic water dissolves soluble rock material, thereby increasing the concentrations of chemical constituents such as calcium, magnesium, chloride, iron, and manganese. As ground water moves slowly through an aquifer the composition of water continues to change, usually by the addition of dissolved constituents (Freeze and Cherry, 1979). A longer residence time will usually increase concentrations of dissolved solids. Because of short residence time, groundwater in recharge areas often contains lower concentrations of dissolved constituents than water occurring deeper in the same aquifer or in shallow discharge areas. Dissolved carbon dioxide, bicarbonate, and carbonate are the principal sources of alkalinity, or the capacity of solutes in water to neutralize acid. Carbonate contributors to alkalinity include atmospheric and biologically-produced carbon dioxide, carbonate minerals, and biologically-mediated sulfate reduction (Clair N. Sawyer, 1994). Non carbonate contributors to alkalinity include hydroxide, silicate, borate, and organic compounds. Alkalinity helps to buffer natural water so that the pH is not greatly altered by addition of acid. The pH of most natural groundwater in North Lebanon is neutral to slightly alkaline. Calcium and magnesium are the major constituents responsible for hardness in water. Their presence is the result of dissolution of carbonate mineralssuch as calcite and dolomite (Kankjoo K., 2005). The weathering of feldspar and clay is a source of sodium and potassium in ground water. Sodium and chloride are produced by the solution of halite (sodium chloride) which can occur as grains disseminated in unconsolidated and bedrock

deposits. Chloride also occurs in bedrock cementing material, connate fluid inclusions, and as crystals deposited during or after deposition of sediment in sea water. High sodium and chloride levels can result from upward movement of saltwater from deeper bedrock in areas of high pumping (Goldenberg et al, 1985). Cation exchange is often a modifying influence of ground-water chemistry. The most important cation exchange processes are those involving sodium -calcium, sodium-magnesium, potassium-calcium, and potassium-magnesium. Concentrations of sulfide, sulfate and manganese depend on geology and hydrology of the aquifer system, amount of dissolved oxygen, pH, minerals available for solution, amount of organic matter, and microbial activity. Mineral sources of sulfate can include pyrite, gypsum, barite, and anhydrite. Sources of manganese include manganese carbonate, dolomite, and limestone. Sources of fluoride in bedrock aquifer systems include fluorite and fluorapatite. Groundwater containing detectable concentrations of fluoride has been found in a variety of geological settings. Natural concentrations of nitrate-nitrite in groundwater originate from the atmosphere and from living and decaying organisms. High nitrate levels can result from leaching of industrial and agricultural chemicals or decaying organic matter such as animal waste or sewage (Jahangir M.M.R., 2012).

By linking geology with the chemical results of our campaigns with the use of PhreeqC software the end result was the determination of the different minerals in the water. The following were determined:

• Anhydrite CaSO₄
• Aragonite CaCO₃
• Calcite CaCO₃
• Dolomite MgCa (CO₃)₂
• Gypsum CaSO₄ 2(H₂O)
• Halite NaCl
• Mirabilite Na₂SO₄ (10H₂O)
• Natron Na₂CO₃ (10H₂O)
• Fluorite CaF₂
• Hydroxyapatite Ca(PO₄)₃ (OH)

The end result was the SI that had positive and negative values that were summarized in the following figure 5.15

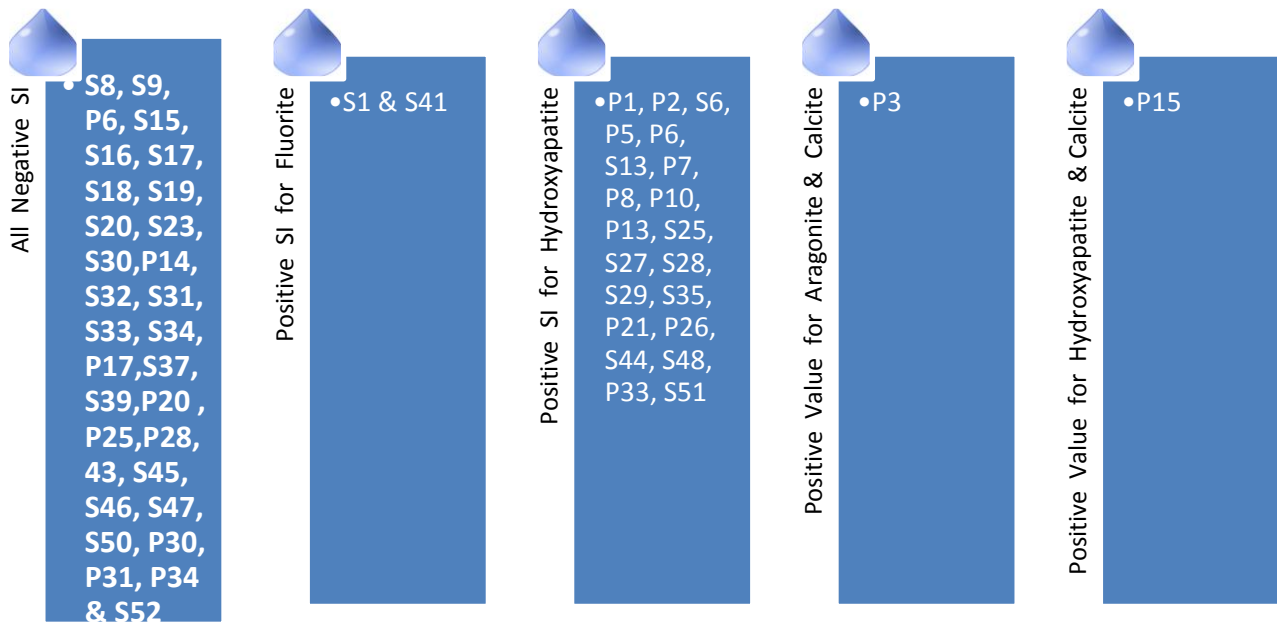


Figure 5.15 Saturation Index of Dry Season 2012

5.2.2.2 Phosphate

According to the Lebanese Standard, the amount of Phosphate is set as 1mg/L. Phosphates sources diverge from urban activities such as laundry or commercial cleaning, to agricultural fertilizers. Figure 5.16 presents the variation of phosphate in the studied locations for dry season 2012. As observed, most samples' concentrations exceed the standard. In general high amount of Phosphate are related to the presence of septic system effluent, (USGS, January 2012) detergents and fertilizers. Therefore a certain amount of Phosphate is beneficial to the health of individuals but any excess could lead to some health problems.

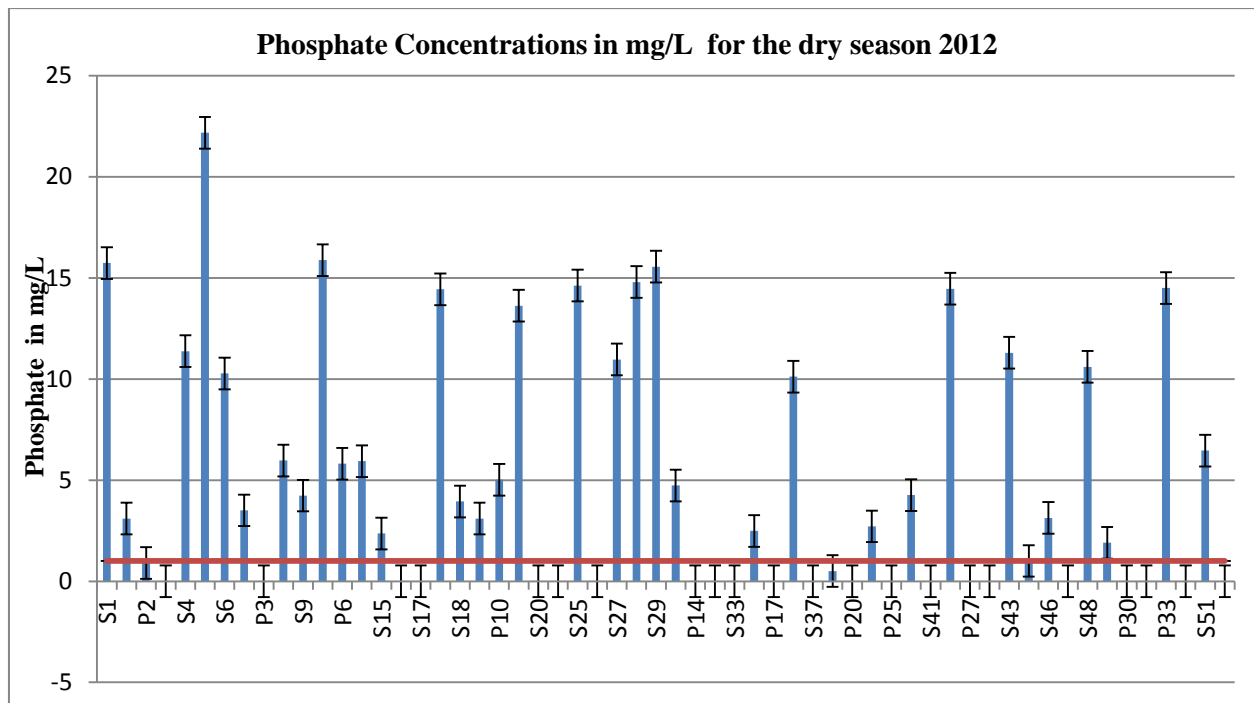


Figure 5.16 Phosphate Variations for Dry Season 2012

5.2.2.3 Fluoride and Fluorite

The determination of Fluorides has become extremely important due to public health concerns. The current MCL set by the Lebanese Standards and WHO are respectively 1.5mg/l and 2 mg/l. We notice that some of the fluoride levels are under the standards and could be explained by the geology of the area. These safe results indicate that citizens using these sources as drinking water are not confronted to problems like Fluorosis. But the high values seen in either wet or dry season are due to corrosion of household plumbing, runoff and infiltration of chemical and erosion of natural deposits .Fig 5.17- 5.18.

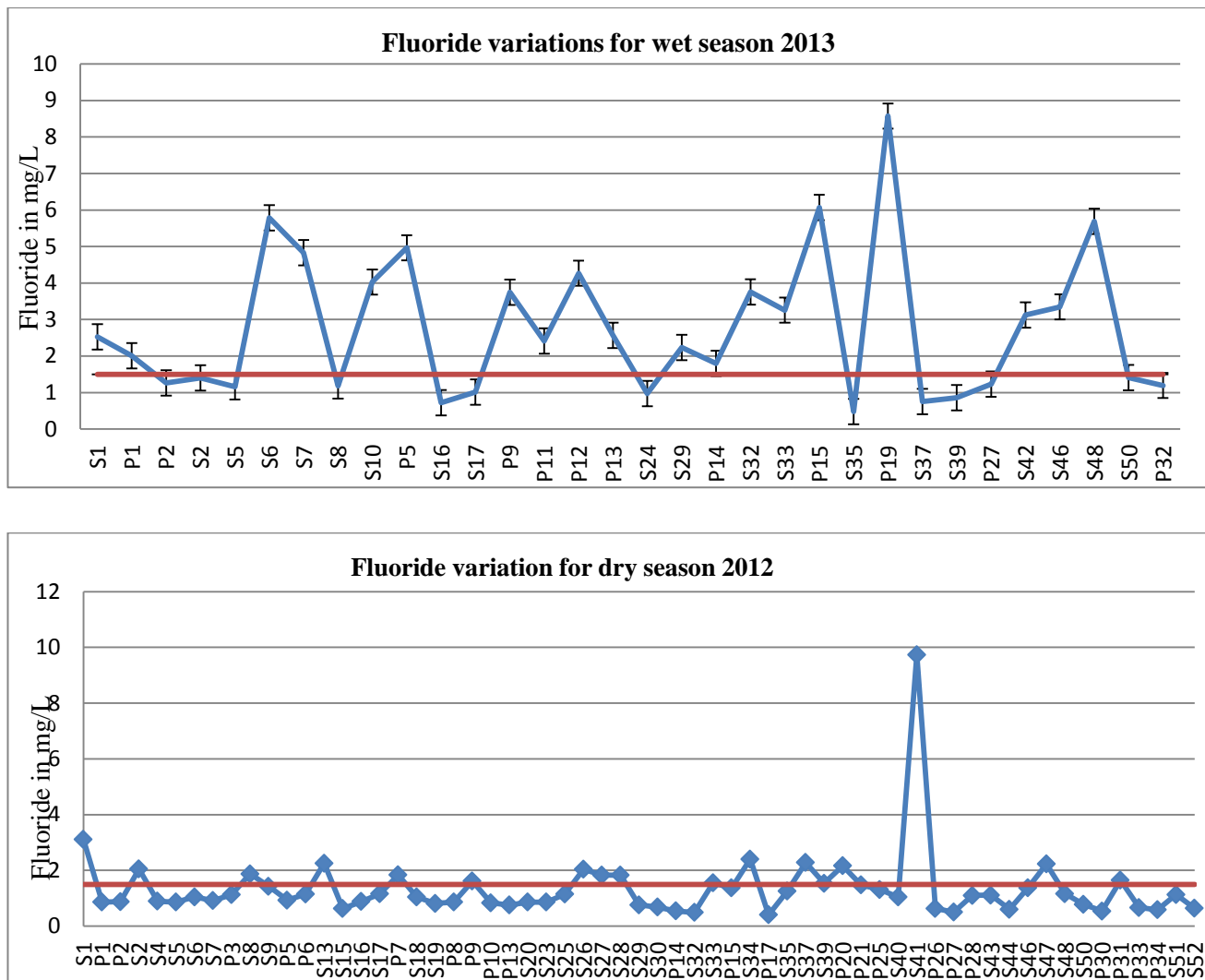


Figure 5.17 & 5.18 Variations of Fluoride Concentrations for Wet and Dry Season

Fluorite CaF_2 the Naturogenic contamination of Fluorite CaF_2 is due to :

Fluoride minerals in fluorite rock that are not readily soluble in water under normal pressure and temperature. But under alkaline conditions and range of specific conductivity between 750 and 1750 $\mu\text{S}/\text{cm}$, dissolution rate of fluorite minerals increases. This is seen in the graph 5.19, wherever we have a high conductivity concentration, a high concentration of Fluoride is seen. It can be explained by the longue residence time in a fractured aquifer containing fluorite rich rocks enhances the fluoride levels in the groundwater. Overall, the natural concentration of fluoride in groundwater depends on the geological, chemical and physical characteristics of the aquifer, the porosity and acidity of the soil and rocks, the surrounding temperature, the action of other chemical elements, depth of the aquifer.

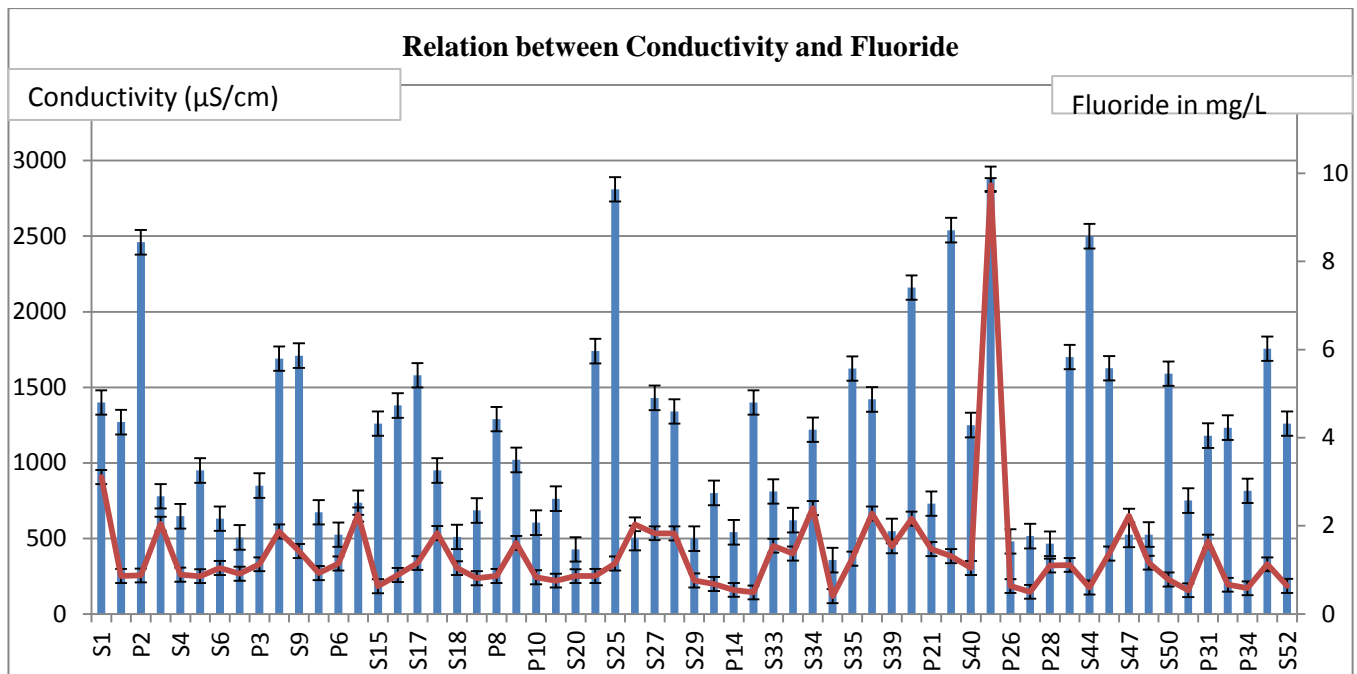


Figure 5.19 Relationships Between Conductivity and Fluoride for Wet Season 2013

The Anthropogenic factor that affect mostly fluoride is phosphate containing fertilizers that add up to the fluoride content in soil and groundwater (Gi-Tak Chae, 2007). It is evident that phosphatic fertilizers such as superphosphate, potash and Nitrogen Phosphorous Potassium (NPK) ; contain remarkable amounts of fluoride . In addition another chemical that exhibits a positive relationship with fluoride; is sodium (See fig 5.20). The highest value noticed was on the coastline of Tripoli that is basically due to seawater intrusion., it can be seen in S27, S28 & S29 circled in orange. While some excess amounts of Fluoride circled in green can explained by the geology and the neighboring activities surrounding these areas.

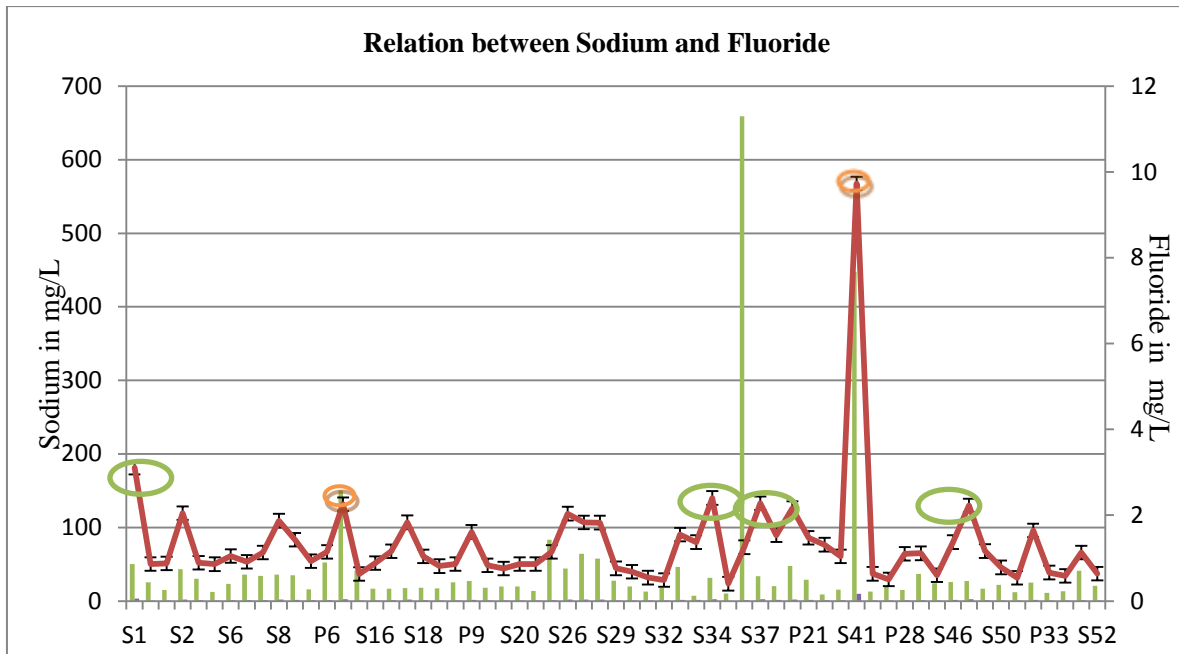


Figure 5.20 Relationship Between Sodium and Fluoride for Dry Season 2012

5.2.2.4 Bromide

The determination of the concentrations of bromide in groundwater has become essential nowadays it is considered as essential nutrients for the growth of organisms. According to the Lebanese Standard, the amount of Bromide is set as 0.34mg/L. Bromide source from urban activities, figure 5.21 presents the variation of phosphate in the studied locations. As observed, most of the samples exceed the standard in the exception of the some locations, which has set a value lower than the standard. In general high amount of Bromide are related to the presence of septic system effluent, detergents and fertilizers.. (Hem, 1992) In addition, the high levels of Bromide could be explained by their location and by the activities occurring around as well as the fact that Bromine is found in seawater and exists as the bromide ion. Therefore the high peaks seen in Tripoli mostly seen Figure 5.21 could be explained by both the sea factor as well as the urbanization aspect.

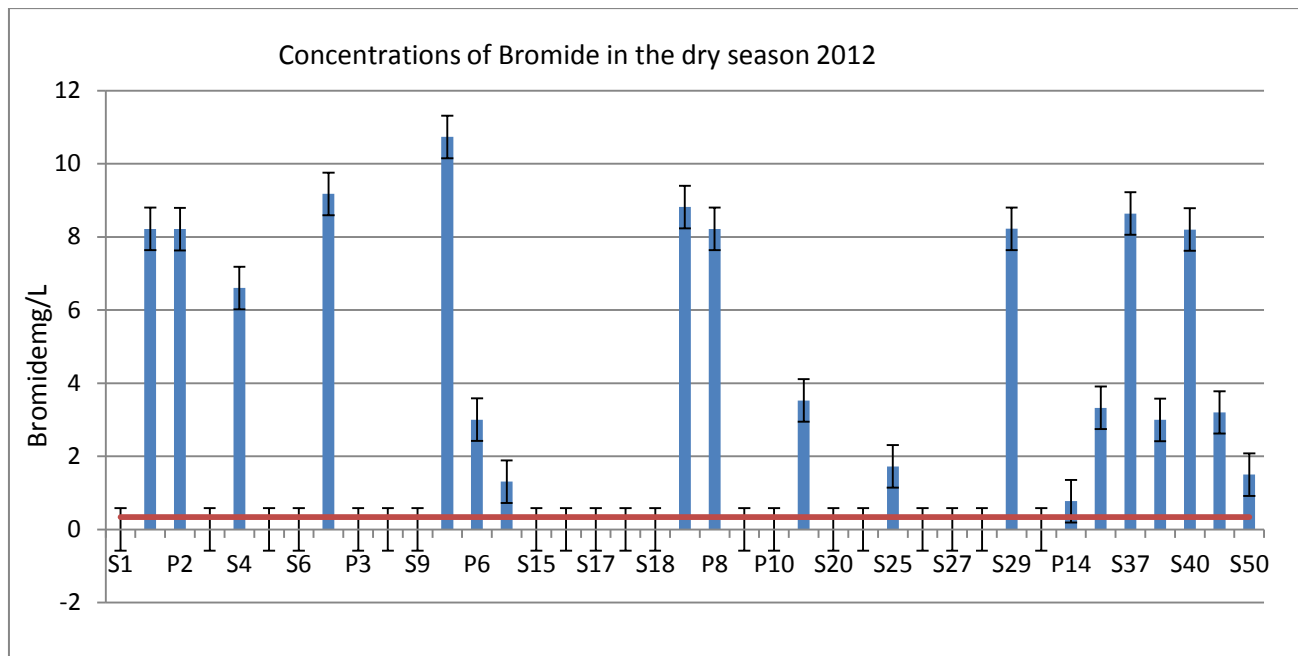


Figure 5.21 Concentrations of Bromide in the Dry Season 2012

5.2.2.5 Nitrate Nitrite and Ammonium

The two most important compounds that result from the reaction of the nitrogen gases available in the atmosphere and rainwater are nitrate (NO_3^- , an anion) and ammonium (NH_4^+ , a cation). In the atmosphere major sources of nitrate include reactions caused by lightning, photochemical oxidation in the stratosphere, chemical oxidation of ammonia, soil production of NO by microbial processes, and fossil fuel combustion (Gaillard J.-F, 1995). Anthropogenic activities have a major impact on the levels of these compounds that are found in both rain water and the atmosphere. Many of the major sources of nitrate and ammonium come from the use and production of fertilizers and the burning of fuels, as listed above.

Nitrate that leaves the atmosphere can be converted back into elemental nitrogen, through the process of denitrification (Jahangir M.M.R., 2012). This often takes place in the soil through the activity of bacteria (such as E.Coli and Coliform) that reduce the nitrate. Ammonium can undergo the process of nitrification, which is an oxidation reaction that converts it to nitrate. Through this mechanism, the nitrogen in the ammonium ion is released back into the atmosphere (Berner, 1987). After the conversion from elemental into nitrogenous ions in solutions of rainwater, the nitrogen in these compounds can be exhausted back to the atmosphere by the pathways previously described, thus completing the cycle. (Jahangir M.M.R., 2012) According to WHO and Lebanese Standards, the MCL for Nitrate is 10 mg/L, whereas for Nitrite is 0.1 mg/l. Analysis for Nitrate and Nitrite is essential to confirm the presence of pollutants in groundwater and identify whether the water could be used for drinking purposes. Nitrate occurs naturally in mineral

deposits, soils, seawater, the atmosphere, and biota. Major sources of Nitrate or Nitrite in drinking water include fertilizers, manure, irrigation of lawns and gardens, sewage, and some other domestic and industrial activities (Salbu E., 1995). In the samples locations, nitrate concentrations in Figure 5.22 and Figure 5.23 are less than the MCL. Geology of the ground affects the groundwater, if the ground is capable of filtrating most of the chemicals; this is due to the low porosity of the ground that is allowing the infiltration of these chemicals into their groundwater. Despite the protection measures applied to protect the drinking water, percolation occurs due to geological factor or agricultural factor that enhances the use of fertilizers containing mostly Nitrate and Nitrite used for olive culture quite famous in the area (Burkartaus M. R., 2008). The amount of Nitrate is lower than the standard, which means that this compound is within the standard and is of no harm; whereas Nitrite concentrations are all greater than the standard, which implies the side effects of Nitrite pollution on humans (see Figure 5.24). To the previous factor, the lack of active waste water treatment plants and the presence of septic tanks in which leaching all leads to infiltration of contaminants into the groundwater. In addition, seawater intrusion and increasing urbanization also have an important role here too, because the sewage of Tripoli city is discharged in the sea; as a consequence when intrusion occurs, sewage mixes with groundwater and directly contaminates water with nutrients and elements such as Nitrate, Nitrite, and Sulfate (Parello F., 2007). Another factor is the condensation of Ammonium in the dry season (mainly due to the excess of sewage discharge) that will be transformed with time to Nitrite than Nitrate; for that reason; we observe a consecutive diminution with seasons of Nitrite .

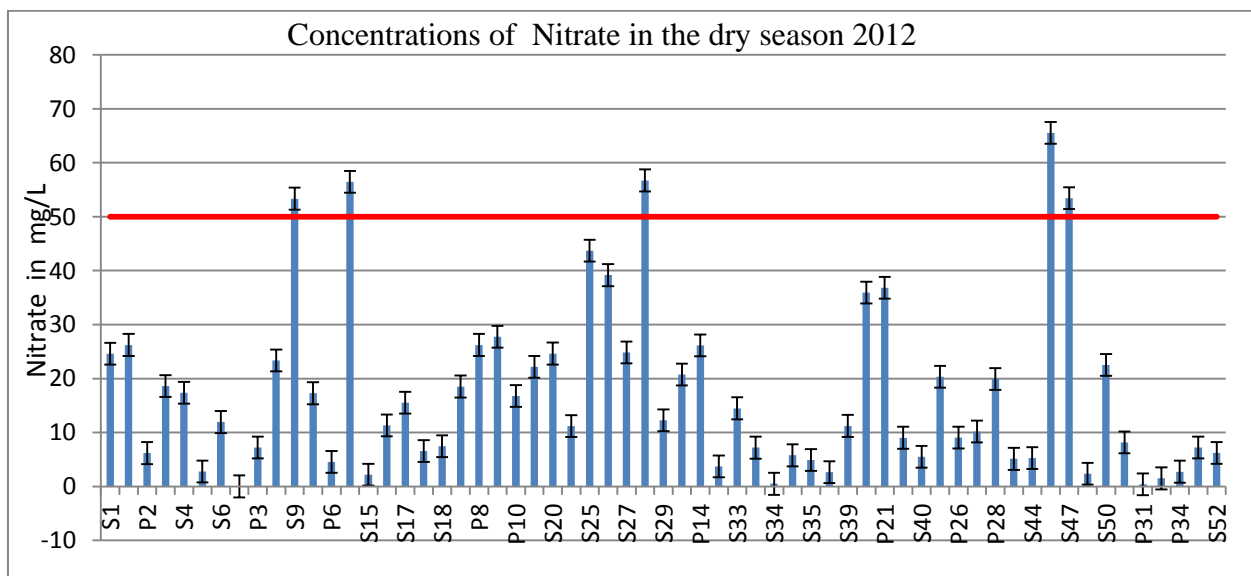


Figure 5.22 Nitrate concentrations in Dry Season 2012

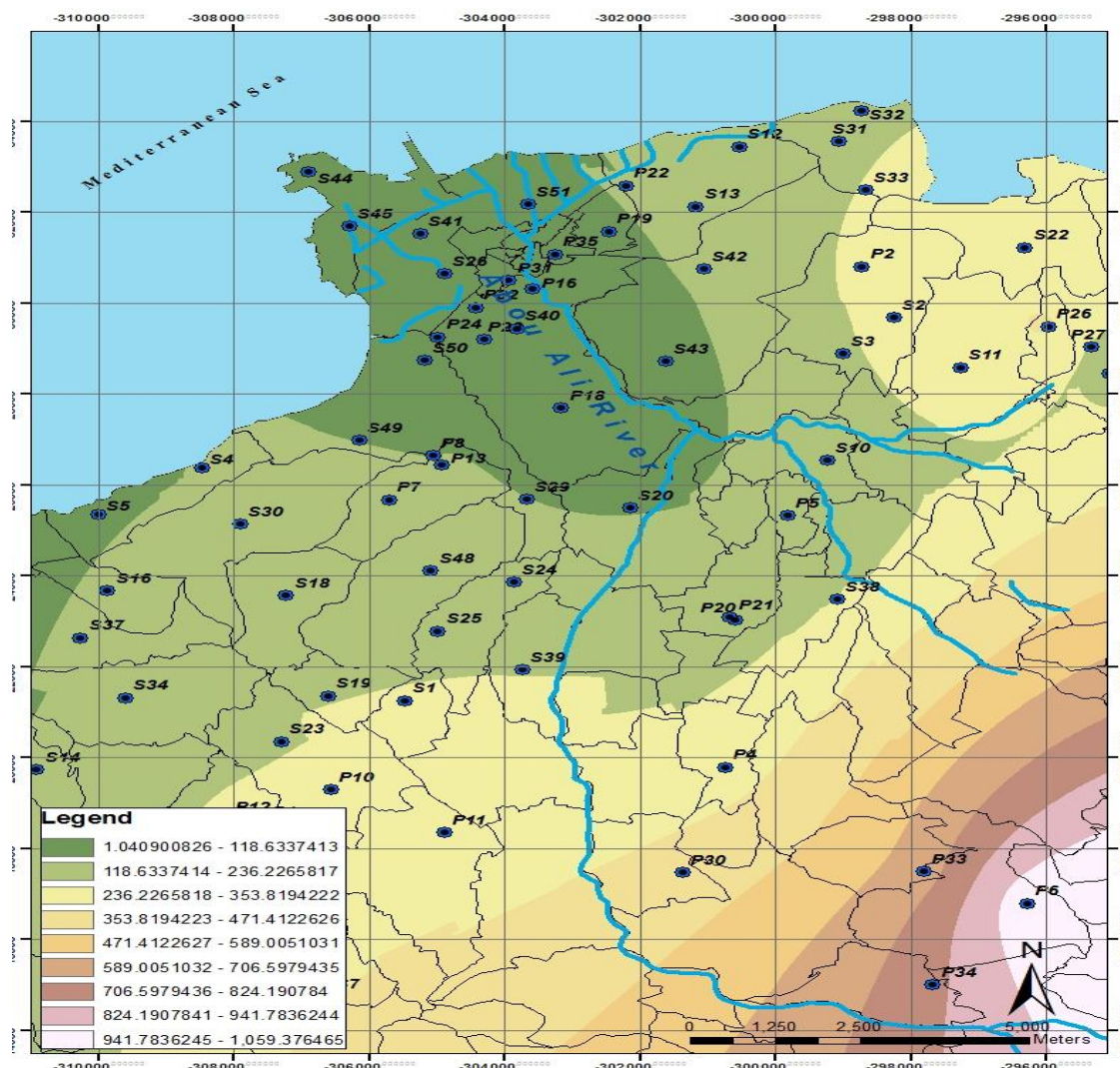


Figure 5.23 Nitrate Concentrations in mg/L for Wet Season 2013 (GIS)

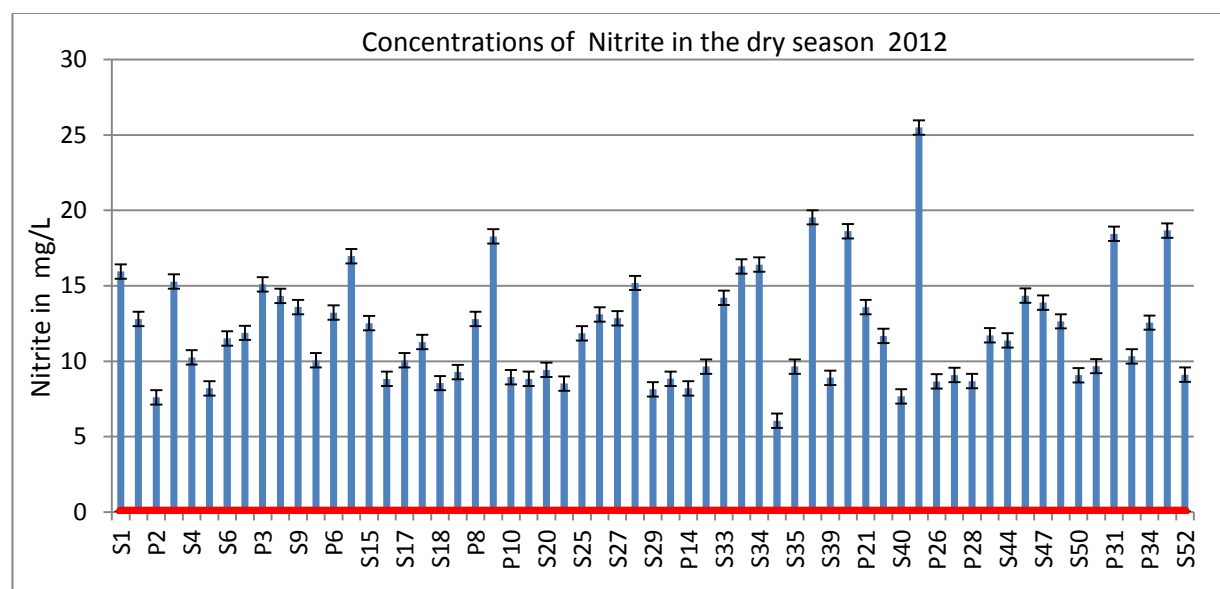


Figure 5.24 Nitrite Concentrations for Dry Season 2012

As for Ammonium and by examining the data, it is observed that the average ammonium is much higher in dry season than in wet season, and only few locations have ammonium concentrations in the dry season. In addition the values seen in dry season are higher than those of the Lebanese standard (0.5 mg/L) and those of dry period. Refer to graphs in figure 5.25 and 5.26. The average level in wet season was 0.7 mg/L whereas the average for dry was of 4.8 mg/L. This is due to the interrelation mentioned previously with Nitrate that shows greater concentration as well in the dry season. As explained formerly, the presence or absence of this element is related to naturogenic and anthropogenic factors. The plants take nitrogen from the soil by absorption through their roots in form of nitrate and ammonium and since our geological structure is most commonly formed in limestone, dolomite, and chalk, i.e. Karst features, therefore percolation to the groundwater is definite (Lindenbaum J., 2012) (Tekin E., September 2012). Consequently, explaining the high levels seen in dry and not in wet season.

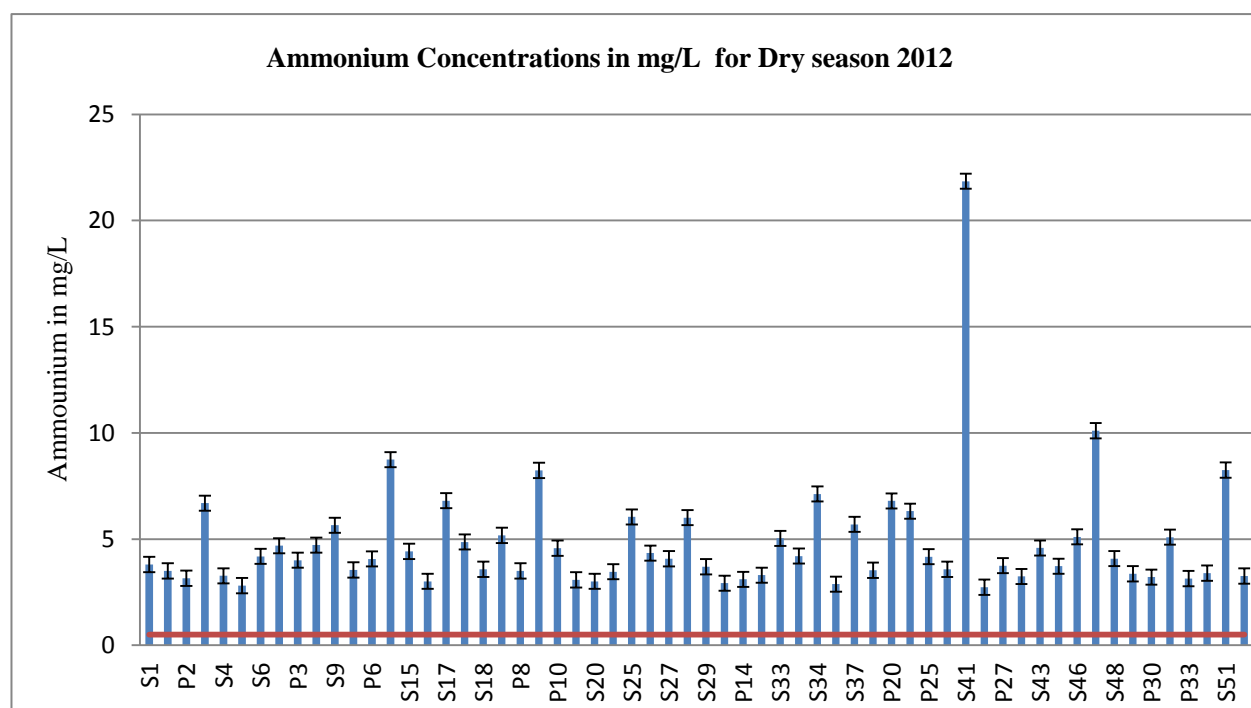


Figure 5.25 Ammonium Concentrations in mg/L for Dry Season 2012

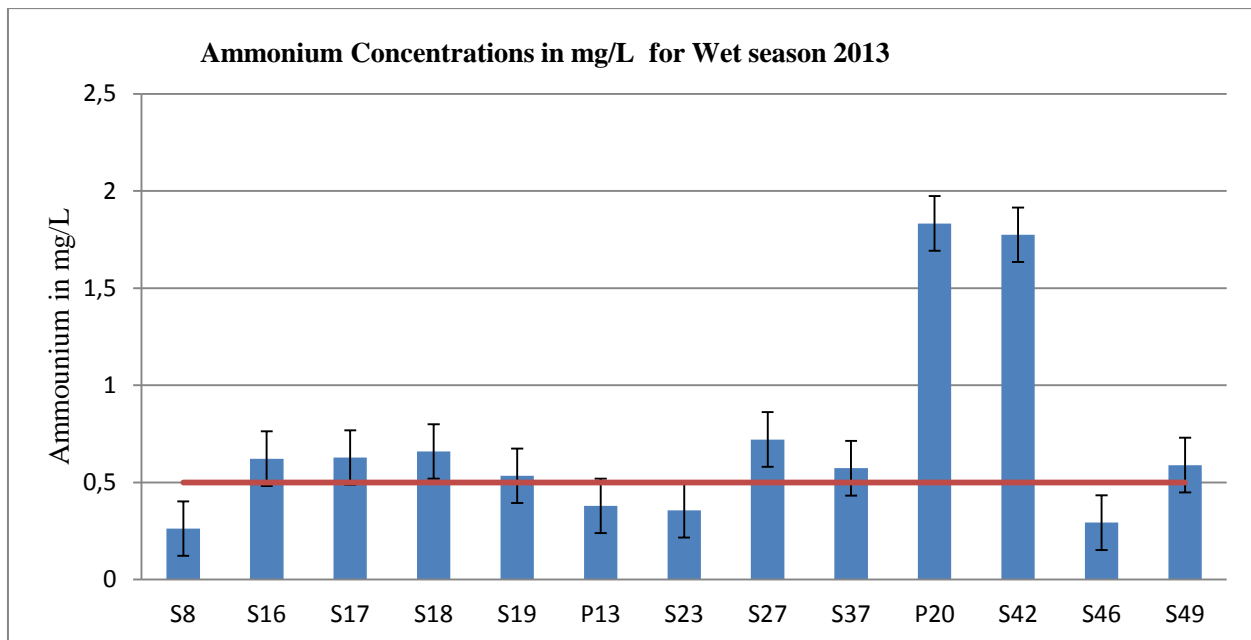


Figure 5.26 Ammonium Concentrations in mg/L for Wet Season 2013

5.2.2.6 Chloride

In general, Chloride concentrations in groundwater are associated with the presence of salts originating from many sources. According to the WHO and Lebanese Standards the MCL of Chloride is 25 mg/l. Therefore, from Figure 5.27 and 5.28, it is noticed that the levels of chloride are almost all above the standard. The results obtained could be explained by many factors (Eriksson, 1969). For instance in the case of Tripoli, over-pumping from wells implies that the rate of water abstraction is higher than the rate of recharge, leading to groundwater mining (Grassi & Cortecchi, 2007). Moreover, the city is driven by drilling countless number of wells as a source of drinking water, consequently the chloride concentrations in coastal groundwater is attributed to seawater intrusion (El-Fadel, Tomaszewicz, & Abou Najm, 2012). This problem has reached a new scale of severity over the last two decades due to the expansion of coastal agglomerations. Rural-urban migration and population growth have increased demand for water all along the coast, and most particularly in Tripoli. In Zgharta and Koura, a new urban development in the villages is occurring which adds the need for water demand and increases the pumping of groundwater. As a result, the increase of extraction of water from deeper ground leads to its infiltration from upper lands. In the absence of strict enforcement of borehole specifications and permissible abstraction rates, the salt-freshwater interface shifts inland (Sayyed J- A., 2011); this explains the higher levels of chloride. In the locations where moderate amounts were seen it was often attributed to fertilizer applications.

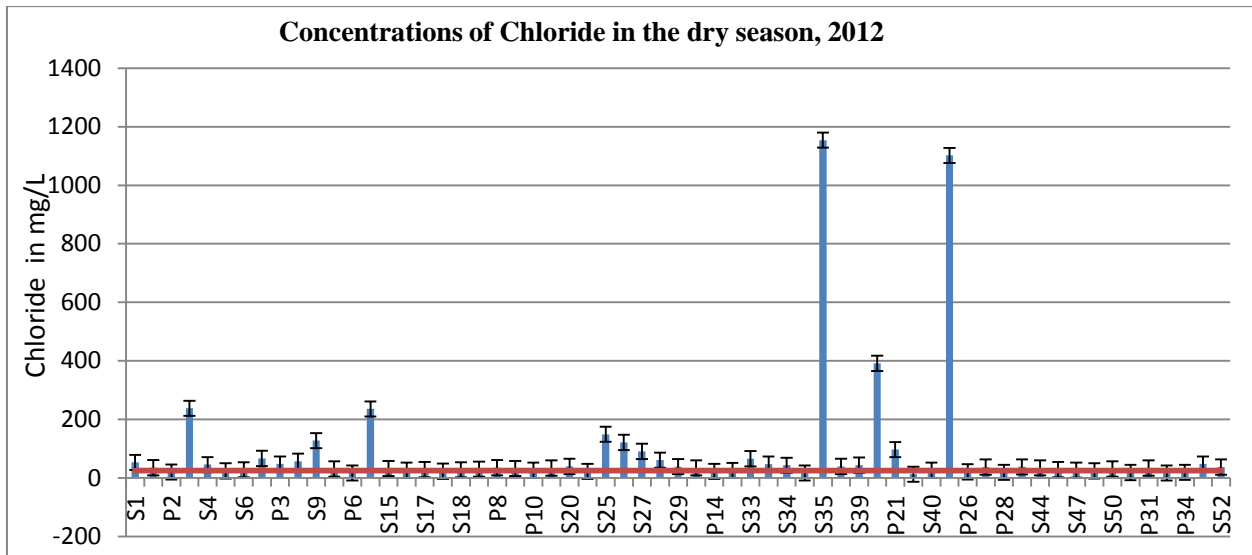


Figure 5.27 Chloride Concentrations for Dry Season 2012

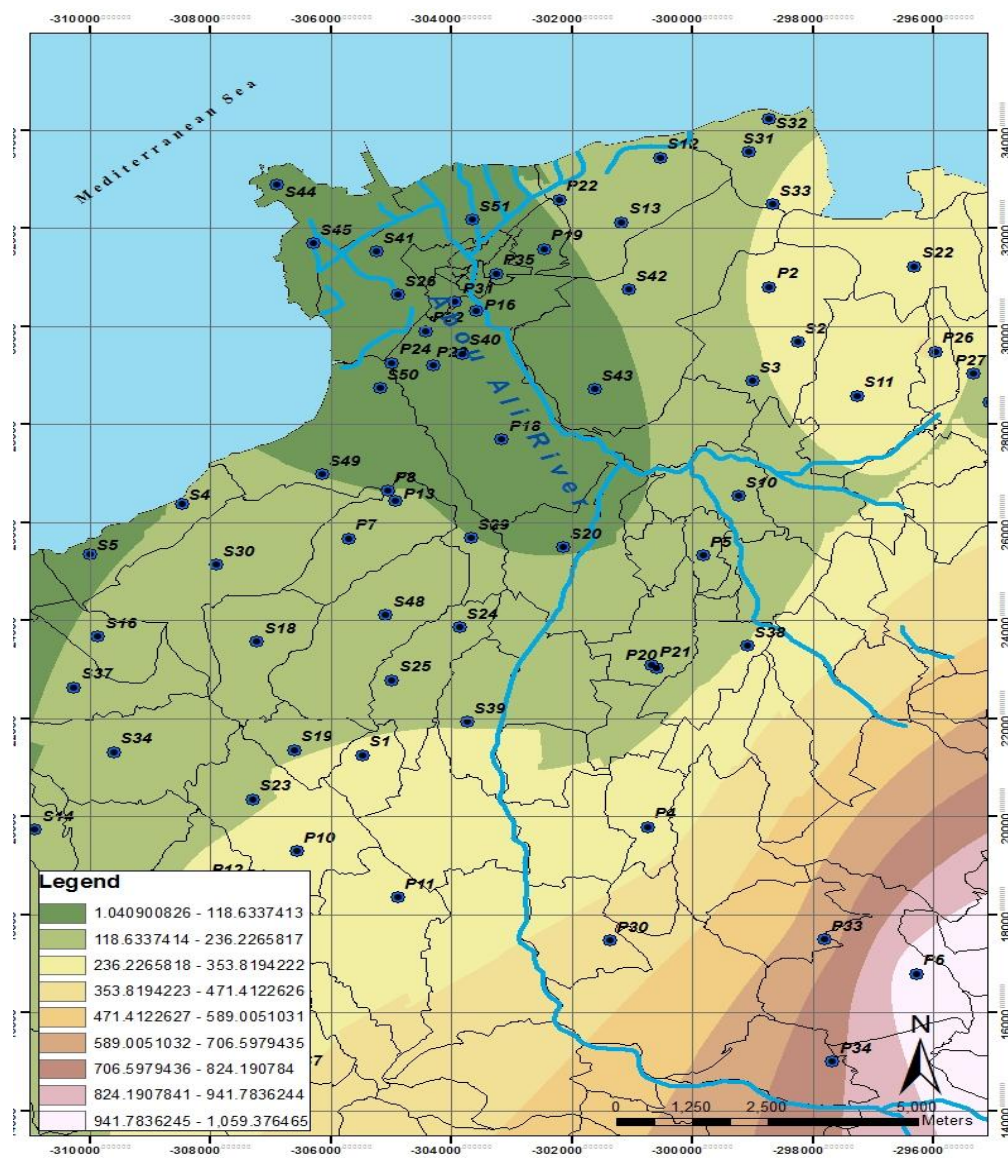


Figure 5.28 Chloride Variations for Wet Season 2013 (in mg/L)

5.2.2.7 Hardness, Calcium and Magnesium

The most common problem associated with groundwater is hardness. It is a term relating to the concentrations of certain ions in water, particularly magnesium and calcium, and is usually expressed as an equivalent concentration of dissolved calcite (CaCO_3) (Ribolz O., 1993). In hard water, the ions of concern may react with soap to produce an insoluble residue. These metallic ions may also react with negatively charged ions to produce a solid precipitate when hard water is heated (Freeze and Cherry, 1979). Hard waters can thus consume excessive quantities of soap, and cause damaging scale in water heaters, boilers, pipes, and turbines. Many of the problems associated with hard water, however, can be mitigated by using water-softening equipment. Durfor and Becker (1964) developed the following classification for water hardness that is useful for discussion purposes: soft water, 0 to 60 mg/L (as CaCO_3); moderately hard water, 61 to 120 mg/L; hard water, 121 to 180 mg/L; and very hard water, over 180 mg/L. A hardness level of about 100 mg/L or less is generally not a problem in waters used for ordinary domestic purposes (Hem, 1992). Lower hardness levels, however, may be required for waters used for other purposes. For example, Freeze and Cherry (1979) suggest that waters with hardness levels above 60-80 mg/L may cause excessive scale formation in boilers. Ground water in the Miocene aquifer of North Lebanon can be generally characterized as hard to very hard in the Durfor and Becker hardness classification system. The measured hardness level is below 180 mg/L (as CaCO_3) in fewer than 10 percent of the ground-water samples. The following graphs of calcium and magnesium concentrations in our sampled groundwater are presented below. Because calcium and magnesium are the major constituents responsible for hardness in water, the highest levels of these ions generally occur in groundwater with high hardness levels. As expected, the concentrations found in the studied area are high due to the contact of water with certain rocks and minerals. Calcium and magnesium are washed from rocks and subsequently ends up in water. These minerals include limestone and gypsum mostly for calcium; as for minerals containing they include dolomite calcium magnesium carbonate; $\text{CaMg}(\text{CO}_3)_2$, Aragonite $\text{CaMg}(\text{CO}_3)$

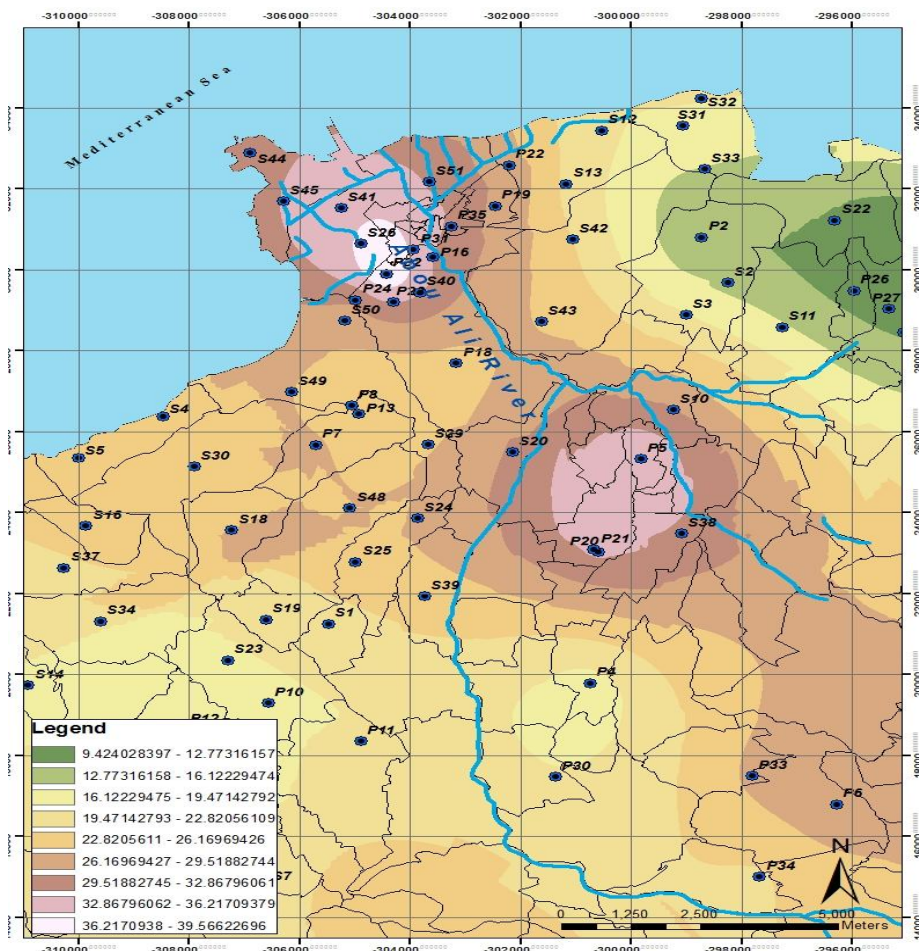
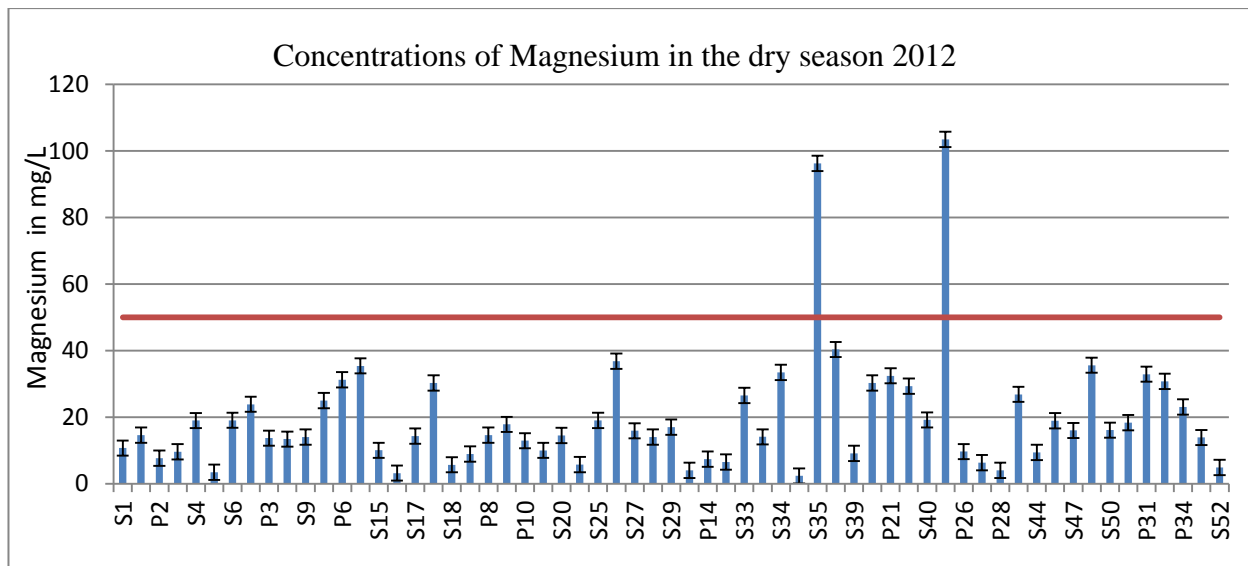


Figure 5.29 Concentrations of Magnesium (in mg/L) for Dry Season 2012

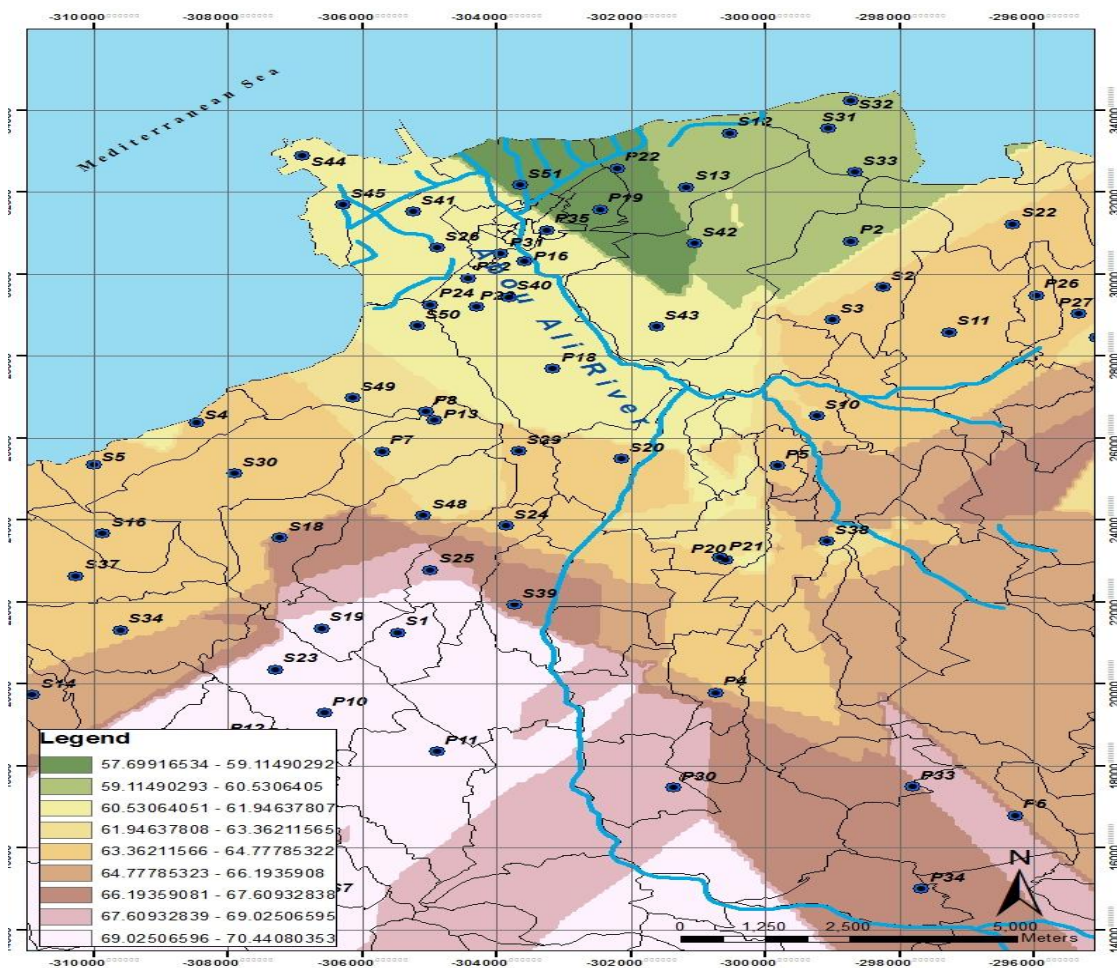
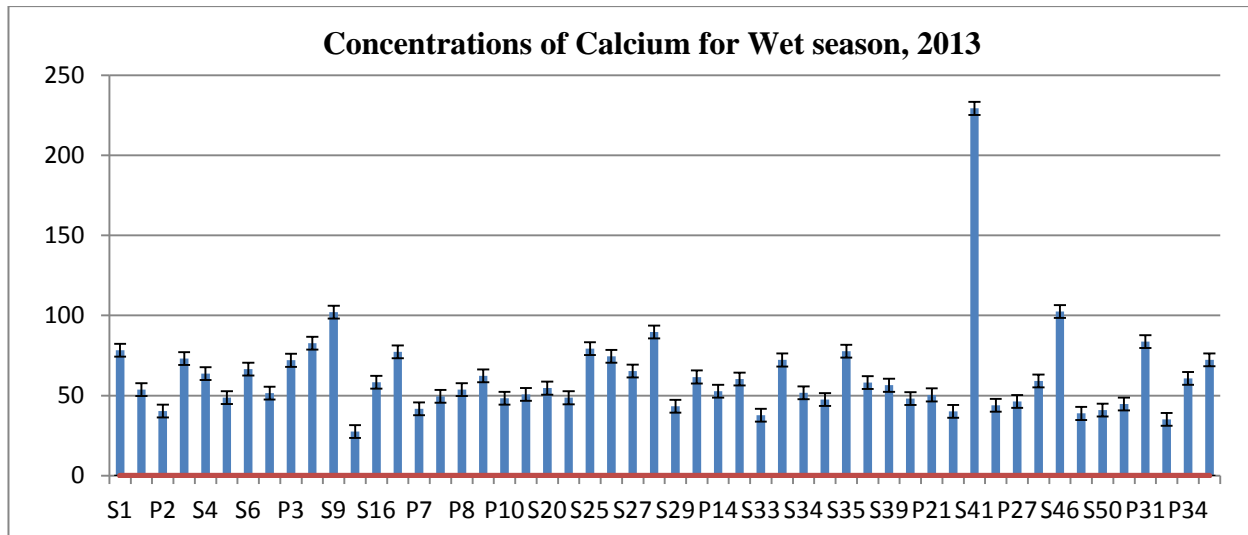


Figure 5.30: Concentrations of Calcium (in mg/L) for Wet Season 2013

5.2.2.8 Sodium and Potassium

- The source of potassium in groundwater samples is likely due to silicate minerals and evaporates deposits of gypsum. In addition, sulfate releases considerable amount of potassium into the groundwater. The presence of potassium is highly due to agricultural activities; mainly potassium nitrate, are popular synthetic fertilizers. 95% of commercially applied potassium that is added to synthetic fertilizers (Sayyed J- A., 2011). To this, saltwater intrusion plays an important factor in the increase of potassium concentration since seawater contains about 400 ppm of potassium. See Figure 5.33.
- As for Sodium, it is washed out from rocks and soils, ending up in our groundwater. Therefore the groundwater samples contain significant amounts of sodium depending on geological conditions and wastewater contamination or even agricultural activities such as sodium nitrate. Sodium compounds are due to the geological formation containing halite, mirabilite, natron etc... As seen in figure 5.31 and 5.32 ; all sodium values are all below standard in the exception of S35 and S41 that are in coastal and thus inducing the possibility of sea water intrusion

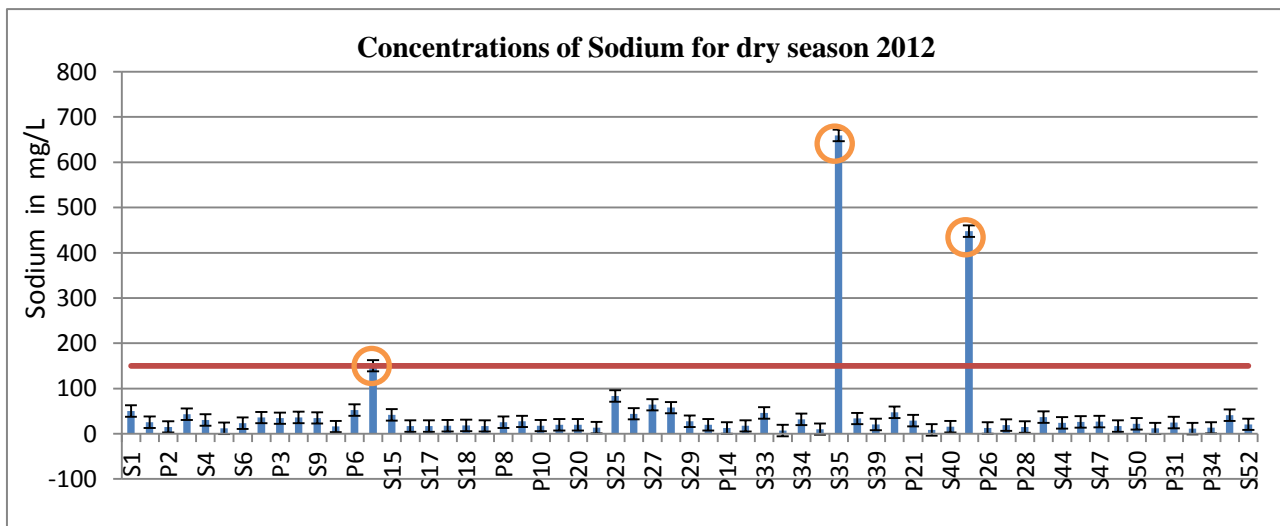


Figure 5.31 Concentrations of Sodium for Dry Season 2012

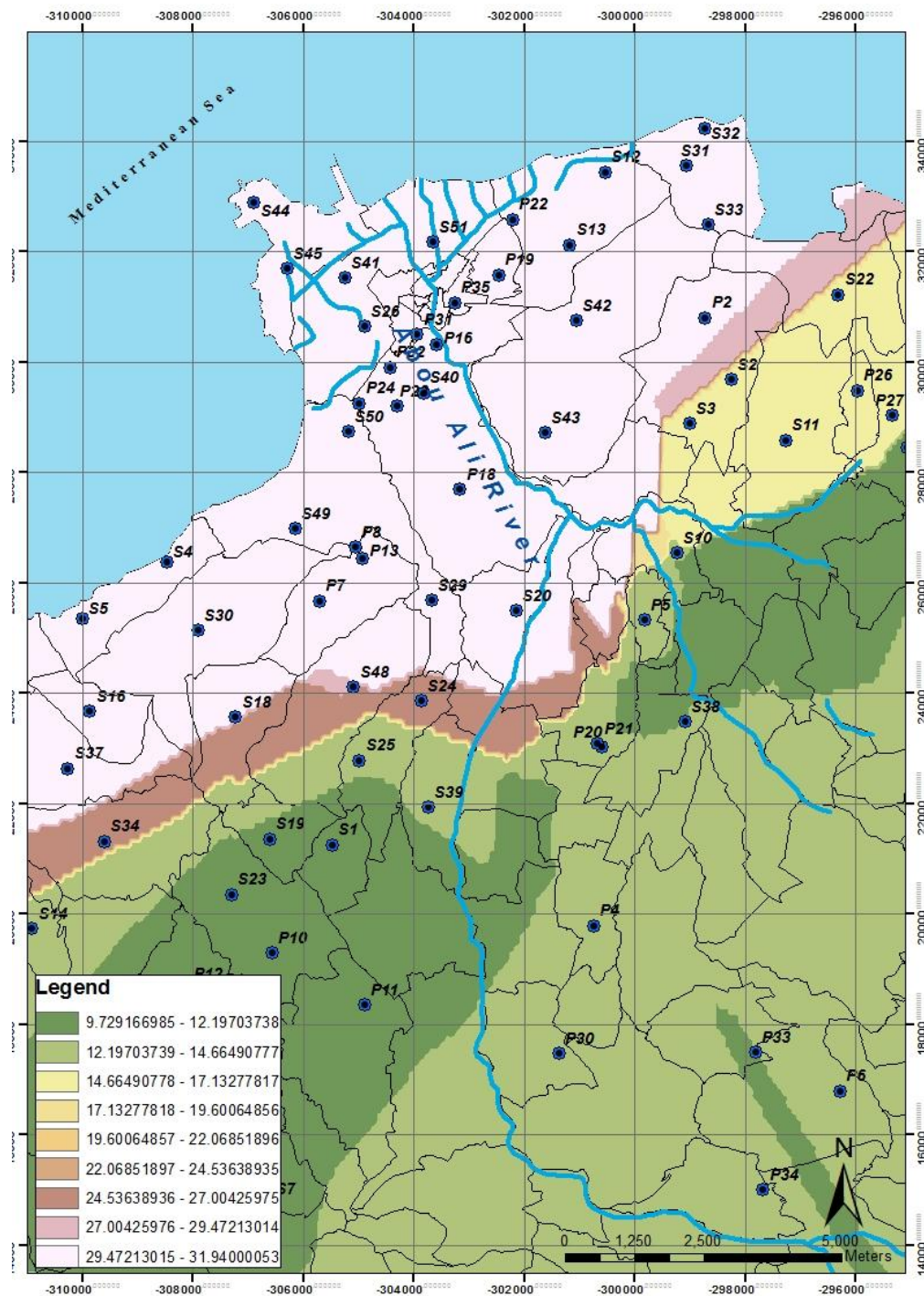


Figure 5.32 Sodium Variations for Wet Season 2013

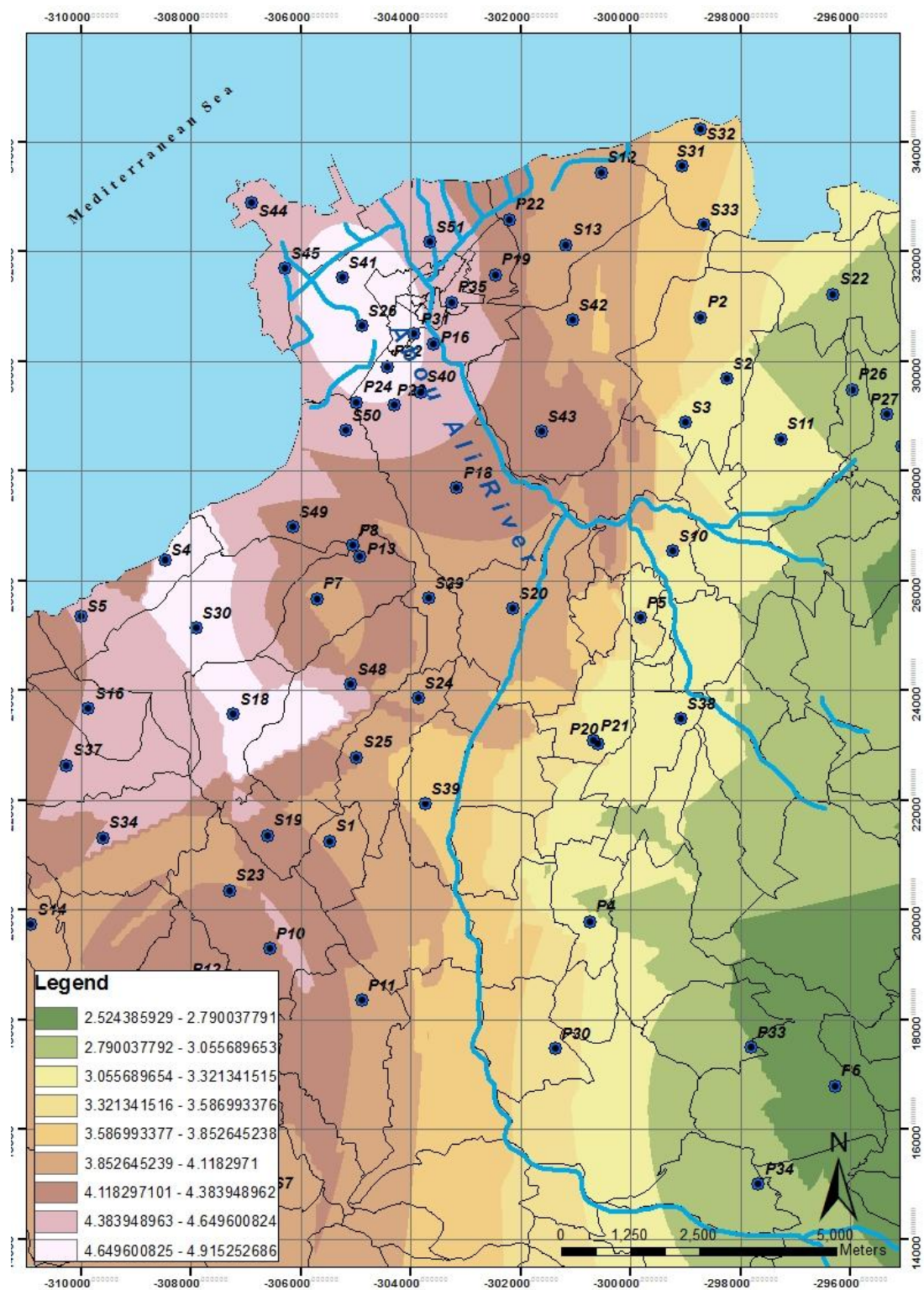


Figure 5.33 Potassium variations for Wet Season 2013

5.2.2.9 Sulfate

Sulfate (SO_4), an anion formed by oxidation of the element sulfur, is commonly observed in ground water. The established secondary maximum contaminant level (SMCL) for sulfate is 250 mg/L. One important source of sulfate and sulfuric acid products are fertilizers, chemicals, dyes, glass, paper, soaps, textiles, fungicides, and fertilizers) (WHO/SDE/WSH/03.04/114, 2004). Sulfate is discharged into the dissolution or weathering of sulfur containing minerals. Two possible mineral sources of sulfate were identified in the studied aquifers. The first includes evaporate minerals, such as gypsum and anhydrite (CaSO_4). Gypsum and anhydrite are the two calcium sulfate minerals occurring in nature. The second possible mineral source of sulfate is pyrite (FeS_2), a mineral present in dolomite. The oxidation of pyrite releases iron and sulfate into groundwater. Therefore, the presence of sulfate groundwater samples taken from our Miocene Limestone aquifer appears to be a result of the dissolution of gypsum deposits. See figure 5.34.

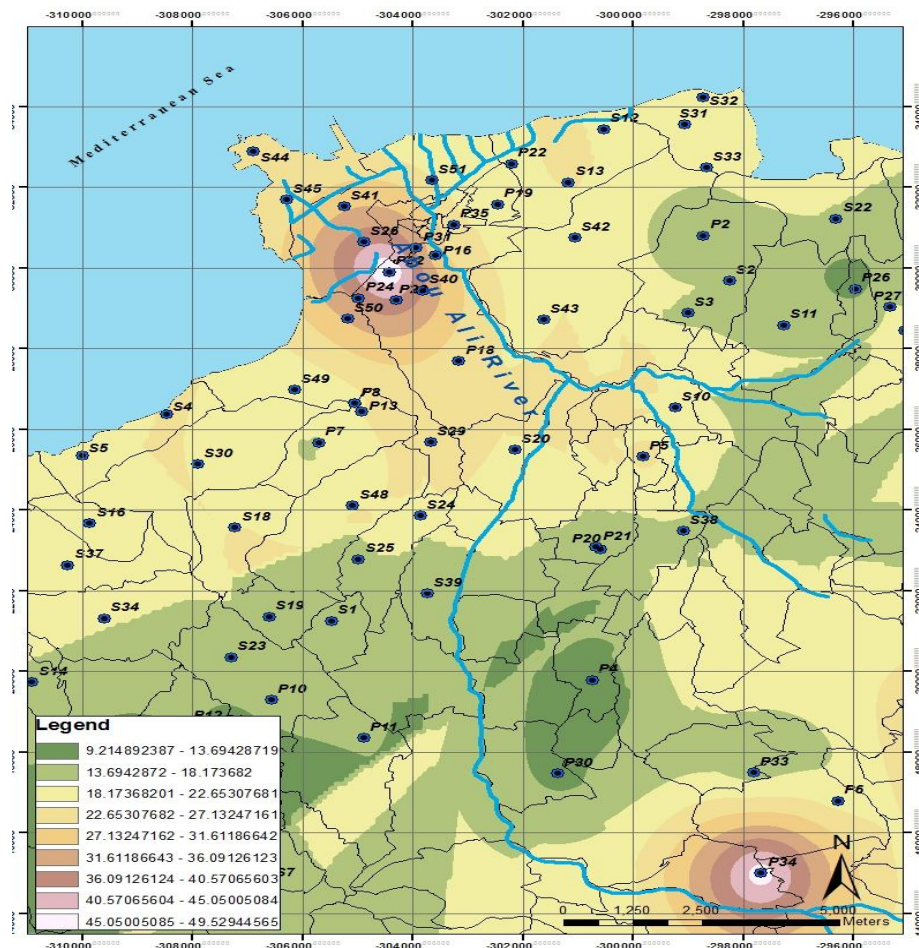


Figure 5.34 Sulfate Variations (in mg/L) for Wet Season 2013

5.2.2.10 Correlation Between Calcium, Sodium and Sulfate

The origin of Calcium, Sodium & Sulfate was determined as naturogenic according to the study handled with PhreeqC software and the discussion made in the previous page. Their presence is primarily due to the sedimentary soil structure containing: Anhydrite, Aragonite, Calcite, Dolomite, Gypsum, Halite, Mirabilite etc...

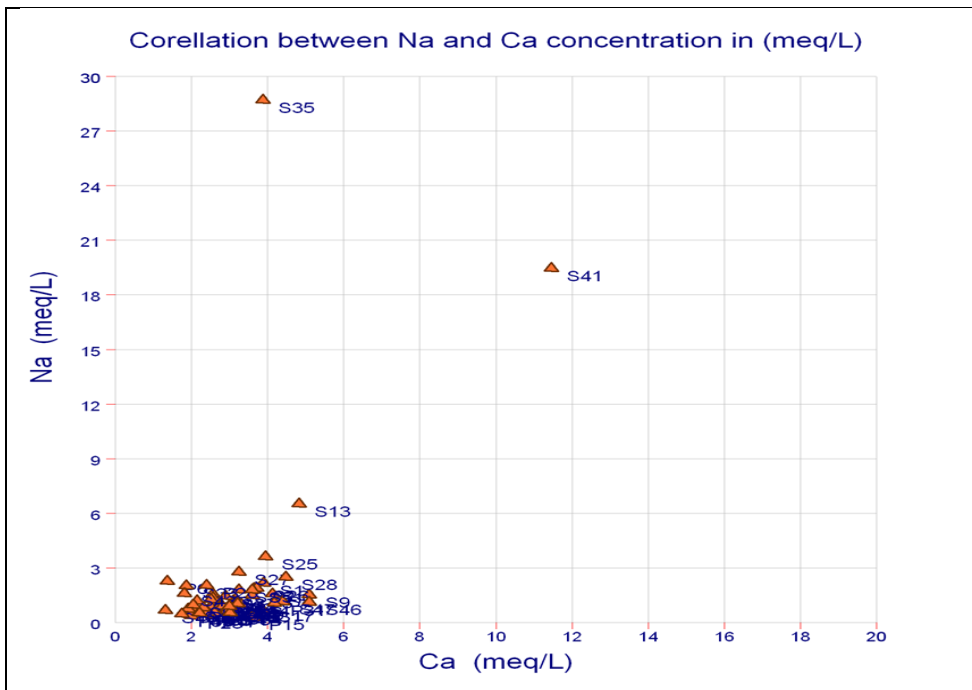


Figure 5.35 Correlation Between Sodium and Calcium (PhreeqC) for Dry Season 2012

The graph represents in figure 5.35 shows that calcium and sodium evolves independently, this indicates that the leaching of these two chemicals occurs from rocks containing calcium carbonate for calcium; and halite and mirabilite for sodium. When coupling calcium and sulphate we observe from figure 5.36 that Ca performs an alignment after sulfates, in two lines (clouds of points) indicating that these two elements have the same origin which is anhydrite (Ca SO_4) and gypsum ($\text{CaSO}_4 \cdot 2(\text{H}_2\text{O})$). In addition, if the SI index of both rock types is to be compared, the values of the two parameters are very similar if not identical for some locations proofing the same origin. The same observation was made when coupling Na and Cl and Na with SO_4 implying a common origin of the elements. The following elements presence is due to the halite (NaCl) in the soil structure and mirabilite ($\text{Na}_2\text{SO}_4 \cdot 10\text{H}_2\text{O}$). The excess values seen in figures 5.37 has been noticed to occur always in the same locations implying a sea water intrusion in these areas which overlay with their closeness to the sea.

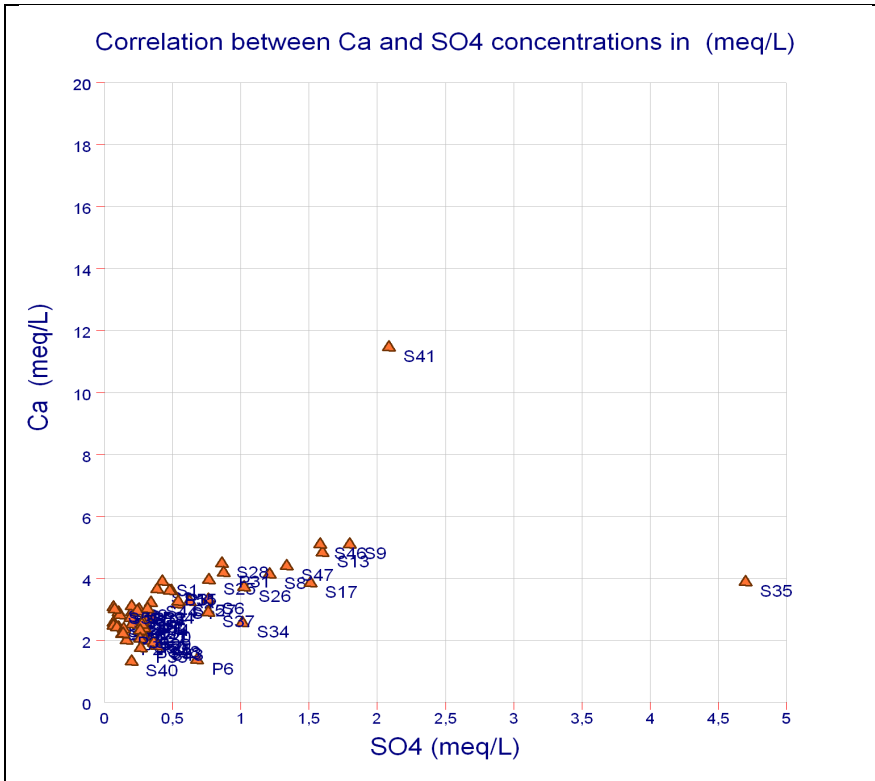


Figure 5.36 Correlation Between Calcium and Sulfate (PhreeqC) for Dry Season 2012

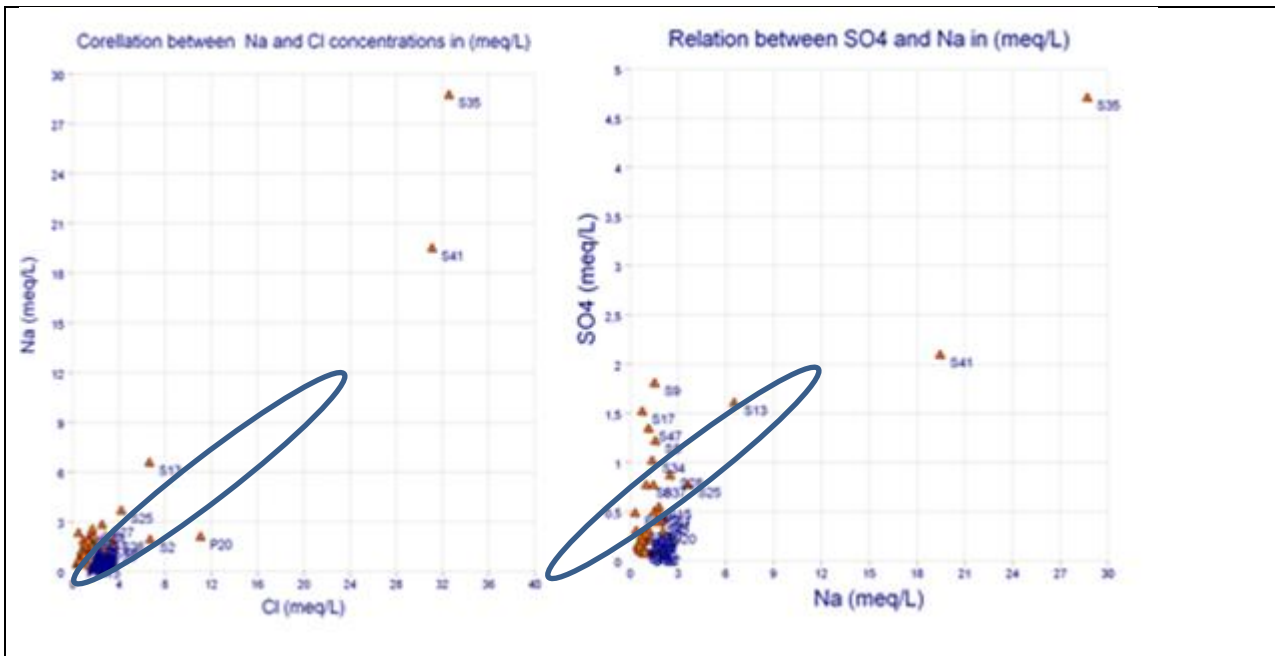


Figure 5.37 Correlation Between Calcium and Chloride and Sulfate and Sodium (PhreeqC) for Dry Season 2012.

5.2.2.11 Magnesium

Magnesium in groundwater originates from the weathering of rock fragments in the unconsolidated deposits and dissolution of the underlying bedrock. Limestone and dolomites calcium magnesium carbonate; $\text{CaMg}(\text{CO}_3)_2$, Aragonite $\text{CaMg}(\text{CO}_3)$ are the major sources of this element in this aquifer according to PhreeqC. Magnesium is washed from rocks and subsequently ends up in water. Figure 5.38 and 5.39

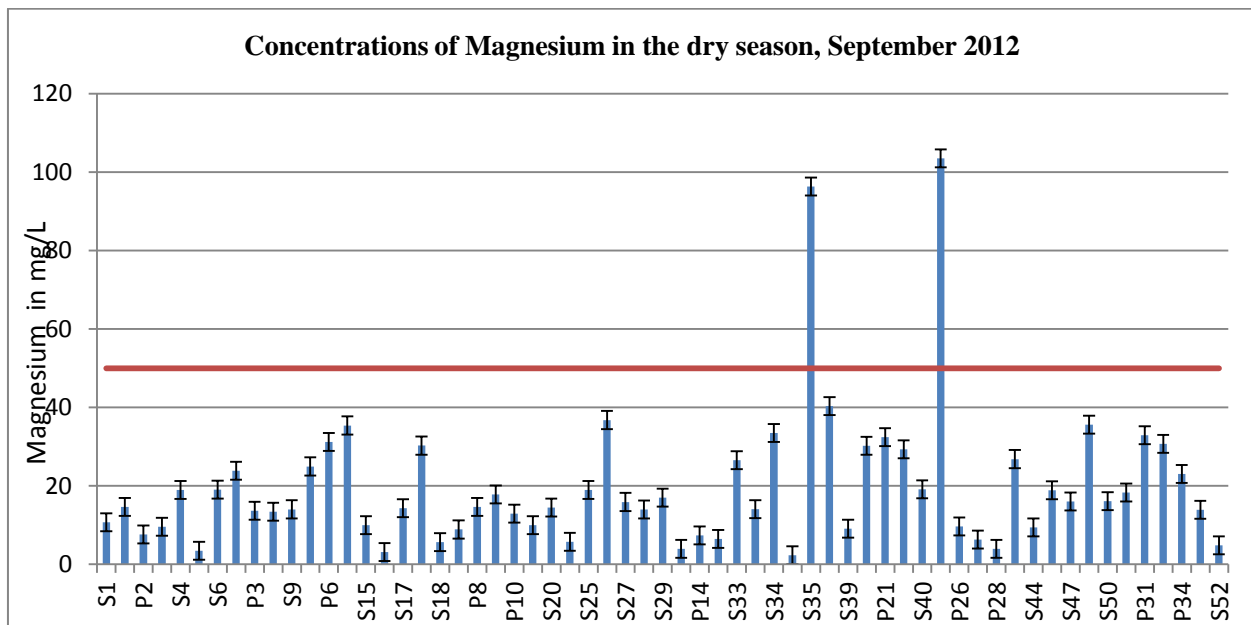


Figure 5.38 Magnesium Variation in mg/L for Dry Season 2012

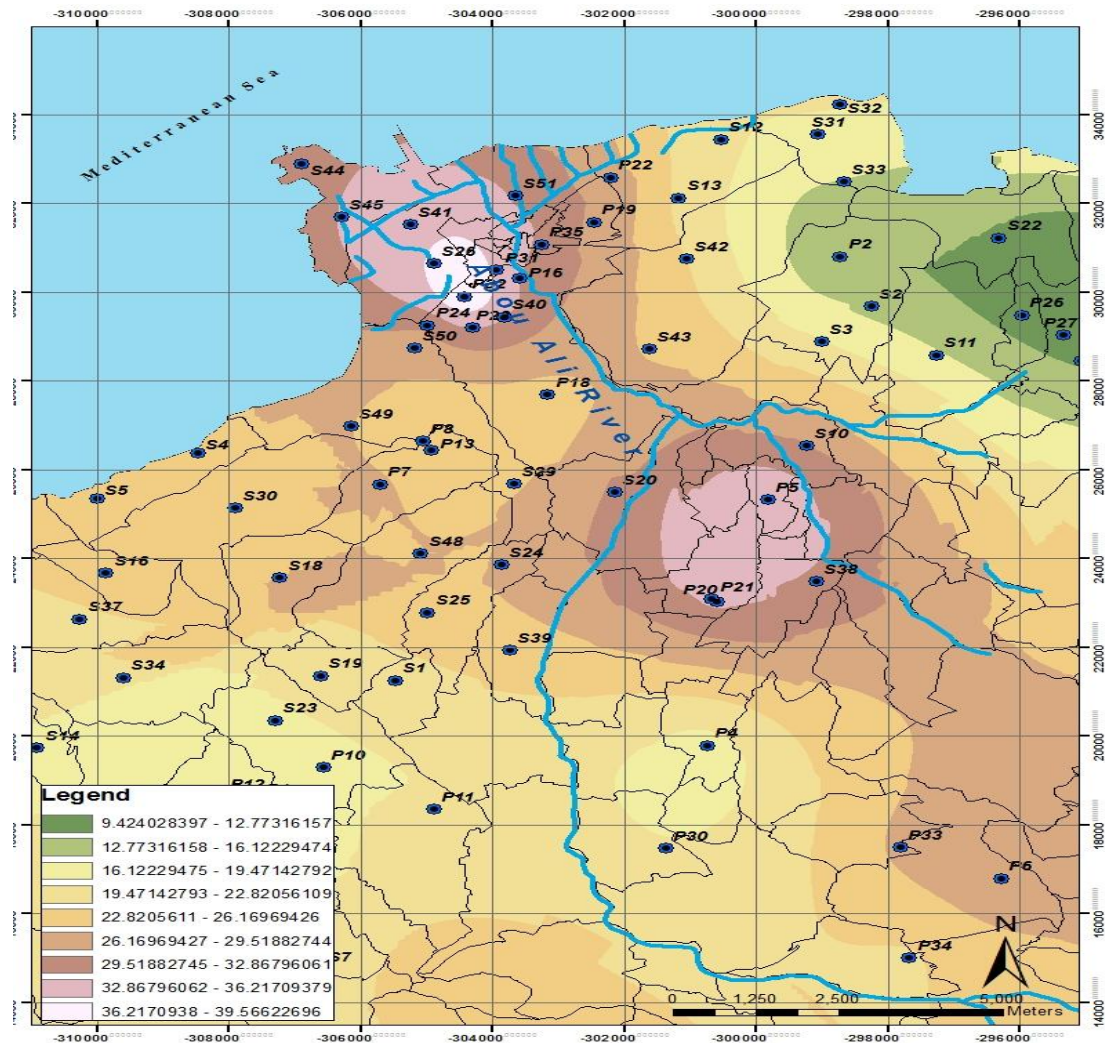


Figure 5.39 Magnesium Variations in mg/L for Wet Season 2013

5.2.2.12 Lithium

Lithium is a natural earth metal, it is found in soils, rocks, dusts, surface water, ground water and seawater. Because of its natural presence it is found in plants, animals, food products and beverages. Manmade products that contain lithium and industrial processes that involve lithium can produce higher concentrations in some areas than would be found under natural conditions (Authority, July 2011). The concentrations see bellow in Figure5.37 turn all around 0 to 1.6 mg/L which means that the source is naturogenic.

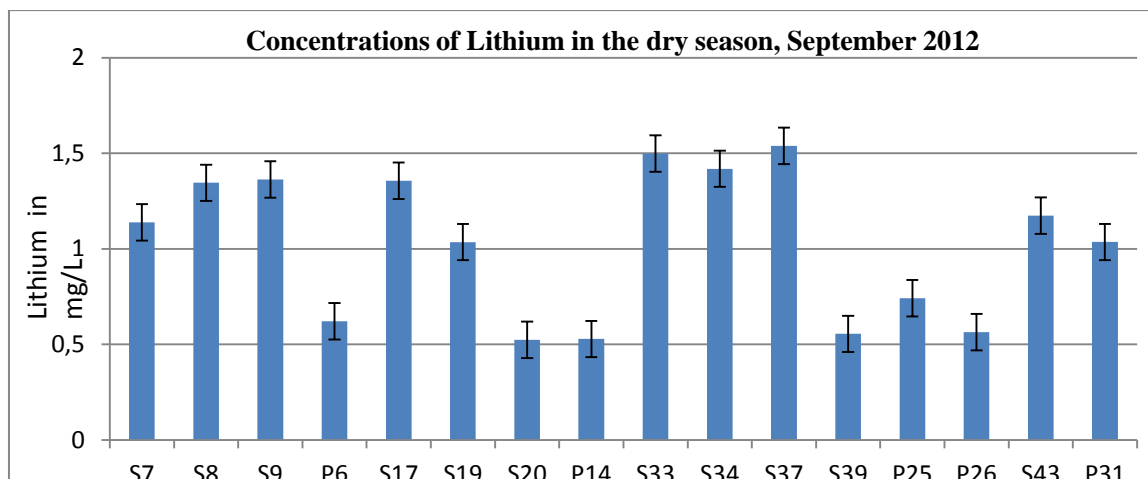


Figure5.40 Lithium Variations for Dry Season 2012

5.2.2.13 Bromide

As known, the main source of bromide in groundwater is derived from atmospherically transported materials that falls as wet precipitation and particular matter (Matthias Raiber a, 2012). In the locations where bromide was detected, the quantitative results obtained show higher levels in dry season rather than in the wet season. Several factors explain the following results; near the coast the mineral bromide is dominated by salts derived from the sea. In addition, the dissolution of evaporate and salt deposits, clay compaction, recrystallization of minerals, connate water and seawater intrusion contribute to additional bromide concentrations in groundwater. As for the anthropogenic factors affecting the increase in bromide levels, they include sewage disposal and so on.

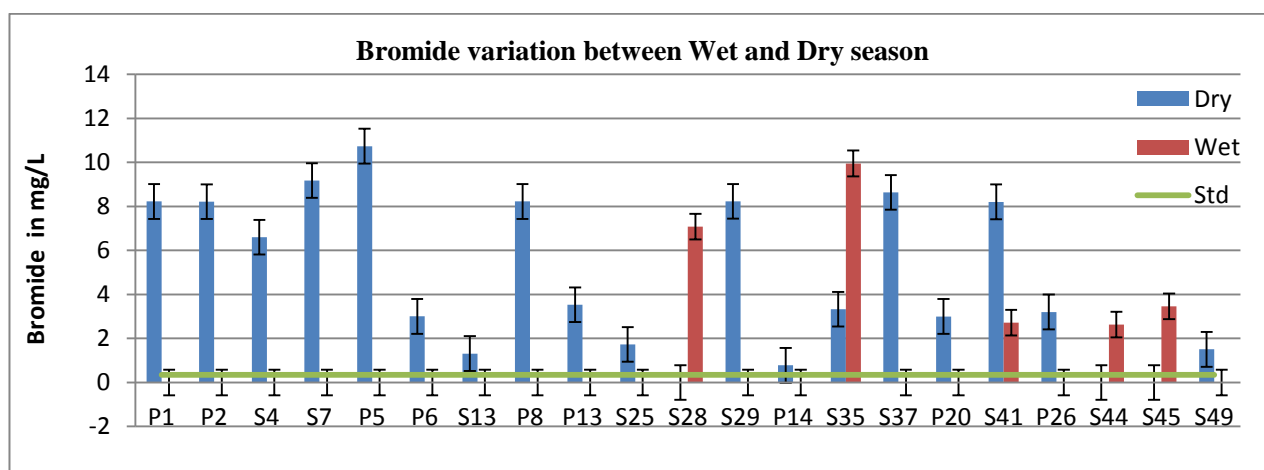


Fig 5.41 Bromide Variation Between Wet and Dry Season

5.2.2.14 E.Coli , Coliform and Salmonella

Groundwater contains a broad spectrum of microbial types similar to those found in surface soils and waters. These microbes encompass bacteria, fungi and protozoa, and are representative of most physiological types. On occasion pathogenic bacteria and protozoans of gastrointestinal origin from domestic, agricultural and other anthropogenic activities, may infiltrate through soils, sediments and rocks to the underlying groundwater (Baskaran S., 2009) (Hamze, Hassan, Thomas, Khawlie, & Kawass, 2005). E.Coli was used as a primary indicator of faecal contamination of drinking water according to the National Health and Medical Research Council (NHMRC, 2003). Therefore E.Coli, Coliform and Salmonella are figured in Fig 5.42; 5.43. In the two main campaigns, salmonella presence was negative (not present) in all samples in the exception of one sampled points S29

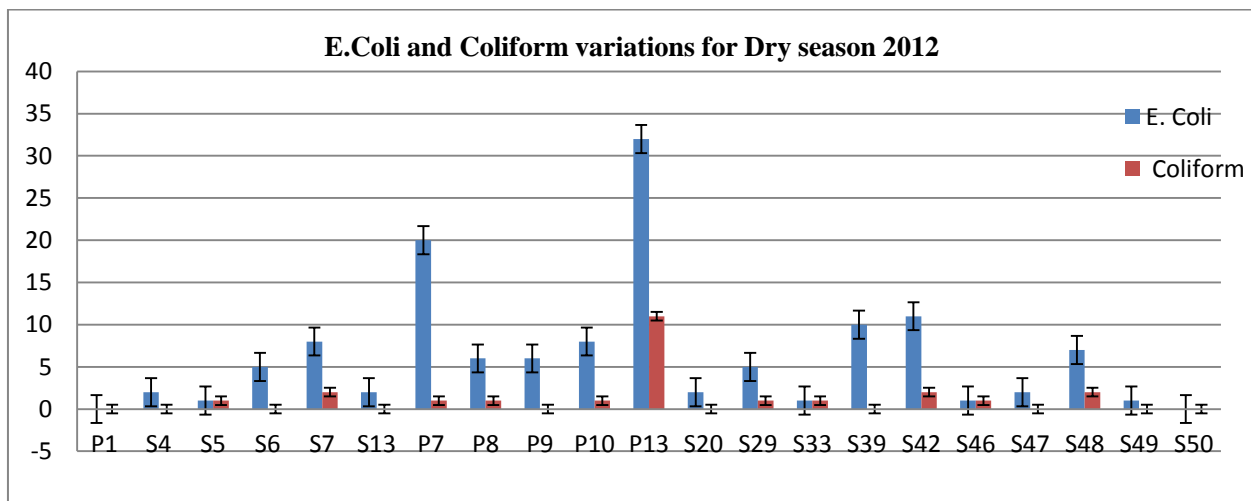


Fig 5.42 E.Coli and Coliform Variations for Dry Season 2012

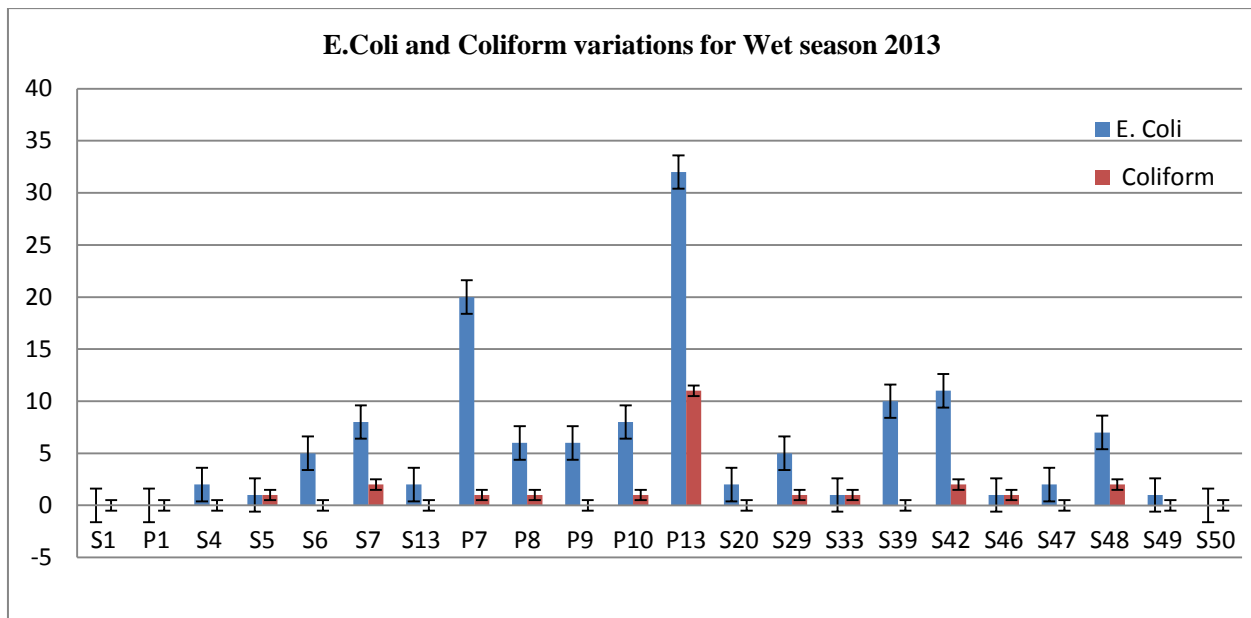


Fig 5.43 E.Coli and Coliform Variations for Wet Season 2013

5.3 Brief Discussion and Conclusion

The Miocene aquifer of North Lebanon is a bedrock aquifer most commonly formed of limestone, dolomite, and chalk. Karst features, such as solution-enlarged fractures, sink holes, and caves, form in these rocks at land surface and in the subsurface. Water parameters studied in this aquifer were shown in this chapter. These values are either due to anthropogenic factors or to the direct and effective recharge flow-paths from the soil cover to and through the aquifers (naturogenic factor).

The groundwater composition in Zgharta, Koura and Tripoli areas show some variations between wet and dry season. The water pattern goes from fresh, unpolluted groundwater in upper areas such as Zgharta and Koura (in the exceptions of some sites where manure occur) to a more saline and polluted water towards the coastline and Tripoli. Meaning we have an increasing pattern of concentration values with the closeness to the sea. This leaning is due to saltwater intrusion that have occurred from the constant and excessive pumping leading to a decrease of the water table during the dry season and so allowing the drift and mixing of fresh and saline water. In addition high evaporation rates in summer times with the salt accumulation in the soils further reduces the potential for rainfall infiltration into the groundwater (Oueida, 1992). Consequently, parameters such as salinity for example have a linear variation with seasons in all the sampled locations. Therefore, it is no coincidence that the groundwater in the Miocene aquifer has high concentrations of sodium, chloride, sulfate, and nitrate. To better understand refer to the illustration below in Figure 5.44 and 5.45.

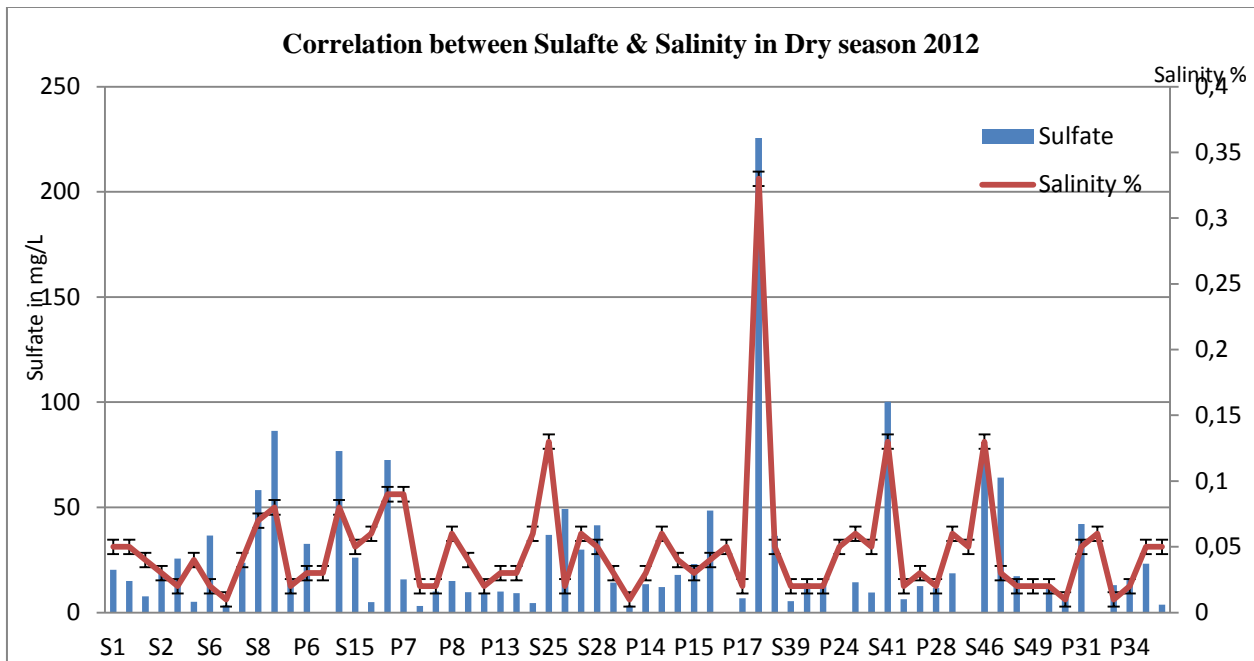


Figure 5.44 Correlation Between Sulfate & Salinity in Dry Season 2012

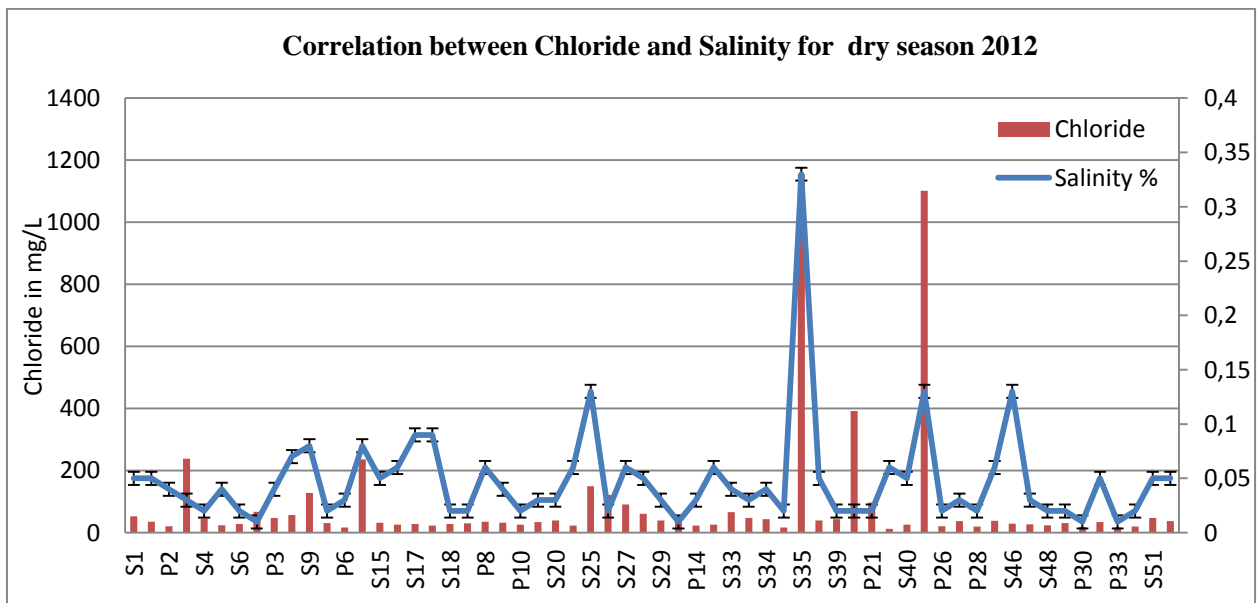


Figure 5.45 Correlation Between Chloride and Salinity for Dry Season 2012

As a conclusion, the composition and existence of the minerals (i.e. magnesium, calcium, sulfate, chlorite, fluoride, etc...) in groundwater is due to two major factors, first the geological formation of the rocks especially limestone and soil types; and second of all the anthropogenic factors.

The geological formations of the studied area belong to middle Cretaceous and quaternary deposits (especially Tripoli). The cretaceous rocks are derived from the Sannine formation, or what we call "C4"; it constitutes the most important karstic system in Lebanon. As for the quaternary deposits enclosing sequence of gravel, sand, slit and clay, this unit holds very little quantities of water. Therefore by linking the geology to celerity of percolation, the fresh water that enters the aquifer (Miocene) will be polluted or not with excess minerals.

CHAPTER 6

ESTIMATION of GROUNDWATER RESOURCES and GROUND WATER FLOW to WELLS (PUMPING TEST ANALYSES)

6.1 Estimation of Groundwater Resources

Use of Analog Models to Simulate Flow Recession of Karstic Springs

Marianne Saba¹, Erick Carlier², Najib Gerges³

¹Université Lille 1, Sciences et Technologies, 59655 Villeneuve d'Ascq Cedex, France and Université de Balamand, Kelhat, P.O.Box 100, Tripoli, Lebanon;

²Université Lille 1, Sciences et Technologies, 59655 Villeneuve d'Ascq Cedex, France;

³Université de Balamand, Kelhat, P.O.Box 100, Tripoli, Lebanon

marianne.saba@balamand.edu.lb; erick.carlier@polytech-lille.fr; najib.gerges@balamand.edu.lb

Abstract

Analog models of reservoirs were developed from the analysis of flow recession for three karst springs in Lebanon. The first source is characterized by a linear relationship between flow and time; while the other two obey a power law. For the first source, the analog model is a reservoir with vertical walls, whereas the reservoirs for the other two consist of curved walls whose geometric equation is a power law with **non-integer dimension. It is shown that for these two types of reservoirs, there is no linear relationship** between the flow and the stored water volume at the same time, and that these analog models enable estimation of the stored water volume.

Keywords

Recession; Analog models; Karstic springs; Reservoir

Introduction

The recession analysis of flow springs permits to estimate the reserves of groundwater used to provide populations need, irrigation and industrial activities. The most frequent analysis method used is based on the linearity between the flow rate and the volume of water stored at the same time. The first published

works on this subject are those of Boussinesq (Boussinesq, 1904) and Maillet (Maillet, 1905), and this linear model approach is still frequently used for karstic environment. To overcome the inability to simulate the recession of a spring flow by a single exponential law, the most common method used is to cut chronic discharge and fit, for each family of flow, an exponential law (Raesi, 2008). Some authors have questioned the linear property because of the inadequacy of the exponential law as a depletion model (Han and Hammond, 2006). Along with the physical approach of the phenomenon, some authors have developed methods for the analysis of probabilistic flow recession (Aksoy, 2004; Ceola et al, 2010). Probabilistic approaches have the advantage of highlighting the Markovian character that is related or not to the possible effect of the karst memory but do not provide information on the geometric characteristics of the aquifer. These characteristics can be determined by the use of analog models (Carlier et al, 2012) even though the proposed model may not be unique (Carlier and Mroueh, 2012).

The objective of this paper is to propose a plausible

recession model from the geometrical definition of analog reservoirs and identify available groundwater reserves.

Geological Setting of Karst Springs and Flood Recession Rates

Even though the values of flow recessions are few since they are done on monthly basis, they help highlighting the different modes of flow recession according to the spring.

Figures 1, 2 and 3 show that the flow recession, from May to September, obeys different laws. The decay law for the Rachiine river appears to be linear, whereas for the sources of Jouaiite and Abou Ali, the decay laws that give the best fit are power laws rather

than exponential laws.

Recession Flow Analysis for the Source of Rachiine

Reservoir Model

The best fit of flow-time has been obtained by a linear relationship of the form:

$$Q(t) = b - at \quad (1)$$

$$b : (L^3T^{-1}); a : T^{-1}$$

Equation (1) is a mathematical model of recession and it is important to understand its physical reality. It has been shown (Carlier et al, 2012) that a linear law of flow

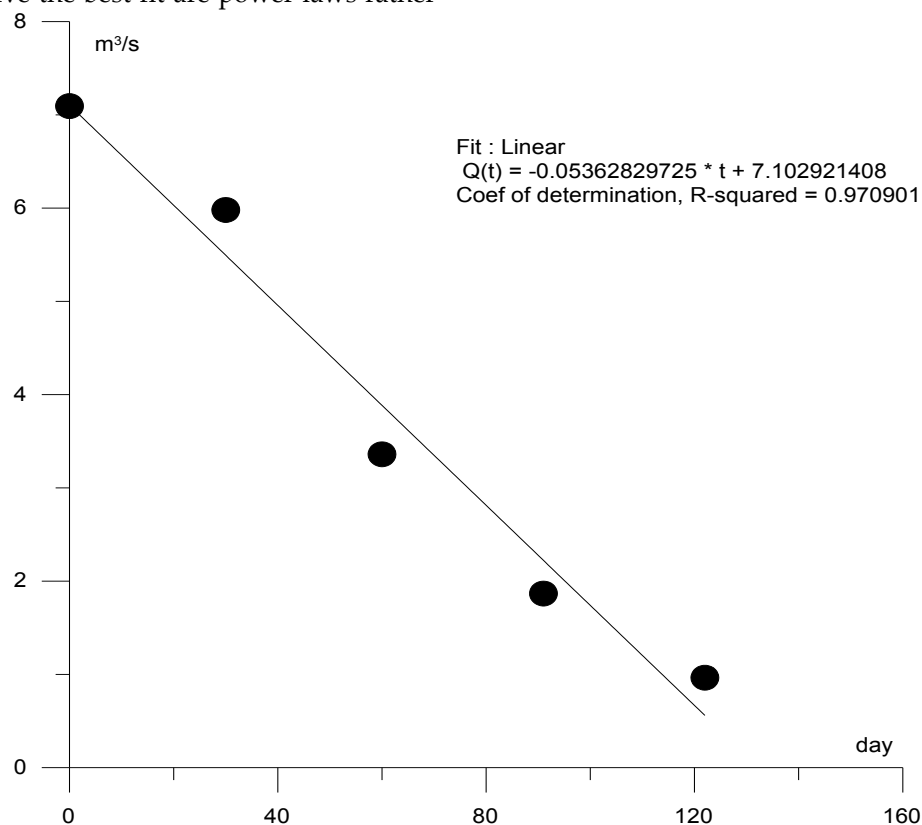


FIG. 1 FLOW RECESSION FOR THE SOURCE OF RACHIINE

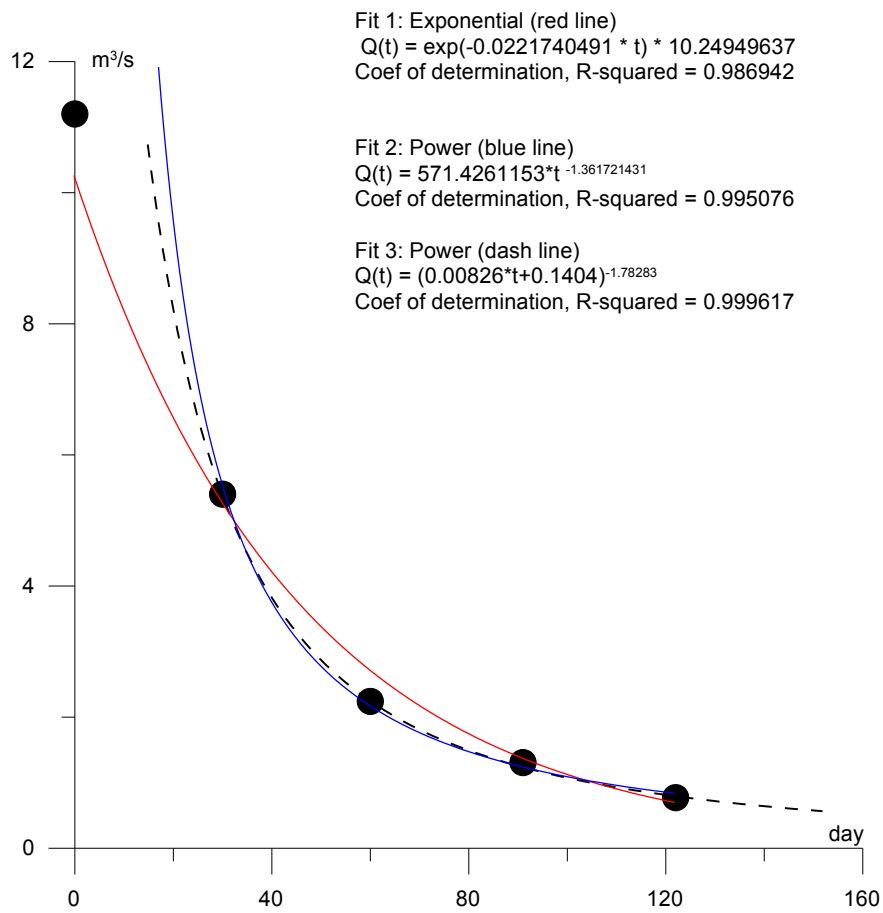


FIG. 2 FLOW RECESSION FOR THE SOURCE OF ABOU ALI

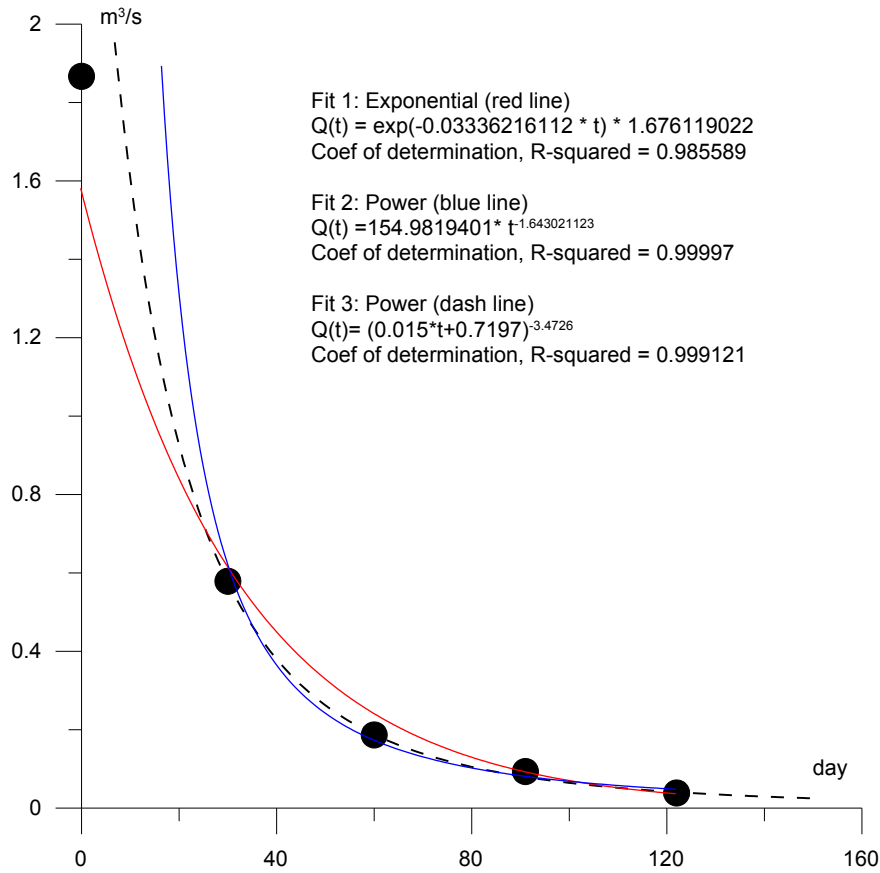


FIG. 3 FLOW RECESSION FOR THE SOURCE OF JOUAAIT

recessions in function of time corresponds to reservoirs with vertical walls (Figure 4).

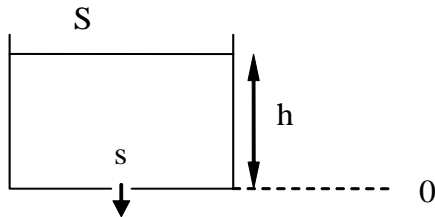


FIG. 4 RESERVOIR WITH VERTICAL WALLS

It has also been shown (Carlier et al, 2012) that by considering Bernoulli's law as a law of behavior (Equation 2) and combining it with the law of continuity in the absence of recharge (Equation 3), a decay law of the height h of water could be determined (equation 4) and that the parameters a and b of the calibration equation could be identified (equation 5).

$$Q(t) = K s \sqrt{2 g h(t)} \quad (2)$$

$$Q(t) = - S(t) \frac{dh(t)}{dt} \quad (3)$$

K : loss coefficient, between 0 and 1, bonded to the irregular geometry and roughness of the outlet orifice of the reservoir

s : area of the outlet orifice of the reservoir (L^2)

g : acceleration due to gravity ($L T^{-2}$)

$h(t)$: height of water above the orifice (L)

$S(t)$: Horizontal surface of the water at time t (L^2)

$$h(t) = \left(-a t \sqrt{2 g s^2} \right)^2 \quad (4)$$

$$Q(t) = Q_0 - \left(\frac{2 g s^2}{a} \right) \sqrt{S} \quad (5)$$

$$S = \left(\frac{2 g s^2}{a} \right)^2 t^2 \quad (6)$$

Estimation of the Stored Water Volume

For this type of reservoir, it has been shown (Carlier et al, 2012) that the emptying time t_v is expressed in the following equation (7).

$$t_v = 2 S h_0^{1/2} / K s (2 g)^{1/2} = 2 S h_0 / K s (2 g h_0)^{1/2} = 2 V_0 / Q_0 \quad (7)$$

V_0 is the volume of water stored in the reservoir at the start of the recession and Q_0 is the initial flow rate.

The emptying time can also be pulled from the equation (5) by considering $Q(t) = 0$:

$$t_v = \left(\frac{Q_0}{a} \right) \sqrt{\frac{2 g s^2}{a}} \quad (8)$$

The relationship between the flow at time t and the volume of groundwater stored at the same time can be established:

$$\begin{aligned} Q(t) &= K s \left(g h(t) \right)^{3/2} = K s \left(g V(t) / S \right)^{3/2} \\ &= A V(t)^{3/2} \\ A &= K s \left(g / S \right)^{3/2} \end{aligned} \quad (9)$$

Reservoirs with vertical walls are therefore called non-linear reservoirs. Attention should be paid to the terminologies since the non-linearity is related to the flow-volume relationship stored at the same time whereas the relationship between speed and time is perfectly linear.

The total stored water volume at the beginning of the recession is determined by the equation (9), for $t=0$ it is written as follow:

$$V_0 = \left(\frac{Q_0}{A} \right)^2 S \left(\frac{g}{K^2 s^2} \right) \quad (10)$$

By combining equations (6) and (10), the volume of water stored is:

$$V_0 = Q_0^2 / \left(\frac{g}{a} \right) b^2 / \left(\frac{g}{a} \right) \quad (11)$$

The parameters a and b are determined from the statistical processing of field measurements.

Interpretation of the Recession and Its Validation

Recession obeys the following linear law:

$$Q(t) = 7.103 - 0.05363 t \quad (12)$$

Time t is per Day, the Flow Q is expressed in $\text{m}^3 \text{s}^{-1}$; therefore, the unit for parameter $a=0.05363$ is in $\text{m}^3 \text{s}^{-1} \text{J}^{-1}$

By expressing the parameter a in $\text{m}^3/\text{s}/\text{s}$, its value will be modified to: $a=6.207 \cdot 10^{-7} \text{ m}^3/\text{s}/\text{s}$

With: $a = K^2 s^2 g / S$

Emptying time in accordance to the equation (8), is equal to $t_v = 132.44$ days.

By setting arbitrary values for the coefficient of loss of charge K and for the section of the outlet s ; the horizontal surface of the reservoir S can be calculated with the equation (6).

The initial height h_0 is calculated by equation (2), and the initial volume V_0 is equal to the product of $h_0 S$.

Table 1 gives some possible models of reservoirs with vertical walls displaying the same recession.

TABLE 1 PLAUSIBLE PHYSICAL MODELS FOR THE RECESSION

$S \text{ m}^2$	$S \text{ m}^2$	$Q_0 \text{ m}^3/\text{s}$	K	$h_0 \text{ m}$	$V_0 \text{ m}^3$	EMPTYING TIME J
1	5689543	7.103	0.6	7.143	40640550	132.44
0.25	355596	7.103	0.6	114.28	40640550	132.44

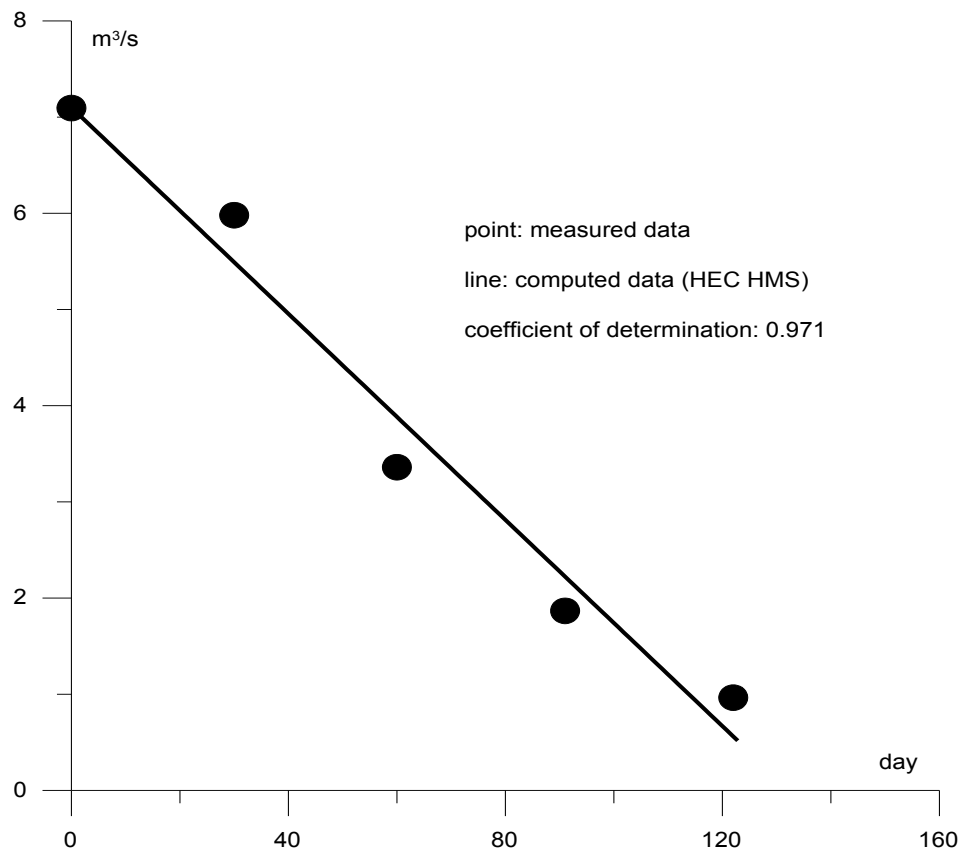


FIG. 5 MODELING FLOW RECESSION WITH THE NUMERICAL CODE HEC-HMS

The numerical code HEC-HMS (Hydrologic Modeling System), developed at the Hydrologic Engineering Center of the United States army, was used, with the purpose to model the drain of the reservoir with vertical walls having an outlet of 1 m², a coefficient of pressure loss of 0.6 and a constant horizontal surface of 5,689,543 m² with an initial water height of 7.14 m relative to the center of the outlet area of 1 m². The comparison between the calculated and measured flow is shown in Figure 5.

Analysis of ABOU ALI and JOUAITE Flow Recession

Reservoir Model

Figures 2 and 3 display that the best fit is associated with the power laws. The power law is as follow:

$$Q = at^{-\beta} \quad (13)$$

With $\beta > 0$, the initial condition $t=0$ states as a problem since the flow tends to go to infinity. In order to satisfy the initial condition $Q(t_0)=Q_0$, the following power law adopts:

$$Q = (at + b)^{-\alpha} \quad (14)$$

with $b = Q_0^{-1/\alpha}$

It has been shown (Carlier et al, 2012) that the equation (14) corresponds to reservoirs with curved walls (Figure 6).

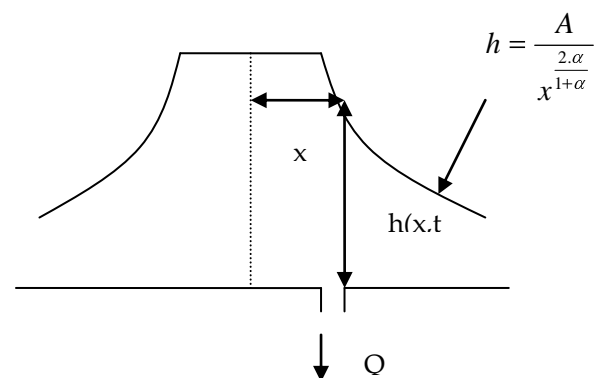


FIG. 6 GEOMETRY OF THE RESERVOIR WITH CURVED WALLS

The equation (15) expresses the relation, for instant t , between the water level of the free surface h and the abscissa x :

$$h = A/x^{2\alpha/(1+\alpha)} \quad (15)$$

With:

$$A = 0.5 \left(\frac{a}{\alpha} \right)^{2\alpha/(1+\alpha)} \left(\frac{2}{s^2 g} \right)^{1/(1+\alpha)} \quad (16)$$

α : non integer dimension

$$B = A^{(\beta+1)/\alpha} = 2^{-(\alpha+1)/\alpha} s^2 g^{(\alpha-1)/\alpha} / \alpha l \quad (18)$$

Similarly

$$x = B/h^{(\beta+1)/\alpha} \quad (17)$$

With:

Equation (15) expresses the geometry of the wall tank.

TABLE 2 STORED WATER VOLUME

NAME	α	a with t in J	a with t in s	Q_0 CALCULATED m ³ /s	V_0 hm ³	Q_0 MEASURED m ³ /s	V_0 hm ³
ABOU ALI	1.78283	0.00826	9.5602E-08	33.1207	62.13	11.20	38.6
JOUAAITE	3.4726	0.015	1.7361E-07	3.1337	5.25	1.8668	3.63

TABLE 3 ESTIMATED PARAMETERS AND NON-INTEGGER POWER

NAME	s (m ²)	l (m)	K	α
ABOU ALI	2	500	0.6	1.78283
JOUAAITE	0.5	500	0.6	3.4726

TABLE 4 CALCULATED PARAMETERS AND INITIAL VALUES OF FLOW AND WATER LEVEL

NAME	A	B	Q_0 m ³ /s	h_0 (m)
ABOU ALI	70956.21	6108.998	33.1207	38.83
JOUAAITE	46647.57	1015.437	3.1337	5.56

TABLE 5 RECESSION EQUATIONS AND GEOMETRIC FUNCTIONS OF RESERVOIRS

NAME	EQUATION	$x=f(h)$
ABOU ALI	$Q = (0.00826t + 0.1404)^{-1.78283}$	$x = 6108.99799/h^{0.78045299}$
JOUAAITE	$Q = (0.015t + 0.7197)^{-3.4726}$	$x = 1015.43651/h^{0.64398433}$

Estimation of the Volume of Water Stored

The volume of water which has flowed out of the reservoir at time t is:

$$V_{out}(t) = \int_0^t Q(\tau) d\tau = \left[\frac{b + \tau^\alpha}{\alpha(1-\alpha)} \right] \left[\frac{1-\alpha}{\alpha(1-\alpha)} \right] \quad (19)$$

Equation (19) can be written with $b = Q_0^{-1/\alpha}$:

$$V_{out}(t) = \frac{Q(t)^\beta}{\beta} - \frac{Q_0^\beta}{\beta} \left[\frac{1-\alpha}{\alpha(1-\alpha)} \right] \quad (20)$$

With $\beta = (\alpha-1)/\alpha$

For both sources, α is greater than 1, it can be deduced that for an infinitely large time t , the total volume of water restored is:

$$V_{out}(\infty) = - \left[\frac{1-\alpha}{\alpha(1-\alpha)} \right] \quad (21)$$

Equation (21) is, in fact, the total volume of water stored at the beginning of the recession, or V_0 .

It can be written that:

$$V_0 = Q_0^\beta / \left[\frac{1-\alpha}{\alpha(1-\alpha)} \right] \quad (22)$$

It is deduced that the volume of water stored at time t is:

$$V(t) = V_0 - V_{out}(t) = Q(t)^\beta / \left[\frac{1-\alpha}{\alpha(1-\alpha)} \right] \quad (23)$$

With $\alpha > 1$ and $\beta > 0$

There is no linear relationship between flow and volume stored at the same time. This type of reservoir is called nonlinear.

Table 2 presents an estimation of available groundwater reserves.

Numerical Modeling

The initial rate calculated Q_0 is estimated by equation (14) for $t=0$.

By setting arbitrary values for the coefficient of loss K , the section of the outlet opening s and the width l of the reservoir, perpendicular to the x coordinate (abscissa), the parameters A and B are calculated by equations (16) and (18). The initial height of the water in the tank, h_0 , is calculated by the equation (2).

Equation (17) permits the calculation of the corresponding x_0 values and its homologue h_0 .

Tables 3, 4 and 5 summarize the estimated and calculated values that have helped define the geometry of the tanks.

Once the geometry of the reservoir has been defined,

and introduced into the code HEC-HMS, the simulation of the emptying of the reservoir can be

simulated. The results are shown in Figures (7) and (8).

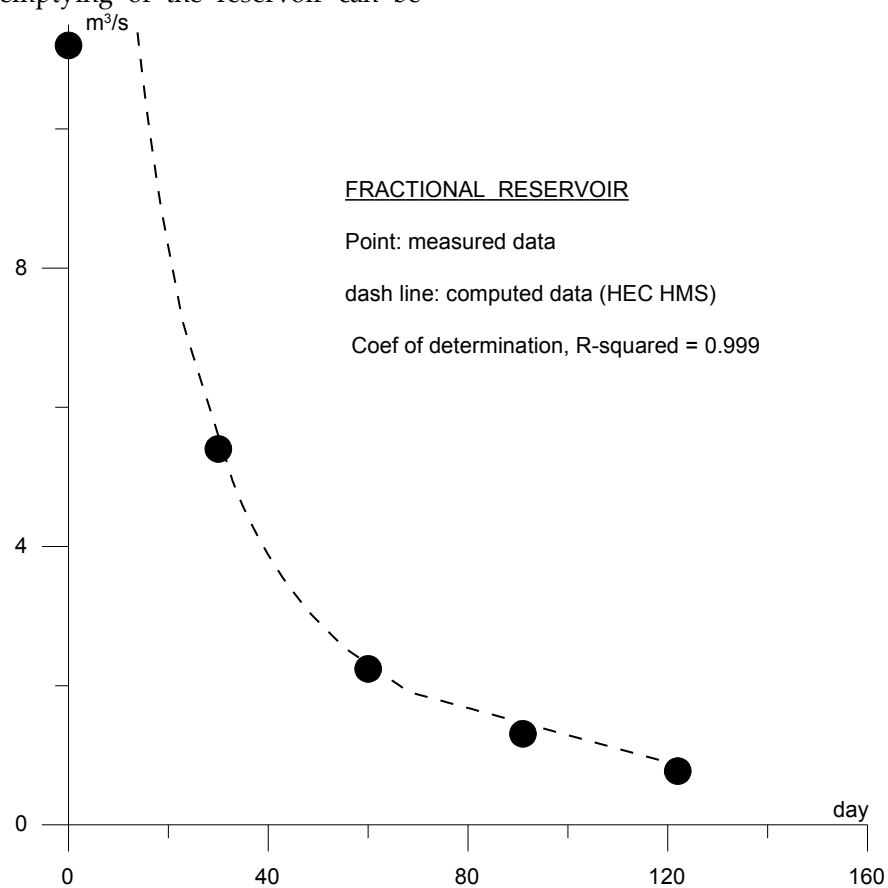


FIG. 7 ABOUT ALI. RECESSION ACCORDING TO A NON-INTEGER DIMENSION TANK

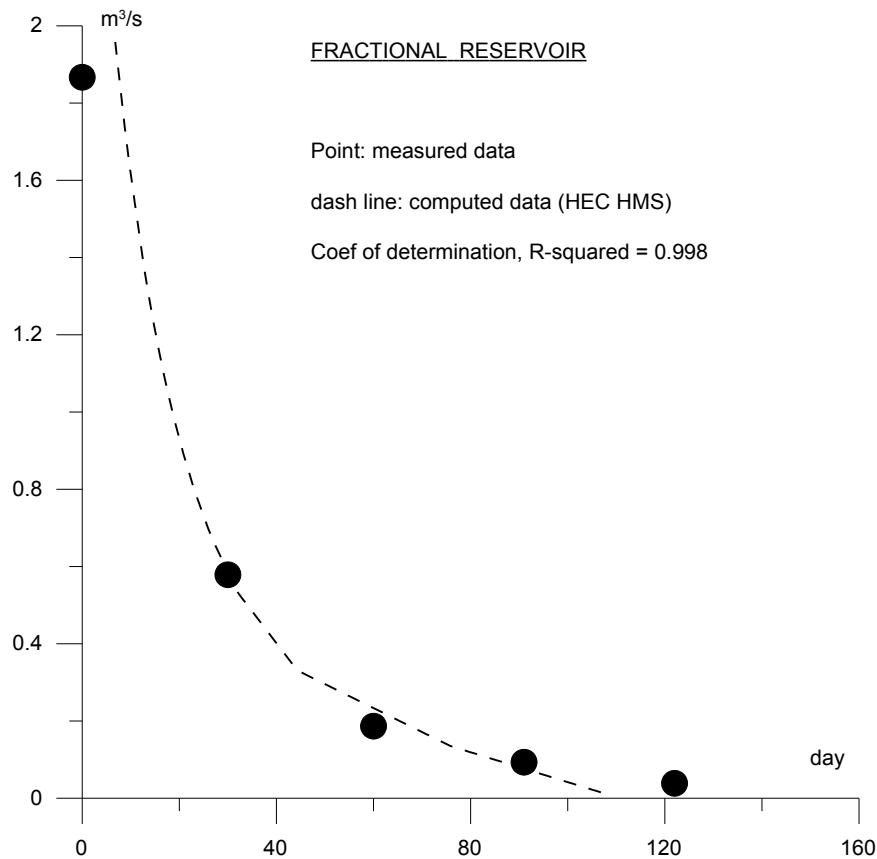


FIG. 8 JOUAIITE RECESSION ACCORDING TO A NON-INTEGGER DIMENSION TANK

Conclusion

The analog models presented have a descriptive function. The proposed approach shows a close relationship between the shape of the flow recession curves and geometry of analog reservoirs. It also shows that even if there is no unique model for a given analogue chronic flow, reservoirs belong to the same geometric family. Following this analysis, it appears that the modeling of flow recessions by exponential law is very questionable, even objectionable for karst environments. Indeed, the exponential law for recession implies a linear relationship between flow and volume stored at the same time, yet the models developed for the three Lebanese sources are highly nonlinear. This prospective analysis of flow opens up new interpretations that should be tested systematically on the karstic sources.

REFERENCES

- Aksoy, H. "Using Markov Chains for Nonperennial Daily Streamflow Data Generation". *Journal of Applied Statistics*, Vol. 31, No. 9, (2004): 1083–1094.
- Boussinesq, J. "Recherches théoretique sur l'écoulement des nappes d'eau infiltrées dans le sol et sur le débit des sources". *J. Math. Pure Appl.* 10 (5), (1904): 5-78.
- Carlier, E., Zouhri, L., Shahrour, I. "Explication de décrues anormales par modèles analogiques de réservoirs". *Hydrological Sciences Journal*, 57 (5), (2012): 913-927.
- Carlier, E., Mroueh, H. "Comment on « Tank-reservoir drainage as a simulation of the recession limb of karst spring hydrographs". *Hydrogeology journal*, Volume 20, Issue 7 (2012): 1427-1428.
- Ceola, S., Botter, G., Bertuzzo, E., Porporato, A., Rodriguez-Iturbe, I., Rinaldo, A. "Comparative study of ecohydrological streamflow probability distributions", *Water Resour. Res.*, 46, W09502, (2010), doi:10.1029/2010WR009102.
- Hammond, M., Han, D. "Recession curve estimation for storm event separations". *Journal*

of Hydrology (330), (2006): 573-585.

Maillet, E. "Essais d'hydraulique souterraine et
fluviale". Librairie Sci. Hermann Paris, 1905, 218

p.

Raeisi, E. "Ground-water storage calculation in
karst aquifers with alluvium or no-flow
boundaries". Journal

6.2 Ground Water Flow to Wells (Pumping Test Analyses)

To be able to study our watershed and consider if it as an aquifer, it has to be permeable enough to store and transmit economic quantities of water; this is related to both transmissivity and storativity of the aquifer. (Kruseman G.P., 2003) Therefore many assumptions have to be made in order to study the groundwater in the selected locations. Here is a list of the essentials.

1. If the aquifer is bounded on the bottom by a confining layer
2. All geological Formations are horizontal and have infinite horizontal extent
3. The potentiometric surface of the aquifer is horizontal and has infinite horizontal extent.
4. The potentiometric surface of the aquifer is not changing with time prior to the start of the pumping.
5. All changes in the position of the potentiometric surface are due to the effect of the pumping well alone.
6. The aquifer is homogeneous and isotropic
7. All the flow is radial towards the well
8. Groundwater flow is horizontal
9. Darcy's law is valid
10. Groundwater has a constant density and viscosity
11. The pumping well are fully penetrating; and screening over the entire thickness of the aquifer
12. The pumping well has a small diameter and 100% efficiency. (in our case the efficiency is not 100% since the conditions of the wells isn't good for all the wells)

The determination of hydrodynamic parameters of the aquifer is done through pumping tests using various methods of interpretation available, most of which branch from the method of Theis (1935) and Cooper-Jacob (1947). Various studies have shown that it is possible to calculate these parameters using short pumping tests or by steps providing pumping levels for each cycle. The minimum number of levels required to achieve satisfactory results is three (3) (Lam Q.D, 2000).

6.2.1 Method to Approach Fractured Medium

There are several ways to approach the fractured medium in the interpretation of pumping tests. The best known are the equivalent porous medium, the double porosity model or mixed model and discontinuous medium or discrete model. Our choice will be on the model of equivalent porous medium because it is the approach most known and most used by hydro-geologists. Equivalent model of porous media is the most classic style. Cracked medium is treated as a continuous porous equivalent medium, isotropic, homogeneous, or not. This representation has been adopted in order to make easier the calculations by applying the average existing calculations for the continuous medium in fractured media. The concept of an equivalent porous medium refers to the concept of Representative Volume Element (RVE).

6.2.2 Determination of Conductivity and Transmissivity

The hydraulic conductivity is given by: (Todd D. K., 2004)

$$K = \frac{k \cdot g}{\nu} \quad (6.1)$$

Where K is the hydraulic conductivity [L/T], g the acceleration due to gravity $\approx 9.81 \text{ m/s}^2$, k the permeability [L^2], and ν the kinematic viscosity [L^2/T], equal to about $1.10 \cdot 10^{-6} \text{ m}^2/\text{s}$ at 20°C ; the kinematic viscosity is given by μ/ρ where μ is the dynamic viscosity [M/LT], equal to about $1.10 \cdot 10^{-3} \text{ Pa}\cdot\text{s}$ at 20°C , and ρ is the density of water, equal to about 1000 kg/m^3 at 20°C . Values of the density, kinematic and dynamic viscosity of water versus temperature are given in Table 6.1.

Table 6.1: Density, Kinematic and Dynamic Viscosity of Water (Kruseman G.P., 2003)

Temperature T (°C)	Density ρ (kg/m ³)	Dynamic viscosity μ (10 ⁻³ Pa·s)	Kinematic viscosity ν (10 ⁻⁶ m ² /s)
0	999,9	1,787	1,787
5	1000,0	1,519	1,519
10	999,7	1,307	1,307
15	999,1	1,140	1,141
20	998,2	1,002	1,004
25	997,1	0,894	0,897
30	995,7	0,801	0,804
35	994,1	0,723	0,727
40	992,2	0,656	0,661
45	990,2	0,599	0,605
50	988,1	0,549	0,556
55	985,7	0,506	0,513
60	983,2	0,469	0,477
65	980,6	0,436	0,444
70	977,8	0,406	0,415
75	974,9	0,380	0,390
80	971,8	0,357	0,367
85	968,6	0,336	0,347
90	965,3	0,317	0,328
95	961,9	0,299	0,311
100	958,4	0,284	0,296

The permeability depends upon the size of the pores, and one would be tempted to relate this to the size of the particles. Unfortunately, the exact relationship is complicated due to the particles size distribution, the packing of the particles, and the shape of the particles. Therefore, only crude

estimations are possible. The first one is the Kozeny-Carman equation, which is valid for a porous material of equal sized spherical grains

$$k \approx n^3 \frac{D^2}{180(1-n)^2} \quad (6.2)$$

Where n is the porosity [L^3/L^3], which represents in this equation the effect of the packing of the grains (dense packing means low porosity and loose packing high porosity), and D is the diameter of the grains [L].

In experimental procedure, conductivity was determined by the insertion of the piezometer in the samples wells. When wells have been pumping for an appreciable time steady state conditions may prevail. It is only under state conditions that continued abstraction of ground water is feasible. If not, groundwater levels will continue to decline, which finally will result in the well falling dry or in a complete exhaustion of the groundwater reservoir. Hence, it is important to understand the relationships under which steady state groundwater flow to pumping wells can occur.

In reality, however, many aquifer tests will never reach the steady state (i.e., the cone of depression will continue to grow over time). These conditions are referred to as non-equilibrium or transient flow conditions. (Fetter C.W., 2001) Here we will only discuss the methods of determining transmissivity and storativity in a confined aquifer under non-equilibrium radial flow conditions. By definition, the transmissivity is the flow of water flowing per unit width of an aquifer under the influence of a hydraulic gradient unit. It is the capacity of the aquifer to pass water through a unit area. It can inform us on the permeability of the medium, accordingly and depending on the value (high or low values) of transmissivity (T), an aquifer can be considered good or bad. All wells in the study are in the fractured, partially karstified Miocene limestone aquifer. For the determination of the T values, several empirical methods have been established such as Theis and Cooper- Jacob ect... In our study, the methods used are Theis and the Cooper- Jacob method even if some of the assumptions of these methods are violated, but it can be generally justified. The assumptions of horizontality, uniform thickness and homogeneity is not always met, however, since it is an overall study of the aquifer, average values within the cone of depression, and therefore it is considered as satisfactory for the study. The resulting values are those obtained from the pumping tests available in the field representing pumping wells, due to

the lack of observation piezometers. Using these data, the transmissivity of the aquifer can be assessed by both data of water recession or lift.

To better assess the distribution of transmissivity, a classification has been established and is as follows (Lam Q.D, 2000) in m^2/s :

- Low class: $T < 10^{-5} \text{ m}^2/\text{s}$
- Mid class: $10^{-5} < T < 10^{-4} \text{ m}^2/\text{s}$
- Large class : $T > 10^{-4} \text{ m}^2/\text{s}$

6.2.3 Theis Method (Unsteady-State Flow)

Theis (1935) was the first to develop a formula for unsteady-state flow that introduces the time factor and the storativity. He noted that when a well penetrating an extensive confined aquifer is pumped at a constant rate, the influence of the discharge extends outward with time. The rate of decline of head, multiplied by the storativity and summed over the area of influence, equals the discharge. The Theis equation is written as follows: (Theis, The source of water derived from wells. Essential Factors controlling the response of an aquifer to development., May 1940)

$$T = \frac{Q}{4\pi (h_0 - h)} W(u) \quad (6.3)$$

Where T is the aquifer transmissivity, Q is the steady pumping rate, $h_0 - h$ is the drawdown, and $W(u)$ is the well function. Likewise, storativity is written as follow:

$$S = \frac{4Tut}{r^2} \quad (6.4)$$

Where S is the aquifer storativity, T is the transmissivity, u is a dimensionless constant, t is the time since pumping starts, and r is the radial distance from the pumping well.

During an aquifer test, water is pumped out at a well for a period of time; the drawdown is then measured as a function of time in the wells. The data are analyzed using different methods to

determine aquifer transmissivity and storativity by using **Aquitest** software.

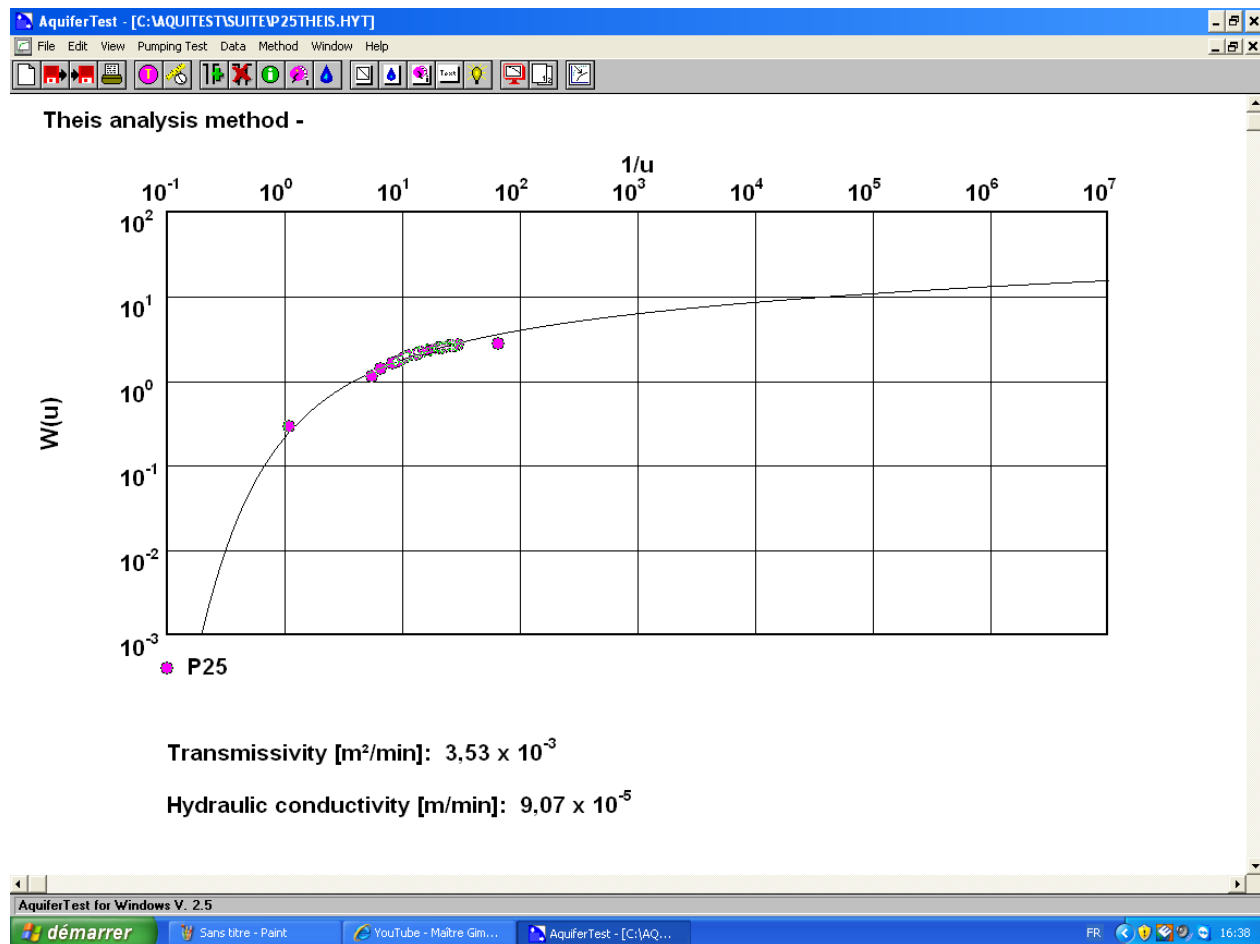


Figure 6.1 Method of Theis Applied for One of the Sampled Location by the Use of Aquitest Software

The Theis method is a graphical method that involves the following steps:

1. Making a plot of $W(u)$ versus $1/u$ on full logarithmic scale. This graph has the shape of the cone of depression near the pumping well and is referred to as the Theis type curve, or the non-equilibrium type curve.
2. Plotting the field drawdown for the studied wells, $(h_0 - h)$, versus t using the same logarithmic scale as the type curve.
3. Laying the type curve over the field-data graph and adjust the two graphs until the data points match the type curve, with the axes of both graphs parallel. the intersection of the line $W(u) = 1$ and the line $1/u = 1$ is selected as the matching point.

4. Transmissivity (T) values and conductivity values (K) are handled as a final step with Aquitest software. As seen in the Figure 6.1 above.

6.2.4 Cooper-Jacob Method (Cooper-Jacob Straight-Line Time-Drawdown Method)

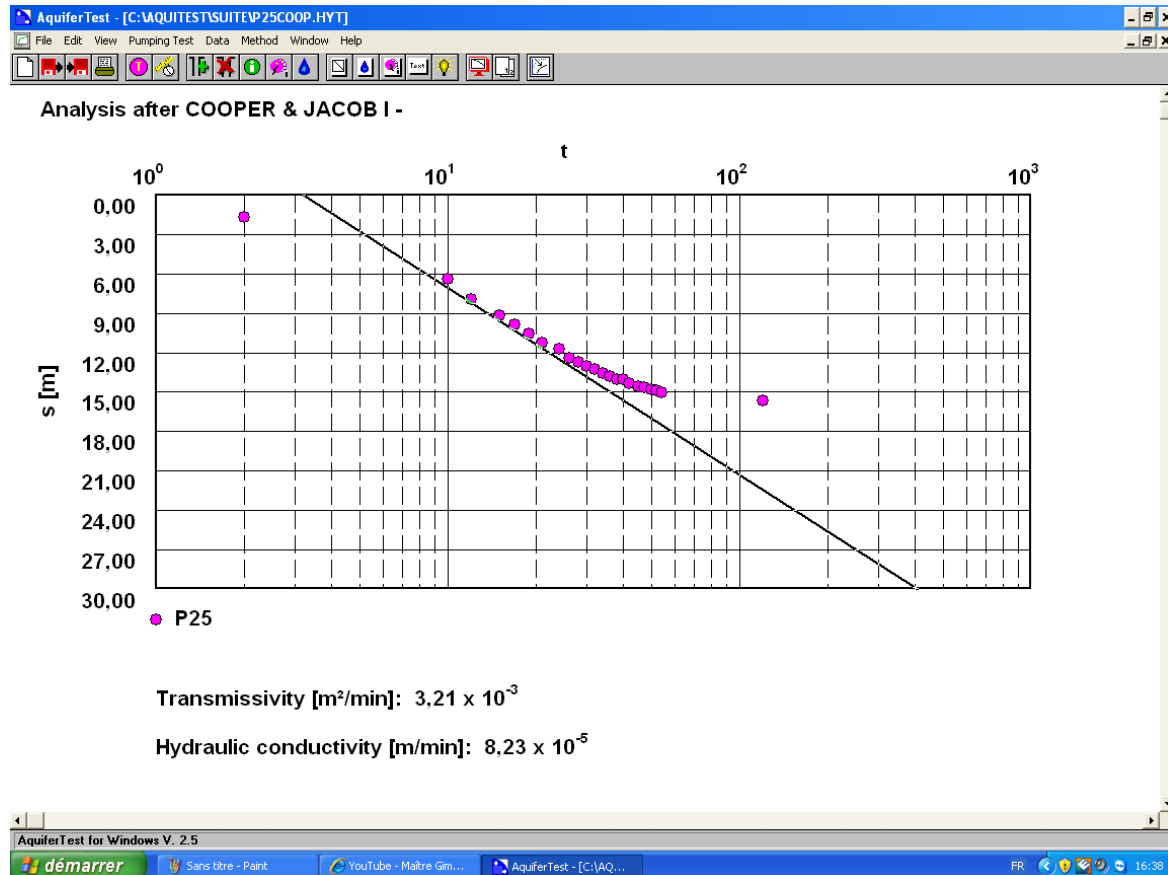


Figure 6.2 Method of Cooper-Jacob Applied for one of the Sampled Location by the Use of Aquitest Software

The determination of transmissivity can also be performed by the method of Cooper-Jacob (Kruseman G.P., 2003). This method of interpretation of well test data is based on the logarithmic approximation of the equation of Theis (1935); and is only valid for $u < 0.05$. In this method a semi-log plot of the field drawdown data versus time is made. A straight line is drawn through the field-data points and extended backward to the zero-drawdown axis. The time at the intercept of the straight line and the zero-drawdown axis is designated t_0 . The value of the drawdown, $\Delta(h_0 -$

h), is obtained from the slope from the graph. The values of transmissivity and storativity can be calculated from the following equations:

$$T = \frac{2.3Q}{4\pi\Delta (h_0-h)} \quad (6.5)$$

$$S = \frac{2.25Tt_0}{r^2} \quad (6.6)$$

The Cooper Jacob method does not apply for all of the studied wells, it was sometimes impossible to determine T and S values by this method for our study. Some conditions apply for the method of Cooper-Jacob. These assumptions and conditions of application are as follows: (Kruseman G.P., 2003)

- The aquifer has an infinite lateral extension;
- The diameter of the well is negligible;
- The well is perfect;
- Aquifer is homogeneous, isotropic, of constant thickness over the entire area affected by the pumping;
- Flow into the well is momentary.

Table 6.2: Method of Cooper-Jacob Applied for One of the Sampled Location by the Use of Aquitest Software

ID	T with Theis in m ² /sec	K with Theis in m/s	Depth in m	Radius in m	Pumping rate in m ³ /h	K with Cooper in m/min	K with Cooper m/s
P16	n.a	7.25E-04	250	0.15	2500	0.045	7.53 E-04
P18	n.a	n.a	120	0.2	4.776	0	0
P19	n.a	n.a	89	inactive		0	0
S47	n.a	n.a	20	0.15	2	0	0
P6	6.97E-07	5.48E-09	150	0.2	0.5	3.89 E-06	6.48E-08
S15	1.67E-05	9.32E-07	85	0.12	2.4	4.87 E-05	8.12E-07
S14	1.77E-05	1.21E-06	26	0.2	0.8	0	0
S50	1.87E-05	3.73E-06	190	0.11	5.33	4.37 E-04	7.28E-06
S10	1.97E-05	2.93E-07	150	0.11	2	1.62 E-05	2.7E-07
S43	2.08E-05	2.78E-07	170	0.15	3	1.64 E-05	2.73E-07
S48	2.08E-05	4.45 E-07	259	0.12	3	2.82 E-05	4.7E-07
P22	2.16E-05	4.52E-07	75	0.15	3.42	4.05 E-05	6.75E-07
P31	2.17E-05	6.66 E-06	125	0.12	1.392	3.75 E-05	6.25E-07
P32	2.58E-05	2.33E-07	160	0.09	3.456	2.24 E-05	3.73E-07
P5	2.73E-05	4.58E-07	125	0.12	4	1.093 E-05	3.22E-07
S32	2.76E-05	4.78E-07	90	0.076	5	2.78 E-05	4.63E-07
S46	2.76E-05	1.97E-06	25	0.15	2.5	8.88 E-05	1.48E-06
S3	3.32E-05	1.07E-06	120	0.08	3	6.58 E-05	1.09E-06
P33	3.32E-05	2.4 E-06	450	0.1	30	1.35 E-05	2.25E-07
S36	3.48E-05	8.73E-07	75	0.15	5	5 E-04	8.33E-07
S37	4.32E-05	4.32E-06	108	0.1	1.1	9.94 E-05	1.66E-06
S52	4.42E-05	1.72E-06	115	0.15	2	0	0
S26	5.27E-05	1.33 E-06	30	0.076	3	4.14 E-03	6.9E-05
S44	5.52E-05	1.23E-05	7	0.2	2.5	0	0
S34	5.67E-05	3.9 E-06	90	0.2	1.8	2.17 E-04	3.62E-06

P25	5.88E-05	1.52E-06	140	0.064	15	8.23 E-05	1.37E-06
S45	6.95E-05	1.26E-05	8	0.2	0.24	2.46 E-04	4.1E-06
P2	8.38E-05	6.98E-07	350	0.15	8.5	4.44 E-05	7.33E-07
P4	9.8E-05	7.72E-07	225	0.051	12.5	1.39 E-05	2.32E-07
P17	9.93E-05	2.62E-06	90	0.2	4.5	0	0
P23	1.11E-04	8.7 E-07	212	0.22	5.04	0	0
P20	1.12E-4	4.03E-06	80	0.11	9	1.53 E-04	2.55E-06
S9	1.14E-04	4.2 E-05	8	0.12	5.143	0	0
P35	1.16E-04	4.28E-06	120	0.12	3.708	2.77 E-04	4.62E-06
S42	1.32E-04	3.58E-06	150	0.15	6	0	0
P21	1.40E-04	5.15 E-06	80	0.07	8	3.25 E-04	5.42E-06
S35	1.42E-04	6.58E-06	45	0.07	7.2	7.94 E-05	1.33E-06
P26	1.58E-04	1.67E-06	250	0.076	18	8.4 E-05	1.4E-06
S4	1.59E-04		9	0.5	7.2	0	0
P13	1.62E-04	2.67E-06	185	0.15	9	1.56 E-04	2.6E-06
S17	1.67E-04	7.72E-06	30	0.13	2.4	4.65 E-04	7.75E-06
P24	1.98E-04	5.52E-06	70	0.12	9	3.42 E-04	5.7E-06
P30	2.08E-04	2.43E-06	300	0.2	30	1.35 E-04	2.25E-06
P34	2.1E-04	5.27E-06	60	0.15	8.5	3.08 E-04	5.13E-06
S51	2.2E-04	3.68E-05	12	0.12	2	1.94 E-03	3.23E-05
P10	2.36E-04	8.73E-07	450	0.1	24	4.97 E-05	8.28E-07
P9	2.58E-04	1.25 E-06	260	0.15	33	5.59 E-05	9.32E-07
P8	2.63E-04	4.0 E-07	150	0.12	3	2.38 E-05	3.97E-07
P3	2.87E-04	2.87E-05	22	0.12	13	0	0
P28	3.62E-04	1.09E-05	60	0.138	10	7.01 E-04	1.16E-05
P27	3.73E-04	9.18E-06	60	0.151	12	5.8 E-04	9.67E-06
P15	4.23E-04	1.44E-06	450	0.15	43	8.9 E-05	1.48E-06
P7	4.72E-04	6.95 E-06	225	0.1	2.4	4.52 E-04	7.53E-06
S2	5.02E-04	3.87E-05	85	0.08	7.2	3.01 E-03	5.02E-05

P12	5.32E-04	2.03E-06	348	0.12	27	1.22 E-04	2.03E-06
P1	5.55E-04	3.33 E-05	260	0.12	36	2.32 E-04	3.85E-06
S5	6.21E-04	6.22 E-04	9	0.1	1	5.14 E-03	8.57E-05
S21	7.08E-04	4.38E-06	220	0.12	36	2.92 E-04	4.87E-06
S27	7.43E-04	6.67E-05	50	0.15	3	3.32 E-03	5.53E-05
P29	1.53E-03	3.9 E-05	55	0.15	15.5	2.18 E-03	3.63E-05
P14	2.72 E-03	5.18E-05	55	0.2	15.5	3.12 E-03	5.2E-05
S31	4.45 E-03	4.53E-05	150	0.12	90	2.22 E-03	3.7E-05
S28	6.61 E-03	3.15 E-03	10	0.5	3	0.018	3 E-03
S30	6.92 E-03	2.65 E-04	220	0.12	140	0.015	2.45 E-03
P11	n.a	n.a	375	0.2	10	0	0
std deviation	1.35 E-03	6.33 E-04				6.23 E-03	1.03 E-04

Table 6.3: Results of Conductivity and Transmissivity Obtained with Aquitest Software for WET Season 2013

ID	T with Theis m ² /s	K with Theis in m/s	Depth of the well in m	Rayon in m	Pumping rate in m ³ /h	T with Cooper m ² /s	K with Cooper m/s
P6	2.77E-06	2.1 E-08	150	0.2	0.5	3.27E-06	2.47E-08
S17	2.97E-06	1.35E-07	30	0.13	2.4	1.32E-06	5.95E-08
S45	4.72E-06	7.87E-07	8	0.2	0.24	4.85E-06	8.03E-07
S37	1.53E-05	9.58 E-07	108	0.1	1.1	1.49E-05	9.33E-07
P5	1.75E-05	3.63 E-07	125	0.12	4	2.9E-05	6.05E-07
S14	1.77E-05	9.82 E-08	26	0.2	0.8	0	n.a
S5	2.2E-05	1.47E-05	9	0.1	1	n.a	n.a
P18	2.35E-05	6.05 E-07	120	0.2	4.776	3.4E-05	8.72E-07
S50	2.63E-05	9.08 E-07	219	0.11	5.33	2.8E-05	9.68E-07
S47	2.78E-05	2.31667E-06	40	0.15	2	2.83E-05	2.35E-06
S2	3.17E-05	1.18 E-06	85	0.08	7.2	5.18E-05	1.95E-06
S3	3.32E-05	1.18E-06	120	0.08	3	4.55E-05	1.63E-06
P21	3.95E-05	1.39 E-05	80	0.07	8	4.23 E-04	1.49E-05
P8	4.18E-05	2.92E-07	150	0.12	3	5E-05	3.5E-07
P11	4.4E-05	2.57 E-07	375	0.2	10	5.1E-05	2.98E-07
S10	4.42E-05	6.3 E-07	150	0.11	2	5.12E-05	7.3E-07
S41	4.42E-05	2.45 E-06	25	0.05	2	1.02 E-04	5.67E-06
S51	4.42E-05	6.8 E-06	12	0.12	2	n.a	n.a
S27	4.68E-05	2.62 E-06	50	0.15	3	5.68E-05	3.17E-06
S15	4.72E-05	1.75 E-06	85	0.12	2.4	4.97E-05	1.83E-06
S49	5.08E-05	1.37E-06	90	0.15	2.3	0	n.a
P32	5.4E-05	6.07E-07	160	0.09	3.456	5.4E-05	6.35E-07
P31	5.47E-05	1.56 E-06	125	0.12	1.392	5.55E-05	1.59E-06
S32	5.53E-05	9.3 E-07	90	0.076	5	6.7E-05	1.13E-06

P13	5.6E-05	6.68 E-07	185	0.15	9	5.88E-05	7.02E-07
S39	5.73E-05	4.58 E-06	160	0.2	1.3	6.03E-05	4.83E-06
S48	5.9E-05	6.08 E-07	259	0.12	3	6.12E-05	6.32E-07
S43	6.62E-05	5.47E-07	170	0.15	3	7.25E-05	5.98E-07
P4	6.93E-05	5.22E-07	225	0.051	12.5	7.52E-05	5.65E-07
S35	7.1E-05	2.62 E-06	45	0.07	7.2	7.67E-05	2.83E-06
P22	7.55E-05	1.57E-06	75	0.15	3.42	8.12E-05	1.68E-06
S42	9.38E-05	1.47 E-06	150	0.15	6	9.45E-05	1.47E-06
P17	9.93E-05	2.25 E-06	90	0.2	4.5	0	n.a
P35	1.03 E-04	3.32E-06	120	0.12	3.708	1.03 E-04	3.52E-06
P34	1.05 E-04	2.5 E-06	60	0.15	8.5	1.02 E-04	2.42E-06
P7	1.06 E-04	8.85 E-07	225	0.1	2.4	1.26 E-04	1.05E-07
P23	1.11 E-04	8.7 E-07	212	0.22	5.04	0	n.a
P15	1.19 E-04	5.62 E-07	450	0.15	43	1.27 E-04	5.97E-07
S46	1.24 E-04	1.12 E-05	25	0.15	2.5	1.23 E-04	1.11E-05
S26	1.32 E-04	6.45 E-06	30	0.076	3	1.32 E-04	6.45E-06
S44	1.39 E-04	2.77 E-05	7	0.2	2.5	1.38 E-04	2.75E-05
P20	1.41 E-04	5.63E-06	80	0.11	9	1.57 E-04	6.28E-06
S52	1.56 E-04	5.07 E-06	115	0.15	2	1.59 E-04	5.15E-06
S4	1.59 E-04	3.17 E-04	9	0.5	7.2	n.a	n.a
P24	1.76 E-04	1.38 E-06	70	0.12	9	1.75 E-04	1.37E-06
S28	1.87 E-04	4.05 E-05	10	0.5	3	2.48 E-04	5.4E-05
P33	2.08 E-04	9.7 E-07	450	0.1	30	2.25 E-04	1.04E-06
P25	2.33 E-04	1.24 E-05	140	0.064	15	2.45 E-04	1.31E-05
P3	2.87 E-04	2.05 E-05	22	0.12	13	n.a	n.a
P27	3.73 E-04	8.08E-06	60	0.151	12	3.88 E-04	8.42E-06
S36	3.92 E-04	8.16E-06	75	0.15	5	3.81 E-04	7.95E-06
P1	3.98 E-04	2.4 E-06	260	0.12	36	1.25 E-03	7.35E-06
P30	4.18 E-04	4.53E-06	300	0.2	30	4.35 E-04	4.73E-06

P26	4.45 E-04	4.62 E-06	250	0.076	18	4.63 E-04	4.82E-06
P9	4.6 E-04	3.93 E-06	260	0.15	33	4.53 E-04	3.88E-06
S34	5.528 E-04	3.1 E-04	90	0.2	1.8	7.8 E-04	4.35E-05
P12	7.5 E-04	2.87E-06	348	0.12	27	8.02 E-04	3.05E-06
P10	8.4 E-04	3.067E-05	450	0.1	24	1.04 E-03	3.82E-06
S21	1.12 E-04	5.85 E-06	220	0.12	36	1.11 E-03	5.75E-06
P2	1.51 E-04	1.08E-05	350	0.15	8.5	2.88 E-03	1.93E-05
S31	1.77 E-03	1.75 E-05	150	0.12	90	2.15 E-03	2.12E-05
S30	1.95 E-03	9.42E-06	220	0.12	140	2.08 E-03	1.01E-05
P14	1.98 E-03	1.36 E-05	55	0.2	15.5	0	n.a
P29	3.83 E-03	9.07E-05	55	0.15	15.5	4.02 E-03	9.5E-05
S9	1.14 E-02	6.3 E-02	8	0.12	5.143	6.55 E-04	3.63 E-04
P16	0.139	8.87 E-04	250	0.15	2500	0.143	9.46 E-04
P28	6.98 E-04	1.46 E-05	60	0.138	10	7.33 E-04	1.53E-05
Std deviation	0.853	7.75 E-04				0.035	4.21 E-04

6.3. Interpretation of Theis and Cooper Jacob

Theis and Cooper-Jacob methods are the conventional methods used for field applications in order to estimate the subsurface flow parameters based on the assumption of homogeneity. As a result of this assumption, these pumping test analysis procedures yield representative single estimates of the flow parameters of the aquifer volume surrounding the pumping well. The two methods were performed on Aqitest software by inserting the drawdown data collected at different times to estimate representative values of the flow parameters. For example, the graphical curve fitting the Theis approach attempts to fit drawdown data observed at different times to normalized drawdown curves. The Cooper-Jacob method is based on a straight line fit to the late drawdown data. Drawdowns from the 66 simulated well tests were interpreted with Theis and Cooper-Jacob methods; therefore giving us transmissivity and conductivity values. In general, transmissivity values in a confined aquifer are more important than storativity.

Water levels measurements for pumping were taken as the following

Time since start of pumping (minutes)	Time intervals (minutes)
0 – 5	0.5
5 – 60	5
60 – 120	20
120 – shut down the pump	60

After the pump has been shut down, the water levels in the well will start to rise again.

These rises can be measured in what is known as recovery test. If the pumping rate was not constant throughout the pumping test, recovery-test data are more reliable than drawdown data because the water table recovers at a constant rate.

Two example applications using Aquitest program for the wet and dry season of the year 2012/2013 was done with the field data gathered during the hydrogeologic investigations of the aquifer. Results obtained by means of the computer program indicate high transmissivity values ($T > 10^{-4} \text{ m}^2/\text{s}$), low transmissivity values ($T < 10^{-6} \text{ m}^2/\text{s}$) and standard transmissivity values ranging in the $10^{-5} \text{ m}^2/\text{s}$. Thus indicating a principal direction of flow, in the range transmissivity and conductivity from upward (low values) towards the sea (increase in values).

To be able to interpret these range values, transmissivity is defined as the measure of how much water can be transmitted horizontally, such as to a pumping well (Krasny J., March-April 1993). When the soil layer is entirely below the water table, its saturated thickness corresponds to the thickness of the soil layer itself. When the water table is inside a soil layer, the saturated thickness corresponds to the distance of the water table to the bottom of the layer. As the water table may behave dynamically, this thickness may change from place to place or from time to time, so that the transmissivity may vary accordingly.

The hydraulic conductivity and transmissivity values in the aquifer are uniformly distributed spatially and fall within a similar range, but since we are in a karstic limestone aquifer, some conductivity and transmissivity values are irregular or higher than the surrounding pumped wells. Those values are due to the presence of the well in bedrock because groundwater flowing in bedrock is controlled primarily by fractures, which are unevenly distributed throughout the aquifer. Most transmissivity and hydraulic-conductivity values were within published ranges for the type of sediment or rock tested. The zones of highest hydraulic conductivity in the aquifer are either in coastal area or in areas where the topologic formation affects the values. In moderately seen values of conductivity and transmissivity, the geologic formations tend to be less karstic such as in Ayto (P6). Therefore; this implies that the differences in hydraulic conductivity and transmissivity values observed amongst the wells is largely due to formation, spatial heterogeneity rather than differences in well construction and installation, or test method. The standard deviation of 7.75×10^{-4} in wet season and 6.3×10^{-4} in dry season for conductivity; as for transmissivity, the standard deviation range from 3.34×10^{-2} in wet season and 1.35×10^{-3} in dry season.

Within the main steps in aquifer-test data interpretation, the analysis of the relationship between

drawdown to time while considering the hydrogeologic setting is an essential key. The characteristic shape of the curves generated by plotting drawdown versus elapsed time using log-log scale and log-linear scale provides clues about the aquifer flow characteristics. As seen in the graphs plotted with Aquitest software, in the earliest part of a drawdown test, the water level in the pumped well will have drawn down enough to create a hydraulic gradient into the well that is sufficient to produce the volume of water being pumped, and the well discharge will be almost entirely water that is stored in the wellbore. Wellbore storage effects are more pronounced the larger the pumping well diameter and the lower the aquifer transmissivity (Moench F., November - December 1993). My analysis of the drawdown response in all 66 wells using the Theis confined aquifer solution (Theis, 1935) with as well Cooper Jacob later on is to certify the values, showed a similar curve pattern for almost all wells. Curve matches from the software program are shown in figure 6.3.

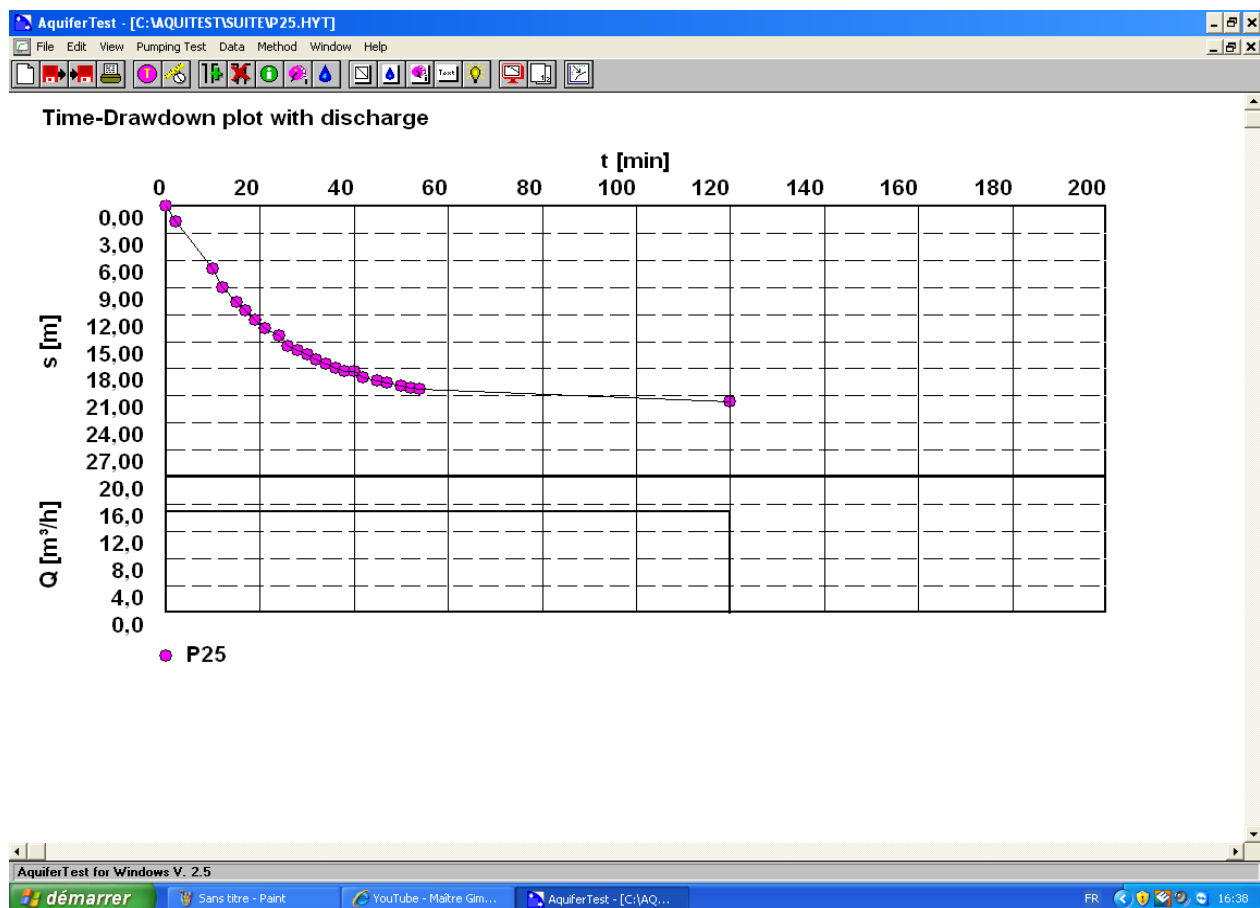


Figure 6.3 Time Drawdown Plot with Discharge

From the table 6.1 and 6.2, the following was concluded; the high transmissivity values are due to the small amount of observed drawdown, which could be a result of:

1. unknown sources of recharge to the aquifer in the vicinity of the observation wells,
2. a semi-permeable barrier to groundwater flow for the pumping which would result in more drawdown on the pumping side of the barrier,
3. Leakage from overlying or underlying units. Leaky aquifer solutions produced similar trends due to the karstic composition of the studied area.
4. Permeability and transmissivity depend on the relation between the rock heterogeneity to the extent of the studied area. (RATS , 1967),

6.4 Conclusion

No homogeneous environment exists under natural conditions; all environments are heterogeneous to a different extent often depending on the extent of the studies area. (Krasny J., March-April 1993).

The proposed explanation for conductivity and transmissivity handled in this chapter aims to provide a basis for quantitative and objective expression and representation of prevailing hydrogeological map of the Miocene limestone aquifer of North Lebanon.

CHAPTER 7

MODELING GROUNDWATER USING VISUAL MODFLOW

7.1 Introduction

In recent years, several numerical and analytical groundwater models are used to simulate the behavior of groundwater structures. Almost in all cases, analytical methods cannot be considered as feasible due to the heterogeneity of the aquifer, irregular shape of the boundaries and spatial distributions of the watershed. On the contrary, numerical models are based on methods of finite elements such as finite element (Modflow) which has been developed and used to simulate the aquifer systems with the boundary and initial conditions. The creation of such a model, also referred to as modeling, is quite time consuming because of the large data entry required to run.

Groundwater models are tools that allow us to develop a representation of the processes that occur in the groundwater environment; in order to predict the behavior of the groundwater system: flow heads, drawdown, pathlines, transport, concentration etc... (Matthias Raiber a, 2012)

- Maps are numbers first, pictures later
- Understanding that a digital map is first and foremost an organized set of numbers is fundamental to analyzing mapped data.
- The concept of “vector” and “raster” are an essential component of the map. Within this context, the location of map features are translated into computer form as organized sets of X,Y coordinates “vector” or grid cells “raster”
- What is the objective of statistical analysis
- The hydrology tools are used to model the flow of water across a surface.
- When modeling the flow of water, you may want to know where the water came from and where it is going. It will give a clearer view on how to use the hydrologic analysis functions to help model the movement of water across a surface.
- It also gives ideas on how the tools can be used to extract hydrologic information from a

digital elevation model (DEM)

- It can be used to determine the values for the points where measurements are not made or are not feasible.
- It can analyze spatial variability and spatial interpolation → Kriging provides the best linear unbiased estimation for spatial interpolation.

7.1.1 Gridding Overview

- Contour maps, image maps, shaded relief maps, vector maps, and wireframe maps all require grids for their generation in Visual Modflow, GIS and Surfer.
- A grid is a regular, rectangular array of values. The [Grid | Data](#) command provides you with several methods for generating a grid file [.GRD] from the X Y Z data.
- Gridding methods produce a regularly spaced, rectangular array of Z values from irregularly spaced X, Y, and Z data.
- A grid is a rectangular region comprised of evenly spaced rows and columns. The intersection of a row and column is called a grid node. Grid file columns and rows are sometimes referred to as X grid lines and Y grid lines, respectively.
- When XYZ data are collected on regular intervals, you may produce a grid file that uses the Z values directly and does not interpolate the values for the grid nodes.
- If we provide Visual Modflow, GIS and Surfer with the locations of the wells (the XY coordinates) and the depth to the water table (the Z value) in the form of an XYZ data file, **the 3 software's** can produce a grid file and, ultimately, a grid-based map from the original data.

7.1.2 Gridding Method

In a scattered groundwater observation net, geostatistical methods can be used to determine the values for the points where measurements are not made or are not feasible. Geostatistics provides a set of statistical tools for analyzing spatial variability and spatial interpolation. Kriging provides the best linear unbiased estimation for spatial interpolation (Esri). Nowadays, Geostatistics has become a popular means to describe spatial patterns and to interpolate the attribute of interest at un-sampled locations. Geostatistical methods have been increasingly used in many disciplines, such as meteorology, hydrology, geology, and environmental sciences. The choice of the interpolation technique depends on the distribution of points in the data set, application domain, approximating function, or the method that is prevalent in the discipline. Differences between the gridding methods are in the mathematical algorithms used to compute the weights during grid node interpolation. Each method can result in a different representation of the data. It is advantageous to test each method with a typical data set to determine the gridding method that provides us with the most satisfying interpretation of the data.

1. Inverse Distance to a Power
2. Kriging
3. Minimum Curvature
4. Modified Shepard's Method
5. Natural Neighbor
6. Polynomial Regression
7. Radial Basis Function
8. Triangulation with Linear Interpolation
9. Moving Average

Along the 9 proposed methods, Kriging method was found to suit us the most. Here is a small briefing on the characteristics of the chosen method for our study.

7.1.3 The Kriging Formula

Kriging is formed as a weighted sum of the data:

$$\hat{Z}(s_0) = \sum_{i=1}^N \lambda_i Z(s_i) \quad (7.1)$$

Where:

$Z(s_i)$ = the measured value at the i location

λ_i = an unknown weight for the measured value at the i location

s_0 = the prediction location

N = the number of measured values

With the Kriging method, the weights λ_i , are based not only on the distance between the measured points and the prediction location but also on the overall spatial arrangement of the measured points. Kriging goes through a 2 step process:

1. It creates the variograms and covariance functions to estimate the statistical dependence (called spatial autocorrelation) values that depend on the model of autocorrelation (fitting a model).
2. It predicts the unknown values (making a prediction).

It is because of these two distinct tasks that it has been said that Kriging uses the data twice: the first time to estimate the spatial auto-correlation of the data and the second to make the predictions (Itanidis P. K, 1997). Below is a representation, with Surfer software; of the area of study.

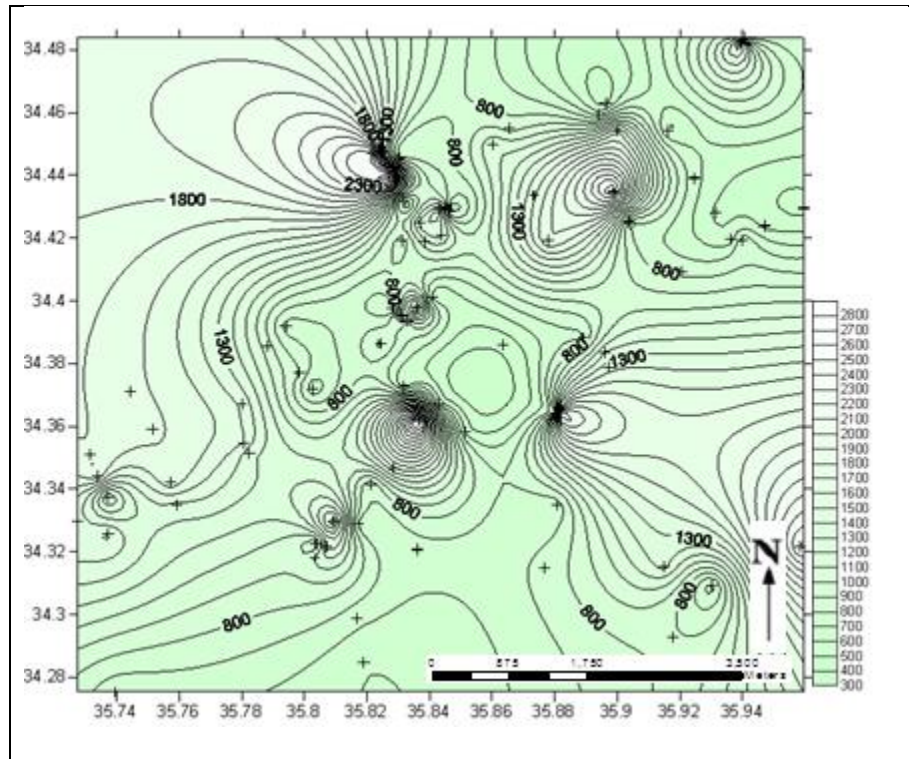


Figure 7.1 Area of Study Applied with Surfer Software using Kriging Method

Kriging was the Interpolation Method used and assumed for the model. In theory, no other method of grid generation can produce better estimates (in the sense of being unbiased and having minimum error.) In practice, the effectiveness of the technique depends on the correct specification of several parameters that describe the semi-variograms and the model of the drift. In this way by Kriging, maps were accomplished for all parameters (chemical and physical parameters) for the 2 seasons studied.

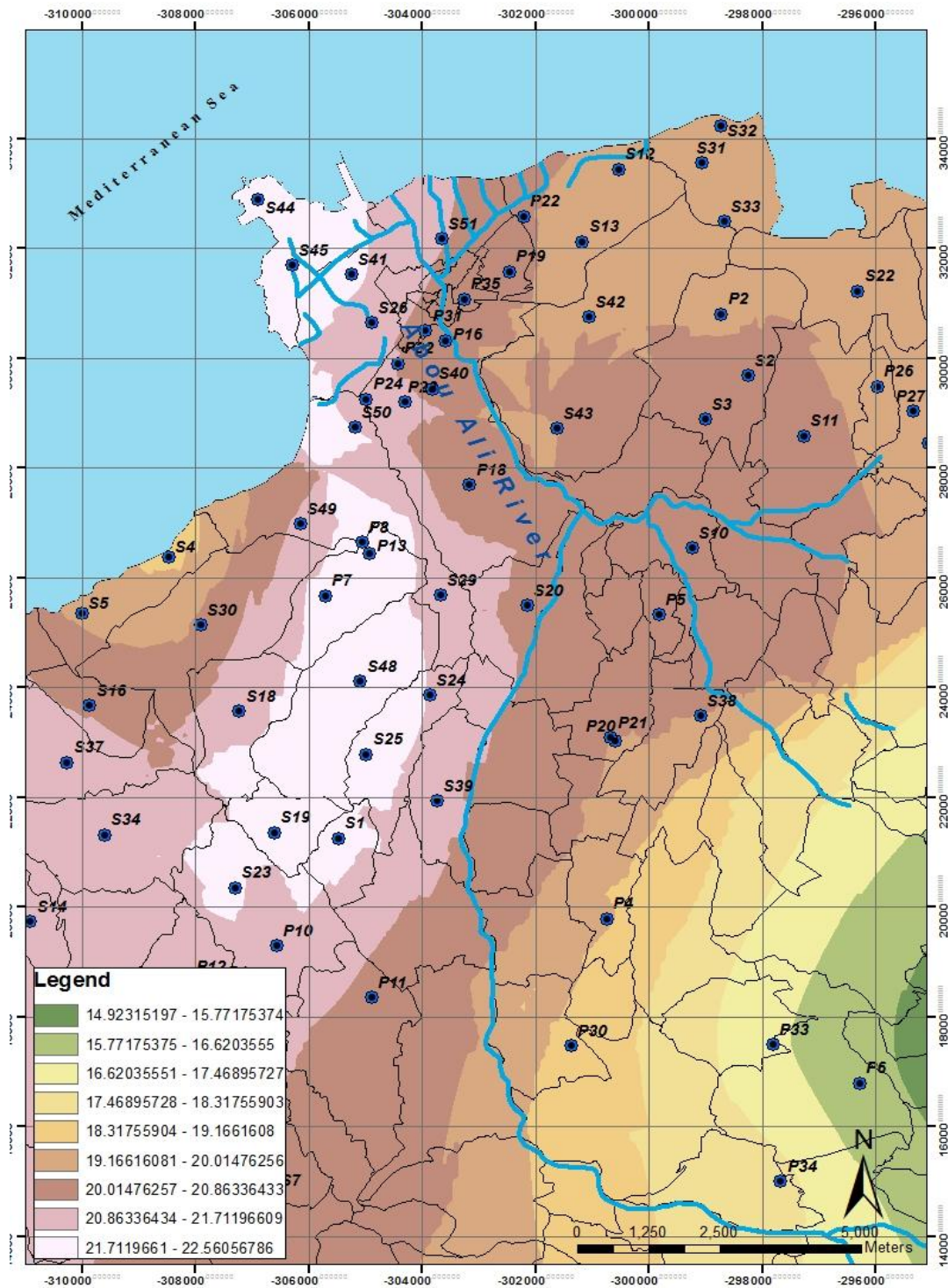


Figure 7.2 Temperature Variations (in °C) for the Studies Area using Kriging Method (GIS)

7.2 Geographical Information System and Visual Modflow for Our Study

Visual Modflow Flex (VMOD Flex) is a powerful software package that provides the tools for building three-dimensional groundwater conceptual and numerical models using raw Geographical Information System (GIS) data objects. (Harbaugh, Banta, & Hill, 2000) .The conceptual model approach to groundwater modeling allows us to do the following:

- Build a conceptual model of the groundwater system, prior to the simulation .The geological formations, property model, and boundary conditions are all designed outside the model grid or mesh; this allows the flexibility to adjust the interpretation of the groundwater system before applying a discretization method and converting it to a numerical model. (AberJ.T., 2007)
- Build the model with minimal data pre-processing required .Working with grid-independent data allows us to maximize the use of the existing GIS data and incorporate physical geology and geographic conditions before designing a grid or mesh.
- Generate and simulate and design local grids around areas of interest, directly within the conceptual model environment.
- Make changes to the model data and immediately see results. The conceptual model environment provides simultaneous 2D and 3D views which are updated whenever changes to the data are made.

All of the data that used within VMOD are referred to as data objects. These can consist of:

- Raw data that was imported either in the form of polyline or polygon shape files, wells from a excel sheet, surfaces from Surfer, GRD, etc.
- Conceptual data objects were generated during the development through the conceptual model, and include: Structural Zones, Property Zones, and Boundary Conditions.
- Numerical model data objects were produced throughout the progress through numerical modeling and include:
 - Input: Numerical Grid, Properties (Conductivity, Initial Heads, etc.), Boundary Conditions (a group of river cells, drain cells, pumping wells, etc.), Observation Wells,

Zone Budget zones.

-Output: Calculated Heads, Drawdown, Pathlines, etc.

The map should have all these files in the same folder to open

- We couldn't work it with WGS UTM as the Hillshade in Lebanon is only Stereo
- Find below the projection :
 - **Lebanon-Stereo**
 - **Projection: Stereographic**
 - **False_Easting: 0.000000**
 - **False_Northing: 22.000000**
 - **Central_Meridian: 39.150000**
 - **Scale_Factor: 0.999534**
 - **Latitude_Of_Origin: 34.200000**
 - **Linear Unit: Meter**
 - **GCS_Clarke_1880**
 - **Datum: D_Clarke_1880**

Visual Modflow is a graphical user interface that allows developing:

- A Modflow model of the groundwater flow system
- A MT3D/RT3D model of solute transport in the Modflow model
- A well calibrated model using WinPest

Therefore VMOD is a mathematical representation of the groundwater environment.

The real world	VMOD world
Stratigraphy	Grid structure (layer bottom elevation)
Geology	Model parameters (K, Sy, n, ...)
Flow boundaries	Boundary conditions (riv, ...)
Field observations	Observation wells (head, concentrations,...)

There are two types of data that we need to collect,

1. Input parameters that are used to construct the model
 - Model geometry, horizontal and vertical extent, layer structure
 - Properties; conductivity, porosity,
 - Boundaries; location, value, time dependence.
2. Observations that are used to calibrate the model

A Conceptual Model refers to a basic, high-level representation of the hydrogeological system being modeled. It will form the foundation for one or more numerical models. In VMOD Flex, the conceptual model is completely grid and simulator independent. This means you define the inputs using your raw data objects (surfaces, polylines, polygons, etc.). The grid or mesh is only introduced at the time of launching a numerical model. This allows you to:

The sequential step in building the conceptual model are presented in the workflow navigator and are summarized below:

Convert the conceptual model to multiple numerical models for uncertainty analysis

Convert the conceptual model to a MODFLOW

Easily update corresponding numerical models as your conceptualization changes

The sequential steps in building the conceptual models are summarized below:

1. Define Modeling Objectives
2. Collect Data Objects (through importing maps in the form of polylines from GIS database or creating)
3. Define the Conceptual Model Area
4. Define Model Structure (vertical layering)

5. Define Property Zones (parameter values for Conductivity, Initial Heads, and Storativity)
6. Define Boundary Conditions (constant heads, drains, pumping wells, rivers, evapotranspiration, etc.)
7. Define Numerical Grid or Finite Element Mesh (Finite Difference Grid used for MODFLOW)
8. Convert to Numerical Model (generate numerical inputs for a MODFLOW model)
9. Translate to Finite Element Model

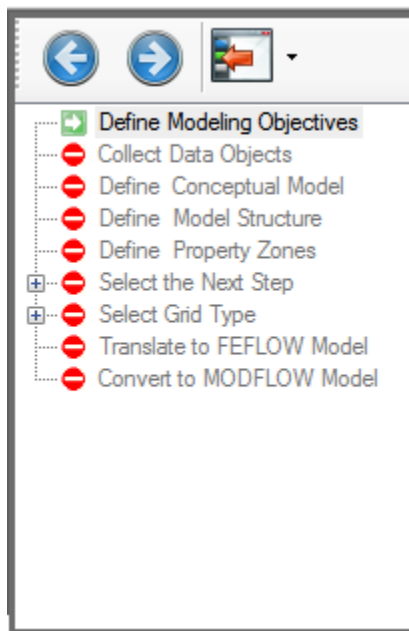


Figure 7.3 Window Appearing in VMOD Upon its Creation

7.2.1 Procedure in Simulation of VMOD

Let us discuss briefly step by step the procedure of the modeling:

Collecting the data object is the first procedure done

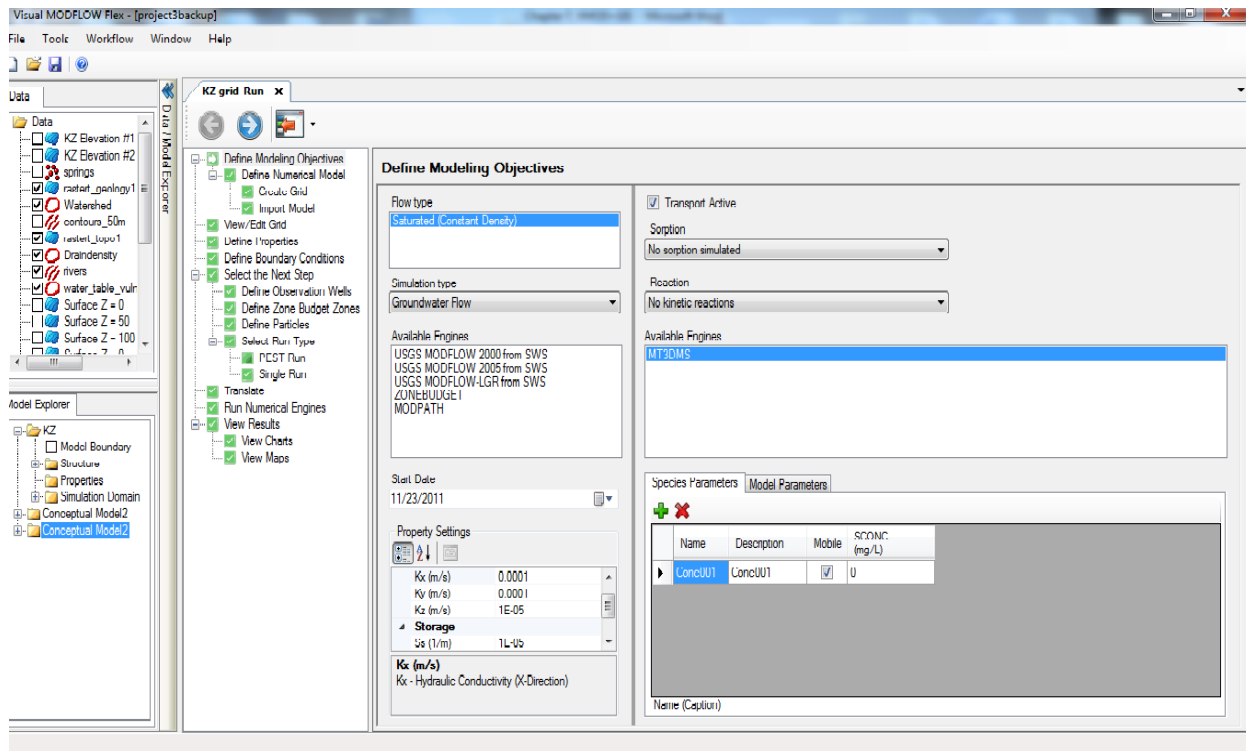


Figure 7.4 Collecting Data with VMOD

In this step, we collect the data wanted to build and interpret the model. This means that the data object as are collected to be used appropriately in order to use these at a particular step in the workflow. The data objects can be collected through several ways:

- Importing data: importing GIS data (shapefiles, polylines, polygons, and CAD files), gridded data, images, points/ wells in excels spreadsheets etc...
- Creating data objects: digitizing new points, polygon or polyline etc...
- Creating Surfaces: interpolating X, Y and Z points using Kriging method in our cases.

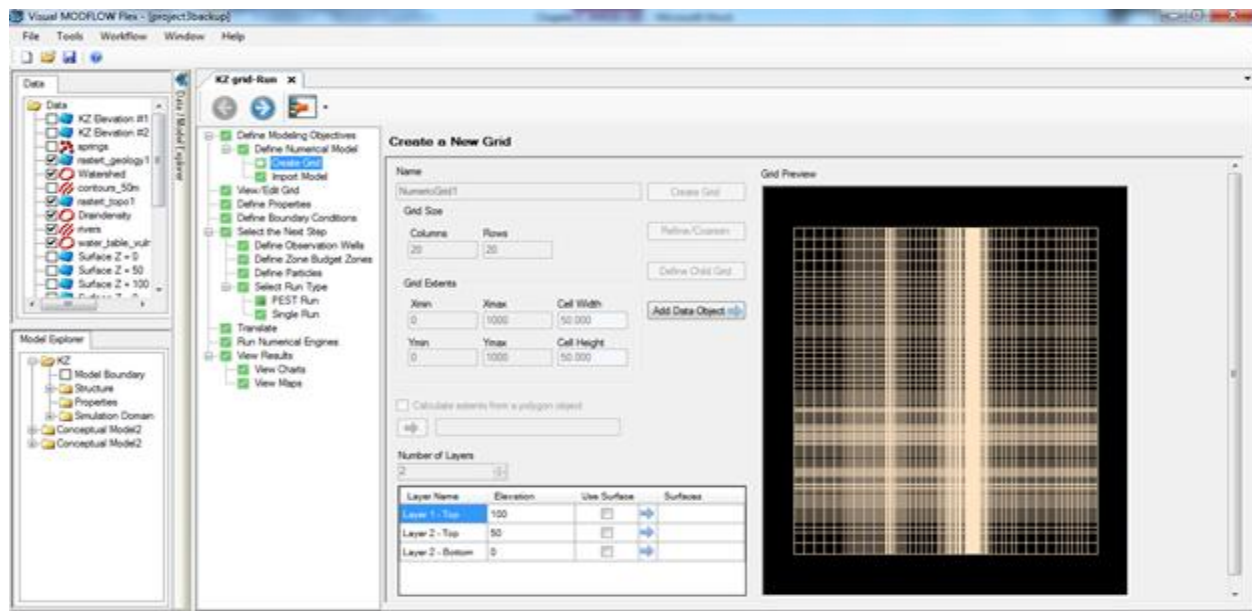


Figure 7.5 Creating Grid System in VMOD

See the following table for some typical data object types and how they are used in the conceptual model workflow. (A. W. Harbaugh, 2000)

Table 7.1 Typical Data Object Used for a Conceptual Model Workflow (Harbaugh, Banta, &

If you have...	First you should..	Then you can..
River locations in a shapefile	1- Import these as Polyline Initial heads.	Select this data object when creating a river boundary condition
Geological layers in a Surfer .GRD or ASCII GRD	Import these as Surface data objects	Select these data objects when defining horizons
Air photo with river location	Import this as a Map image Then Create a new Polyline data object Digitize the polyline in a 2D Viewer	Select this new polyline data object when creating a river boundary condition
XYZ points for geological contacts	Import these as Points data objects Then "Create Surfaces" from these data objects	Select these surfaces when defining horizons or numerical model layers
Raster Grid of Kx or Recharge data (from Surfer, ESRI .GRD)	Import these as surface data objects	Select these data objects when defining properties or Recharge boundary conditions

Hill, 2000)

The elevation in the model area was inserted as a DEM from ArcMap, where the high and low values of top and bottom elevation were used.

7.2.1.1 Defining Properties

At this step Defining properties Zones for the model where each zone is assigned appropriate attributes, such as conductivity, storage, and initial heads. In the groundwater flow modeling, many different types of data to simulate the hydrogeological processes influencing the flow of groundwater are needed. The hydrogeological characteristics of the model are classified into the

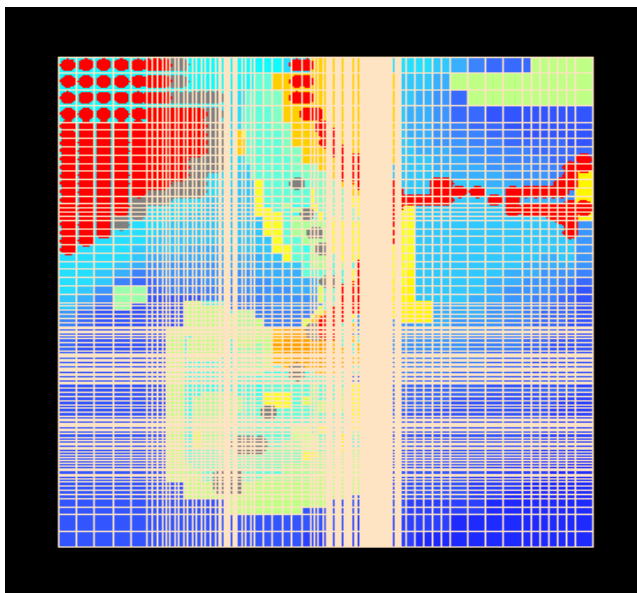
following parameters:

- Conductivity (K_x , K_y , K_z)
- Storage S_s , S_y , P_{eff} ,
- Initial Heads

See figure below, where conductivity values are set for each zone of the modeling area.

1-Conductivity (K_x , K_y , K_z)

Hydraulic conductivity describes the ease with which a fluid (usually water) can move through pore spaces or fractures. It depends on the intrinsic permeability of the material and on the degree of saturation, and on the density and viscosity of water (Vieux E. B., 2004). The hydraulic conductivity varies according to the geological unit, in particular fractured rocks aquifer. Hydraulic conductivity in our study was determined by Theis and Cooper Jacob results according to the sampling campaigns and was assigned and entered into visual Modflow as excel sheets. In addition from precious studies, (Programme des Nations Unies pour le Développement F. C., 1971) the area was divided into different zones with different geological formation, therefore in addition to the excel spreadsheets, a surface file (with Surfer) was applied with the different zones containing different hydraulic conductivity values. Refer to figure below.



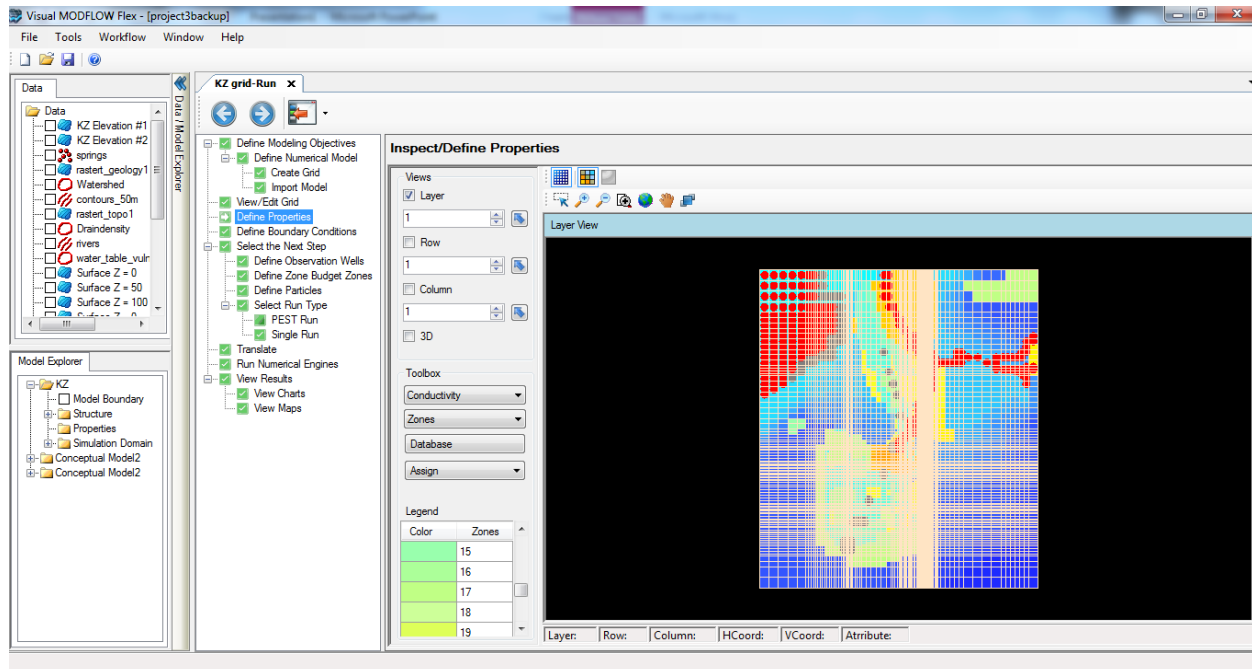


Figure 7.6 Defining Model Properties for the Studied Area

2- Effective Porosity and Specific Yield

Porosity is defined as the volume of pore space; it is the volume of pores divided by the total volume (including pore volume and solid volume) (Fetter C.W., 2001). It controls the volume of water that can be stored in the saturated zone. These parameters are used in Visual Modflow to calculate the average velocity of flow through the porous medium (AberJ.T., 2007). The table 7.2 indicates the total porosity values for all geological material, and shows that the values available are not constant quantities because the soil, specially soil containing clay swells, shrinks, compacts and cracks. The effective porosity, n_e , referred to as kinematic porosity is defined as the ratio of the part of the pore volume where the water can circulate to the total volume of representative sample of the medium (Fetter C.W., 2001). It is essential in VMOD because it estimates the mean velocity of the

flow of water through the porous medium of our modeling.

Table 7.2: Representative Porosity Values (Wortter & Sunada, 1977)

Material	Total Porosity, pt	Arithmetic Mean	Effective Porosity, a pe	Arithmetic Mean
	Range		Range	
Sedimentary material				
Sandstone (fine)	-b	-	0.02 - 0.40	0.21
Sandstone (medium)	0.14 - 0.49	0.34	0.12 - 0.41	0.27
Siltstone	0.21 - 0.41	0.35	0.01 - 0.33	0.12
Sand (fine)	0.25 - 0.53	0.43	0.01 - 0.46	0.33
Sand (medium)	-	-	0.16 - 0.46	0.32
Sand (coarse)	0.31 - 0.46	0.39	0.18 - 0.43	0.3
Gravel (fine)	0.25 - 0.38	0.34	0.13 - 0.40	0.28
Gravel (medium)	-	-	0.17 - 0.44	0.24
Gravel (coarse)	0.24 - 0.36	0.28	0.13 - 0.25	0.21
Silt	0.34 - 0.51	0.45	0.01 - 0.39	0.2
Clay	0.34 - 0.57	0.42	0.01 - 0.18	0.06
Limestone	0.07 - 0.56	0.3	~0 - 0.36	0.14

Specific yield S_y , is defined as the volume of water drained from a saturated sample of unit volume with a unit decrease of the water table (Masters, 1994). Specific yield is not necessarily equal to porosity and is not necessarily inserted in the modeling.

3- Initial Heads

Initial head is the height of water in a well relative to a datum (sea level). It is measured as the depth below the natural surface (Eisenlohra L Bouzelboudjena M., 1997). Groundwater will always move from high to low hydraulic (initial) head. The depth of the well and water level where accomplished in the sampling campaigns accomplished for this study and were inserted as excel worksheets for VMOD simulation.

7.2.2. Boundary Conditions

The first step involves selecting the boundary condition type and specifying the location of the boundary condition on the simulation domain.

Constant Head
River
General Head
Drain

Recharge
Evapotranspiration
Lake
Specified Flux

In VMOD Flex, boundary condition types are separated into three categories:

- Boundary condition (standard) (Constant Head, Rivers, Drains, General Head, Recharge, EVT, etc.)
- pumping wells

1- Constant Head

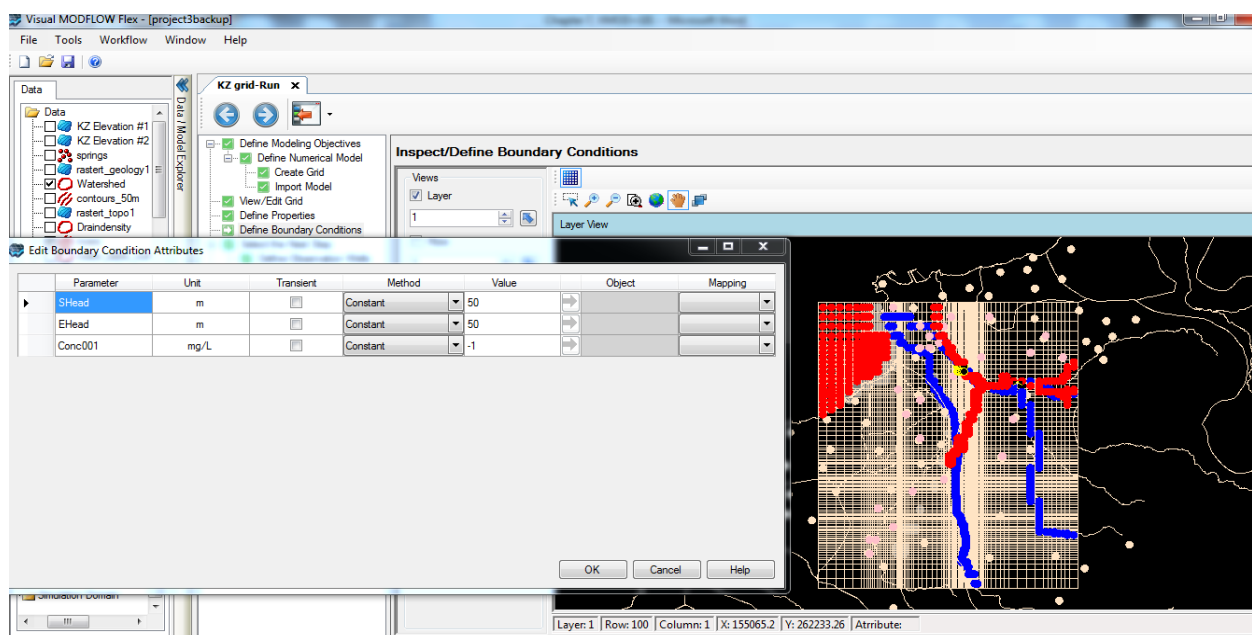


Figure 7.7 Defining Boundary Conditions

The boundary conditions were inserted in the model step by step. The constant head condition was divided into 3 scenarios. The first one were the grid cells of the model were kept untouched, this means that the hydraulic head was computed as 1 (its concentration) and therefore the cells were active cells. The second set-up is inserting a constant head, with concentration of (-1), this is the case of the river and the sea such as presented in the figure 7.7. The third setting was a no flow within the cell, meaning a cell value of zero (inactive cells).

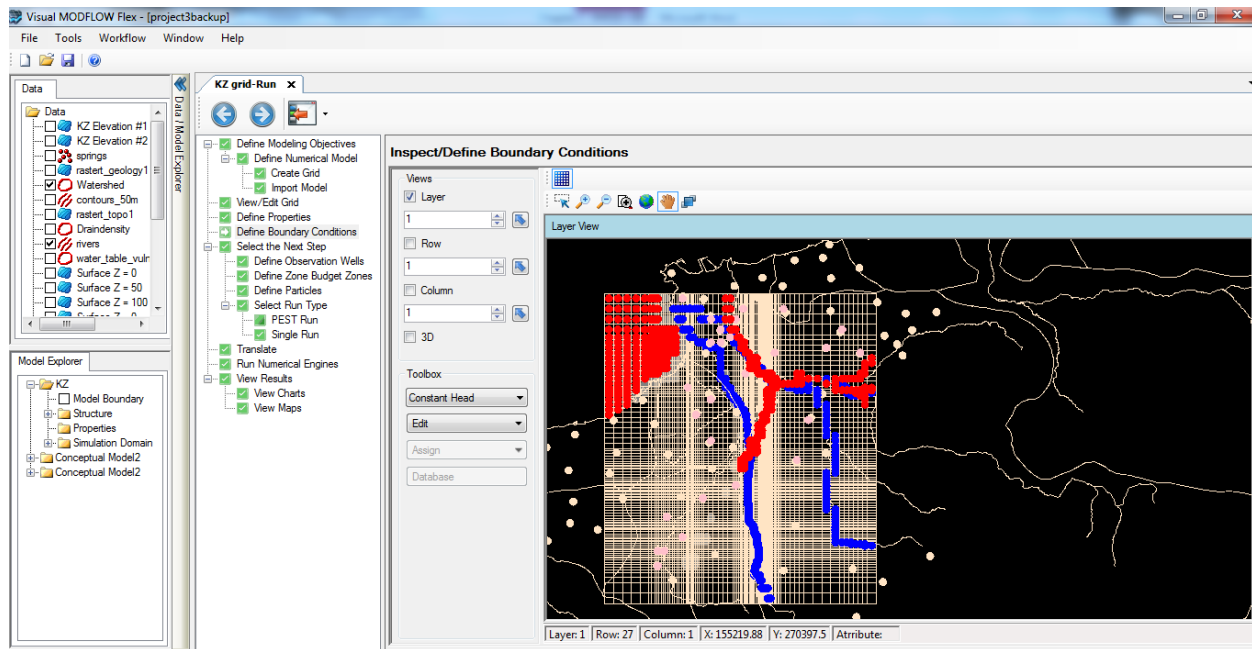


Figure 7.8 Constant Head Condition with VMOD

2- River

The River boundary condition is used to simulate the influence of a surface water body on the groundwater flow. Surface water bodies such as rivers, streams, may either contribute water to the groundwater system, or act as groundwater discharge zones, depending on the hydraulic gradient between the surface water body and the groundwater system (A. W. Harbaugh, 2000). The MODFLOW River Package simulates the surface water/groundwater interaction via a seepage layer separating the surface water body from the groundwater system (see following figure 7.9).

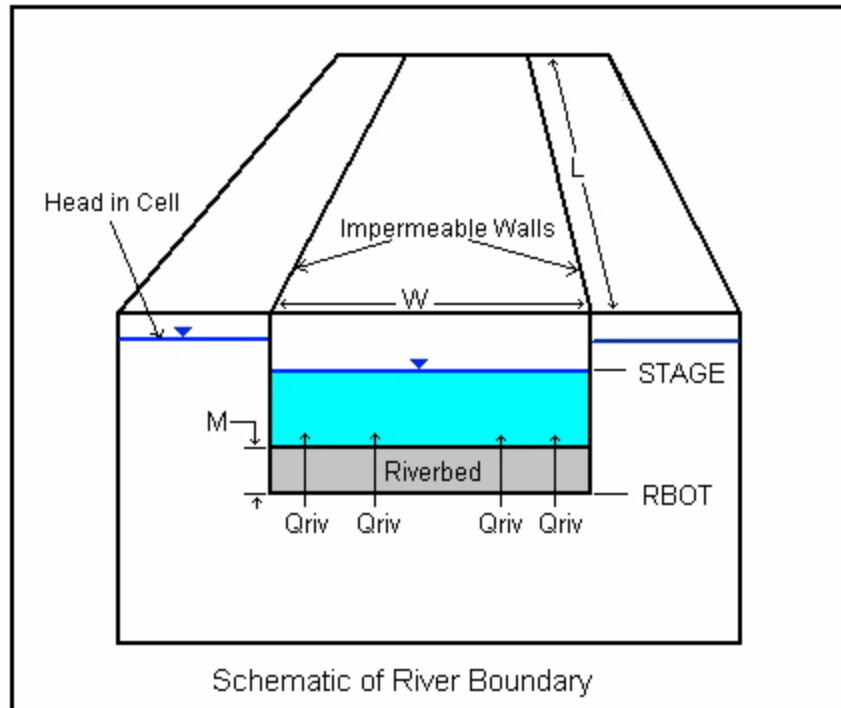


Figure 7.9 River Boundary Condition as Seen in VMOD (A. W. Harbaugh, 2000)

To stimulate the effect of flow between the surface water features and groundwater systems, different types of data are required for each grid cell containing a river boundary (A. W. Harbaugh, 2000). When a river boundary condition is assigned, the default leakance option is automatically selected. If the default Leakance option is selected, the river boundary condition requires the following data:

- River Stage: The free water surface elevation of the surface water body.
- Riverbed Bottom: The elevation of the bottom of the seepage layer (bedding material) of the surface water body.
- Riverbed Thickness: Thickness of the riverbed
- Leakance also referred to as conductance of the riverbed: A numerical parameter representing the resistance to flow between the surface water body and the aquifer (this field is read-only and is calculated using the formula described below).
- Riverbed K_z : Vertical hydraulic conductivity of the riverbed material.
- River Width: Width of the river.

According to the previous studies, UN booklet 1971 and the study on sustainable management of scarce resources in the coastal zone (Hakim B., 1977) ; these are the following data inserted in VMOD:

- Hydraulic Conductivity is considered as 0.25 m/d. this values is needed to calculate the conductance of the riverbed.
- River width= 12 m
- Average depth at midpoint = 1 m
- Cross-section area= 7.70 m²
- Depth at the South-West side =1.25m
- Depth at the North-West side= 0.75 m
- Length = 3km
- Leakance also referred to as conductance of the riverbed The Leakance value (C) may be calculated from the length of a reach (L) through a cell, the width of the river (W) in the cell, the thickness of the riverbed (M), and the vertical hydraulic conductivity of the riverbed material (K) using the following formula:

$$C = \frac{K \times L \times W}{M}$$

$$C = 0.25 \times 200 \times 12 / 1 = 6 \text{ m}^2/\text{d}$$

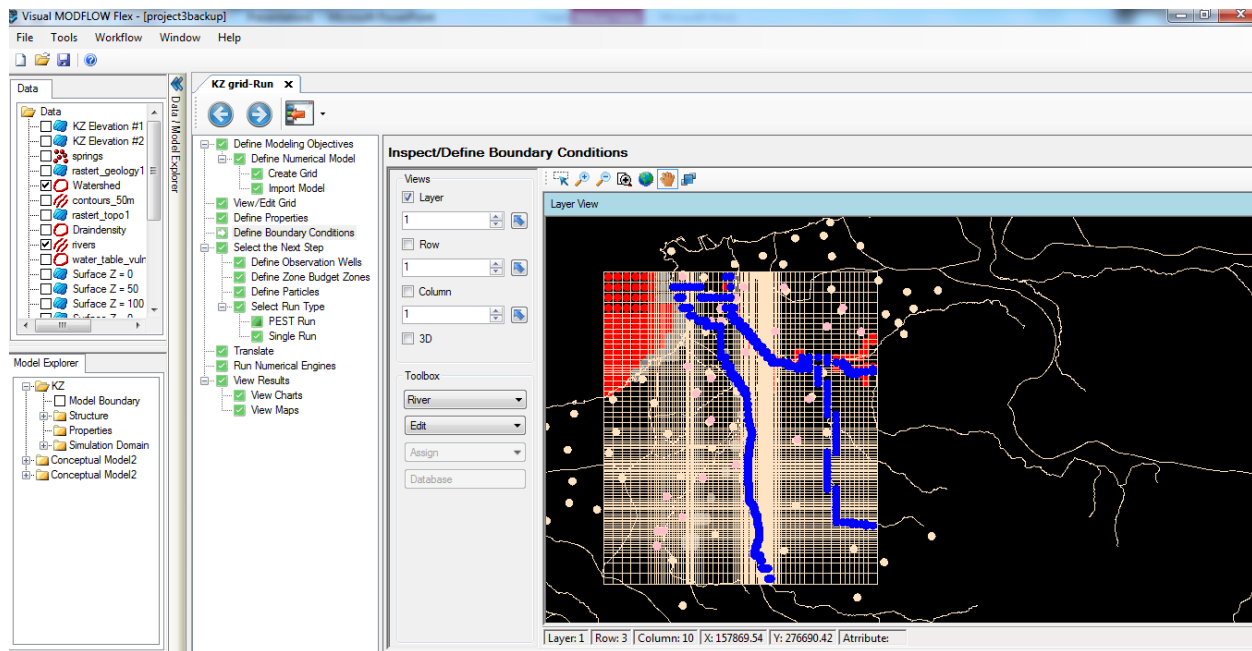


Figure 7.10 Layer View of the River Studied in Our Study in VMOD

3-Drain

Modflow's drain condition is designed to simulate the effects of drains. A drain removes water from the aquifer at a rate proportional to the difference between the head in the aquifer and elevation. The drain condition requires the following information as input for each cell containing this boundary condition:

- **Elevation:** The drain elevation of the free surface of water within the drain. The drain is assumed to run only partially full, so that the head within the drain is approximately equal to the median elevation of the drain.
- **Leakance:** The drain leakance is a lumped coefficient describing the head loss between the drain and the groundwater system. This loss is caused by converging flow patterns near the drain, the presence of foreign material around the drain, channel bed materials, the drain wall, and the degree to which the drain pipe openings may be blocked by chemical precipitates, plant roots, etc. When a polyline is used to define the boundary condition geometry, the default formula for the leakage is as follows: (Harbaugh, Banta, & Hill, 2000)

$$\text{\$COND} = \text{\$RCHLNG} \times \text{\$LCOND}$$

- \$COND: is the Leakance
- \$RCHLNG: is the reach length of the drain in each grid cell
- \$LCOND: is the Leakance per unit length of the drain in each grid cell

2- Recharge

The recharge boundary condition is typically used to simulate surface recharge to the groundwater system. Most commonly, recharge occurs as a result of precipitation percolating into the groundwater system. In our study, the precipitation ranges from 640 to 1240 mm with an average range of 821 mm (ELARD, 2010) (MOE, 2011) (MOE U. , 2010). Since the recharge rate is assumed to be a percentage of the precipitation. This percentage typically ranges from 5% to 20% depending on many different factors including the surface topography (slope), and the soil cover material. In the case of our soil composition the groundwater recharge consists of 10% from precipitation. Therefore the recharge values inserted in VMOD= 2.2×10^{-4} m/day. It comes from the following formula:

$$\text{Recharge} = 10\% \times \text{precipitation}$$

$$\text{Recharge} = 10\% \times 0.821\text{m/year} \times (1\text{year}/365 \text{ days})$$

$$\text{Recharge} = 2.2 \times 10^{-4} \text{ m/day (because this is the SI unit inserted)}$$

- Recharge is only applied to the top grid layer: if any grid cells in layer 1 are dry, or if they are designated as no-flow cells; the inactive or dry cells act like an impermeable barrier to the recharge .Therefore we inserted the top elevation for the top layer as the surface area for the study.

3- Evapotranspiration

The evapotranspiration boundary condition simulates the effects of plant transpiration, direct evaporation, and seepage at the ground surface by removing water from the saturated groundwater regime the surface characteristics of the upper layer were inserted as the surface shape file for our model. (Matthias Raiber a, 2012) The rate of evapotranspiration is entered as it

occurs when the water table elevation is equal to the top of the grid cell elevation. This value should be entered in the units set for Recharge meaning in m/day; therefore the value is $2.73790926 \times 10^{-6}$ meters / day is multiplied by the yearly RTP values we have obtained in the Thornthwaite formula for the year 2012. We get a mean value of 2.655×10^{-3} meters / day.

4- Pumping Wells

The pumping data extracted during our two main sample campaigns are summed up in the form of excel (xls) sheets. In order to be able to map the pumped wells, the excel sheets are imported as pumping wells points. VMOD Flex provides us with various options for importing wells, and associated well data. For example, we can choose to import well heads (Well ID, X, Y, Elevation, and Bottom), or we can choose to import wells heads along with related screen locations, pumping schedules, etc...

If this option is selected, you must first map the well heads under the Well Heads tab. Next, click on the Screens tab, and map the appropriate columns from the source data to the following target fields:

- Well ID
- X
- Y
- Elevation
- Bottom
- Screen ID
- Screen Bottom Z (elevation of bottom of screen)
- Screen Top Z (elevation of top of screen)
- Pumping Start Date, in MM/DD/YYYY HH:MM:SS format, time
- Pumping End Date, in MM/DD/YYYY HH:MM:SS format, time
- Pumping Rate

For each well in the source data, the Screen ID must be unique. Also, screens should not overlap within a single well. These requirements will be validated in the final step of the well import process.

7.2.3 Proceed to Run or Define Optional Model Elements

After defining the properties and the boundary conditions, we come to screen; some of the non-essential inputs for the model, such as observation wells etc... (See figure 7.11). Afterwards, we proceed by running the simulation.

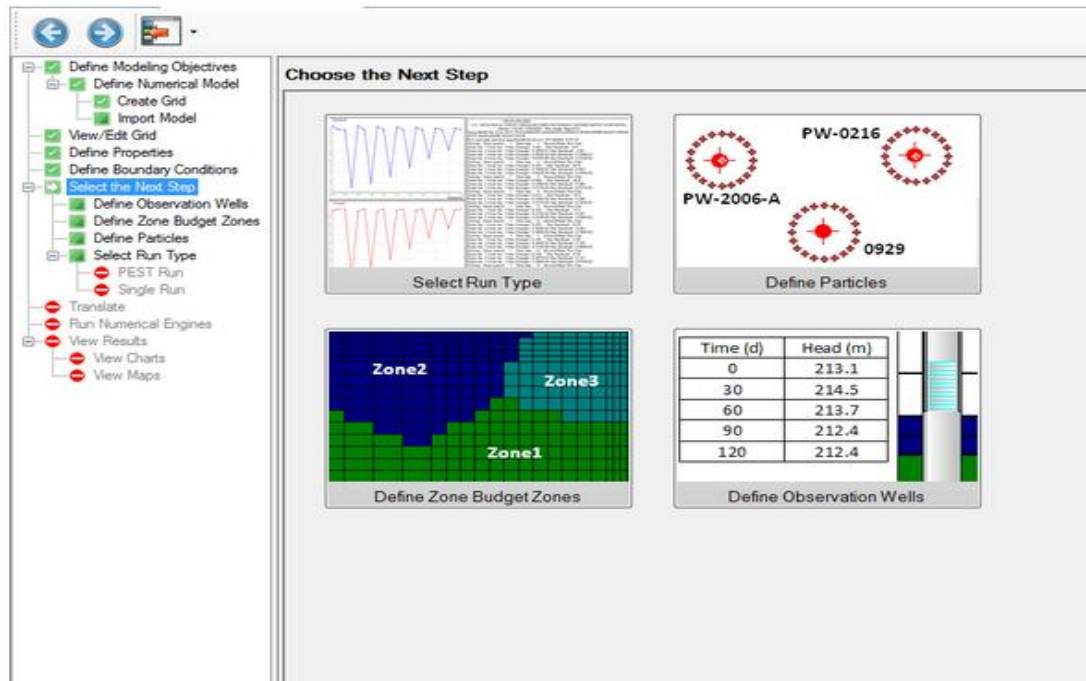


Figure 7.11 Running the Simulation

The “Compose Engines” button to proceed is necessary; the “Next step” button will take us to the following step (see figure 7.12) as it is pre-defined as the default step.

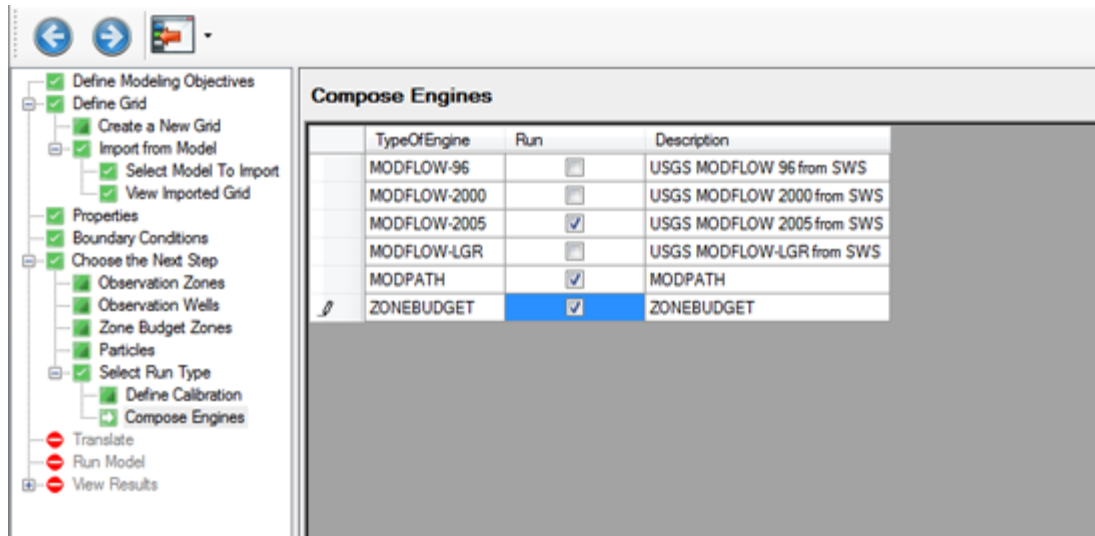


Figure 7.12 Engines Used to Proceed With VMOD

MODFLOW-2005 should be selected by default; we also MODPATH and Zone Budget, to run the selected engines. We will reach:

1 . The “Translation Step”.

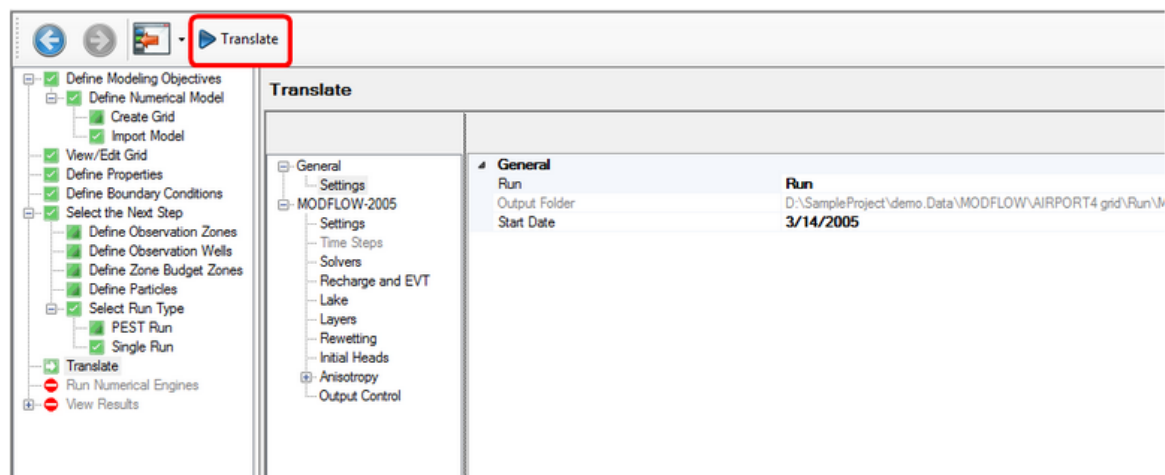


Figure 7.13 Translating with VMOD

2- Run Engines

By clicking the button on the main workflow toolbar, we start running the engines. The engine progress in the scrolling window. After a successful run, the Heads and Pathlines items will be added the tree in the model explorer.

7.3 Results

We then choose to view results in the form of Maps ;contours and color shading are options in the map settings that help us edit the results in the esthetic way we desire for instance to see the head observation map. We will then see color shading of the calculated heads, in layer view.

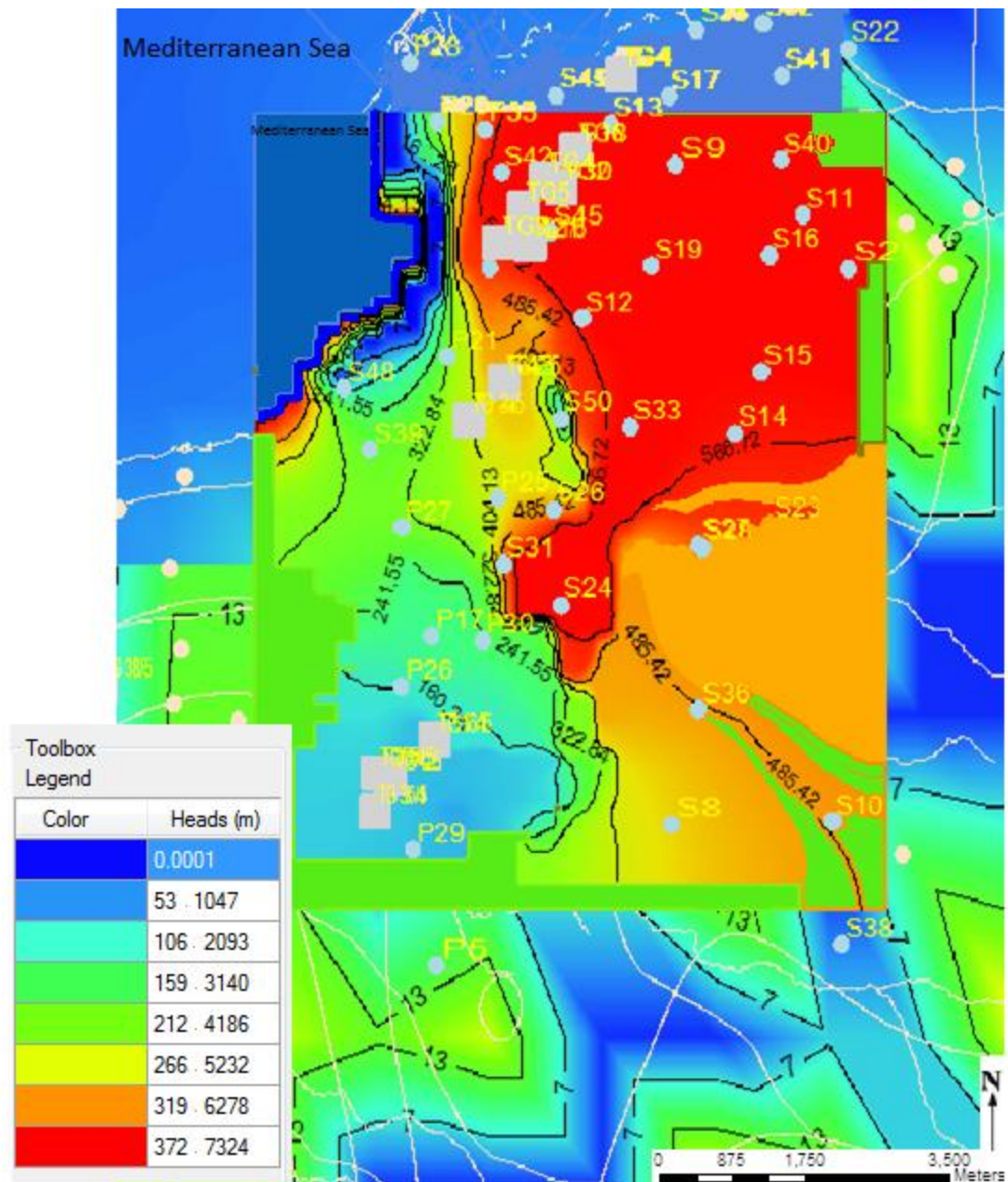


Figure 7.14 Potentiometric Map of Koura Zgharta and Tripoli Area

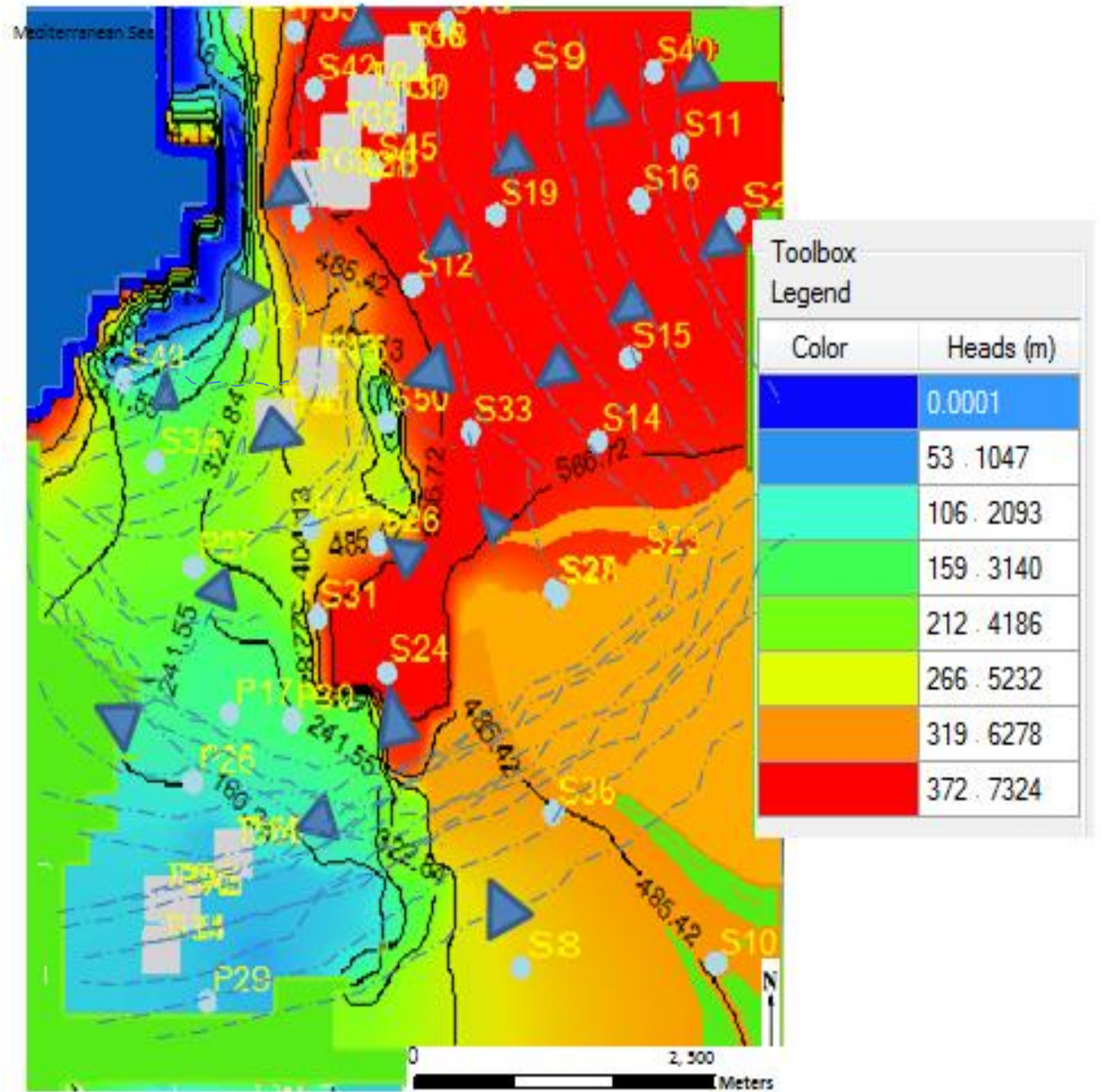


Figure 7.15 Closer View of Potentiometric Map of Koura Zgharta and Tripoli Area

The ground-water system as a whole is actually a three-dimensional flow field; therefore, it is important to understand how the vertical components of ground-water movement affect the interaction of ground water and surface water. A vertical section of a flow field indicates how potential energy is distributed beneath the water table in the ground-water system and how the energy distribution can be used to determine vertical components of flow near a surface-water body. The term hydraulic head, which is the sum of elevation and water pressure divided by the weight density of water, is used to describe potential energy in ground-water flow systems. For example, Figure above shows a generalized vertical section of subsurface water flow. Water that infiltrates at land surface moves vertically downward to the water table to become ground water. The ground water then moves both vertically and laterally within the ground-water system.

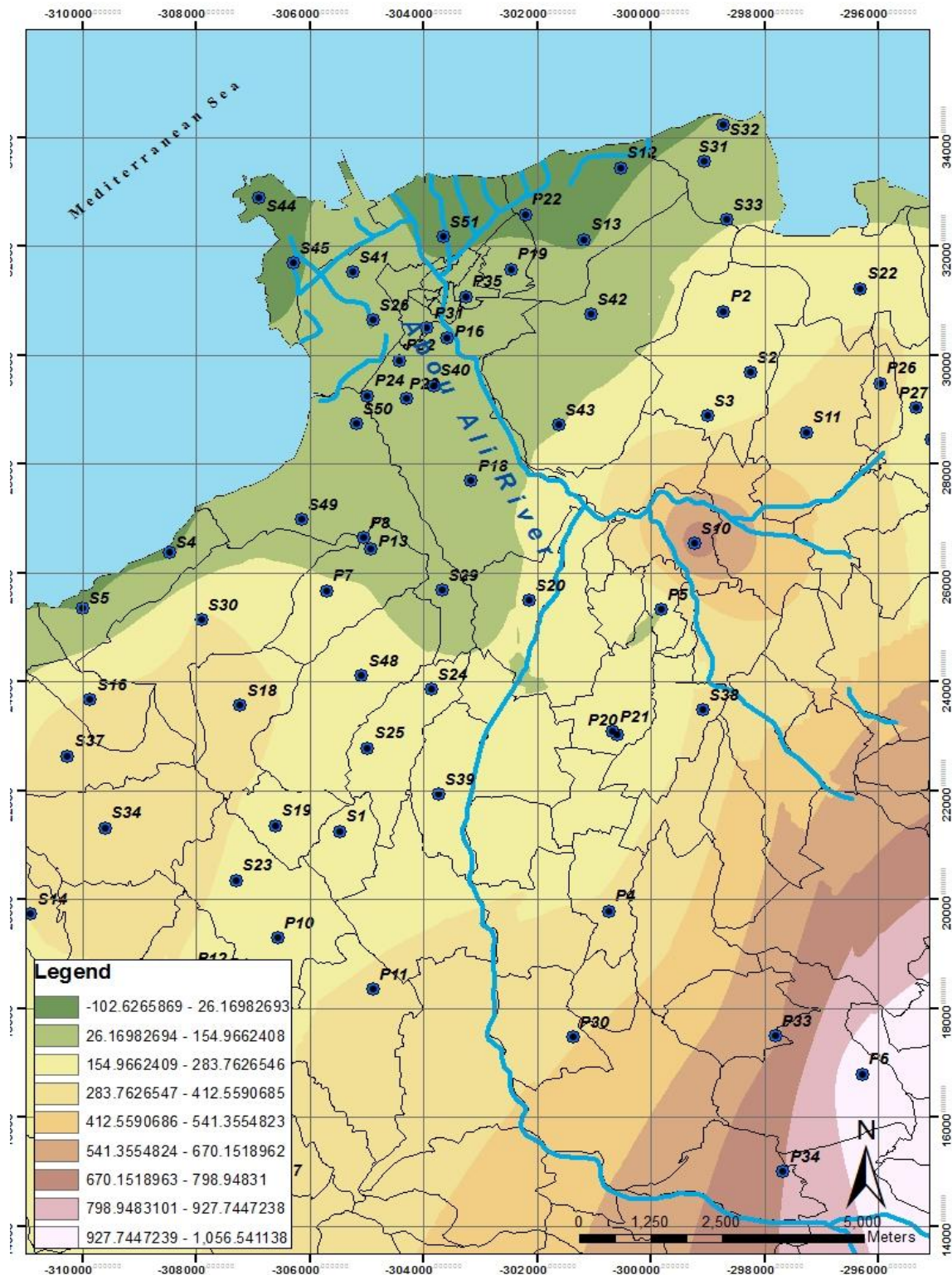
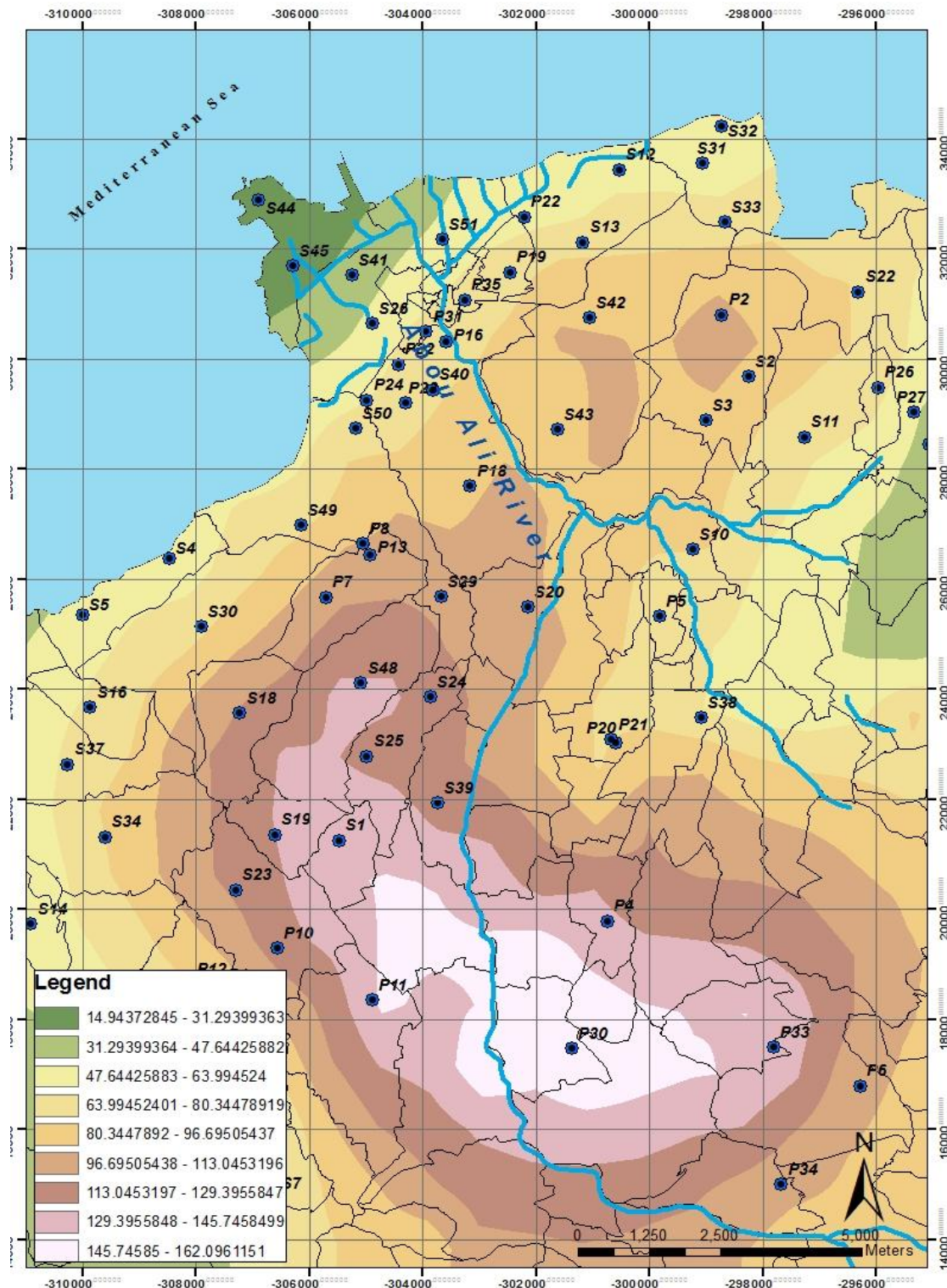


Figure 7.16 Dynamic Water Level Map (in meters below ground) of Koura Zgharta and Tripoli Region



As known, water flowing in an aquifer is driven by groundwater recharge from precipitation, by flow from adjacent regions, by exchange with river, and by pumping. Anticipating the results of the simulation, the major effect of pumping is actually quite important in a Karstic aquifer.

In our case, the hydraulic parameter fields' Transmissivity T and Conductivity K of the groundwater model are specified based on our sampling campaigns. Obviously, the situation is much more complicated in reality, since it is a karstic aquifer, water is not all stored since it works like a cave system and water tends to seep from the aquifer towards the sea.

In general, the information available than the hydrogeologic map obtained however; in particular the hydraulic heads map is quite essential. Figure 7.16 and 7.17 shows an example of such data: contour lines interpolated from measured hydraulic heads in our studied limestone aquifer.

Groundwater flow in Koura, Zgharta and Tripoli region is obtained with the simulated groundwater model that is shown in Figure 7.15. The streamlines reveal a quite complicated flow with flow directions from east to west towards the sea. Generally, water flow is from the upper aquifer Zgharta area where heads as high as 400 meters MSL, 300 meters MSL are seen to the lower, shallower aquifer where most of the water is thrown away in the Mediterranean Sea. This transfer occurs mostly through the hydraulic spaces in the aquifer where the thickness is decreasing and the material contains a high fraction and karstified limestone. Such conditions prevail in the northern and southern east part of the region specially Zgharta area. There, the streamlines indicate that water infiltrates from the river into the aquifer, travels westward towards the sea.

CHAPTER 8

MANAGEMENT of GROUNDWATER in MIOCENE LIMESTONE AQUIFER of NORTH LEBANON

The study of the hydrogeological, hydrochemical and hydraulic properties (such as recharge, discharge, etc...) of the Miocene limestone aquifer of North Lebanon allows a proper assessment and management of the water in the area. In order to evaluate the groundwater management, two major terminologies are essential: groundwater budget and safe yield. Nevertheless, the amount of water that recharges from confined aquifers is determined by 3 factors; (1) the amount of precipitation that is not lost by evapotranspiration and runoff and therefore is available for recharge; (2) the hydraulic conductivity; and (3) the transmissivity of the aquifer. (Fetter C.W., 1999)

8.1. Recharge and Evapotranspiration

Recharge to confined aquifer as discussed earlier in this chapter is due to 3 main factors. In our case the main source of recharge for Koura-Zgharta Miocene aquifer is due to the precipitation that recharges it. However, precipitation, evapotranspiration, runoff and recharge rate data must be available in order to calculate the amount of recharge.

A previous climatological study on the area from the year 1971 up to 2001 was accomplished, as well as data collected from the United Nation booklet of 1971 and the Tripoli Weather Station from 1962 to 2001. The rest of the data up to 2011-2012 was entered either from weather data from the international airport of Beyrouth or from National Climatic Data Center (<http://www.ncdc.noaa.gov/>). This included mostly the study of the evapotranspiration on Tripoli Area, Abou Ali, Rachiine and Jouit's Rivers. Many formulas are available to calculate the ET_p , such as Turc's formula, Thornthwaite etc. (Fetter C.W., 2001). But according to the parameters present below, the Thornthwaite equation was the one that fitted us the most. The Thornthwaite's method which is used in this study, is based upon the assumption that potential

evapotranspiration was dependent only upon meteorological conditions and ignored the effect of vegetative density. The factors included are temperature, latitude and months. Thornthwaite's formula is expressed by the following equation (D.G, 1986).

$$ET_p = 16(10\theta/I)^a \times F(\lambda) \text{ in (mm/month)} \quad (8.1)$$

Here, ET_p is the potential evapotranspiration and is given in millimeters per month

θ mean temperature of the period in question ($^{\circ}\text{C}$) measured under shelter

$$a = (6.75 \times 10^{-7})I^3 - (7.71 \times 10^{-5})I^2 + (1.79 \times 10^{-2})I + 0.49239$$

I annual thermal index, sum of twelve monthly thermal indexes, i

$$i = (\theta/5)^{1.514}$$

$F(\lambda)$ correction coefficient, function of latitude and month

From the data taken from the Tripoli weather station between 1962 and 1999, the 34 years average for the total yearly precipitation was found to be 820.6 mm. in addition, and according to Khair (Zaahruddine K., 1992), the average recharge percent from precipitation was found to be 36% which gives a recharge of 13.02MCM/year for the year 1992.

In the total area of study that cover 165.8 km^2 of land, the volume of precipitation was $1.36 \times 10^8 \text{ m}^3/\text{yr}$. By applying the 36% average recharge, the aquifer recharge value was established as $49 \text{ Mm}^3/\text{yr}$.

These values couldn't be inserted in Visual Modflow since the SI unit required was in m/days, therefore the recharge data was obtained by TEDO 2010 and UNICEF file 2011. Most commonly, recharge occurs as a result of precipitation percolating into the groundwater system. In our study, the precipitation ranges from 640 to 1240 mm with an average range of 821 mm (MOE U. , 2010) and (UNDP, 2011). Since the recharge rate is assumed to be a percentage of the precipitation. This percentage typically ranges from 5% to 20% depending on many different factors including the surface topography (slope), and the soil cover material. In the case of our soil composition the groundwater recharge consists of 10% from precipitation. Therefore the recharge values inserted in VMOD= $2.2 \times 10^{-4} \text{ m/day}$. It comes from the following formula of Woodward-Clyde (1999):

Recharge = 10% x precipitation

Recharge = 10% x 0.821m/year x (1year/365 days)

Recharge = 2.2×10^{-4} m/day (because this is the SI unit inserted)

Recharge = 13.32 MCM/year

If we compare it with the 1992 value of El Khair it has increased of 0.3 MCM/year for the year 2013.

As for evapotranspiration, the rate of evapotranspiration is as well required for VMOD in m/day; therefore the value is $2.73790926 \times 10^{-6}$ meters / day is multiplied by the yearly RTP values we have obtained in the Thornthwaite formula for the year 2012.

We get a mean value of 2.655×10^{-3} meters / day.

8.2 Discharge

The main discharges sources available in the studied aquifer are the discharge of ground water by pumping wells and the outflow of the groundwater towards the sea. One is designated as artificial discharge (pumping) and the natural throughout of water in the sea is the natural discharge. The groundwater losses to the sea in Lebanon are estimated to 880 MCM per year (ECODIT, The State and Trends of the Lebanese Environment , 2011). According to the Bureau techniques de developement BTd, (1994), the estimated natural discharge to the sea is 35.3MCM/year in the 165.8 km² of studied area, more specifically Tripoli, Haab surrounding; 3.5MCM/year spreaded discharge in the Tripoli area to the sea and 22.1 MCM/year discharge from Haab underground source to the sea. Assuming an estimate of 25.6 MCM/year in the 165.8 km² of land studied.

The pumping well rate between private and public wells is assumed to be 26.4MCM/ year (15 MCM/year private and 11.4 MCM public); the ETP is 0.012 m/year which give a total of 61.7 MCM /year.

8.3 Groundwater Budget

A water budget for all resources of recharge for an aquifer is quite useful for the determination of groundwater recharge. The advantage of studying groundwater budget is that the aquifer doesn't necessarily require dynamic equilibrium. It is even essential to avoid groundwater mining. A groundwater budget attempts to account for all sources of water that enters or leaves the aquifer, meaning all the amount of water that recharge the aquifer as well as the discharge. A water budget is essential to avoid water exploitation and fall in a mining situation in which the withdrawal of water is greater than the recharge rate of the aquifer. The groundwater balance equation can be summarized by the following equation (Fetter C.W., 2001):

$$I - O = \Delta S \quad (8.2)$$

$$\Delta S = 13.32 - 61.7 = -48.38 \text{ MCM/ year}$$

Where I is the inflow of the aquifer, O is the outflow and ΔS is the change in storage of groundwater.

Inflow has many components such as precipitation, irrigation, influent seepage from rivers, inflow (subsurface) from neighbour aquifers and run-off recharge. Outflow occurs when effluent is percolating to the rivers, to the sea or even to other basins. It also includes pumping wells (most common) and evapotranspiration (occurs mostly in shallow unconfined aquifers). In the case of the Miocene aquifer of North Lebanon, pumping by wells usually accounts for most of the outflow in the aquifer. Since the result from the applied equation was negative, we can conclude that the aquifer is being mined at a rate of 48.38 MCM/ year. Nevertheless it is very difficult to model accurately the water balance equation “...one of the most challenging Rubik Cubes of nature, one in which the ‘squares’ change colours, shapes and sizes as they are being moved around by the different forces, and in which even the structural setup changes with time...” Klemes (1988), A hydrological perspective.

8.4 Lifetime of the Aquifer

The lifetime of the aquifer is the time it takes to deplete the storage of the aquifer. It is calculated using two equations listed below (Khayat Z., 2001) :

Lifetime of the aquifer= (Storage of aquifer) / (annual decline of storage)

Lifetime of the aquifer= $(A \times h \times S) / (\text{groundwater budget})$ which is used in this study

A= horizontal area of the aquifer 200 m below the surface of the ground

H = saturated thickness between 100 and 200 meters

S= Storativity of aquifer will be taken as $3.3 \times 10^{-4} / \text{m}^3$ as minimum value and $1.4 \times 10^{-2} / \text{m}^3$ as maximum value.

Groundwater budget =18.38 MCM/year

Min Lifetime of the aquifer= 0.54 year

Max Lifetime of the aquifer= $200 \times 150 \times 1.4 \times 10^{-2} / 18.38 \text{ MCM/year} = 22.85 \text{ years}$

In a confined aquifer, the concept of aquifer has 2 main gears:

1. Lowering the potentiometric surface beneath the top of the aquifer or the base of the confined layer.
2. Calculation of lifetime of the aquifer as an unconfined aquifer , since as we know we have a convergence from confined to unconfined subsidence

Therefore , the time to lower the potentiometric surface bellow the base of the confined area was calculated and believed to be between half a year and 23 years. This range can be used as follow: in areas such as in Tripoli, with high abstraction rate and a potentiometric surface height above the confining layer base , an immediate danger of damaging the aquifer is seen. This danger is perceived by the regionnal seawater intrusion. However, in areas where low pumping occurs and the potentiometric surface height is above the confining layer, no immediate danger will be seen. This is the case of the central part of the aquifer, specially in areas such as in Zgharta.

As for the second part of the lifetime calculations, it is present when the potentiometric surface drops below the bottom of the confining layer, therefore the aquifer becomes an unconfined aquifer. According to (FetterC.W., 1999), in such a case, the storativity becomes the specific yield and consequently ranges between 0.02 to 0.30. The results are as follow:

Min Lifetime of the aquifer = 32.64 years

Max Lifetime of the aquifer = 489.66 years

The total lifetime of the aquifer is between 33.18 years and 509.51 years, as a result the aquifer is expected to sustain its current yield for at least 33 years.

8.5 What is the Future?

8.5.1 Water Law

The development and management of water resources should proceed within a framework of legal obligations, rights and limitations. These factors differ from one country to another. Common traditionally water laws have risen concerning the quantity of water available, nevertheless, nowadays; many new laws are written and allocated to protect the quality of water. The concept of protecting the quality of water is relatively recent. It is important for groundwater management that responsibilities are clearly defined, coordinated and accepted by each agency in our country; furthermore, there is a “duty of care” responsibility on all agencies. (Boëdec P. F., 2009).

Table 8.1: Water Sector Institutional Mapping of Responsibilities (ECODIT, Integrated Groundwater – Surface Water Management, 2003)

	Policy formulation	CAPEX planning and execution			Service provision (O&M)
		Donor financed	Budget financed	Cash-flow	
Water	MoEW	CDR	MoEW, CoS, CFD	RWA	RWA; MoEW
Wastewater	MoEW	CDR	MoEW	-	Municipalities, private operators
Irrigation/ WRM	MoEW	CDR	MoEW, LRA	-	Local committees, farmer groups

Source: Bank staff analysis. CoS = Council of the South; CFD = Central Fund for the Displaced.

8.5.2 Fundamental Principles

A fundamental principle underlying groundwater protection is the identification and maintenance of current or potential groundwater beneficial use. These include ecosystem protection, parks and recreational area (only present in Tripoli city), raw water for drinking water supply, agricultural water, and industrial water. In many cases groundwater protection is not implemented because there is no clear understanding or definition of the basis for protection, and as a consequence no identification of the beneficial use to be protected. The remediation of polluted groundwater also requires specified clean-up goals and these can be set most clearly following identification of the current groundwater uses.

Groundwater quality protection can also be promoted by increasing public awareness. This can not only promote best practice by individuals but also encourage acceptance of, and improved compliance with, regulatory measures. Currently, public awareness of groundwater quality issues and best practices is still in its infancy. None of these measures alone will improve groundwater quality protection. An integrated approach is required. In protecting groundwater quality, the interactions between surface water and groundwater and between water quality and quantity must be taken into account.

8.5.3 Water Shortage

“Lebanon is poised to face chronic water shortages from 2020, unless severe steps are taken to increase supply and manage demand” (UNDP, 2011). Serious shortages during the dry season which extends over the four months of July and October are starting to appear, therefore; contributing to the seasonal water imbalance. The water imbalance symptoms are due to the very low water storage capacity; the high amount of water lost to the sea and last but not least the growing demand for water and the deficiency of the existing water networks. According to the World Bank and the United Nation (UNESCWA, 2012 ; MOE U. , 2010)it is estimated that the seasonal imbalance of water resources will lead to chronic water shortages by 2020, if no actions are taken to improve efficiency and increase storage capacity. (Figure 8.1)

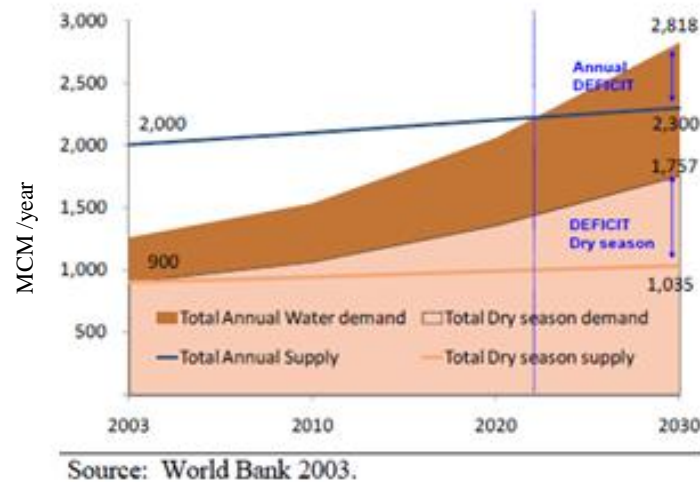


Figure 8.1: Annual Water Demand-Supply Balance, Total and Dry Seasons, 2003-2030 (World Bank, 2003)

The composition of water demand is expected to change significantly over the next 20 years. Domestic water demand, which represents 25 percent of total demand, is expected to exceed irrigation demand by 2030, reaching 45 percent of total water use (UNDP, 2011). Domestic water demand is largely driven by increase in income and population, forecasted at 2.5 percent per year. See figure 8.2 below.

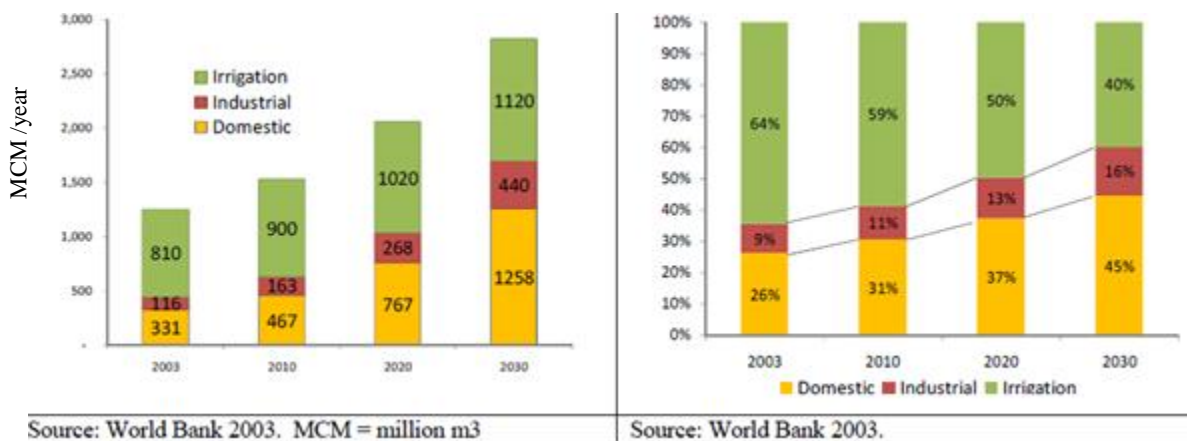


Figure 8.2: Annual Water Demand by Water Usage Category one in (MCM/year) and the other in Percentage

8.5.4 Social Impact Analysis

Reliability of water supply, rather than affordability, is the main constraint for consumer welfare. Reliability of public water supply is a widespread concern across all household expenditure groups, regardless of their level of income. The North Water Authority has the best performance in term of continuity of supply, with no unmet demand.

The North water establishment has managed to reduce water losses in Tripoli. The area has contracted the water authority delegated to a French company the management of water Distribution Ondo-Liban between 2003 and 2007. The most remarkable achievement of the private operator has been the significant reduction of water losses and the extension of 24 hours of daily supply to the entire urban area of Tripoli due to upgrade and rehabilitation of the network. However, the private operator was unable to re-negotiation. “Some of the obstacles faced by Ondo-Liban can be attributed to the unstable political phase in Lebanon during the duration of the contract, which according to the company itself reduced its ability to collect customer fees (Halwani J., Assessment of the Water Situation in Lebanon, 2008). The sustainability of the efficiency improvements is therefore at risk, as management of the Tripoli urban water supply network is transferred back to the North WA. The inability to renew the partnership with the private operator proves that the institutional reality of the WSS sector, characterized by government interference and lack of clear responsibilities, is a significant deterrent for sustainable partnerships with international private operators” According to CDR 2007; North Lebanon RWA-Ondo Liban 2006.

Improving water and sanitation services is one of Lebanon’s essential concerns . Many efforts to rebuild after the war are done, but the critical situation and economy have slow down the significant advancement in the direction of new piping systems and drinkable potable water; in addition to the scarcity of up-to-date and reliable hydrological data that makes it very difficult to plan adequate and sustainable management of the country's water resources into the 21st century. This data deficiency is critical, because economic-development planning must consider the current hydrological picture to make sensible projections about growth and water needs. Reliance on 1930s data and 1950s infrastructure and instruments for gathering water data is an

obstacle to the sustainable management of Lebanon's water resources (Darwish T. M., 2008).

The effectiveness of groundwater quality management and protection relies on enforcement and a comprehensive, targeted monitoring program. There is a growing trend for companies and individuals to self-monitor groundwater where there is a potential for contamination (ECODIT, The State and Trends of the Lebanese Environment , 2011). For the monitoring to be of value and to serve its purpose, there should be regular reporting, review and analysis of the monitoring results. Both government agencies and the potential polluters should be subject to duty of care requirements. (Masciopinto C., 2013) Some tools can be used to protect groundwater resources wellhead protection plans such as educational awareness, community awareness and involvement, land use planning. In particular, there is a need for development of an approach to the establishment and operation of pumping the groundwater out of the sea where it is being flashed away. Since it is a karstic aquifer and water cannot be preserved, it is better for the consumers to stop pumping from the licensed and unlicensed pumping wells and encourage more and more the North water establishment to create another source than Abou Halka to pump water from the sea. In the last decade, the NLWE has been able to reduce the pumping from wells inside Tripoli (Abou Samra) and instead builded a water pumping station in the sea that pumps into a tank the groundwater that is thrown away in the sea. Further plans such as this one should be implemented in the region to reduce the risk of drying out our aquifer.

CHAPTER 9

CONCLUSION AND RECOMMENDATIONS

Groundwater is considered as a precious resource for mankind as it is perceived as the only source of drinking water. The uncontrolled and unlicensed exploitation of this resource never stops thus leading to sea water intrusion specifically in coastal areas. The deterioration of groundwater quality and the whole aquifer progressively became alterable. North Lebanon and more specifically the Koura, Zgharta and Tripoli areas were studied for the Miocene Limestone Aquifer. This confined, fractured aquifer has shown a general water flow from its upper side located in Zgharta region where some of the highest heads were observed towards the lower, shallower aquifer (Koura and then Tripoli) where most of the groundwater will be withdrawn towards the Mediterranean Sea. The hydrochemical, hydrophysical and water level methodologies achieved in this research provided detailed physiochemical and bacteriological on the water quality, potentiometric contour of the watershed. Based on qualitative analysis of 86 artesian wells spread within the research area, it was found that groundwater is clearly affected by pollution mostly due to salinization and agricultural activities; thus indicating that sea water intrusion is a direct effect of human uncontrolled and unsupervised pumping of wells. The integration of the numerical model by the use of Visual Modflow and the GIS gave a scientific approach and analysis on the aquifer condition. The calculations indicated that the aquifer recharge value was established as $49 \text{ Mm}^3/\text{year}$, and discharge value of $61.7 \text{ Mm}^3/\text{year}$. A large deficit was evident between what is infiltrating to the ground and what is going out of it. To this, the total lifetime of the aquifer was found to range between 33.18 years and 509.51 years, as a result the aquifer is expected to sustain its current yield for at least 33 years. This will become problematic as the aquifer in coastal areas covering Tripoli and its surrounding areas will face a lower aquifer lifespan. This problem will increase in intensity due to political and demographic reasons such as the clustering of Syrian immigrant along the Lebanese coastal line. In the last decade, and especially in the past few years, The North Water Lebanon Establishment (NWLE)

became more alerted and aware of the problem of scarce water resource and the excessive drilling and pumping. This led to an increase in measures taken by the NWLE authority by implementing many laws. Stating few: the renewal of Tripoli underground water network; the filtration of ground water from the sea; the establishment of new water filtration centers. These measures should hypothetically decrease the pumping and mining of groundwater from the wells. Many recommendations are set to enactment in the North, but more needs to be done to achieve a holistic solution for this emergent problem.

The recommendations of this research are:

- ✚ Continual physiochemical, bacteriological and water level analysis.
- ✚ Law enforcement of unlicensed wells closure.
- ✚ Renewal and installation of the public water network in Koura and Zgharta
- ✚ Installation of waste water treatment plants with their conduit to the consumers in the entire region.
- ✚ Build dams in the less fractured area in the North to store the excess water during the winter season.
- ✚ Plant the seed for citizen involvement in order to better manage the water resource: this can be accomplished by awareness campaigns starting from the youngsters within schools, to the whole population through conferences and ads.

These recommendations will constitute a backbone for future research in the field. The bigger umbrella is to save the water resources to our future generation in a hope to sustain it.

BIBLIOGRAPHY

- A. W. Harbaugh, E. R. (2000). *MODFLOW-2000, THE U.S. GEOLOGICAL SURVEY MODULAR GROUND-WATER MODEL—USER GUIDE TO MODULARIZATION CONCEPTS AND THE GROUND-WATER FLOW PROCESS*. U.S. GEOLOGICAL SURVEY.
- Abbud M., N. A. (1986). The Study of the Aquiferous Formations of Lebanon through the Chemistry of their typical Springs. *Lebanese Science Bulletin Volume 2, Number 2*.
- AberJ.T., S. D. (2007). *Modeling Groundwater Flow using PMWIN and ArcGIS*. Water Resources Research Lab, Kansas State University.
- Abi Ghanem K. (décembre 2008). *Speciation" des trois elements trace mercure, plomb et cadmium dans les sediments marins des zones cotieres libanaises*. . L'Institut des Sciences et Industries du Vivant et de l'Environnement (Agro Paris Tech) est un Grand Etablissement dépendant du Ministère de l'Agriculture et de la Pêche, composé de l'INA PG, de l'ENGREF et de l'ENSIA.
- Al Saud M. (2010, April). Mapping potential areas for groundwater storage in Wadi Ayrnah Basin, Western Arabian Peninsula, using remote sensing and geographic information system techniques. *Hydrogeology journal*(18), 1481-1495.
- Al-Charideh. (July 2010). Environmental isotope study of groundwater discharge from the large Karst springs in west Syria: a case study of Figh and Al-Sin springs. *Springer-Verlag 2010. Environmental Earth Science*, 63, p: 1-10.
- Al-Mooji Y. (2010). Shared water resources in the western Asia region:An inventory of shared aquifers and aquifer systems. International Conference “Transboundary Aquifers: Challenges and New Directions”. *An inventory of shared aquifers and aquifer systems. International Conference “Transboundary Aquifers: Challenges and New Directions”(ISARM2010)*. (ISARM2010).
- Al-Mooji Y., R. A. (2010). Shared water resources in the western Asia region:.
- Al-Sibai. (2006)). Managerial outputs of mathematical groundwater models: case studies. *The 2nd international conf. on water resources & arid environment*.
- Anderson M.P., W. W. (1992). *Applied Groundwater Modeling, Simulation of flow and Advective*

Transport . . Academic press.

Andreo B., C. F. (2010). Advances in Research in Karst Media . *Environmental Earth Science; Springer*.

APHA. (1998). *Standard Monethods for the Examination of Water and Wastewater,20th edition*.
Washington: American Public Health Association .

Appelo, D. L. (1999). *USER'S GUIDE TO PHREEQC* . Denver- Colorado: Water-Resources
Investigations Report.

Aquilina L., B. M. (2003, November-December). Deep Water Circulation, Residence time and Chemistry
in Karst Complex. *Ground Water*, 41(3), p.790-805.

Arfib B., G. d. (February 2007). Locating the Zone of Saline Intrusion in a Coastal Karst Aquifer Using
Springflow Data. *Groundwater*, Vol. 45, No. 1, p:28–35.

ArfibB., M. G. (2007, January- February). Locating the Zone of Saline Intrusion in a Coastal Kastic
Aquifer using Spring flow Data. *Ground Water*, 45(1), 28-35.

Association, A. P. (1999). *Standard Methods for the Examination of Water and Wastewater, MICROBIOLOGICAL EXAMINATION*. American Public Health Association, American Water
Works Association, Water Environment Federation.

Atlas of water resources in the black hills area. (n.d.). Definition of terms. South Dakota.

Authority, O. H. (July 2011). *Health effects information Lithium* . Office of Environmental Public Health.

Awad S. (30 may-1th june 2006,. Darcy 02:Recharging conditions and ages of the groundwater of the
Bekaa's valey (Lebanon), Hydrogeologic, Hydrochemical and isotopic studies. *International
symposium -Aquifers Systems Management*. Dijon, France.

Baba A., T. G. (2011). Climate Change and its Effects on Water Resources . *Issues of national and global
security. Springer* .

Bakalowicz M. (2005). Karst groundwater: a challenge for new resources. *Hydrogeology Journal*, 13,
148-160.

Bakalowicz M. (20078). Le milieu karstique : études et perspectives, identification et caractérisation de la
resource. *Colloque Hydrogéologie et karst au travers des travaux de Michel Lepiller*.

- Bakalowicz M. (2010). Karst et ressources en eau souterraine : un atout pour le développement des pays Méditerranéens. *Sécheresse*, 21(2).
- Bakalowicz M., E. H.-H. (2008). Karst groundwater resources in the countries of eastern Mediterranean: the example of Lebanon. *Environmental Geology*, 54, 597-604.
- Bakalowicz M., E.-H. A. (2012). Les sources karstiques sous-marines de Méditerranée sont-elles des ressources non conventionnelles exploitables . *Dix-huitièmes journées techniques du Comité Français d'Hydrogéologie*. Cassis : Ressources et gestion des aquifères littoraux.
- Bank, U. (May 17, 2010). *Water Sector: Public Expenditure Review* . World Bank .
- Barlow P-M., A. F. (1999). *WTAQ A Computer Program for Calculating Drawdowns and Estimating Hydraulic Properties for Confined and Water-Table Aquifers*. USGS, Water-Resources Investigations Report 99-4225.
- Baskaran S., A. J. (2009). *Groundwater Sampling and Analysis – A Field Guide*. Geoscience Australia, Department of Resources Energy and Tourism Australia.
- Bayari C. S., O. N. (2010, November). Submarine and coastal Karstic groundwater discharges along the southwestern Mediterranean coast of Turkey. *Hydrogeology journal* , 19, 399-414.
- Beck, H. E. (October 2013). *Linkages between streamflow , climate and catchment characteristics:a global analysis*. VU University Amsterdam.
- Bellos G. S.G. (2011, February). Sedimentology Diagenesis Stratigraphy and Paleontology of the lower cretaceous rock sequence in Lebanon. *Search and discovery article N° 50380*.
- Berner, B. a. (1987).
- Bingqi Zhu, X. Y. (2011). Hydrogeochemistry of three watersheds (the Erlqis, Zhungarer and Yili) in northern Xinjiang, NW China. *Applied Geochemistry*, 26, p: 1535–1548.
- Bitar Al-A. (2007). *Modélisation des écoulements en milieu poreux hétérogènes 2D / 3D, avec couplages surface / souterrain et densitaires*. L'INSTITUT NATIONAL POLYTECHNIQUE DE TOULOUSE.
- Blondel Th. (décembre 2008). *Traçage spatial et temporel des eaux Souterraines dans les hydrosystèmes Karstiques par les matières organiques Dissoutes*. ACADÉMIE D'AIX-MARSEILLE ,

l'Université d'Avignon et des Pays de Vaucluse.

Boëdec P. F., B. P. (2009, 3e Trimestre). L'Eau dans les relations internationales. *Défense et Stratégie*.

Bou-Zeid E., M. E.-F. (September- October 2002). Climate Change and Water Resources in Lebanon and the Middle East. *JOURNAL OF WATER RESOURCES PLANNING AND MANAGEMENT*.

Bradbur C.G., .. R. (1998). Estimating runoff-recharge in southern Lincolnshire limestone catchment. *Journal of Hydrology*, 211, 9,,86-99.

Bradbury, K. a. (1985). A computerized technique for estimating hydraulic conductivity of aquifers from specific capacity data. *Groundwater*, 23(2).

BRGM. (2011). *Guide des prescriptions techniques pour la surveillance physico-chimique des milieux aquatiques*. BRGM.

Brooks D.B., M. O. (2000). *Water Balances in the Eastern Mediterranean*. Published by the International Development Research Centre.

Burkartaus M. R., D. J. (2008). Chapter 7. Nitrogen in Groundwater Associated with Agricultural Systems.

Cahdam J. C., T. R. (2005). Environmental Management of the Waters of the El-Kabir river and the associated Akkar watershed. *Lakes and reservoirs: research and management*, 10, p, 141-146.

Carrera J., A. A. (2005). Inverse problem in hydrogeology. *Hydrogeol Journal*, Vol 13, p: 206–222.

Carton H., S. S. (2004, December). Miocene to Quaternary Folding and Thrusting Offshore Lebanon from Shalimar Seismic Profiles. *Eos Trans. San Francisco, USA: AGU Fall meeting*, 85(47).

Chapuis, R. P. (2007). *Guide des essais de pompage et leurs interprétations*. Gouvernement de Quebec.

Chapuis, R. P. (June 1992). Using Cooper-Jacob Approximation to Take Account of Pumping Well Pipe Storage Effects in Early Drawdown Data of Confined Aquifer. *Groundwater*, Vol 3, p:331-337.

Charideh AL- A.R. ((2007)). Environmental isotopic and Hydrochemical study of water in the Karst aquifer and submarine of the Syrian coast. *Hydrogeology Journal*, 15, 351-364.

Chin-Shung Yang, S.-P. K.-B.-S. (n.d.). TWELVE DIFFERENT INTERPOLATION METHODS: A

CASE STUDY.

- Clair N. Sawyer, P. L. (1994). *Chemistry For Environmental Engineering*. Mc Graw Hill, Fourth Editions.
- Cooper H.H, C. J. (January 1953). A generalized Graphical methof of Evaluating Formation Constants and Summarizing well-field History. *USGS*.
- D.G, M. (1986). *Quantitative Hydrogeology: Groundwater Hydrology for Engineers*.
- Dafny E., A. . (2010). Effects of Karst and geological structure on groundwater flow: The case of Yarqon-Tananim Aquifer. *Journal of Hydrology*, Vol 389, p:260–275.
- Dafny, E. B. (2010). Effects of Karst and geological structure on groundwater flow: The case of Yarqon-Tananim Aquifer, Israel. *Journal of Hydrology*, 389, p, 260–275.
- Darwish T. M., S. R. (2008, June). Assessment of Abandoned Quarries for Revegetation and Water Harvesting in Lebanon, East Mediterranean.
- Debieche T.H. (2002). *Évolution de la qualité des eaux (salinite, azote et Métaux lourds) sous l'effet de la pollution saline, Agricole et industrielle*. U. F. R. des Sciences et Techniques de l'Université de Franche-Comté, Ecole Doctorale Homme, Environnement, Santé.
- DEP. (2012). *DRINKING WATER STANDARDS, MONITORING AND REPORTING*.
- DEP. (2012). *DRINKING WATER STANDARDS, MONITORING CHAPTER 62-550*.
- Dhiman S.C., D. T. (n.d.). Ground Water Management in Coastal Areas. *Ground Water*.
- Dhont D., A. D. (2005). 3-D Geologic Modeling from Remote Surface Information: Application to Underground Water Resources in Lebanon. *IEEE*.
- Dhont D., D. A. (2005). 3-D Geologic Modeling from Remote Surface Information: Application to Underground Water Resources in Lebanon. *IEEE*, p.2172-2174.
- Dingman, S. L. (1994). *Physical hydrology*. New York : Maxwell Macmillan International.
- Dionex, C. (2003). *Cromleon Manual for Installing the ICS-2000 Ion Chromatography System*.
- Drever, J. (1997). *The geochemistry of natural waters: surface and groundwater environments*. New

Jersey: Prentice-Hall.

Drobinski P., D. V. (February 2008). *Hydrological cycle in Mediterranean Experiement*. WHITE BOOK.

Dubertret, L. (1955). *Carte Géologique du Liban au 1: 200,000e*. Notes et Memoires sur le Moyen-Orient.

Dubertret, L. a. (1951). *Carte Géologique au 50000 Feuille de Tripoli avec notice explicative*. Republic Libanaise.

ECODIT, M. (2003). *Integrated Groundwater – Surface Water Management*. NGC ISSUE 1.DOC.

ECODIT, M. (2011). *The State and Trends of the Lebanese Environment* . MOE/UNDP/ ECODIT.

Edgell H.S. (n.d.). *Karst and Hydrogeology of Lebanon*.

Eisenlohra L Bouzelboudjena M. (1997). Numerical versus statistical modelling of natural response of a karst hydrogeological system. *Journal of Hydrology*, 202, p,244–262.

ELARD. (2010). *Vulnerability, Adaptation and Mitigation Chapters of Lebanon's Second National Communication: Climate Risks, Vulnerability & Adaptation assessment*. MOE/UNDP.

El-Fadel M. (2002, June). Draft environmental impact assessment cultural heritage and urban development project.

El-Fadel, M., Tomaszkiwicz, M., & Abou Najm, M. (2012). Sustainable coastal aquifer management in urban areas: The role of groundwater quality indices. *Proceedings of the Resilient Cities 2013 Congress*.

El-Hajj A. (2008, Novembre). *L'aquifère carbonate karstique de Chekka (Liban) et ses exutoires sous-marins. Caractéristiques hydrogéologiques et fonctionnement*.Hydrogéologie de Chekka, Liban. Thèse A. El-Hajj, 2008.

El-Hoz M. (May 2007). Environmental and Development Situation in Tripoli. *Environmental Problems in Lebanon. Conference held at the Institute of Engineering, North Lebanon*.

El-Hoz, M. (2007, May). Environmental and development situation in Tripoli: Environmental problems in Lebanon. *Conference held at the Institute of Engineering, North Lebanon*.

Environment, M. o. (2009). *Compendium statistique national sur les statistiques de l'environnement*

- Fourth national report Of Lebanon To the Convention on biological diversity.* MoE/GEF/UNDP .
- EPA. (2012). *2012 Edition of the Drinking Water Standards and Health Advisories.* Office of Water U.S. Environmental Protection Agency Washington, DC.
- EPA. (2012). *Ground Water and Drinking Water* . US Environmental Protection Agency.
- EPA. (February 2002). *A lexicon of cave and Karst terminology with special reference to environmental Karst hydrology.* United States Environmental Protection Agency, Office of Research and Development Washington, D. C. 20460 .
- Eriksson, E. K. (1969). Chloride concentration on Groundwater , recharge rate and rate of deposition of Chloride in the Israel Coastal Plain. *Journal of Hydrology* , 7, p:178-197 .
- Esri. (n.d.). *www.esri.com*. Retrieved from GIS best practices: GIS for Karst.
- Essink, G. O. (April 1996). *Impact of Sea Level Rise on Groundwater Flow Regimes* (Vol. Vol 7). Delft: Delft Studies in Integrated Water Management , Delft University of Technology.
- Fadoua Hamzaoui-Azaza, M. K. (2011). Hydrogeochemical characteristics and assessment of drinking water quality in Zeuss–Koutine aquifer,southeastern Tunisia. *Environ Monit Assess*, 174, p::283–298.
- FAO. (1971). *Etude géologique de la region de Koura-Zgharta (HG 17)*. Beirut: FAO.
- Faulkner J., B. X. (2009). Laboratory analog and numerical study of groundwater flow and solute transport in a karst aquifer with conduit and matrix domains. *Journal of Contaminant Hydrology*, Vol 110 , p:34–44.
- Faulkner, J. (2009). Laboratory analog and numerical study of groundwater flow and solute transport in a karst aquifer with conduit and matrix domains. *Journal of Contaminant Hydrology*, 110, p:34–44.
- Fawaz. (2006-2009). *Water Supply Sector Lebanon, Development Program 2006 – 2009*. L0538-RPT-ENV 01-REV B.
- Fetter C.W. (2001). *Applied Hydrogeology (4th ed.)*. New Jersey: Pearson Education,Upper Saddle River.
- FetterC.W. (1999). *Contaminant Hydrogeology, Second Edition*. New Jersey: Prentice Hall,Upper Saddle River.

- Fleury P., B. L. (2009). Modelling the hydrologic functions of a karst aquifer under active water management – The Lez spring. *Journal of Hydrology*, Vol 365 , p:235–243.
- Fleury P., L. B. (2009). Modelling the hydrologic functions of a karst aquifer under active water management – The Lez spring. *Journal of Hydrology*, 365, p:235–243.
- Foley D., M. G. (2009). *Investigations in Environmental Geology (3rd edition)*. New Jersey: Pearson, Prentice Hall Upper Saddle River.
- Foster S. S. D., A. C.-C. (2011). Nitrate Leaching to Groundwater. *Royal Society publishing*, p:477-480.
- Fried, J. J. (n.d.). Groundwater, Chapter 3. In Groundwater, *Groundwater Pollution* (pp. p:185-225).
- Gaillard J.-F., .. P. (1995). *Principes et Processus Chimiques. In Limnologie Générale*. Masson, Paris, 115-156.
- Garassino A., D. A. (2009). A new hermit crab (Crustacea, Anomura, Paguroidea) from the Late Cretaceous (Cenomanian) of Lebanon. *Stor. nat. Milano,; Atti Soc. it. Sci. nat. Museo civ.*
- GIS. (2012-2013-2014). Maps accomplished at the GIS. University of Balamand.
- Gi-Tak Chae, S.-T. Y.-H. (2007). Fluorine geochemistry in bedrock groundwater of South Korea. *Science of the Total Environment*, 385, p: 272–283.
- Goldenberg et al, M. ., (1985). Surface water groundwater interaction: water quality aspects .
- Gopalakrishnan, C., Tortajada, K., & Biswas, A. (2005). Water Institutions: Policies, Performance and Prospects. *Water Resources Development and Management; Springer*.
- Gorelick S.M. (1993). *Groundwater contamination: Optical capture and containment*. Ann Arbor: Lewis Publishers.
- Grassi S., G. P. (April, 2007). *Groundwater resource degradation in coastal plains: The example of the Cecina area (Tuscani-Central Italy)*. Institute of Geosciences and Earth Resources, Italy.
- Grassi, S., & Cortecchi, G. &. (2007). Groundwater resource degradation in coastal plains: The example of the Cecina area (Tuscani-Central Italy). *Applied Geochemistry*, 22(11), p:2273-2289.
- (n.d.). *Ground-Water Resource Availability, West Fork and White River Basin*.

- Group, A. ((2007, September).). *Geological and hydrogeological study for the location & design of water well in the village of Assia*. ABS Group .
- Gundogdu K.S, I. G. (February 200). Spatial analyses of groundwater levels using universal kriging. *Journal of Earth Syst. Sci., Vol 116, No. 1*, pp. 49–55.
- Gvt, A. (2002). *Groundwater Quality Protection*. COMMONWEALTH OF AUSTRALIA 2002.
- Hakim B. (1977). Problèmes Hydrologiques et Hydrochimiques du Kart du Liban central. *Norois, Numéro 95 bis, Karstologie*, p: 213-227.
- Halford J., K. (May-June 1995). Effects of Unsaturated Zone on Aquifer Test Analysis in a Shallow – Aquifer System. *Groundwater, Vol 35*.
- Halwani J. (2008). Assessment of the Water Situation in Lebanon. *The 3rd International Conference on Water Resources and Arid Environments (2008)*.
- Halwani J. (2009). Climate change and water resources in Lebanon. *IOP Conf. Series: Earth and Environmental Science 6* .
- Hamze, M., Hassan, S., Thomas, L. R., Khawlie, M., & Kawass, I. (2005). Bacterial indicators of Faecal pollution in the waters of El- Kabir river and Akkar watershed in Syria and Lebanon. *Lakes & reservoirs: research and management*, 10, p:117-125.
- Hamzeh, M. (2000). *Groundwater conditions in south Lebanon between the Awali and Litani Rivers*. MS Thesis. Beirut: Department of Geology, American University of Beirut.
- Harbaugh, A. W., Banta, E. R., & Hill, M. C. (2000). *MODFLOW-2000, THE U.S. GEOLOGICAL SURVEY MODULAR GROUND-WATER MODEL—USER GUIDE TO MODULARIZATION CONCEPTS AND THE GROUND-WATER FLOW PROCESS*. Reston, Virginia: U.S. GEOLOGICAL SURVEY.
- Hem, J. (1992). *Study and interpretation of the chemical characteristics of natural waters*. Washington: . Unites States government Printing Office.
- Hess J.W, W. B. (1993). Groundwater geochemistry of the carbonate karst aquifer,southcentral Kentucky, U.S.A. *Applied Geochemistry, Vol. 8*, p:189-204.
- Hessenauer M., , C. (Décembre 2001). Prospection d’eau souterraine par forages. *Bulletion de Géologie*

appliqué, vol. 6, p: 147 – 164.

Hongyan LI, Z. G. (20012). Spatial Characteristics of Water Quality of Wetland inNortheast China– the Case of Zhalong Wetland. *Procedia Environmental Sciences*, 12, p: 1024 – 1029.

Hydrogeologic cycle. (n.d.). Retrieved from <http://www.rmbel.info/Reports/Static/WaterCycle.aspx>

Hydrotechnik. (2012). *Hydrotechnik*. Retrieved from http://www.ht-hydrotechnik.com/cms/front_content.php?idcat=26&lang=2

Ian J. Fairchilda, G. W. (2006). Modelling of dripwater hydrology and hydrogeochemistry In a weakly karstified aquifer (Bath, UK): Implications For climate change studies. *Journal of Hydrology*, 321, p: 213–231.

IDRC, A. H. (n.d.). *Assessing Lebanon's water balance*, (document 4 of 14).

Itanidis P. K. (1997). *Introduction to Geostatistics: Application to hydrogeology*. . Cambridge University press.

J. I. (1997). *The Geochemistry of Natural Waters, Surface and Groundwater Environments* . Third Edition . Drever, University of Wyoming : Prentice Hall Upper Saddle River.

Jahangir M.M.R., P. J. (2012). Linking hydrogeochemistry to nitrate abundance in groundwater in agricultural settings in Ireland. (Elsevier, Ed.) *Journal of Hydrology*, Vol 449, p:212–222.

Jermar M.K. (1987). Developments in Water Science 28. *Water Resources and Water Management*.

Joerin C. (2000). *Etude des processus hydrologiques Par l'application du traçage environnemental. Association à des mesures effectuées À l'échelle locale et analyse d'incertitude*. ÉCOLE POLYTECHNIQUE FÉDÉRALE DE LAUSANNE.

JSene, K., J., M., & Hachache A. (1999, February). An assessment of the difficulties in qualifying the surface water resources of Lebanon. *Hydrological sciences journal*, 44(1) , p.79-96.

Julien Walter, A. R. (2011). Hydrogéochimie des eaux souterraines de la région du Saguenay-Lac-Saint-Jean : résultats préliminaires. *Geo- Hydro 2011*.

Kankjoo K., N. R.-J.-H. (2005). Evaluation of geochemical processes affecting groundwater chemistry based on mass balance approach: A case study in Namwon, Korea. *Geochemical Journal*, Vol.

39, p: 357 - 369.

Karst, S. G. (2002). "A Lexicon of Cave and Karst Terminology with Special to Environmental Karst Hydrology" EPA/600/R-02/003. EPA: Washington, DC.

Katisfarakis K.L., M. M. (2009). OPTIMIZATION OF GROUNDWATER RESOURCES MANAGEMENT IN POLLUTED AQUIFERS. *Global NEST Journal*, Vol 11, No 3, p: 283-290.

Kaufmann G. (2003). Modelling unsaturated flow in an evolving karst aquifer. *Journal of Hydrology*, 276, P:53-70.

Kaufmann G. (2009). Modelling unsaturated flow in an evolving karst aquifer. *Journal of Hydrology* 2, Vol 276, p:53–70.

Kaufmann G., D. T. (2010). Modeling three-dimensional karst aquifer evolution using different matrix-flow contributions. *Journal of Hydrology*, Vol 388, p:241–250.

Kaufmann G., R. D., & T., H. (2010). Modeling three-dimensional karst aquifer evolution using different matrix-flow contributions. *Journal of Hydrology*, 388 , p:241–250.

Keith J. Halford, W. D. (2000). Interpretation of Transmissivity Estimates from Single-Well Pumping Aquifer Tests. *Groundwater*, Vol 44, no. 3, p: 467–471.

Khair, K., Aker, N., Hadda, F., Jurdi, M., & Hchach, A. (1994, November). The environmental impacts of humans on groundwater in Lebanon. *Water, Air, & Soil Pollution*, 78(1-2), pp. p:37-49.

Khater, C., & M. Arnaud. (2007). Application of Restoration Ecology principles to the practice of limestone quarry rehabilitation in Lebanon. *Lebanese Science journal*, vol. 8(no.1).

Khawlie, M., Shaban, A., Abdallah, C., Darwish, T., & Kawass, I. (2005). Watersheds Characteristics, Land Use and Fabric: the Application of Remote Sensing and Geographical InformationS.M. *Lakes & Reservoirs: Research and Management*, 10, p:85-92.

Khayat Z. (2001). *Groundwater Condition in the Koura- Zgharta Miocene Limestone Aquifer*. Lebanon: American University of Beirut.

Kiely, G. (1998). *KielyEnvironmental Engineering*. McGraw-Hill. International Edition 1998.

Kirsch R. (2006). *Groundwater Geophysics: A tool for Hydrogeology*. Springer.

- Klein J. (2009). *L'Eau dans les relations internationales*.
- Konikow L.F. (2000). *UTILISATION DE MODELES NUMERIQUES POUR SIMULER LES PROCESSUS D'ECOULEMENT ET DE TRANSPORT DANS LES EAUX SOUTERRAINES*. US Geological Survey, Reston, Virginia, USA.
- Korfali S.I., & Jurdi M.J. (2010, October). Deterioration of Coastal Water Aquifers: Causes and Impacts. *European Water*, 29, p: 3-10.
- Krasny J. (March-April 1993). Classification of Transmissivity Magnitude and Variation. *Groundwater*.
- Kriging, t. u. (1996). Spatial modeling and interpolation of monthly temperature using kriging. *CLIMATE RESEARCH*.
- Kruseman G.P., D. R. (2003). *Analysis and Evaluation of Pumping Test Data, Second Edition*. International Institute for Land Reclamation and Improvement.
- Lanini S., Bakalowicz M., El-Hajj A., & Dorfliger N. (2008). Construction of a Water Management Support System for the Chekka Bay area (Lebanon). *Lanini et al., WWC*.
- Lam Q.D, (2000) , Assesing the impact of point and diffuse source pollution on nitrate load in a rural lowland catchement using SEWAT model. Kiel University, Germany.
- Lebanon, R. o. (May 17, 2010). *Water Sector: Public Expenditure Review*. Lebanon: World Bank.
- Leibundgut, C., Maloszewski, P., & Kulls C. (2009). *Tracers in Hydrology*. Wiley- Blackwell, John Wiley & sons, Ltd.
- Li Y., M. K. (2011). *Water Quality Concepts, Sampling, and Analyse*. CRC press Taylor and Francis group LLC.
- Libanaise, R. (2006). *Compendium statistique national sur les statistiques de l'environnement au Liban 2006*. Ministère de l'Environnement.
- Lindenbaum J. (2012). *Identification of sources of ammonium in groundwater using stable nitrogen and boron isotopes in Nam Du, Hanoi*. Dissertations in Geology at Lund University.
- Linsley, R., & Kohler, M. (1998). *Hydrogeology for Engineers. SI Metric Edition*. McGraw-Hill Book Company.

- Lucia F.J. (2007). Carbonate Reservoir Characterization, an Integrated Approach, Second Edition, Chapter 1 Petrophysical Rock Properties. Springer.
- LWMD. (2010). *General Guidelines for Calculating a Water Budget*. Land and Water Management Division.
- Makush D. S, C. D. (1995). Scale behavior of hydraulic conductivity during a pumping test. *Effects of Scale on Interpretation and Management of Sediment and Water Quality (Proceedings of*
- Mangin A, S. J. (1994). Karst hydrogeology in Groundwater Ecology. (N. Y. Press, Ed.)
- Markner-Jager B. (2008). *Technical English for Geosciences (a Text/ Work Book)*. Springer.
- Marsily D.G. (1986). *Quantitative Hydrogeology: Groundwater Hydrology for Engineers*.
- Masaad, H., & Bakalowicz M. (2007). Significance and origin of very large regulating power of some karst aquifers in the Middle East. Implication on karst aquifer classification. *Journal of Hydrology*, 333, p:329– 339.
- Masciopinto C. (2013). Management of aquifer recharge in Lebanon by removing seawater intrusion from coastal aquifers. *Journal of Environmental Management*, Vol 130, p:306-312.
- Massoud M.A. (2006). Factors influencing development of management strategies for the Abou Ali River in Lebanon: Spatial variation and land. *Science of the Total Environment*, 362, p:15– 30.
- Masters, G. M. (1994). *Introduction to Environmental Engineering and Science*. Department of Civil Engineering Stanford University.
- Mathevet, T. (Septembre 2002). *Analyse du fonctionnement du système karstique de Bange-L'eau-Morte (Bauges, Savoie & Haute-Savoie, France)*. Université Pierre et Marie Curie, Université Paris-Sud, École des Mines de Paris & École Nationale du Génie Rural des Eaux et des Forêts.
- Matthias Raiber a, ♂. P. (2012). Three-dimensional geological modelling and multivariate statistical analysis of Water chemistry data to analyse and visualise aquifer structure and Groundwater composition in the Wairau Plain, Marlborough District, New Zealand. *Journal of Hydrology*, 436-437, p:13–34.
- May A. Massoud, M. E.-F. (2006). Factors influencing development of management strategies for the Abou Ali River in Lebanon I: Spatial variation and land use. *Science of the Total Environment*,

Vol 362, p:15– 30.

Mayer J., B. J. (2002). Groundwater Quality Implications of Bank- Storage in a Crystalline-Rock Setting. *Environmental Geosciences, Volume 9, Number 2*, p.74–80.

Mazzullo S. J. (2004). Overview of Porosity Evolution in Carbonate Reservoirs. *Search and Discovery Article N .40134* .

McCuen R. H. (1998). *Hydrologic Analysis and Design (2nd edition)*. New Jersey: Pearson Education, Prentice Hall Upper Saddle River.

MEDITATE. (December, 2007). *Final report of MEDITATE project. BRGM*.

Mehnert E., A. J. (1985). THE EFFECT OF SALINITY-DEPENDENT HYDRAULIC CONDUCTIVITY ON SALTWATER INTRUSION EPISODES. *Journal of Hydrology*,, 80, p:297 283.

Mehnert, E., & Jennings, A. (1985). The effect of salinity-dependent hydraulic conductivity on saltwater intrusion episodes. *Journal of Hydrology, vol. 80*, p: 283-297.

Mijatović B. (2006, august). The Groundwater discharge in the Mediterranean Karst Coastal Zones and freshwater tapping: set problems and adopted solutions. *Environmental Geology, 51*, p:737-742.

Mineral saturation index,. (n.d.). Retrieved from <http://www.water-research.net/corrosion.htm>

MOE. (2011). *LEBANON'S SECOND NATIONAL COMMUNICATION TO THE UNFCCC*. MOE.

MOE, A. C. (2006). *COMPENDIUM STATISTIQUE NATIONAL SUR LES STATISTIQUES DE L'ENVIRONNEMENT AU LIBAN 2006*. Eurostat.

MOE, U. (2010). *TEDO 2010*. Lebanon: MOE.

MoE/GEF/UNDP. (July 2009). *FOURTH NATIONAL REPORT of LEBANON to the CONVENTION ON BIOLOGICAL DIVERSITY* . MoE/GEF/UNDP.

Moench F., A. (November - December 1993). Computation of Type Curves for flow to partially penetrating wells in Water-Table Aquifers. *Groundwater*, p:966-971.

Mohammadi Z., R. E. ((January) 2010). Mise en évidence d'un karst à partir de fonctionnement de l'aquifère des calcaires Asmari, au site du Barrage de Khersan 3, sud de l'Iran. *Hydrological*

Sciences Journal , p.205 -220.

- Moore J.P. (2009). Geochemical and statistical evidence of recharge, mixing, and controls on spring discharge in an eogenetic karst aquifer. *Journal of Hydrology Elsevier*, 376 , p:443–455.
- Mores. (June 2010). Hydrological Analysis and Vulnerability Mapping of Qammoua and the Surrounding Area.
- Morhange C., A., P. P., N., M., F., M. L., & T., N. (2006). Late Holocene relative sea-level changes in Lebanon, eastern Mediterranean. *Elsevier Marine geology*, 230, p:99-114.
- Morhange C., P. P. (2006). Late Holocene relative sea-level changes in Lebanon, eastern Mediterranean. *Elsevier Marine geology*, 230, p: 99-114.
- Moujabber M. EL, B. B. (2006). Comparison of Different Indicators for Groundwater Contamination by Seawater Intrusion on the Lebanese Coast. *Water Resources Management*, Vol 20, p:161–180.
- Murray, C. (1960). Origin of porosity in carbonate rocks. *Journal of Sedimentary Petrology*, vol 30, p: 59-84.
- Nader F. H., S. R. (2003). *Karst-Meteoric Dedolomitization in Jurassic carbonates, Lebanon*. Geologica Belgica.
- Nader F.H. (2007). Petrographic and geochemical study on cave pearls from Kanaan Cave (Lebanon). (I. 0392-6672., Ed.) *International Journal of Speleology*, Vol 36 (1), p:39-50.
- Nathanson, J. A. (200). *Basic Environmental Technology. Water Supply, Water Management and Pollution Control. Third Edition* .
- Nations Unies. (1970). *Etude des eaux souterraines*. New York: Nations Unies.
- Nations Unies. (1970). *Liban, Etudes des eaux souterraines*.
- Neuman S. P., A. B. (2007). Type curve interpretation of late-time pumping test data in randomly heterogeneous aquifers. *WATER RESOURCES RESEARCH*, VOL. 43.
- Oueida, R. (1992). *Terrain Analysis and Geological Studies for Land-Use Planning in and around Tripoli-North Lebanon*. MS Thesis. Department of Geology, American University of Beirut,.
- Parello F., A. H. (2007). Geochemical characterization of the surface waters and groundwater resources in

the Managua area (Nicaragua, Central America).

Parello, F., Aaiuppa, A., Calderon, H., Calvi, F., Cellura, D., Martinez, V., et al. (2008). Geochemical characterization of the surface waters and groundwater resources in the Managua area (Nicaragua, Central America). *Applied geochemistry*, 23(4), p:914-931.

Programme des Nations Unies pour le Développement, F. C. (1971). *Etude Geologique de la Region de Koura- Zgharta*. Beirut.

Programme des Nations Unies pour le Développement, F. C. (1972). *Etude Geologique de la Region de Koura- Zgharta* . Beirut: FAO.

Québec, G. d. (Juillet 2008). *Guide d'échantillonnage à des fins d'analyses environnementales*. Centre d'expertise en analyse environnementale du Québec.

Quinlan F.J. ((February)1989). *Ground water monitoring in Karst terrains (recommended protocols & implicit assumption)*. EPA.

Rai S.N, M. A. (1999). *Modelling of water table variation in response to time-varying recharge from multiple basins using the linearised Boussinesq equation*. Journal of Hydrology.

Rai S.N., A. M. (1999). Modelling of water table variation in response to time-varying recharge from multiple basins using the linearised Boussinesq equation. *Journal of Hydrology*, Vol 220, p:141–148.

Record, G. A. (2008). *A Review of Spatial Interpolation Methods for Environmental Scientists*. Australian Gvt.

Ribolz O., v. V. (1993). Contrôle géochimique des eaux par la formation de calcite en milieu méditerranéen et en milieu tropical Arguments d'équilibre et argument de bilan. *SCIENCE DU SOL*, Vol. 31, 1/2, p:77-95.

Robins S.N. (1998). *Groundwater pollution, aquifer recharge and vulnerability*. London: Geologic Society London.

Saad Z., K. V. (2005). A hydrochemical and isotopic study of submarine Fresh water along the coast in lebanon. *The Electronic Journal of the International Association for Environmental Hydrology*.

Saadeh M. (February 2008). *Influence of overexploitation and seawater intrusion on the quality of*

- groundwater in greater Beirut*. Dissertation Master of Science Mark Saadeh AUS Beirut, Lebanon.
- Salbu, B. &. (1995). Trace elements in natural waters. *Boca Raton, Florida: CRC Press*.
- Sawyer, C. N., McCarty, P. L., & Parkin, G. F. (1994). *Chemistry for environmental engineering*. (4th ed.). New York: N.Y.: McGraw-Hill.
- Sayyed J- A., B. A. (2011). *Analysis of Chloride, Sodium and Potassium in Groundwater Samples of Nanded City in Mahabharata, India*. European Journal of Experimental Biology.
- Schoeller H. (n.d.). Les modification de la composition chimique de l'eau dans une meme nappe . p: 124-129 .
- Schoeller H. (n.d.). Salinite des eaux souterraines. Evapotranspiration et alimntation des nappes.
- SCHOELLER, H. (n.d.). *LA CLASSIFICATION GÉOCHIMIQUE DES EAUX*.
- SCS. (1972). *Calculating Effective Rainfall*. <http://www.alanasmith.com/theory-Calculating-Effective-Rainfall-The-SCS-Method.htm>.
- Shaban A. (2008). . Identification of groundwater storage and flow through the analysis of fracture systems from space. *The 3rd International conference onwater resources and arid environments and the 1st Arab water forum*.
- Shaban A. (December 2010). Trans-boundary water resources of Lebanon: monitoring and assessment. *International Conference "Transboundary Aquifers: Challenges and New Directions"*.
- Shaban A. (February 2010). Support of space techniques for groundwater exploration in Lebanon,. *JWARP*.
- Shaban A., K. M. (November 2004). *Geologic Controls of Submarine Groundwater Discharge: application of remote sensing to North Lebanon*.
- Shaban A., K. M. (2005). Hydrological and Watershed Characteristics of the El-Kabir river, North Lebanon. *Lakes & Reservoirs: Research and Management*, 10, p:93-101.
- Shaban A., K. M. (2006). Use of remote sensing and GIS to determine recharge potential zones: the case of occidental Lebanon. . *Springer Hydrogeology Journal* , p:433-433.

- Singhal, B. a. (2007). *Applied Hydrogeology of Fractured Rocks*. (Vol. 47). Kluwer Academic Publishers, Dordecht,.
- Sipes J. L. (2010). . *Sustainable Solutions for Water Resources (Policies, Planning, Design, and Implementation)*. Wiley; John Wiley & Sons, Inc.
- Smyth R.C., L. J. (2000). *Transmissivity , Hydraulic Conductivity and Storativity of The Carrizo-Wilcox Aquifer in Texas*.
- Snoeyink V. L., J. D. (1980). *Water Chemistr*. New York: John Wiley & sons.
- Soliman M., L. P. (1998). *Environmental Hydrogeology*. .Lewis Publishers.
- Stephan R. (2010). *State and trends of the Lebanese environment 6 land resources*. Lebanon.
- Stiff, H. J. (1951). The interpretation of chemical water analysis by means of patterns. *Journal of petroleum technology*, vol. 3, p. 15-17.
- Survey, G. a. (2011). *Definition and Classification of Limestone*. Missouri Department of Natural Resources, Division of Geology and Land Survey.
- Taniguchi M., T. (2011). *Groundwater and Subsurface Environments (Human Impacts in Asian Coastal Cities)* . Springer.
- Tekin E. (September 2012). *Anaerobic ammonium oxidation in groundwater contaminated by fertilizers*. Thesis Submitted to the Faculty of Graduate and Postdoctoral Studies ,University of Ottawa.
- Theis, C. (1938). The significance and nature of the cone of depression in ground-water bodies. *Economic Geology*, vol. 38, p. 889-902.
- Theis, C. (May 1940). The source of water derived from wells. Essential Factors controlling the response of an aquifer to development. *Civil Engineering, Volume 10, N5*.
- Thomas R. L., K. M. (2005). The Assessment and Management of the Water Quality of the Akkar Watershed on the Northern Boundary of Lebanon with Syria. *Lakes & reservoirs: Research and Management*, 10, p:83-84.
- Thomas R. L., S. A. (n.d.). Geology of the Sediments of the El-Kabir River and Akkar Watershed in Syria and Lebanon. *Lakes and reservoirs: research and management, Vol 10*, p:127-134.

- Thompson S. A. (1999). *Hydrology for Water Management*. A.A. Balkema, Rotterdam Brookfield.
- Todd D. K., M. L. (2004). *Groundwater Hydrology (3rd edition)*. Wiley; John Wiley & Sons, Inc. .
- Toth J.,T. (2009). *Gravitational systems of groundwater flow: Theory, evaluation, utilization*. Cambridge.
- Traboulsi M. (2010). La pluviometrie moyenne annuelle au Liban Interpolation et cartographie Automatique. *Lebanese Science Journal*, Vol. 11, No. 2.
- Traboulsi M., H. B. (2012). Fortes chaleurs et circulation atmosphérique associée autour de la Méditerranée orientale : cas du littoral tunisien et syro-libanais. *Territoire en mouvement*, p:106-119.
- Tracey A. Spencer, L. D. (2000). *Water-Quality and Water-Level Data for a FreshwaterTidal Wetland, West Branch Canal CreekAberdeen Proving Ground, Maryland*. Baltimore, Maryland.
- UNDP, M. &. (2011). *State and Trends of the Lebanese Environment 2010*.
- UNESCWA. (2012). *WATER IN LEBANON STRATEGIC MANAGEMENT DATA NATIONAL ASSESSMENT MATRIX*. MOE -UNESCWA.
- USGS. (January 2012). *Phosphorus and Groundwater: Establishing Links BetweenAgricultural Use and Transport to Streams*. USGS.
- Usharni K., U. K. (June 2010). Physico-Chemical and Bacteriological Characteristics of Noyyal River and Ground Water Quality of Perur, India. *Journal of Applied Science and Environmental Management*, Vol. 14 (2) , p:29 - 35.
- Van Beynen P. E. (2011). *.Karst Management*. Springer.
- Van Dongen P. G., V. D. (October 1966). *Paleomagnetism and the alpine tectonics of Eurasia III: Paleomagnetic research in the central Lebanon Mountains and in the Tartous area (Syria)*. Tectonophysics- Elsevier Publishing Company, Ams.
- Vieux E. B. (2004). *Distributed Hydrologic Modeling using GIS (2nd edition)*. Kluwer Academic Publishers .
- Vivier J.P, G. T. (October 1997). An Analytical method for the analysis of pumping tests in fracture aquifers. *Water SA*.

- Walley C. D. (n.d.). the Geology and Hydrogeology of the AAMMIQ Wetlands Region.
- Walley C. D. (1998). *Notes on the Geology of Lebanon*. AUB : Beirut .
- Walley C.D. (1997). The Lithostratigraphy of Lebanon: A Review. *Lebanese Science Bulletin* vol. 10.1, p. 81-108 .
- Walley C.D. (1997). *The lithostratigraphy of Lebanon: A review*. Lebanese Science Bulletin.
- Walley C.D. (1998). Some outstanding issues in the geology of Lebanon and their importance in the tectonic evolution of the Levantine region. *Tectonophysics* vol. 298, p. 37-62.
- Walley C.D. (1998). *The Geology of Lebanon: A Summary*. AUB : Beirut.
- Water, N. O. (October 2011). *General purpose water accounting reports Groundwater methodologies*. Sydney: NSW Office of Water.
- Watershed*. (n.d.). Retrieved from <http://ga.water.usgs.gov/edu/watercycleinfiltration.html>
- White W.B. (2002). Karst hydrology: recent developments and open questions. *Elsevier Engineering Geology* 65 ; p.85–105.
- WHO. (2006). *Guidelines of drinking water quality recommendation:3rd edition*. Geneva.
- WHO/SDE/WSH/03.04/114. (2004). *Sulfate in Drinking-water*. Background document for development of WHO Guidelines for Drinking-water Quality. World Health Organization .
- Wikipedia. (n.d.).
- World Health Organization. (2011). *Guidelines for Drinking-water Quality*. Switzerland: World Health Organization.
- Worter, M., & Sunada. (1977).
- Wright, D. K. (May 2002). *AN ASSESSMENT OF GROUNDWATER QUALITY IN SOUTH CORK* . Cork County Council (Southern Division).
- Zaahrudine K., K. K. (1992). Hydrologic units of Lebanon. *Applied Hydrogeology* vol. 2, p. 34-49.
- Zeinati M., E.-F. M. (2000). Water Ressources in Lebanon: Characterization , Water Balance and

Contamination. *Water resource Development*, Vol 16(No 4), p,625-658.

Zektzer I.S., V. I. (1973). THE PROBLEM OF DIRECT GROUNDWATER DISCHARGE TO THE SEAS. *Journal of Hydrology*, p:1-36.

APPENDIX 1- WATER PROPERTIES

Table A.2.4

Temperature (°C)	Specific Weight (kN/m ³), $\gamma = \rho g$	Mass per unit volume, ρ (kg/m ³)	Dynamic viscosity, μ (10 ³ /Pa s)	Kinematic viscosity, $\nu (= \mu/\rho)$ (10 ⁻⁶ m ² /s)	Latent heat of vaporization (J/g)
0	9.805	999.8	1.781	1.785	2500.3
5	9.807	1000.0	1.518	1.519	2488.6
10	9.804	999.7	1.307	1.306	2476.9
15	9.798	999.1	1.139	1.139	2465.1
20	9.789	998.2	1.002	1.003	2453.0
25	9.777	997.0	0.890	0.893	2441.3
30	9.764	995.7	0.798	0.800	2429.6
40	9.730	992.2	0.653	0.658	2405.7
50	9.689	988.0	0.547	0.553	2381.8
60	9.642	983.2	0.466	0.474	2357.6
70	9.589	977.8	0.404	0.413	2333.3
80	9.530	971.8	0.354	0.364	2308.2
90	9.466	965.3	0.315	0.326	2282.6
100	9.399	958.4	0.282	0.294	2256.7

Table A.2.5

Properties of Seawater at 34 kg/m³

Temperature °C	Mass per unit volume, ρ (kg/m ³)	Specific heat, c (J/kg K)	Kinematic viscosity, ν (10 ⁶ m ² /s)
0	1027.32	3989	1.8
5	1026.91	3992	1.6
10	1026.19	3995	1.4
15	1025.22	3997	1.2
20	1024.02	4000	1.1
25	1022.61	4002	0.94

Table A.2.6**Properties of Saltwater at Various Concentrations**

Concentration of NaCl (kg/m ³)	Mass of NaCl per mass of solution at 20°C (%)	Mass per unit volume of the solution at 15°C (kg/m ³)	The same at 20°C	Specific heat at 20°C (J/kg K)
0	0	999.13	998.23	4182
10	0.995	1006.30	1005.30	4127
20	1.976	1013.39	1012.29	4075
30	2.943	1020.41	1019.22	4024
40	3.898	1027.35	1026.07	3975
50	4.841	1034.25	1032.88	3929
60	5.772	1041.05	1039.60	3884
70	6.690	1047.83	1046.32	3841

Table A.2.4

Temperature (°C)	Specific Weight (kN/m ³), $\gamma = \rho g$	Mass per unit volume, ρ (kg/m ³)	Dynamic viscosity, μ (10 ³ /Pa s)	Kinematic viscosity, $\nu (= \mu/\rho)$ (10 ⁻⁶ m ² /s)	Latent heat of vaporization (J/g)
0	9.805	999.8	1.781	1.785	2500.3
5	9.807	1000.0	1.518	1.519	2488.6
10	9.804	999.7	1.307	1.306	2476.9
15	9.798	999.1	1.139	1.139	2465.1
20	9.789	998.2	1.002	1.003	2453.0
25	9.777	997.0	0.890	0.893	2441.3
30	9.764	995.7	0.798	0.800	2429.6
40	9.730	992.2	0.653	0.658	2405.7
50	9.689	988.0	0.547	0.553	2381.8
60	9.642	983.2	0.466	0.474	2357.6
70	9.589	977.8	0.404	0.413	2333.3
80	9.530	971.8	0.354	0.364	2308.2
90	9.466	965.3	0.315	0.326	2282.6
100	9.399	958.4	0.282	0.294	2256.7

APPENDIX 2- DATA REQUIRED FOR VISUAL MODFLOW

sampling name	Location	North	Easr	X	CODE	x	y	Elevation	Depth of the well in m
S1	Aaba (private)	N 34° 20' 48.0"	E 035° 49'42.8"	0	34	-305475	21248	241	150
P1	Agrotech	N 34° 19' 17.7"	E 035° 48' 25.0"	0	34	-307554	18531	256	240
S2	Alma 1	N 34° 25' 29.0"	E 035° 54' 14.9"	0	34	-298248	29679	198	198
S3	Alma 2	N 34° 25' 31.6"	E 035° 54' 13.2"	0	34	-299002	28884	220	85
P2	Alma Dawle	N 34° 26' 05.0"	E 035° 53' 55.2"	0	34	-298716	30804	254	120
S4	Almoun 1	N 34° 23' 31.0"	E 035° 47'38.9"	0	34	-308475	26371	7	5
S5	Almoun 2	N 34°23' 07.6"	E 035° 47' 18.1"	0	34	-310008	25351	20	9
S6	Amioun 1	N 34° 17' 55.3"	E 035° 49' 00.9"	0	34	-307100	17059	295	30
S7	Amioun 2	N 34° 17' 05.2"	E 035° 49' 08.3"	0	34	-306616	14736	298	25
P3	Anfe , Jrade	N 34° 20' 14.7"	E 035° 44' 13.9"	0	34	-313912	20499	20	22
S8	Anfeh 1	N 34° 21' 03.3"	E 035° 43'53.8"	0	34	-314268	22942	10	7.5
S9	Anfeh 2	N 34° 20' 39.1"	E 035°44' 02.3"	0	34	-314445	21796	14	8

S10	Arabech	N 34° 23' 01.0"	E 035° 53' 45.6"	0	34	-299225	26535	770	150
S11	Arde	N 34° 24' 33.0"	E 035° 55'14.1"	0	34	-297260	28578	145	50
P4	Arges	N 34° 20' 05.2"	E 035° 52' 50.1"	0	34	-300732	19775	299	225
P19	aser el maei			0	0	-302463	31580	0	125
P5	Asnoun 2	N 34° 23' 17.3"	E 035° 53' 20.4"	0	34	-299822	25314	149	150
P6	Ayto	N 34° 18' 32.6"	E 035° 55' 48.3"	0	34	-296269	16778	1028	35
S12	Badawi 1	N 34° 27' 17.4"	E 035° 51' 56.1"	0	34	-300526	33444	10	22
S13	Badawi 2	N 34° 26' 43.8"	E 035°49'49.1"	0	34	-301168	32123	15	26
S14	Badebhoon 1	N 34° 20' 05.3"	E 035°45' 32.8"	0	34	-310917	19725	199	85
S15	Badebhoon 2	N 34° 20' 05.8"	E 035° 45' 33.6"	0	34	-312337	20085	216	76
S16	Balamand	N 34° 22' 01.9"	E 035° 46'48.0"	0	34	-309866	23670	302	30
S17	Barghon	N 34° 20' 31.9"	E 035°45' 25.8"	0	34	-312153	21194	153	115
P7	Barsa	N 34° 23' 11.11"	E 035° 49' 28.4"	0	34	-305699	25667	164	145
S18	Batromine	N 34°22' 19.3"	E 035°48' 09.2"	0	34	-307223	23559	318	150
S19	Bdebba	N 34° 20' 28.6"	E 035°49' 16.5"	0	34	-306607	21350	247	150
P8	Bir Al- Ahdab (Ras Maska)	N 34° 23' 43.3"	E 035° 49' 52.3"	0	34	-305057	26639	114	99
P9	Bir Bechmezzine, Snoubar	N 34° 19' 04.3"	E 035° 48' 12.0"	0	34	-307899	17843	270	145

P10	Bir Bterram	N 34° 19' 43.3"	E 035° 49' 02.8"	0	34	-306562	19288	260	250
P11	Bir El mazraa – Kferaka	N 34° 19' 14.3"	E 035° 50' 09.6"	0	34	-304884	18339	319	308
P12	Bir Kfarhazir, (Ain el Bakar)	N 34° 19' 20.6"	E 035° 48' 13.4"	0	34	-307847	18630	260	185
P13	Bir Ras Maska	N 34° 23' 36.8"	E 035° 49' 58.0"	0	34	-304918	26434	149	132
S20	Bkeftine	N 34° 23' 08.9"	E 035° 51' 48.0"	0	34	-302137	25484	170	220
S21	Borj Hayodiyeh (Dawle Well)	N 34° 27' 15.8"	E 035° 54' 58.5"	0	34	-297198	33006	198	50
S22	Boussit	N 34° 26' 20.9"	E 035° 55' 29.0"	0	34	-296306	31217	596	85
S23	Bteram (private)	N 34° 19' 46.5"	E 035° 48'33.6"	0	34	-307305	20345	268	155
S24	Btouratij , Adnan Hassan	N 34° 22' 01.8"	E 035° 50' 34.7"	0	34	-303864	23848	215	130
S25	Btouratij 2 , Mokhtar	N 34° 21' 42.7"	E 035° 50'11.0"	0	34	-304982	22777	227	30
S26	Chahal Building (Dam & Farez)	N 34° 25' 53.6"	E 035°49' 53.7"	0	34	-304891	30651	23	29
S27	Chekaa 1	N 34° 19' 32.4"	E 035° 44' 14.2"	0	34	-313499	19196	52	10
S28	Chekaa 2	N 34° 19' 47.1"	E 035°43'38.9"	0	34	-315299	18535	11	7
S29	Dahel El Ain , private 1	N 34° 24' 04.4"	E 035° 50' 27.0"	0	34	-303667	25675	79	88
P14	Deir Achach	N 34° 25' 09.3"	E 035° 56' 23.4"	0	34	-295049	28439	187	55
S31	Deir Amar 1	N 34° 27' 33.8"	E 035° 53' 38.2"	0	34	-299062	33553	46	40

S32	Deir Amar 2	N 34° 27' 46.8"	E 035° 53' 46.5"	0	34	-298733	34228	37	35
S33	Deir amar, kassarat	N 34° 27' 15.8"	E 035° 53'59.7"	0	34	-298667	32490	146	90
S30	Didde, Gaz Station	N 34° 22' 37.5"	E 035° 47' 54.3"	0	34	-307902	25137	306	250
P15	Ejed Ebrin	N 34° 16' 30.9"	E 035° 44' 22.9"	0	34	-313912	13598	247	90
S34	Fih	N 34° 21' 05.1"	E 035° 46' 56.5"	0	34	-309603	21311	412	250
P16	Hawouz	N 34° 25' 44.3"	E 035° 50' 45.5"	0	34	-303578	30322	56	50
P17	Hellan	N 34° 25' 46.2"	E 035° 57' 34.2"	0	34	-293267	30659	312	45
S35	Hraiche 1	N 34° 22' 15.7"	E 035° 44' 39.6"	0	34	-312016	24658	40	75
S36	Hraiche 2	N 34° 17' 33.5"	E 035° 55' 03.6"	0	34	-313488	24028	0	120
P18	Jisir			0	0	-303158	27696	0	89
S37	Kelhat	N 34° 21' 16.9"	E 035° 46' 50.1"	0	34	-310263	22626	410	108
S38	Kfarhat, Jedeide	N 34° 22' 43.3"	E 035° 53' 50.5"	0	34	-299090	23474	129	56
S39	Kfarkahel	N 34° 21' 30.0"	E 035° 51' 05.3"	0	34	-303731	21926	220	160
P20	Kferzayna 1	N 34° 21' 50.6"	E 035° 52' 51.3"	0	34	-300597	23020	182	80
P21	Kferzayna 2	N 34° 21' 51.5"	E 035° 52' 49.2"	0	34	-300668	23085	190	80
P22	Malloule	N 34° 26' 59.1"	E 035° 51' 36.5"	0	34	-302202	32583	16	8
P23	Manar	N 34° 25' 07.3"	E 035° 50' 18.9"	0	34	-304294	29204	70	212

P24	Massafi 7	N 34° 25' 08.7"	E 035° 49' 52.9"	0	34	-304981	29250	28	70
P25	Mazra3et el Tefeh	N 34° 19' 17.3"	E 035° 57' 29.7"	0	34	-293810	18063	1031	140
S40	Mervat , Abou Samra	N 34° 25' 15.4"	E 035° 50' 37.0"	0	34	-303824	29438	138	52
S41	Mervat , House	N 34° 26' 21.6"	E 035° 49' 38.8"	0	34	-305243	31526	99	15
P26	Meryata 1- El Blat	N 34° 25' 41.0"	E 035° 55' 53.5"	0	34	-295964	29480	370	250
P27	Meryata 2	N 34° 25' 11.2"	E 035° 56' 10.2"	0	34	-295322	29038	225	60
P28	Meryata 3	N 34° 25' 25.4"	E 035° 56' 49.2"	0	34	-294856	30605	219	60
P29	Meryata 4 (Youn Achech)	N 34° 25' 27.0"	E 035° 56' 49.7"	0	34	-294533	29737	219	55
S42	Mijdlaya 1	N 34° 26' 00.8"	E 035° 52' 23.9"	0	34	-301050	30749	146	136
S43	Mijdlaya 2	N 34° 25' 09.2"	E 035° 52' 39.9"	0	34	-301625	28711	148	144
S44	Mina 1	N 34° 26' 51.1"	E 035° 49' 19.2"	0	34	-306892	32899	2	3
S45	Mina 2	N 34° 26' 51.11"	E 035° 49' 32.2"	0	34	-306289	31689	10	8
S46	Minieh 1			0	0	-296683	34656	0	25
S47	Minieh 2			0	0	-294911	35898	0	20
S51	Miteen			0	0	-303655	32180	0	60
S48	Nakhle	N 34° 22' 21.0"	E 035° 49' 54.2"	0	34	-305091	24102	227	180
S49	Ras Maska , Private 1	N 34° 23' 51.1"	E 035° 49' 41.6"	0	34	-306149	26970	108	109

S50	Ras Maska , Private 2	N 34° 23' 52.7"	E 035° 50' 09.3"	0	34	-305188	28739	78	300
P30	Raskifa	N 34° 18' 53.0"	E 035° 52' 36.6"	0	34	-301368	17463	405	125
P31	Saadoun	N 34° 25' 47.4"	E 035° 50' 34.1"	0	34	-303938	30497	66	60
P32	Sankari	N 34° 25' 29.7"	E 035° 50' 12.9"	0	34	-304424	29899	80	45
P33	Seb3el	N 34° 18' 54.3"	E 035° 54' 53.5"	0	34	-297802	17480	653	60
P34	Sereel	N 34° 17' 33.5"	E 035° 55' 03.6"	0	34	-297666	14994	794	12
P35	Willey	N 34° 25' 45.6"	E 035° 50' 36.8"	0	34	-303248	31076	80	120
S52	Zakroun	N 34° 21' 32.5"	E 035° 45' 05.3"	0	34	-312376	22816	96	99

Well Points

Sample ID	Abreviation	x	y	X	Y	Z
Aaba (private)	S1	N 34° 20' 48.0"	E 035° 49'42.8"	35.828556	34.346667	241
Agrotech	S2	N 34° 19' 17.7"	E 035° 48' 25.0"	35.806944	34.321583	256
Alma dawle	S3	N 34° 26' 05.0"	E 035° 53' 55.2"	35.898667	34.434722	254
Alma 1	S4	N 34° 25' 29.0"	E 035° 54' 14.9"	35.904139	34.424722	198
Alma 2	S5	N 34° 25' 31.6"	E 035° 54' 13.2"	35.903667	34.425444	220
Almoun 1	S6	N 34° 23' 31.0"	E 035° 47'38.9"	35.794139	34.391944	7
Almoun 2	S7	N 34°23' 07.6"	E 035° 47' 18.1"	35.788361	34.385444	20
Amioun 1	S8	N 34° 17' 55.3"	E 035° 49' 00.9"	35.816917	34.298694	295
Amioun 2	S9	N 34° 17' 05.2"	E 035° 49' 08.3"	35.818972	34.284778	298
Anfe , Jade	S10	N 34° 20' 14.7"	E 035° 44' 13.9"	35.737194	34.337417	20
Anfeh 1	S11	N 34° 21' 03.3"	E 035° 43'53.8"	35.731611	34.350917	10
Anfeh 2	S12	N 34° 20' 39.1"	E 035°44' 02.3"	35.733972	34.344194	14
Arabech	S13	N 34° 23' 01.0"	E 035° 53' 45.6"	35.896	34.383611	770
Arde	S14	N 34° 24' 33.0"	E 035° 55'14.1"	35.920583	34.409167	145

Arges	S15	N 34° 20' 05.2"	E 035° 52' 50.1"	35.880583	34.334778	299
Asnoun	S16	N 34° 23' 17.3"	E 035° 53' 20.4"	35.889	34.388139	149
Ayto	S17	N 34° 18' 32.6"	E 035° 55' 48.3"	35.930083	34.309056	1028
Badawi 1	S18	N 34° 26' 43.8"	E 035°49'49.1"	35.865583	34.454833	15
Badawi 2	S19	N 34° 27' 15.8"	E 035° 53'59.7"	35.830306	34.4455	146
Badebhoon 1	S20	N 34° 20' 05.3"	E 035°45' 32.8"	35.759111	34.334806	199
Badebhoon 2	S21	N 34° 20' 05.8"	E 035° 45' 33.6"	35.759333	34.334944	216
Balamand	S22	N 34° 22' 01.9"	E 035° 46'48.0"	35.78	34.367194	302
Barghon	S23	N 34° 20' 31.9"	E 035°45' 25.8"	35.757167	34.342194	153
Barsa	S24	N 34° 23' 11.11"	E 035° 49' 28.4"	35.824556	34.386419	164
Batromine	S25	N 34°22' 19.3"	E 035°48' 09.2"	35.802556	34.372028	318
Bdebba	S26	N 34° 23' 08.9"	E 035° 51' 48.0"	35.82125	34.341278	170
Bir Al- Ahdab (Ras Maska)	S27	N 34° 23' 43.3"	E 035° 49' 52.3"	35.831194	34.395361	114
Bir Bechmezzine, Snoubar	S28	N 34° 19' 04.3"	E 035° 48' 12.0"	35.803333	34.317861	270
Bir Bterram	S29	N 34° 19' 43.3"	E 035° 49' 02.8"	35.817444	34.328694	260
Bir El mazraa – Kferaka	S30	N 34° 19' 14.3"	E 035° 50' 09.6"	35.836	34.320639	319

Bir Kfarhazir, (Ain el Bakar)	S31	N 34° 19' 20.6"	E 035° 48' 13.4"	35.803722	34.322389	260
Bir Ras Maska	S32	N 34° 23' 36.8"	E 035° 49' 58.0"	35.832778	34.393556	149
Bkeftine	S33	N 34° 27' 15.8"	E 035° 54' 58.5"	35.863333	34.385806	198
Borj Hayodiyeh (Dawle Well)	S34	N 34° 26' 20.9"	E 035° 55' 29.0"	35.91625	34.454389	596
Boussit	S35	N 34° 22' 01.8"	E 035° 50' 34.7"	35.924722	34.439139	215
Bteram (private)	S36	N 34° 19' 46.5"	E 035° 48'33.6"	35.809333	34.329583	268
Btouratij 1 , Adnan Hassan	S37	N 34° 21' 42.7"	E 035° 50'11.0"	35.842972	34.367167	227
Btouratij 2 , Mokhtar	S38	N 34° 26' 51.1"	E 035° 49' 19.2"	35.836389	34.361861	2
Chahal Building (Dam & Farez)	S39	N 34° 23' 51.1"	E 035° 49' 41.6"	35.831583	34.431556	108
Chekaa 1	S40	N 34° 19' 32.4"	E 035° 44' 14.2"	35.737278	34.325667	52
Chekaa 2	S41	N 34° 19' 47.1"	E 035°43'38.9"	35.727472	34.32975	11
Dahel El Ain , private 1	S42	N 34° 24' 04.4"	E 035° 50' 27.0"	35.840833	34.401222	79
Dédde, Gaz Station	S43	N 34° 28' 56.2"	E 035° 56' 22.6"	35.939833	34.41925	38
Deir Achach	S44	N 34° 25' 09.3"	E 035° 56' 23.4"	35.893944	34.459389	187
Deir Amar 1	S45	N 34° 27' 33.8"	E 035° 53' 38.2"	35.89625	34.463	46
Deir Amar 2(kasser balade)	S46	N 34° 27' 46.8"	E 035° 53' 46.5"	35.899917	34.454389	37

Deir amar 3, Kassarat	S47	N 34° 29' 01.9"	E 035° 56' 26.6"	35.798417	34.377083	26
Ejed Ebrin	S48	N 34° 16' 30.9"	E 035° 44' 22.9"	35.739694	34.27525	247
Fih	S49	N 34° 21' 05.1"	E 035° 46' 56.5"	35.782361	34.351417	412
Hawouz	S50	N 34° 25' 44.3"	E 035° 50' 45.5"	35.845972	34.428972	56
Hellan	S51	N 34° 25' 46.2"	E 035° 57' 34.2"	35.9595	34.4295	312
Hraiche 1	S52	N 34° 22' 15.7"	E 035° 44' 39.6"	35.744333	34.371028	40
Hraiche 2	S53	N 34° 17' 33.5"	E 035° 55' 03.6"	35.917667	34.292639	not taken
Jisr	S54	-303353	30343,48			28
Kasser Mae	S55	N 34° 26' 12.2"	E 035° 51' 06.8"			89
Kelhat	S56	N 34° 21' 16.9"	E 035° 46' 50.1"	35.780583	34.354694	410
Kfarhat, Jedeide	S57	N 34° 22' 43.3"	E 035° 53' 50.5"	35.897361	34.378694	129
Kfarkahel (private)	S58	N 34° 21' 30.0"	E 035° 51' 05.3"	35.851472	34.358333	220
Kferzayna 1	S59	N 34° 21' 50.6"	E 035° 52' 51.3"	35.880917	34.364056	182
Kferzayna 2	S60	N 34° 21' 51.5"	E 035° 52' 49.2"	35.880333	34.364306	190
Malloule	S61	N 34° 26' 59.1"	E 035° 51' 36.5"	35.860139	34.44975	16
Manar	S62	N 34° 25' 07.3"	E 035° 50' 18.9"	35.838583	34.418694	70
Massafi 7	S63	N 34° 25' 08.7"	E 035° 49' 52.9"	35.831361	34.419083	28

Mazraet el Tefeh	S64	N 34° 19' 17.3"	E 035° 57' 29.7"	35.95825	34.321472	1031
Mervat , Abou Samra	S65	N 34° 25' 15.4"	E 035° 50' 37.0"	35.843611	34.420944	138
Mervat , House	S66	N 34° 26' 21.6"	E 035° 49' 38.8"	35.827444	34.439333	99
Meryata 1- El Blat	S67	N 34° 25' 41.0"	E 035° 55' 53.5"	35.931528	34.428056	370
Meryata 2	S68	N 34° 25' 11.2"	E 035° 56' 10.2"	35.936167	34.419778	225
Meryata 3	S69	N 34° 25' 25.4"	E 035° 56' 49.2"	35.947	34.423722	219
Meryata 4 (Youn Achech)	S70	N 34° 25' 27.0"	E 035° 56' 49.7"	35.947139	34.424167	219
Mijdlaya 1	S71	N 34° 26' 00.8"	E 035° 52' 23.9"	35.873306	34.433556	146
Mijdlaya 2	S72	N 34° 25' 09.2"	E 035° 52' 39.9"	35.87775	34.419222	148
Mina 1	S73	N 34° 26' 51.11"	E 035° 49' 32.2"	35.822	34.447528	10
Mina 2	S74	N 34° 25' 53.6"	E 035° 49' 53.7"	35.825611	34.447531	23
Minieh 1	S75	N 34° 27' 17.4"	E 035° 51' 56.1"	35.939611	34.482278	10
Minieh 2 - Saleh Kheir	S76	N 34° 20' 28.6"	E 035° 49' 16.5"	35.940722	34.483861	247
Nakhle (private)	S77	N 34° 22' 21.0"	E 035° 49' 54.2"	35.831722	34.3725	227
Ras Maska , Private 1	S78	N 34° 23' 52.7"	E 035° 50' 09.3"	35.828222	34.397528	78
Ras Maska , Private 2	S79	N 34° 22' 37.5"	E 035° 47' 54.3"	35.835917	34.397972	306

Raskifa	S80	N 34° 18' 53.0"	E 035° 52' 36.6"	35.876833	34.314722	405
Saadoun	S81	N 34° 25' 47.4"	E 035° 50' 34.1"	35.842806	34.429833	66
Sankari	S82	N 34° 25' 29.7"	E 035° 50' 12.9"	35.836917	34.424917	80
Sebeel	S83	N 34° 18' 54.3"	E 035° 54' 53.5"	35.914861	34.315083	653
Sereel	S84	N 34° 17' 33.5"	E 035° 55' 03.6"	35.917667	34.292639	794
Tripoli (200)	S85	N 34° 17' 05.2"	E 035° 49' 49.1"	35.843556	34.429333	15
Willey	S86	N 34° 25' 45.6"	E 035° 50' 36.8"	35.751472	34.359028	80
Zakroun	S87	N 34° 21' 32.5"	E 035° 45' 05.3"			96

Well Pumping Characteristics for Dry Season

Nom	Libellé	Depth of the well in m	Radius in m	Pumping rate in m ³ /h	Theis T m ² /min	Theis K m/min	Cooper T m ² /min	Cooper K m/min
S1	Aaba (private)							
P1	Agrotech	260	0.12	36	3,33*10 ⁻²	2*10 ⁻⁴	3,91*10 ⁻²	2,31*10 ⁻⁴
P2	Alma dawle	350	0.15	8.5	5,03*10 ⁻³	4,19*10 ⁻⁵	5,28*10 ⁻³	4,4*10 ⁻⁵
S2	Alma 1	85	0.08	7.2	3,01*10 ⁻²	2,32*10 ⁻³	3,92*10 ⁻²	3,01*10 ⁻³
S3	Alma 2	120	0.08	3	1,99*10 ⁻³	6,43*10 ⁻⁵	2,04*10 ⁻³	6,58*10 ⁻⁵
S4	Almoun 1	9	0.5	7.2	9,54*10 ⁻³	n.a	n.a	n.a
S5	Almoun 2	9	0.1	1	3,73*10 ⁻²	3,73*10 ⁻²	5,14*10 ⁻³	5,14*10 ⁻³
P3	Anfe , Jrade	22	0.12	13	1,72*10 ⁻²	1,72*10 ⁻³	n.a	n.a
S9	Anfeh 2	8	0.12	5.143	6,82*10 ⁻³	2,52*10 ⁻³	n.a	n.a
S10	Arabech	150	0.11	2	1,18*10 ⁻³	1,76*10 ⁻⁵	1,09*10 ⁻³	1,62*10 ⁻⁵
S11	Arde							
P4	Arges	225	0.051	12.5	5,88*10 ⁻³	4,63*10 ⁻⁵	1,77*10 ⁻³	1,39*10 ⁻⁵
P5	Asnoun	125	0.12	4	1,64*10 ⁻³	2,75*10 ⁻⁵	1,17*10 ⁻³	1,93*10 ⁻⁵
P6	Ayto	150	0.2	0.5	4,18*10 ⁻⁵	3,29*10 ⁻⁷	4,94*10 ⁻⁴	3,89*10 ⁻⁶
S14	Badebhoon 1	26	0.2	0.8	1,06*10 ⁻³	7,21*10 ⁻⁵	n.a	n.a
S15	Badebhoon 2	85	0.12	2.4	1*10 ⁻³	5,59*10 ⁻⁵	8,78*10 ⁻⁴	4,87*10 ⁻⁵
S16	Balamand							
S17	Barghon	30	0.13	2.4	1*10 ⁻²	4,63*10 ⁻⁴	1*10 ⁻²	4,65*10 ⁻⁴
P7	Barsa	225	0.1	2.4	2,83*10 ⁻²	4,17*10 ⁻⁴	3,07*10 ⁻²	4,52*10 ⁻⁴
P8	Bir Al- Ahdab (Ras Maska)	150	0.12	3	1,58*10 ⁻³	2,40*10 ⁻⁵	1,57*10 ⁻³	2,38*10 ⁻⁵
P9	Bir Bechmezzine, Snoubar	260	0.15	33	1,55*10 ⁻²	7,50*10 ⁻⁵	1,50*10 ⁻²	5,59*10 ⁻⁵
P10	Bir Bterram	450	0.1	24	1,42*10 ⁻²	5,24*10 ⁻⁵	1,34*10 ⁻²	4,97*10 ⁻⁵
P11	Bir El mazraa – Kferaka	375	0.2	10	n.a	n.a	n.a	n.a
P12	Bir Kfarhazir, (Ain el Bakar)	348	0.12	27	3,19*10 ⁻²	1,22*10 ⁻⁴	3,19*10 ⁻²	1,22*10 ⁻⁴

P13	Bir Ras Maska	185	0.15	9	9,74*10 ⁻³	1,60*10 ⁻⁴	9,48*10 ⁻³	1,56*10 ⁻⁴
S20	Bkeftine							
S21	Borj Hayodiyeh (Dawle Well)	220	0.12	36	4,25*10 ⁻²	2,63*10 ⁻⁴	4,72*10 ⁻²	2,92*10 ⁻⁴
S26	Chahal Building (Dam & Farez)	30	0.076	3	3,16*10 ⁻³	7,98*10 ⁻⁵	1,04*10 ⁻⁴	4,14*10 ⁻³
S27	Chekaa 1	50	0.15	3	4,46*10 ⁻²	3,14*10 ⁻³	4,72*10 ⁻²	3,32*10 ⁻³
S28	Chekaa 2	10	0.5	3	3,97*10 ⁻¹	1,89*10 ⁻¹	3,78*10 ⁻²	1,8*10 ⁻²
S29	Dahel El Ain , private 1							
S30	Dédde, Gaz Station	220	0.12	140	4,15*10 ⁻¹	1,59*10 ⁻²	3,83*10 ⁻¹	1,47*10 ⁻²
P14	Deir Achach	55	0.2	15.5	1,63*10 ⁻¹	3,11*10 ⁻³	1,63*10 ⁻¹	3,12*10 ⁻³
S31	Deir Amar 1	150	0.12	90	2,67*10 ⁻¹	2,72*10 ⁻³	2,17*10 ⁻¹	2,22*10 ⁻³
S32	Deir Amar 2(kasser balade)	90	0.076	5	1,66*10 ⁻³	2,87*10 ⁻⁵	1,61*10 ⁻³	2,78*10 ⁻⁵
S33	Deir amar 3, Kassarat							
P15	Ejed Ebrin	450	0.15	43	2,54*10 ⁻²	8,63*10 ⁻⁵	2,62*10 ⁻²	8,9*10 ⁻⁵
S34	Fih	90	0.2	1.8	3,37*10 ⁻³	2,34*10 ⁻⁴	3,12*10 ⁻³	2,17*10 ⁻⁴
P16	Hawouz	250	0.15	2500	6,61*10 ⁰	4,35*10 ⁻²	6,93*10 ⁰	4,52*10 ⁻²
P17	Hellan	90	0.2	4.5	5,96*10 ⁻³	1,57*10 ⁻⁴	n.a	n.a
S35	Hraiche 1	45	0.07	7.2	8,51*10 ⁻³	3,95*10 ⁻⁴	1,70*10 ⁻³	7,94*10 ⁻⁵
S36	Hraiche 2	75	0.15	5	2,09*10 ⁻³	5,24*10 ⁻⁵	2,04*10 ⁻³	5,10*10 ⁻⁵
P18	Jisr	120	0.2	4.776				
P19	Kasser Mae	89	inactive		n.a	n.a	n.a	n.a
S37	Kelhat	108	0.1	1.1	2,59*10 ⁻³	2,59*10 ⁻⁴	9,94*10 ⁻⁴	9,94*10 ⁻⁵
P20	Kferzayna 1	80	0.11	9	6,71*10 ⁻³	2,42*10 ⁻⁴	4,25*10 ⁻³	1,53*10 ⁻⁴
P21	Kferzayna 2	80	0.07	8	8,42*10 ⁻³	3,09*10 ⁻⁴	8,86*10 ⁻³	3,25*10 ⁻⁴
P22	Malloule	75	0.15	3.42	1,27*10 ⁻³	2,71*10 ⁻⁵	1,90*10 ⁻³	4,05*10 ⁻⁵
P23	Manar	212	0.22	5.04	6,68*10 ⁻³	5,22*10 ⁻⁵	n.a	n.a
P24	Massafi 7	70	0.12	9	1,19*10 ⁻²	3,31*10 ⁻⁴	1,23*10 ⁻²	3,42*10 ⁻⁴
P25	Mazraet el Tefeh	140	0.064	15	3,53*10 ⁻³	9,07*10 ⁻⁵	3,21*10 ⁻³	8,23*10 ⁻⁵

P26	Meryata 1- El Blat	250	0.076	18	9,50*10 ⁻³	1,00*10 ⁻⁴	7,98*10 ⁻³	8,40*10 ⁻⁵
P27	Meryata 2	60	0.151	12	2,24*10 ⁻²	5,51*10 ⁻⁴	2,36*10 ⁻²	5,80*10 ⁻⁴
P28	Meryata 3	60	0.138	10	2,16*10 ⁻²	6,59*10 ⁻⁴	3,15*10 ⁻²	7,01*10 ⁻⁴
P29	Meryata 4 (Youn Achech)	55	0.15	15.5	9,18*10 ⁻²	2,34*10 ⁻³	8,55*10 ⁻²	2,18*10 ⁻³
S42	Mijdlaya 1	150	0.15	6	7,95*10 ⁻³	2,15*10 ⁻⁴	n.a	n.a
S43	Mijdlaya 2	170	0.15	3	1,25*10 ⁻³	1,67*10 ⁻⁵	1,23*10 ⁻³	1,64*10 ⁻⁵
S44	Mina 1	7	0.2	2.5	3,31*10 ⁻³	7,36*10 ⁻⁴	n.a	n.a
S45	Mina 2	8	0.2	0.24	4,17*10 ⁻³	7,58*10 ⁻⁴	1,35*10 ⁻³	2,46*10 ⁻⁴
S46	Minieh 1	25	0.15	2.5	1,66*10 ⁻³	1,18*10 ⁻⁴	1,24*10 ⁻³	8,88*10 ⁻⁵
S47	Minieh 2 - Saleh Kheir	20	0.15	2				
S48	Nakhle (private)	259	0.12	3	1,25*10 ⁻³	2,67*10 ⁻⁵	1,32*10 ⁻³	2,82*10 ⁻⁵
S50	Ras Maska , Private 2	190	0.11	5.33	1,12*10 ⁻³	2,24*10 ⁻⁴	2,18*10 ⁻³	4,37*10 ⁻⁴
P30	Raskifa	300	0.2	30	1,25*10 ⁻²	1,46*10 ⁻⁴	1,16*10 ⁻²	1,35*10 ⁻⁴
P31	Saadoun	125	0.12	1.392	1,30*10 ⁻³	3,96*10 ⁻⁵	1,23*10 ⁻³	3,75*10 ⁻⁵
P32	Sankari	160	0.09	3.456	1,55*10 ⁻³	1,40*10 ⁻⁵	1,84*10 ⁻³	2,24*10 ⁻⁵
P33	Sebeel	450	0.1	30	1,99*10 ⁻³	1,44*10 ⁻⁵	1,87*10 ⁻³	1,35*10 ⁻⁵
P34	Sereel	60	0.15	8.5	1,26*10 ⁻²	3,16*10 ⁻⁴	1,23*10 ⁻²	3,08*10 ⁻⁴
S51	Tripoli (200)	12	0.12	2	1,32*10 ⁻²	2,21*10 ⁻³	1,16*10 ⁻²	1,94*10 ⁻³
P35	Willey	120	0.12	3.708	6,94*10 ⁻³	2,57*10 ⁻⁴	7,48*10 ⁻³	2,77*10 ⁻⁴
S52	Zakroun	115	0.15	2	2,65*10 ⁻³	1,03*10 ⁻⁴	n.a	n.a

Well Pumping Characteristics for Wet Season

No m	Libellé	Depth of the well in m	Radius in m	Pumping rate in m ³ /h	T values with Theis m ² /min	K values with Theis m/min	K values with Theis in m/s	T values for Cooper m ² /min	K values for Cooper m/min
S1	Aaba (private)								
P1	Agrotech	260	0.12	36	2.39×10^{-2}	0.000144	2.40E-06	7.50×10^{-2}	4.41×10^{-4}
P2	Alma dawle	350	0.15	8.5	9.04×10^{-2}	0.00065	1.08333E-05	1.73×10^{-1}	1.16×10^{-3}
S2	Alma 1	85	0.08	7.2	1.90×10^{-3}	0.0000705	1.18E-06	3.11×10^{-3}	1.17×10^{-4}
S3	Alma 2	120	0.08	3	1.99×10^{-3}	0.0000712	1.18667E-06	2.73×10^{-3}	9.76×10^{-5}
S4	Almoun 1	9	0.5	7.2	9.54×10^{-3}	0.019	3.17E-04	n.a	n.a
S5	Almoun 2	9	0.1	1	1.32×10^{-3}	0.000884	1.47333E-05	n.a	n.a
S6	Amioun 1								
S7	Amioun 2								
P3	Anfe , Jrade	22	0.12	13	1.72×10^{-2}	0.00123	2.05E-05	n.a	n.a
S8	Anfeh 1								
S9	Anfeh 2	8	0.12	5.143	6.82×10^{-1}	0.378	6.30E-03	3.93×10^{-2}	2.18×10^{-2}
S10	Arabech	150	0.11	2	2.65×10^{-3}	0.0000378	0.00000063	3.07×10^{-3}	4.38×10^{-5}
S11	Arde								
P4	Arges	225	0.051	12.5	4.16×10^{-3}	0.0000313	5.21667E-07	4.51×10^{-3}	3.39×10^{-5}
P5	Asnoun	125	0.12	4	1.05×10^{-3}	0.0000218	3.63E-07	1.76×10^{-3}	3.63×10^{-5}
P6	Ayto	150	0.2	0.5	1.66×10^{-4}	0.00000126	0.000000021	1.96×10^{-4}	1.48×10^{-6}
S12	Badawi 1								
S13	Badawi 2								
S14	Badebhoon 1	26	0.2	0.8	1.06×10^{-3}	0.0000589	9.82E-07	n.a	n.a
S15	Badebhoon 2	85	0.12	2.4	2.83×10^{-3}	0.000105	0.00000175	2.98×10^{-3}	1.10×10^{-4}

S16	Balamand								
S17	Barghon	30	0.13	2.4	1.78×10^{-4}	0.00000813	1.355E-07	7.87×10^{-5}	3.57×10^{-6}
P7	Barsa	225	0.1	2.4	6.35×10^{-3}	0.0000531	8.85E-07	7.55×10^{-3}	6.32×10^{-5}
S18	Batromine								
S19	Bdebba								
P8	Bir Al- Ahdab (Ras Maska)	150	0.12	3	2.51×10^{-3}	0.0000175	2.91667E-07	3×10^{-3}	2.10×10^{-5}
P9	Bir Bechmezzine, Snoubar	260	0.15	33	2.76×10^{-2}	0.000236	3.93E-06	2.72×10^{-2}	2.33×10^{-4}
P10	Bir Bterram	450	0.1	24	5.04×10^{-2}	0.00184	3.06667E-05	6.29×10^{-2}	2.29×10^{-4}
P11	Bir El mazraa – Kferaka	375	0.2	10	2.64×10^{-3}	0.0000154	2.57E-07	3.06×10^{-3}	1.79×10^{-5}
P12	Bir Kfarhazir, (Ain el Bakar)	348	0.12	27	4.50×10^{-2}	0.000172	2.86667E-06	4.81×10^{-2}	1.83×10^{-4}
P13	Bir Ras Maska	185	0.15	9	3.36×10^{-3}	0.0000401	6.68E-07	3.53×10^{-3}	4.21×10^{-5}
S20	Bkeftine								
S21	Borj Hayodiyeh (Dawle Well)	220	0.12	36	6.74×10^{-2}	0.000351	5.85E-06	6.63×10^{-2}	3.45×10^{-4}
S22	Boussit								
S23	Bteram (private)								
S24	Btouratij 1 , Adnan Hassan								
S25	Btouratij 2 , Mokhtar						0.00E+00		
S26	Chahal Building (Dam & Farez)	30	0.076	3	7.93×10^{-3}	0.000387	0.00000645	7.93×10^{-3}	3.87×10^{-4}
S27	Chekaa 1	50	0.15	3	2.81×10^{-3}	0.000157	2.62E-06	3.41×10^{-3}	1.90×10^{-4}
S28	Chekaa 2	10	0.5	3	1.12×10^{-2}	0.00243	0.0000405	1.49×10^{-2}	3.24×10^{-3}

S29	Dahel El Ain , private 1						0.00E+00		
S30	Dédde, Gaz Station	220	0.12	140	$1.17 \cdot 10^{-1}$	0.000565	9.41667E-06	$1.25 \cdot 10^{-1}$	$6.06 \cdot 10^{-4}$
P14	Deir Achach	55	0.2	15.5	$1,19 \cdot 10^{-1}$	0.000813	1.36E-05	n.a	n.a
S31	Deir Amar 1	150	0.12	90	$1.06 \cdot 10^{-1}$	0.00105	0.0000175	$1.29 \cdot 10^{-1}$	$1.27 \cdot 10^{-3}$
S32	Deir Amar 2(kasser balade)	90	0.076	5	$3.32 \cdot 10^{-3}$	0.0000558	9.30E-07	$4.02 \cdot 10^{-3}$	$6.79 \cdot 10^{-5}$
S33	Deir amar 3, Kassarat								
P15	Ejed Ebrin	450	0.15	43	$7.17 \cdot 10^{-3}$	0.0000337	5.62E-07	$7.63 \cdot 10^{-3}$	$3.58 \cdot 10^{-5}$
S34	Fih	90	0.2	1.8	$3,35 \cdot 10^{-2}$	0.00186	0.000031	$4.70 \cdot 10^{-2}$	$2,61 \cdot 10^{-3}$
P16	Hawouz	250	0.15	2500	$8.32 \cdot 10^0$	0.0532	8.87E-04	$8.90 \cdot 10^0$	$5.68 \cdot 10^{-2}$
P17	Hellan	90	0.2	4.5	$5,96 \cdot 10^{-3}$	0.000135	0.00000225	n.a	n.a
S35	Hraiche 1	45	0.07	7.2	$4.26 \cdot 10^{-3}$	0.000157	2.62E-06	$4.60 \cdot 10^{-3}$	$1.70 \cdot 10^{-4}$
S36	Hraiche 2	75	0.15	5	$2,35 \cdot 10^{-2}$	0.00049	8.16667E-06	$2.29 \cdot 10^{-2}$	$4.77 \cdot 10^{-4}$
P18	Jisr	120	0.2	4.776	$1.41 \cdot 10^{-3}$	0.0000363	6.05E-07	$2.04 \cdot 10^{-3}$	$5.23 \cdot 10^{-5}$
P19	Kasser Mae	89	inactive		n.a			n.a	n.a
S37	Kelhat	108	0.1	1.1	$9.2 \cdot 10^{-4}$	0.0000575	9.58E-07	$8.96 \cdot 10^{-4}$	$5.60 \cdot 10^{-5}$
S38	Kfarhat, Jedeide								
S39	Kfarkahel (private)	160	0.2	1.3	$3.44 \cdot 10^{-3}$	0.000275	4.58E-06	$3.62 \cdot 10^{-3}$	$2.90 \cdot 10^{-4}$
P20	Kferzayna 1	80	0.11	9	$8.45 \cdot 10^{-3}$	0.000338	5.63333E-06	$9.43 \cdot 10^{-3}$	$3.77 \cdot 10^{-4}$
P21	Kferzayna 2	80	0.07	8	$2.37 \cdot 10^{-3}$	0.000833	1.39E-05	$2.54 \cdot 10^{-2}$	$8.94 \cdot 10^{-4}$
P22	Malloule	75	0.15	3.42	$4.53 \cdot 10^{-3}$	0.0000944	1.57333E-06	$4.87 \cdot 10^{-3}$	$1.01 \cdot 10^{-4}$
P23	Manar	212	0.22	5.04	$6,68 \cdot 10^{-3}$	0.0000522	8.70E-07	n.a	n.a
P24	Massafi 7	70	0.12	9	$1.06 \cdot 10^{-2}$	0.0000831	0.000001385	$1.05 \cdot 10^{-2}$	$8.20 \cdot 10^{-5}$

P25	Mazraet el Tefeh	140	0.064	15	$1.40 \cdot 10^{-2}$	0.000741	1.24E-05	$1.48 \cdot 10^{-2}$	$7.83 \cdot 10^{-4}$
S41	Mervat , House	25	0.05	2	$2.65 \cdot 10^{-3}$	0.000147	0.00000245	$6.12 \cdot 10^{-3}$	$3.40 \cdot 10^{-4}$
P26	Meryata 1- El Blat	250	0.076	18	$2.67 \cdot 10^{-2}$	0.000277	4.62E-06	$2.78 \cdot 10^{-2}$	$2.89 \cdot 10^{-4}$
P27	Meryata 2	60	0.151	12	$2,24 \cdot 10^{-2}$	0.000485	8.08333E-06	$2,33 \cdot 10^{-2}$	$5.05 \cdot 10^{-4}$
P28	Meryata 3	60	0.138	10	$4.19 \cdot 10^{-2}$	0.000873	1.46E-05	$4.40 \cdot 10^{-2}$	$9.17 \cdot 10^{-4}$
P29	Meryata 4 (Youn Achech)	55	0.15	15.5	$2.30 \cdot 10^{-1}$	0.00544	9.06667E-05	$2.41 \cdot 10^{-1}$	$5.70 \cdot 10^{-3}$
S42	Mijdlaya 1	150	0.15	6	$5.63 \cdot 10^{-3}$	0.000088	1.47E-06	$5.67 \cdot 10^{-3}$	$8.86 \cdot 10^{-5}$
S43	Mijdlaya 2	170	0.15	3	$3.97 \cdot 10^{-3}$	0.0000328	5.46667E-07	$4.35 \cdot 10^{-3}$	$3.59 \cdot 10^{-5}$
S44	Mina 1	7	0.2	2.5	$8.32 \cdot 10^{-3}$	0.00166	2.77E-05	$8.29 \cdot 10^{-3}$	$1.65 \cdot 10^{-3}$
S45	Mina 2	8	0.2	0.24	$2.83 \cdot 10^{-4}$	0.0000472	7.86667E-07	$2.91 \cdot 10^{-4}$	$4.85 \cdot 10^{-5}$
S46	Minieh 1	25	0.15	2.5	$7.42 \cdot 10^{-3}$	0.000674	1.12E-05	$7.36 \cdot 10^{-3}$	$6.69 \cdot 10^{-4}$
S47	Minieh 2 - Saleh Kheir	40	0.15	2	$1.67 \cdot 10^{-3}$	0.000139	2.31667E-06	$1.70 \cdot 10^{-3}$	$1.41 \cdot 10^{-4}$
S48	Nakhle (private)	259	0.12	3	$3.54 \cdot 10^{-3}$	0.0000365	6.08E-07	$3.67 \cdot 10^{-3}$	$3.79 \cdot 10^{-5}$
S49	Ras Maska , Private 1	90	0.15	2.3	$3.05 \cdot 10^{-3}$	0.0000824	1.37333E-06	n.a	n.a
S50	Ras Maska , Private 2	219	0.11	5.33	$1.58 \cdot 10^{-3}$	0.0000545	9.08E-07	$1.68 \cdot 10^{-3}$	$5.81 \cdot 10^{-5}$
P30	Raskifa	300	0.2	30	$2.51 \cdot 10^{-2}$	0.000272	4.53333E-06	$2.61 \cdot 10^{-2}$	$2.84 \cdot 10^{-4}$
P31	Saadoun	125	0.12	1.392	$3.28 \cdot 10^{-3}$	0.0000938	1.56E-06	$3.33 \cdot 10^{-3}$	$9.53 \cdot 10^{-5}$
P32	Sankari	160	0.09	3.456	$3.24 \cdot 10^{-3}$	0.0000364	6.06667E-07	$3.24 \cdot 10^{-3}$	$3.81 \cdot 10^{-5}$
P33	Sebeel	450	0.1	30	$1.25 \cdot 10^{-2}$	0.0000582	9.70E-07	$1.35 \cdot 10^{-2}$	$6.27 \cdot 10^{-5}$
P34	Sereel	60	0.15	8.5	$6.33 \cdot 10^{-3}$	0.00015	0.0000025	$6.10 \cdot 10^{-3}$	$1.45 \cdot 10^{-4}$
S51	Tripoli (200)	12	0.12	2	$2.65 \cdot 10^{-3}$	0.000408	6.80E-06	n.a	n.a
P35	Willey	120	0.12	3.708	$6.19 \cdot 10^{-3}$	0.000199	3.31667E-06	$6.55 \cdot 10^{-3}$	$2.11 \cdot 10^{-4}$
S52	Zakroun	115	0.15	2	$9.41 \cdot 10^{-3}$	0.000304	5.07E-06	$9.55 \cdot 10^{-3}$	$3.09 \cdot 10^{-4}$

Hydraulic Conductivity Values for wells as inserted on VMOD for Dry season

ID	X	Y	Ky m/d	Kx m/d	Kz m/d
P22	163139.75837800000	278806.65477300000	6.98333E-07	6.98333E-07	6.98333E-07
P16	161804.07338800000	276522.27149800000	3.86667E-05	3.86667E-05	3.86667E-05
P24	160420.01442000000	275426.45483600000	1.07167E-06	1.07167E-06	1.07167E-06
P31	161440.97774900000	276690.97039700000	0.000621667	0.000621667	0.000621667
P32	160965.37624700000	276085.13848500000	2.86667E-05	2.86667E-05	2.86667E-05
P35	162120.69690600000	277282.34169500000	0.000042	0.000042	0.000042
P23	161108.10173700000	275392.88176100000	2.93333E-07	2.93333E-07	2.93333E-07
P11	160707.40971500000	264524.89737900000	7.71667E-07	7.71667E-07	7.71667E-07
P8	160390.14701200000	272816.10953100000	4.58333E-07	4.58333E-07	4.58333E-07
P13	160532.72528200000	272613.79207800000	5.48333E-09	5.48333E-09	5.48333E-09
P7	159765.01466600000	271833.90902700000	1.20167E-06	1.20167E-06	1.20167E-06
P1	158035.97931300000	264670.10732900000	9.31667E-07	9.31667E-07	9.31667E-07
P12	157740.94385400000	264764.01307100000	7.71667E-06	7.71667E-06	7.71667E-06
P10	159013.91507800000	265443.77120400000	0.00000695	0.00000695	0.00000695
P9	157702.41979500000	263976.84341400000	0.0000004	0.0000004	0.0000004
P3	151647.48389700000	266526.10210900000	0.00000125	0.00000125	0.00000125
P15	151767.27734800000	259629.98307800000	8.73333E-07	8.73333E-07	8.73333E-07
S48	160400.48693500000	270280.73377900000	2.03333E-06	2.03333E-06	2.03333E-06
S39	161797.32939000000	268129.76609200000	2.66667E-06	2.66667E-06	2.66667E-06
S34	155939.63205900000	267412.79169000000	4.38333E-06	4.38333E-06	4.38333E-06
S37	155257.02040900000	268715.00003200000	0.00000133	0.00000133	0.00000133
P2	166654.73577300000	277088.79667600000	6.66667E-05	6.66667E-05	6.66667E-05

P26	169427.54194900000	275813.83641000000	0.00315	0.00315	0.00315
P27	170076.67609400000	275382.91435000000	0.000265	0.000265	0.000265
P28	170515.74038900000	276957.67862700000	5.18333E-05	5.18333E-05	5.18333E-05
P29	170853.51279300000	276095.41655000000	4.53333E-05	4.53333E-05	4.53333E-05
P17	172102.91093500000	277038.99246500000	4.78333E-07	4.78333E-07	4.78333E-07
P14	170360.87723100000	274789.24566800000	1.43833E-06	1.43833E-06	1.43833E-06
P5	165645.03053800000	271583.63810200000	0.0000039	0.0000039	0.0000039
P20	164909.79301900000	269277.48013600000	0.000725	0.000725	0.000725
P21	164838.27221500000	269340.90115300000	2.61667E-06	2.61667E-06	2.61667E-06
P4	164831.74558000000	266031.80370100000	6.58333E-06	6.58333E-06	6.58333E-06
P30	164236.32733200000	263710.49972700000	8.73333E-07	8.73333E-07	8.73333E-07
P33	167799.98281400000	263789.06080300000	4.31667E-06	4.31667E-06	4.31667E-06
P6	169344.64268600000	263114.65078900000	4.03333E-06	4.03333E-06	4.03333E-06
P25	171779.73629400000	264441.05252700000	0.00000515	0.00000515	0.00000515
P34	167978.63973100000	261307.18303400000	4.51667E-07	4.51667E-07	4.51667E-07
S42	164322.89403700000	276993.36995900000	0.00000087	0.00000087	0.00000087
S43	163783.39296300000	274946.88396300000	5.51667E-06	5.51667E-06	5.51667E-06
S31	166260.34633100000	279829.97702100000	1.51167E-06	1.51167E-06	1.51167E-06
S32	166577.23823000000	280510.54522500000	1.66667E-06	1.66667E-06	1.66667E-06
S21	168133.08451800000	279316.28475900000	9.18333E-06	9.18333E-06	9.18333E-06
S44	158447.12821000000	279040.41675700000	1.09833E-05	1.09833E-05	1.09833E-05
S45	159070.74407400000	277841.75501600000	0.000039	0.000039	0.000039
S26	160486.37296800000	276828.59275500000	3.58333E-06	3.58333E-06	3.58333E-06
S49	159292.57343600000	273128.11707800000	2.78333E-07	2.78333E-07	2.78333E-07
S50	160222.61515900000	274912.63757600000	1.22667E-05	1.22667E-05	1.22667E-05
S24	161630.87373400000	270047.48189100000	1.26333E-05	1.26333E-05	1.26333E-05
S30	157572.78248500000	271266.13294000000	1.96667E-06	1.96667E-06	1.96667E-06
S18	158278.66003200000	269700.85539600000	0.000000445	0.000000445	0.000000445
S12	164799.68269100000	279695.74862100000	3.73333E-06	3.73333E-06	3.73333E-06

S13	164181.39239800000	278364.23426500000	2.43333E-06	2.43333E-06	2.43333E-06
S4	156978.43983600000	272489.22350200000	0.00000066	0.00000066	0.00000066
S5	155464.73271300000	271443.28611400000	2.33333E-07	2.33333E-07	2.33333E-07
S33	166673.99785000000	278775.41511500000	0.00000024	0.00000024	0.00000024
S19	158933.05997000000	267504.09691600000	5.26667E-06	5.26667E-06	5.26667E-06
S17	153393.73715000000	267251.02289300000	3.68333E-05	3.68333E-05	3.68333E-05
S8	151249.00214700000	268961.42240600000	4.28333E-06	4.28333E-06	4.28333E-06
S9	151091.99140100000	267813.32353400000	1.71667E-06	1.71667E-06	1.71667E-06
S35	153470.12110300000	270715.54500600000	3.33333E-06	3.33333E-06	3.33333E-06
S36	152009.50455000000	270060.57113700000	6.98333E-07	6.98333E-07	6.98333E-07
S27	152082.47988100000	265231.04645400000	3.86667E-05	3.86667E-05	3.86667E-05
S28	150295.22393500000	264539.60293000000	1.07167E-06	1.07167E-06	1.07167E-06
S14	154654.01884600000	265805.12410100000	0.000621667	0.000621667	0.000621667
S15	153228.32156300000	266140.26360100000	2.86667E-05	2.86667E-05	2.86667E-05
S52	153142.19690700000	268867.96843200000	0.000042	0.000042	0.000042
S16	155636.07104500000	269765.32237200000	2.93333E-07	2.93333E-07	2.93333E-07
S23	158253.07751400000	266487.20103300000	7.71667E-07	7.71667E-07	7.71667E-07
S1	160066.16278000000	267420.97531500000	4.58333E-07	4.58333E-07	4.58333E-07
S40	161573.84543200000	275635.42660100000	5.48333E-09	5.48333E-09	5.48333E-09
S41	160119.13511300000	277696.58574200000	1.20167E-06	1.20167E-06	1.20167E-06
S11	168148.02148500000	274890.32023300000	9.31667E-07	9.31667E-07	9.31667E-07
S10	166220.56378400000	272813.48667200000	7.71667E-06	7.71667E-06	7.71667E-06
S38	166408.70311400000	269757.19007600000	0.00000695	0.00000695	0.00000695
S22	169055.37736100000	277544.36016100000	0.0000004	0.0000004	0.0000004
S2	167141.54757600000	275972.83340400000	0.00000125	0.00000125	0.00000125
S3	166402.03400700000	275165.64105500000	8.73333E-07	8.73333E-07	8.73333E-07
S29	161796.25980900000	271877.43165400000	2.03333E-06	2.03333E-06	2.03333E-06
S20	163328.54290100000	271712.66827300000	2.66667E-06	2.66667E-06	2.66667E-06
S25	160532.33848300000	268957.70797500000	4.38333E-06	4.38333E-06	4.38333E-06

S6	158514.86563400000	263206.92354700000	0.00000133	0.00000133	0.00000133
S7	159039.19406600000	260893.40749300000	6.66667E-05	6.66667E-05	6.66667E-05
P19	162896.49899000000	277799.36139100000	0.00315	0.00315	0.00315
P18	162269.66099900000	273906.05275700000	0.000265	0.000265	0.000265
S47	170368.34071100000	282246.82410700000	5.18333E-05	5.18333E-05	5.18333E-05
S46	168618.80148700000	280973.98125400000	4.53333E-05	4.53333E-05	4.53333E-05
S51	161694.63149900000	278378.57678300000	4.78333E-07	4.78333E-07	4.78333E-07

Hydraulic Conductivity Values for wells as inserted on VMOD for Wet season

Nom	Libellé	Kx m/d	Ky m/d	Kz m/d
S1	Aaba (private)			
P1	Agrotech	0.00336	0.00336	0.00336
P2	Alma dawle	0.01516667	0.01516667	0.01516667
S2	Alma 1	0.001645	0.001645	0.001645
S3	Alma 2	0.00166133	0.00166133	0.00166133
S4	Almoun 1	0.44333333	0.44333333	0.44333333
S5	Almoun 2	0.02062667	0.02062667	0.02062667
S6	Amioun 1			
S7	Amioun 2			
P3	Anfe , Jrade	0.0287	0.0287	0.0287
S8	Anfeh 1			
S9	Anfeh 2	8.82	8.82	8.82
S10	Arabech	0.000882	0.000882	0.000882
S11	Arde	0	0	0
P4	Arges	0.00073033	0.00073033	0.00073033
P5	Asnoun	0.00050867	0.00050867	0.00050867

P6	Ayto	0.0000294	0.0000294	0.0000294
S12	Badawi 1			
S13	Badawi 2			
S14	Badebhoon 1	0.00137433	0.00137433	0.00137433
S15	Badebhoon 2	0.00245	0.00245	0.00245
S16	Balamand			
S17	Barghon	0.0001897	0.0001897	0.0001897
P7	Barsa	0.001239	0.001239	0.001239
S18	Batromine			
S19	Bdebba			
P8	Bir Al- Ahdab (Ras Maska)	0.00040833	0.00040833	0.00040833
P9	Bir Bechmezzine, Snoubar	0.00550667	0.00550667	0.00550667
P10	Bir Bterram	0.04293333	0.04293333	0.04293333
P11	Bir El mazraa – Kferaka	0.00035933	0.00035933	0.00035933
P12	Bir Kfarhazir, (Ain el Bakar)	0.00401333	0.00401333	0.00401333
P13	Bir Ras Maska	0.00093567	0.00093567	0.00093567
S20	Bkeftine			
S21	Borj Hayodiyeh (Dawle Well)	0.00819	0.00819	0.00819
S22	Boussit			
S23	Bteram (private)			
S24	Btouratij 1 , Adnan Hassan			
S25	Btouratij 2 , Mokhtar			
S26	Chahal Building (Dam & Farez)	0.00903	0.00903	0.00903
S27	Chekaa 1	0.00366333	0.00366333	0.00366333
S28	Chekaa 2	0.0567	0.0567	0.0567
S29	Dahel El Ain , private 1			

S30	Dédde, Gaz Station	0.01318333	0.01318333	0.01318333
P14	Deir Achach	0.01897	0.01897	0.01897
S31	Deir Amar 1	0.0245	0.0245	0.0245
S32	Deir Amar 2(kasser balade)	0.001302	0.001302	0.001302
S33	Deir amar 3, Kassarat			
P15	Ejed Ebrin	0.00078633	0.00078633	0.00078633
S34	Fih	0.0434	0.0434	0.0434
P16	Hawouz	1.24133333	1.24133333	1.24133333
P17	Hellan	0.00315	0.00315	0.00315
S35	Hraiche 1	0.00366333	0.00366333	0.00366333
S36	Hraiche 2	0.01143333	0.01143333	0.01143333
P18	Jisr	0.000847	0.000847	0.000847
P19	Kasser Mae			
S37	Kelhat	0.00134167	0.00134167	0.00134167
S38	Kfarhat, Jedeide			
S39	Kfarkahel (private)	0.00641667	0.00641667	0.00641667
P20	Kferzayna 1	0.00788667	0.00788667	0.00788667
P21	Kferzayna 2	0.01943667	0.01943667	0.01943667
P22	Malloule	0.00220267	0.00220267	0.00220267
P23	Manar	0.001218	0.001218	0.001218
P24	Massafi 7	0.001939	0.001939	0.001939
P25	Mazraet el Tefeh	0.01729	0.01729	0.01729
S41	Mervat , House	0.00343	0.00343	0.00343
P26	Meryata 1- El Blat	0.00646333	0.00646333	0.00646333
P27	Meryata 2	0.01131667	0.01131667	0.01131667
P28	Meryata 3	0.02037	0.02037	0.02037
P29	Meryata 4 (Youn Achech)	0.12693333	0.12693333	0.12693333
S42	Mijdlaya 1	0.00205333	0.00205333	0.00205333

S43	Mijdlaya 2	0.00076533	0.00076533	0.00076533
S44	Mina 1	0.03873333	0.03873333	0.03873333
S45	Mina 2	0.00110133	0.00110133	0.00110133
S46	Minieh 1	0.01572667	0.01572667	0.01572667
S47	Minieh 2 - Saleh Kheir	0.00324333	0.00324333	0.00324333
S48	Nakhle (private)	0.00085167	0.00085167	0.00085167
S49	Ras Maska , Private 1	0.00192267	0.00192267	0.00192267
S50	Ras Maska , Private 2	0.00127167	0.00127167	0.00127167
P30	Raskifa	0.00634667	0.00634667	0.00634667
P31	Saadoun	0.00218867	0.00218867	0.00218867
P32	Sankari	0.00084933	0.00084933	0.00084933
P33	Sebeel	0.001358	0.001358	0.001358
P34	Sereel	0.0035	0.0035	0.0035
S51	Tripoli (200)	0.00952	0.00952	0.00952
P35	Willey	0.00464333	0.00464333	0.00464333
S52	Zakroun	0.00709333	0.00709333	0.00709333

Well Data inserted for Wet season:

ID	X	Y	well bottom	screen ID	Radius in m	Pumping rate	Conductivity m/d	Elevation	Screen top Z	Screen bottom Z
S48	156978	272489	60	51	0.15	120		75	35	44
S39	157572	271266	100	47	0.2	43.2	0.3816	306	75.6	80
S34	157702	263976	150	13	0.051	300	0.0018	300	98	111
S37	157740	264764	125	11	0.11	48	0.002928	280	85	92
P2	158035	264670	15	10	0.12	123.432	0.000007896	300	5.3	5.5
P26	158253	266487	60	65	0.151	288		268	19.2	21.6
P27	158278	269700	150	48	0.15	60000		318	98	99
P28	158447	279040	20	41	0.12	2940	0.017664	22	18	14
P29	158514	263206	125	78	0.12	33.408		295	92	96
P17	158933	267504	135	53	0.1	26.4		247	98	106
P14	159013	265443	150	12		15	0.0012576	280	12.9	16
P5	159039	260893	160	79	0.09	82.944		298	78	83
P20	159070	277841	5.5	42	0.2	372	0.018192	10	2.6	3.1
P21	159292	273128	90	44	0.076	125	0.002832	108	32	47
P4	159765	271833	20	9			0.010008	170	5.5	5.5
P30	160066	267420	55	66	0.138	240		241	15	16
P33	160119	277696	126	68	0.15	144		150	113	118
P6	160222	274912	60	45		23.1	0.005376	88	82	85
P25	160400	270280	150	16		10	0.0006408	237	46	47
P34	160420	275426	240	3	0.15	204	0.007944	255	230	238
S42	160486	276828	55	43	0.12	2160	0.0019152	63	52	54
S43	160532	272613	30	8	0.12	312	0.00384	150	12	12

S31	160532	268957	235	77	0.2	720		250	214	229
S32	160965	276085	100	5	0.08	72	0.000336	150	89	96
S21	161108	275392	20	7	0.1	24	0.0012528	120	n.a	8
S44	161440	276690	85	4	0.08	172.8	0.0009504	120	72	77.7
S45	161573	275635	55	67	0.15	372		138	15.8	16.8
S26	161630	270047	175	46	0.15	1032		215	155	161
S49	161694	278378	102	84	0.15	48	0.05304	110	89.3	89.3
S50	161796	271877	55	75		6.2		79	53	53
S24	161797	268129	120	17		25		230	82	85
S30	161804	276522	98	2	0.12	864	1.044	120	92.4	91
S18	162120	277282	19	6	0.5	172.8	0.006168	100	9	9
S12	162269	273906	60	81	0.15	204		60	20	25
S13	162896	277799	400	80	0.1	720		450	312	380
S4	163139	278806	148	1			0.0006504	170	147.15	146
S33	163328	271712	190	76	0.11	127.92		199	n.a	198
S19	163783	274946	30	37	0.076	63	0.0004008	148	2.5	11
S17	164181	278364	45	50	0.07	172.8		55	23.5	46
S8	164236	263710	180	31			0.003504	405	144	145
S9	164322	276993	10	36		60	0.00516	146	2.5	4
S35	164799	279695	90	49	0.2	108		68	52	52
S36	164831	266031	185	30	0.15	216	0.0011112	299	124.5	127
S27	164838	269340	115	29	0.12	648	0.007416	190	88	90
S28	164909	269277	220	28	0.2	240	0.005808	250	212	230
S14	165645	271583	200	27	0.1	576	0.00066	230	179	186.5
S15	166220	272813	7	70	0.2	60	0.0004224	770	2.5	n.a
S52	166260	279829	50	38	0.15	63	0.06528	66	35.8	36
S16	166402	275165	235	74	0.12	72	0.0015432	260	212	225.5
S23	166408	269757	8	71	0.2	5.76		129	2.5	11
S1	166577	280510	15	39	0.5	63	0.0006888	37	7.9	8

S40	166654	277088	180	20		36	0.002928	265	150	158
S41	166673	278775	120	52	inactive			146	92	102
S11	167141	275972	50	73	0.15	48	0.05568	198	18	25
S10	167799	263789	189	32	0.12	864		653	145.5	160
S38	167978	261307	200	35		54	0.007584	794	154	165
S22	168133	279316	90	40		30	0.006312	198	64	71.5
S2	168148	274890	144	69	0.15	72		176	95	108
S3	168618	280973	112	83	0.12	88.992		120	93	96

APPENDIX 3- INPUT DATA FOR VISUAL MODFLOW

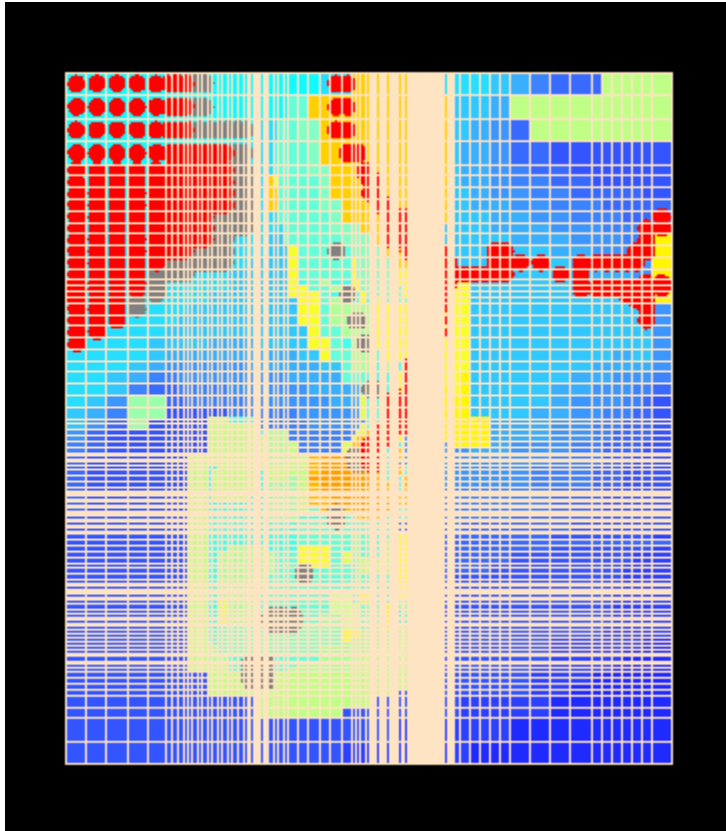
Geological Legend for the polygon file inserted :

Geology Class	NAPPES D'EAU SOUTERRAINE	LITHOLOGIE FACIES	AGE	DEBITS DES SOURCES l/sec.	DEBITS INSTANTANES PROBABLES DES OUVRAGES l/sec.	TRANSMISSIVITE m ² /sec	EXTENSION DES AFFLEUREMENTS Km ²	
1	EN FORMATIONS KARSTIQUES Nappes étendues et riches	Calcaires massifs et calcaires dolomitiques avec intercal. de marnes Epaisseur: >1000 m.	JURASSIQUE Bathonien-Portlandien	<100 100-1000 >1000	>100	10 ⁻² ≤ T ≤ 1 Le plus souvent élevée	1290	6100
2		Calcaires régulièrement lités Epaisseur: 800 à 1000 m.	CRETACE Cénomanien-Turonien	<100 100-1000 >1000	>100	10 ⁻² ≤ T ≤ 1 Le plus souvent élevée	4290	
3		Calcaires et marno-calcaires à lits de silex Epaisseur: ~ 200m.	CRETACE Turonien	100-1000 >1000	>100	Le plus souvent élevée	100	
4		Calcaires subrécifaux Epaisseur: 100 à 800 m.	NUMMULITIQUE Eocène	100-1000	<100	10 ⁻⁴ ≤ T ≤ 10 ⁻² Souvent élevée	317	
5		Calcaires récifaux Epaisseur: 200 à 250 m.	NEOGENE Miocène	100-1000	<100	Souvent élevée	103	
6	EN FORMATIONS MEROKARSTIQUES Nappes étendues	Calcaires, marnes Epaisseur: 100 à 300 m.	NUMMULITIQUE Eocène	<100	<50	10 ⁻⁴ ≤ T ≤ 10 ⁻³ Médiocre	536	536

7	EN FORMATIONS POREUSES	Nappes étendues	Poudingues grossiers torrentiels- Conglomérats marneux Epaisseur: 500 à 600 m.	NEOGENE Miocène et Pliocène (faciès continental)	<100 OU DECHARGE DISPERSEE DIFFUSE	<30	<10 ⁻³ Médiocre ou changeante	746	1644
8			Alluvions anciennes	QUATERNAIRE	DECHARGE DIFFUSE	<30	10 ⁻⁴ ≤ T ≤ 10 ⁻³ Médiocre	68	
9			Limons et "terra rossa" Epaisseur: 600 m.	QUATERNAIRE	DECHARGE DIFFUSE	<10	Médiocre à faible très changeante	830	
10		Nappes locales ou discontinues	Grès Epaisseur: 150 à 250 m.	CRETACE Grès de base	<10	<10	10 ⁻⁵ ≤ T ≤ 10 ⁻⁴ Médiocre à faible	275	431
11			Décollements cailloutis de pentes et coulées boueuses Epaisseur: variable	QUATERNAIRE	–	<10	Médiocre à faible	122	
12			Sols rouges Epaisseur: variable	QUATERNAIRE	DECHARGE DIFFUSE	<10	Médiocre à faible	14	
13			Sables littoraux Epaisseur: variable	QUATERNAIRE	DECHARGE DIFFUSE	<10	Médiocre à faible	12	
14			Alluvions actuelles Epaisseur: variable	QUATERNAIRE	DECHARGE DIFFUSE	<10	Médiocre à faible	7	
15			Grès littoraux Epaisseur: variable	QUATERNAIRE	DECHARGE DIFFUSE	<10	Médiocre à faible	1	
16		REGIONS GENERALEMENT SANS NAPPES OU A NAPPES TRES LOCALES	Alternances de terrains argilo-sableux, de bancs calcaires et de marnes Epaisseur: 300 à 400 m.	CRETACE Aptien_Albien	<5 (Sources intermittentes)	<5	Faible à très faible	552	1489
17			Marnes et marno-calcaires Epaisseur: 100 à 200 m.	CRETACE Sénonien et base de l'Eocène	–	Très faible	Très faible	416	

18	Marnes Epaisseur: 50 m.	NUMMULITIQUE Eocène				
19	Marnes Epaisseur: 50 m.	NEOGENE Miocène_Faciès marin	–	Très faible	Faible à très faible	83
20	Marnes et marno-calcaires Epaisseur: ~ 900 m.	NEOGENE Faciès continental				
21	Argiles, marnes sableuses et calcaires Epaisseur: 250 à 400 m.	NEOGENE Pliocène Faciès marin	–	Très faible	Faible à très faible	73
22	Basaltes Epaisseur: variable	CRETACE INF. MIOCENE PLIOCENE QUATERNAIRE	–	Très faible	Très faible	365

Conductivity Values Inserted :



Conductivity Value Ranges:

Visual MODFLOW Flex - [project 3 latest]

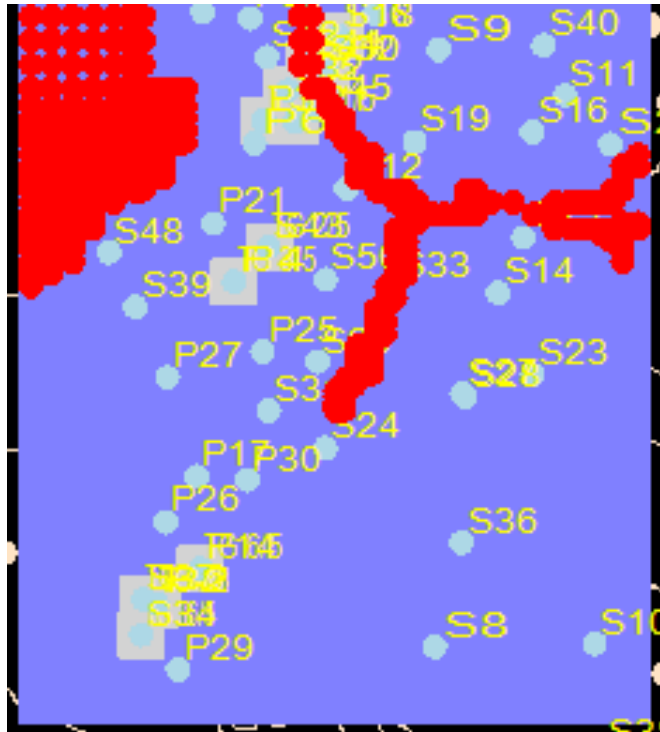
Conductivity

	Zone	Color	Kx	Ky	Kz
4		Blue	Distributed Values	Distributed Values	Distributed Values
5		Blue	Distributed Values	Distributed Values	Distributed Values
6		Blue	Distributed Values	Distributed Values	Distributed Values
7		Blue	Distributed Values	Distributed Values	Distributed Values
8		Blue	Distributed Values	Distributed Values	Distributed Values
9		Blue	Distributed Values	Distributed Values	Distributed Values
10		Blue	Distributed Values	Distributed Values	Distributed Values
11		Blue	Distributed Values	Distributed Values	Distributed Values
12		Blue	Distributed Values	Distributed Values	Distributed Values
13		Blue	0.001	0.001	0.001
14		Blue	Distributed Values	Distributed Values	Distributed Values
15		Blue	Distributed Values	Distributed Values	Distributed Values
16		Blue	Distributed Values	Distributed Values	Distributed Values
17		Blue	Distributed Values	Distributed Values	Distributed Values
18		Blue	Distributed Values	Distributed Values	Distributed Values
19		Blue	0.01	0.01	0.01
20		Blue	Distributed Values	Distributed Values	Distributed Values
21		Blue	8E-08	8E-08	8E-08
22		Blue	0.09	0.09	0.09
23		Blue	0.05	0.05	0.05
24		Blue	0.25	0.25	0.25
25		Blue	0.8	0.8	0.8
44		Red	2.44110217838256E-06	2.44110217838256E-06	2.44110217838256E-06

OK Cancel

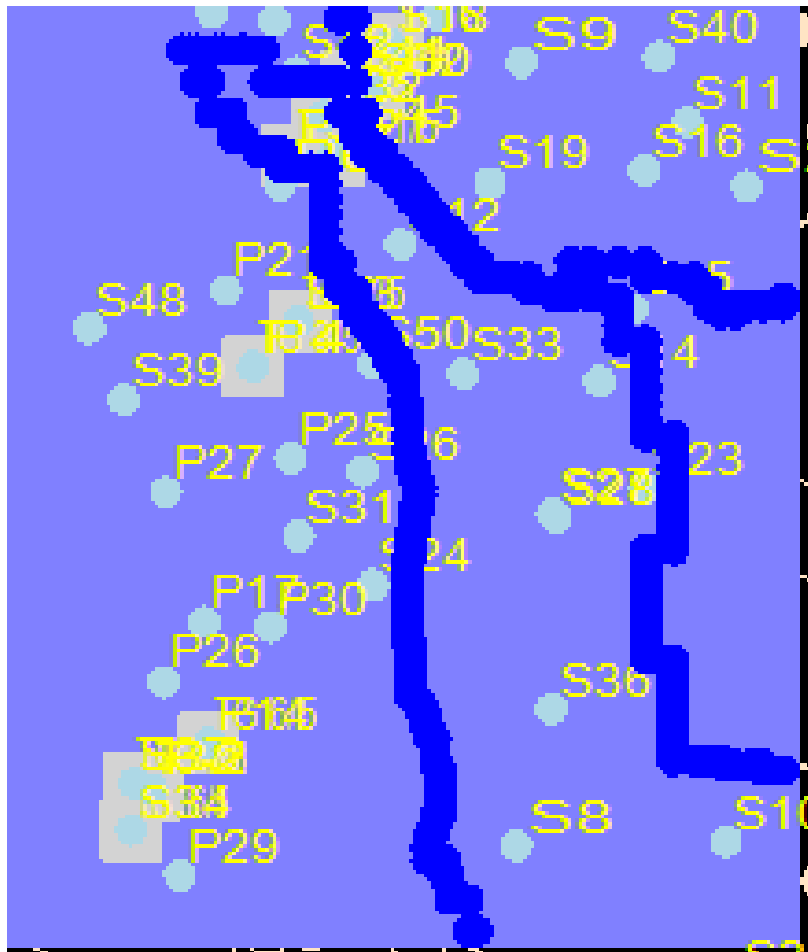
Windows taskbar: 10:17 PM 5/11/2014

Constant Head Assigned for the River and the Sea

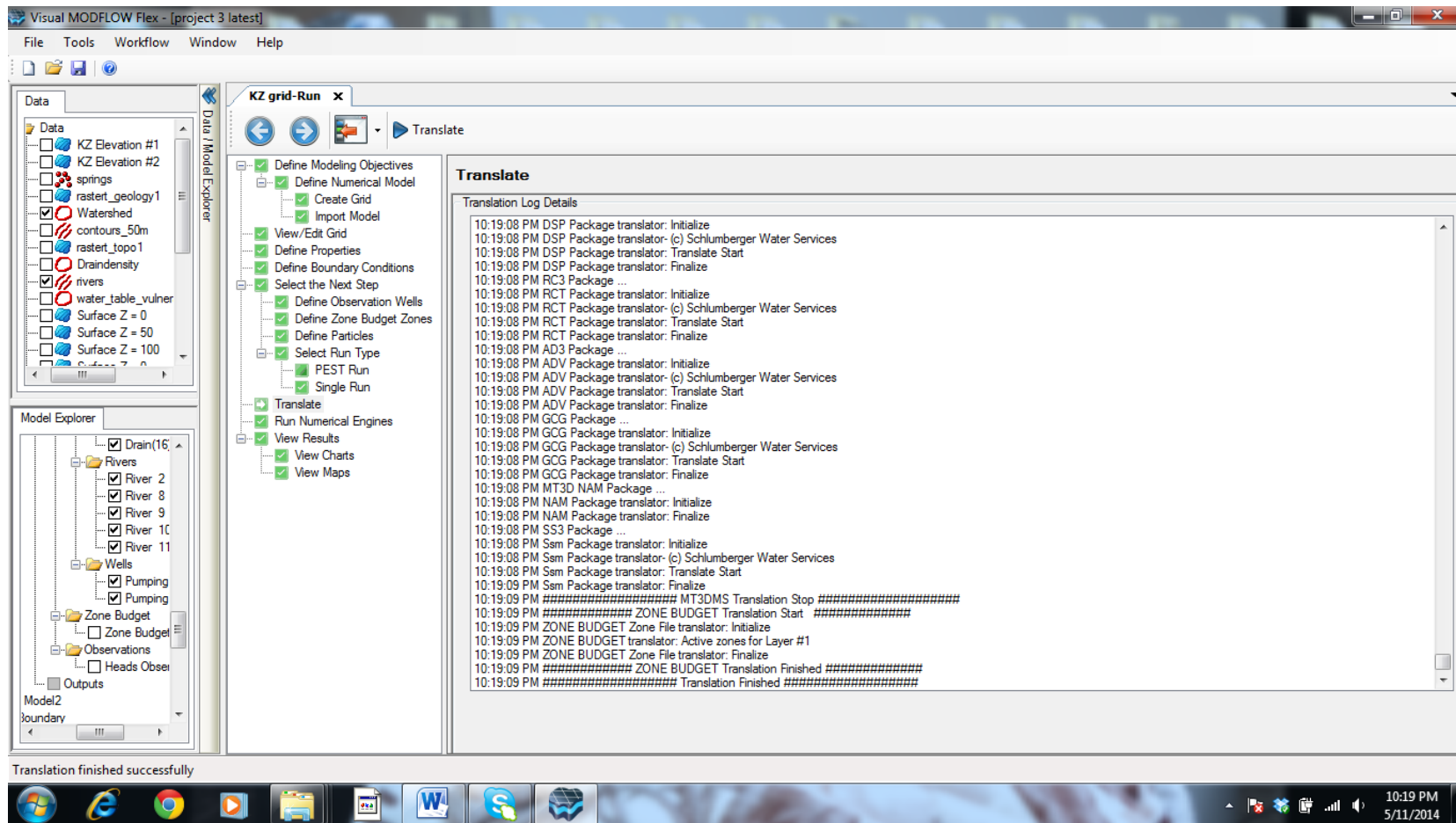


River Characteristics Inserted as Excel sheet on VMOD

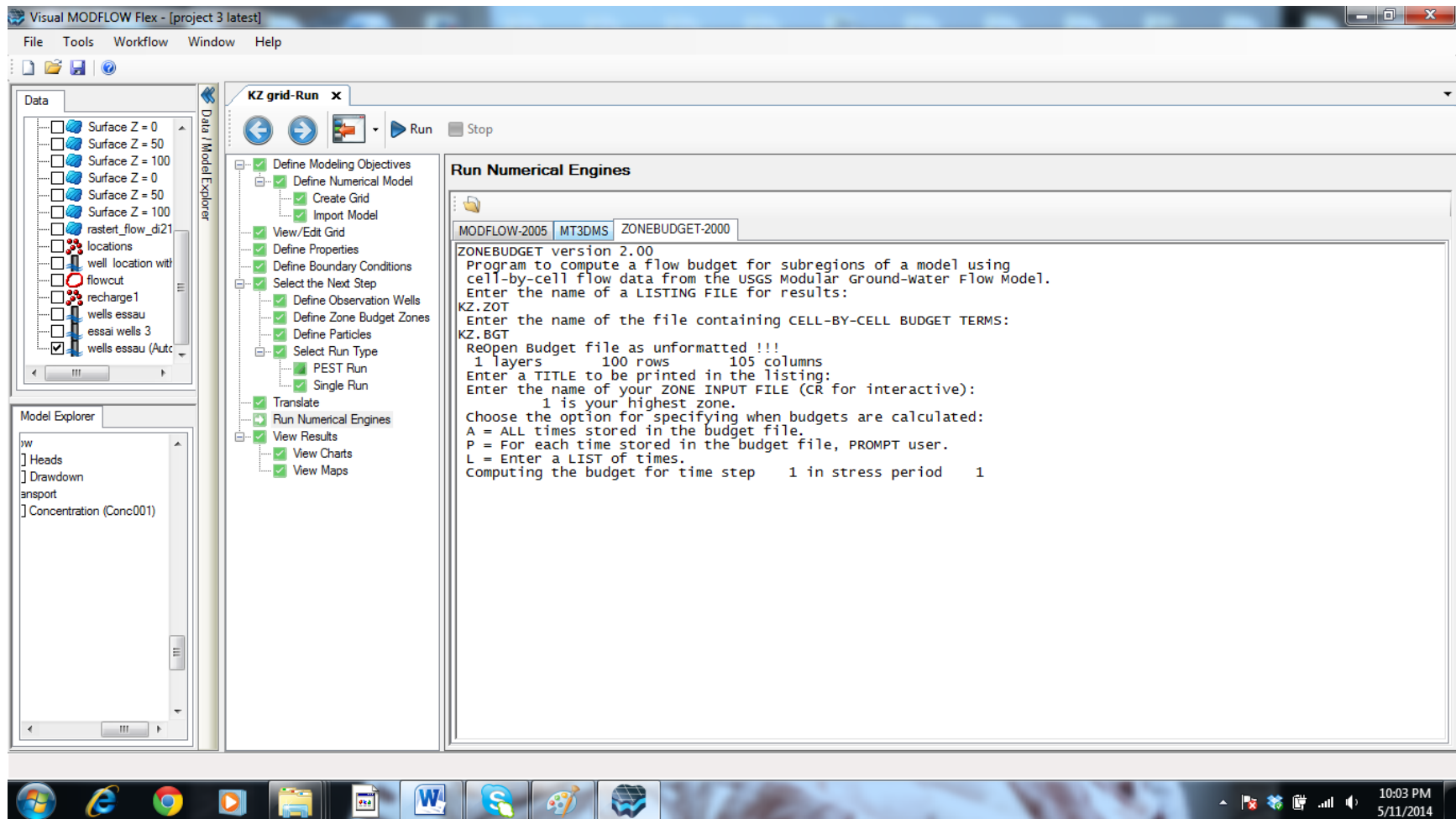
Abou Ali	
Flow	137.8 Mm/year
Coordonnées Abou Ali River	
Latitude	34°20'41, 32'N
Longitude	35°55'29,18'E
Distance	19224 m
Longueur	42 km
Surface	484 km2



Translate function in order to run the model :



Running the model:



Cross section indicating water flow in the model:

